

UNCLASSIFIED

AD NUMBER

AD877587

LIMITATION CHANGES

TO:

Approved for public release; distribution is unlimited. Document partially illegible.

FROM:

Distribution authorized to U.S. Gov't. agencies and their contractors; Critical Technology; SEP 1970. Other requests shall be referred to Army Aviation Material Laboratory, Fort Eustis, VA 23604. This document contains export-controlled technical data.

AUTHORITY

usaamrdl ltr, 10 sep 1971

THIS PAGE IS UNCLASSIFIED

AD 877587

AD No. \_\_\_\_\_

DDC FILE COPY

USAAVLABS TECHNICAL REPORT 70-31

500-POUND CONTROLLED AIRDROP CARGO SYSTEM

By

Robert G. Slayman  
Herbert Q. Bair  
Thomas W. Rathbun

September 1970



U. S. ARMY AVIATION MATERIEL LABORATORIES  
FORT EUSTIS, VIRGINIA

CONTRACT DAAJ02-C-0040

NEW

GOODYEAR AEROSPACE CORPORATION  
AKRON, OHIO

This document is subject to special export controls, and each transmittal to foreign governments or foreign nationals may be made only with prior approval of U.S. Army Aviation Materiel Laboratories, Fort Eustis, Virginia 23604.



Sponsored By

Advanced Research Projects  
Agency - ARPA Order No. 294

256

# DISCLAIMER NOTICE

THIS DOCUMENT IS THE BEST  
QUALITY AVAILABLE.

COPY FURNISHED CONTAINED  
A SIGNIFICANT NUMBER OF  
PAGES WHICH DO NOT  
REPRODUCE LEGIBLY.

MISSING PAGE  
NUMBERS ARE BLANK  
AND WERE NOT  
FILMED



### DISCLAIMERS

The findings in this report are not to be construed as an official Department of the Army position unless so designated by other authorized documents.

When Government drawings, specifications, or other data are used for any purpose other than in connection with a definitely related Government procurement operation, the United States Government thereby incurs no responsibility nor any obligation whatsoever; and the fact that the Government may have formulated, furnished, or in any way supplied the said drawings, specifications, or other data is not to be regarded by implication or otherwise as in any manner licensing the holder or any other person or corporation, or conveying any rights or permission, to manufacture, use, or sell any patented invention that may in any way be related thereto.

### DISPOSITION INSTRUCTIONS

Destroy this report when no longer needed. Do not return it to the originator.

1. WHITE SECTION <input type="checkbox"/>		
2. BUFF SECTION <input checked="" type="checkbox"/>		
3. <input type="checkbox"/>		
4. <input type="checkbox"/>		
5. <input type="checkbox"/>		
6. <input type="checkbox"/>		
7. <input type="checkbox"/>		
8. <input type="checkbox"/>		
9. <input type="checkbox"/>		
10. <input type="checkbox"/>		
11. <input type="checkbox"/>		
12. <input type="checkbox"/>		
13. <input type="checkbox"/>		
14. <input type="checkbox"/>		
15. <input type="checkbox"/>		
16. <input type="checkbox"/>		
17. <input type="checkbox"/>		
18. <input type="checkbox"/>		
19. <input type="checkbox"/>		
20. <input type="checkbox"/>		
21. <input type="checkbox"/>		
22. <input type="checkbox"/>		
23. <input type="checkbox"/>		
24. <input type="checkbox"/>		
25. <input type="checkbox"/>		
26. <input type="checkbox"/>		
27. <input type="checkbox"/>		
28. <input type="checkbox"/>		
29. <input type="checkbox"/>		
30. <input type="checkbox"/>		
31. <input type="checkbox"/>		
32. <input type="checkbox"/>		
33. <input type="checkbox"/>		
34. <input type="checkbox"/>		
35. <input type="checkbox"/>		
36. <input type="checkbox"/>		
37. <input type="checkbox"/>		
38. <input type="checkbox"/>		
39. <input type="checkbox"/>		
40. <input type="checkbox"/>		
41. <input type="checkbox"/>		
42. <input type="checkbox"/>		
43. <input type="checkbox"/>		
44. <input type="checkbox"/>		
45. <input type="checkbox"/>		
46. <input type="checkbox"/>		
47. <input type="checkbox"/>		
48. <input type="checkbox"/>		
49. <input type="checkbox"/>		
50. <input type="checkbox"/>		
51. <input type="checkbox"/>		
52. <input type="checkbox"/>		
53. <input type="checkbox"/>		
54. <input type="checkbox"/>		
55. <input type="checkbox"/>		
56. <input type="checkbox"/>		
57. <input type="checkbox"/>		
58. <input type="checkbox"/>		
59. <input type="checkbox"/>		
60. <input type="checkbox"/>		
61. <input type="checkbox"/>		
62. <input type="checkbox"/>		
63. <input type="checkbox"/>		
64. <input type="checkbox"/>		
65. <input type="checkbox"/>		
66. <input type="checkbox"/>		
67. <input type="checkbox"/>		
68. <input type="checkbox"/>		
69. <input type="checkbox"/>		
70. <input type="checkbox"/>		
71. <input type="checkbox"/>		
72. <input type="checkbox"/>		
73. <input type="checkbox"/>		
74. <input type="checkbox"/>		
75. <input type="checkbox"/>		
76. <input type="checkbox"/>		
77. <input type="checkbox"/>		
78. <input type="checkbox"/>		
79. <input type="checkbox"/>		
80. <input type="checkbox"/>		
81. <input type="checkbox"/>		
82. <input type="checkbox"/>		
83. <input type="checkbox"/>		
84. <input type="checkbox"/>		
85. <input type="checkbox"/>		
86. <input type="checkbox"/>		
87. <input type="checkbox"/>		
88. <input type="checkbox"/>		
89. <input type="checkbox"/>		
90. <input type="checkbox"/>		
91. <input type="checkbox"/>		
92. <input type="checkbox"/>		
93. <input type="checkbox"/>		
94. <input type="checkbox"/>		
95. <input type="checkbox"/>		
96. <input type="checkbox"/>		
97. <input type="checkbox"/>		
98. <input type="checkbox"/>		
99. <input type="checkbox"/>		
100. <input type="checkbox"/>		
101. <input type="checkbox"/>		
102. <input type="checkbox"/>		
103. <input type="checkbox"/>		
104. <input type="checkbox"/>		
105. <input type="checkbox"/>		
106. <input type="checkbox"/>		
107. <input type="checkbox"/>		
108. <input type="checkbox"/>		
109. <input type="checkbox"/>		
110. <input type="checkbox"/>		
111. <input type="checkbox"/>		
112. <input type="checkbox"/>		
113. <input type="checkbox"/>		
114. <input type="checkbox"/>		
115. <input type="checkbox"/>		
116. <input type="checkbox"/>		
117. <input type="checkbox"/>		
118. <input type="checkbox"/>		
119. <input type="checkbox"/>		
120. <input type="checkbox"/>		
121. <input type="checkbox"/>		
122. <input type="checkbox"/>		
123. <input type="checkbox"/>		
124. <input type="checkbox"/>		
125. <input type="checkbox"/>		
126. <input type="checkbox"/>		
127. <input type="checkbox"/>		
128. <input type="checkbox"/>		
129. <input type="checkbox"/>		
130. <input type="checkbox"/>		
131. <input type="checkbox"/>		
132. <input type="checkbox"/>		
133. <input type="checkbox"/>		
134. <input type="checkbox"/>		
135. <input type="checkbox"/>		
136. <input type="checkbox"/>		
137. <input type="checkbox"/>		
138. <input type="checkbox"/>		
139. <input type="checkbox"/>		
140. <input type="checkbox"/>		
141. <input type="checkbox"/>		
142. <input type="checkbox"/>		
143. <input type="checkbox"/>		
144. <input type="checkbox"/>		
145. <input type="checkbox"/>		
146. <input type="checkbox"/>		
147. <input type="checkbox"/>		
148. <input type="checkbox"/>		
149. <input type="checkbox"/>		
150. <input type="checkbox"/>		
151. <input type="checkbox"/>		
152. <input type="checkbox"/>		
153. <input type="checkbox"/>		
154. <input type="checkbox"/>		
155. <input type="checkbox"/>		
156. <input type="checkbox"/>		
157. <input type="checkbox"/>		
158. <input type="checkbox"/>		
159. <input type="checkbox"/>		
160. <input type="checkbox"/>		
161. <input type="checkbox"/>		
162. <input type="checkbox"/>		
163. <input type="checkbox"/>		
164. <input type="checkbox"/>		
165. <input type="checkbox"/>		
166. <input type="checkbox"/>		
167. <input type="checkbox"/>		
168. <input type="checkbox"/>		
169. <input type="checkbox"/>		
170. <input type="checkbox"/>		
171. <input type="checkbox"/>		
172. <input type="checkbox"/>		
173. <input type="checkbox"/>		
174. <input type="checkbox"/>		
175. <input type="checkbox"/>		
176. <input type="checkbox"/>		
177. <input type="checkbox"/>		
178. <input type="checkbox"/>		
179. <input type="checkbox"/>		
180. <input type="checkbox"/>		
181. <input type="checkbox"/>		
182. <input type="checkbox"/>		
183. <input type="checkbox"/>		
184. <input type="checkbox"/>		
185. <input type="checkbox"/>		
186. <input type="checkbox"/>		
187. <input type="checkbox"/>		
188. <input type="checkbox"/>		
189. <input type="checkbox"/>		
190. <input type="checkbox"/>		
191. <input type="checkbox"/>		
192. <input type="checkbox"/>		
193. <input type="checkbox"/>		
194. <input type="checkbox"/>		
195. <input type="checkbox"/>		
196. <input type="checkbox"/>		
197. <input type="checkbox"/>		
198. <input type="checkbox"/>		
199. <input type="checkbox"/>		
200. <input type="checkbox"/>		
201. <input type="checkbox"/>		
202. <input type="checkbox"/>		
203. <input type="checkbox"/>		
204. <input type="checkbox"/>		
205. <input type="checkbox"/>		
206. <input type="checkbox"/>		
207. <input type="checkbox"/>		
208. <input type="checkbox"/>		
209. <input type="checkbox"/>		
210. <input type="checkbox"/>		
211. <input type="checkbox"/>		
212. <input type="checkbox"/>		
213. <input type="checkbox"/>		
214. <input type="checkbox"/>		
215. <input type="checkbox"/>		
216. <input type="checkbox"/>		
217. <input type="checkbox"/>		
218. <input type="checkbox"/>		
219. <input type="checkbox"/>		
220. <input type="checkbox"/>		
221. <input type="checkbox"/>		
222. <input type="checkbox"/>		
223. <input type="checkbox"/>		
224. <input type="checkbox"/>		
225. <input type="checkbox"/>		
226. <input type="checkbox"/>		
227. <input type="checkbox"/>		
228. <input type="checkbox"/>		
229. <input type="checkbox"/>		
230. <input type="checkbox"/>		
231. <input type="checkbox"/>		
232. <input type="checkbox"/>		
233. <input type="checkbox"/>		
234. <input type="checkbox"/>		
235. <input type="checkbox"/>		
236. <input type="checkbox"/>		
237. <input type="checkbox"/>		
238. <input type="checkbox"/>		
239. <input type="checkbox"/>		
240. <input type="checkbox"/>		
241. <input type="checkbox"/>		
242. <input type="checkbox"/>		
243. <input type="checkbox"/>		
244. <input type="checkbox"/>		
245. <input type="checkbox"/>		
246. <input type="checkbox"/>		
247. <input type="checkbox"/>		
248. <input type="checkbox"/>		
249. <input type="checkbox"/>		
250. <input type="checkbox"/>		
251. <input type="checkbox"/>		
252. <input type="checkbox"/>		
253. <input type="checkbox"/>		
254. <input type="checkbox"/>		
255. <input type="checkbox"/>		
256. <input type="checkbox"/>		
257. <input type="checkbox"/>		
258. <input type="checkbox"/>		
259. <input type="checkbox"/>		
260. <input type="checkbox"/>		
261. <input type="checkbox"/>		
262. <input type="checkbox"/>		
263. <input type="checkbox"/>		
264. <input type="checkbox"/>		
265. <input type="checkbox"/>		
266. <input type="checkbox"/>		
267. <input type="checkbox"/>		
268. <input type="checkbox"/>		
269. <input type="checkbox"/>		
270. <input type="checkbox"/>		
271. <input type="checkbox"/>		
272. <input type="checkbox"/>		
273. <input type="checkbox"/>		
274. <input type="checkbox"/>		
275. <input type="checkbox"/>		
276. <input type="checkbox"/>		
277. <input type="checkbox"/>		
278. <input type="checkbox"/>		
279. <input type="checkbox"/>		
280. <input type="checkbox"/>		
281. <input type="checkbox"/>		
282. <input type="checkbox"/>		
283. <input type="checkbox"/>		
284. <input type="checkbox"/>		
285. <input type="checkbox"/>		
286. <input type="checkbox"/>		
287. <input type="checkbox"/>		
288. <input type="checkbox"/>		
289. <input type="checkbox"/>		
290. <input type="checkbox"/>		
291. <input type="checkbox"/>		
292. <input type="checkbox"/>		
293. <input type="checkbox"/>		
294. <input type="checkbox"/>		
295. <input type="checkbox"/>		
296. <input type="checkbox"/>		
297. <input type="checkbox"/>		
298. <input type="checkbox"/>		
299. <input type="checkbox"/>		
300. <input type="checkbox"/>		
301. <input type="checkbox"/>		
302. <input type="checkbox"/>		
303. <input type="checkbox"/>		
304. <input type="checkbox"/>		
305. <input type="checkbox"/>		
306. <input type="checkbox"/>		
307. <input type="checkbox"/>		
308. <input type="checkbox"/>		
309. <input type="checkbox"/>		
310. <input type="checkbox"/>		
311. <input type="checkbox"/>		
312. <input type="checkbox"/>		
313. <input type="checkbox"/>		
314. <input type="checkbox"/>		
315. <input type="checkbox"/>		
316. <input type="checkbox"/>		
317. <input type="checkbox"/>		
318. <input type="checkbox"/>		
319. <input type="checkbox"/>		
320. <input type="checkbox"/>		
321. <input type="checkbox"/>		
322. <input type="checkbox"/>		
323. <input type="checkbox"/>		
324. <input type="checkbox"/>		
325. <input type="checkbox"/>		
326. <input type="checkbox"/>		
327. <input type="checkbox"/>		
328. <input type="checkbox"/>		
329. <input type="checkbox"/>		
330. <input type="checkbox"/>		
331. <input type="checkbox"/>		
332. <input type="checkbox"/>		
333. <input type="checkbox"/>		
334. <input type="checkbox"/>		
335. <input type="checkbox"/>		
336. <input type="checkbox"/>		
337. <input type="checkbox"/>		
338. <input type="checkbox"/>		
339. <input type="checkbox"/>		
340. <input type="checkbox"/>		
341. <input type="checkbox"/>		
342. <input type="checkbox"/>		
343. <input type="checkbox"/>		
344. <input type="checkbox"/>		
345. <input type="checkbox"/>		
346. <input type="checkbox"/>		
347. <input type="checkbox"/>		
348. <input type="checkbox"/>		
349. <input type="checkbox"/>		
350. <input type="checkbox"/>		
351. <input type="checkbox"/>		
352. <input type="checkbox"/>		
353. <input type="checkbox"/>		
354. <input type="checkbox"/>		
355. <input type="checkbox"/>		
356. <input type="checkbox"/>		
357. <input type="checkbox"/>		
358. <input type="checkbox"/>		
359. <input type="checkbox"/>		
360. <input type="checkbox"/>		
361. <input type="checkbox"/>		
362. <input type="checkbox"/>		
363. <input type="checkbox"/>		
364. <input type="checkbox"/>		
365. <input type="checkbox"/>		
366. <input type="checkbox"/>		
367. <input type="checkbox"/>		
368. <input type="checkbox"/>		
369. <input type="checkbox"/>		
370. <input type="checkbox"/>		
371. <input type="checkbox"/>		
372. <input type="checkbox"/>		
373. <input type="checkbox"/>		
374. <input type="checkbox"/>		
375. <input type="checkbox"/>		
376. <input type="checkbox"/>		
377. <input type="checkbox"/>		
378. <input type="checkbox"/>		
379. <input type="checkbox"/>		
380. <input type="checkbox"/>		
381. <input type="checkbox"/>		
382. <input type="checkbox"/>		
383. <input type="checkbox"/>		
384. <input type="checkbox"/>		
385. <input type="checkbox"/>		
386. <input type="checkbox"/>		
387. <input type="checkbox"/>		
388. <input type="checkbox"/>		
389. <input type="checkbox"/>		
390. <input type="checkbox"/>		
391. <input type="checkbox"/>		
392. <input type="checkbox"/>		
393. <input type="checkbox"/>		
394. <input type="checkbox"/>		
395. <input type="checkbox"/>		
396. <input type="checkbox"/>		
397. <input type="checkbox"/>		
398. <input type="checkbox"/>		
399. <input type="checkbox"/>		
400. <input type="checkbox"/>		
401. <input type="checkbox"/>		
402. <input type="checkbox"/>		
403. <input type="checkbox"/>		
404. <input type="checkbox"/>		
405. <input type="checkbox"/>		
406. <input type="checkbox"/>		
407. <input type="checkbox"/>		
408. <input type="checkbox"/>		
409. <input type="checkbox"/>		
410. <input type="checkbox"/>		
411. <input type="checkbox"/>		
412. <input type="checkbox"/>		
413. <input type="checkbox"/>		
414. <input type="checkbox"/>		
415. <input type="checkbox"/>		
416. <input type="checkbox"/>		
417. <input type="checkbox"/>		
418. <input type="checkbox"/>		
419. <input type="checkbox"/>		
420. <input type="checkbox"/>		
421. <input type="checkbox"/>		
422. <input type="checkbox"/>		
423. <input type="checkbox"/>		
424. <input type="checkbox"/>		
425. <input type="checkbox"/>		
426. <input type="checkbox"/>		
427. <input type="checkbox"/>		
428. <input type="checkbox"/>		
429. <input type="checkbox"/>		
430. <input type="checkbox"/>		
431. <input type="checkbox"/>		
432. <input type="checkbox"/>		
433. <input type="checkbox"/>		
434. <input type="checkbox"/>		
435. <input type="checkbox"/>		
436. <input type="checkbox"/>		
437. <input type="checkbox"/>		
438. <input type="checkbox"/>		
439. <input type="checkbox"/>		
440. <input type="checkbox"/>		
441. <input type="checkbox"/>		
442. <input type="checkbox"/>		
443. <input type="checkbox"/>		
444. <input type="checkbox"/>		
445. <input type="checkbox"/>		
446. <input type="checkbox"/>		
447. <input type="checkbox"/>		
448. <input type="checkbox"/>		
449. <input type="checkbox"/>		
450. <input type="checkbox"/>		
451. <input type="checkbox"/>		
452. <input type="checkbox"/>		
453. <input type="checkbox"/>		
454. <input type="checkbox"/>		
455. <input type="checkbox"/>		
456. <input type="checkbox"/>		
457. <input type="checkbox"/>		
458. <input type="checkbox"/>		
459. <input type="checkbox"/>		
460. <input type="checkbox"/>		
461. <input type="checkbox"/>		
462. <input type="checkbox"/>		
463. <input type="checkbox"/>		
464. <input type="checkbox"/>		
465. <input type="checkbox"/>		
466. <input type="checkbox"/>		
467. <input type="checkbox"/>		
468. <input type="checkbox"/>		
469. <input type="checkbox"/>		
470. <input type="checkbox"/>		
471. <input type="checkbox"/>		
472. <input type="checkbox"/>		
473. <input type="checkbox"/>		
474. <input type="checkbox"/>		
475. <input type="checkbox"/>		
476. <input type="checkbox"/>		
477. <input type="checkbox"/>		
478. <input type="checkbox"/>		
479. <input type="checkbox"/>		
480. <input type="checkbox"/>		
481. <input type="checkbox"/>		
482. <input type="checkbox"/>		
483. <input type="checkbox"/>		
484. <input type="checkbox"/>		
485. <input type="checkbox"/>		
486. <input type="checkbox"/>		
487. <input type="checkbox"/>		
488. <input type="checkbox"/>		
489. <input type="checkbox"/>		
490. <input type="checkbox"/>		
491. <input type="checkbox"/>		
492. <input type="checkbox"/>		
493. <input type="checkbox"/>		
494. <input type="checkbox"/>		
495. <input type="checkbox"/>		
496. <input type="checkbox"/>		
497. <input type="checkbox"/>		
498. <input type="checkbox"/>		
499. <input type="checkbox"/>		
500. <input type="checkbox"/>		
501. <input type="checkbox"/>		
502. <input type="checkbox"/>		
503. <input type="checkbox"/>		
504. <input type="checkbox"/>		
505. <input type="checkbox"/>		
506. <input type="checkbox"/>		
507. <input type="checkbox"/>		
508. <input type="checkbox"/>		
509. <input type="checkbox"/>		
510. <input type="checkbox"/>		
511. <input type="checkbox"/>		
512. <input type="checkbox"/>		
513. <input type="checkbox"/>		
514. <input type="checkbox"/>		
515. <input type="checkbox"/>		
516. <input type="checkbox"/>		
517. <input type="checkbox"/>		
518. <input type="checkbox"/>		
519. <input type="checkbox"/>		
520. <input type="checkbox"/>		
521. <input type="checkbox"/>		
522. <input type="checkbox"/>		
523. <input type="checkbox"/>		
524. <input type="checkbox"/>		
525. <input type="checkbox"/>		
526. <input type="checkbox"/>		
527. <input type="checkbox"/>		
528. <input type="checkbox"/>		
529. <input type="checkbox"/>		
530. <input type="checkbox"/>		
531. <input type="checkbox"/>		
532. <input type="checkbox"/>		
533. <input type="checkbox"/>		
534. <input type="checkbox"/>		
535. <input type="checkbox"/>		
536. <input type="checkbox"/>		
537. <input type="checkbox"/>		
538. <input type="checkbox"/>		
539. <input type="checkbox"/>		
540. <input type="checkbox"/>		
541. <input type="checkbox"/>		
542. <input type="checkbox"/>		
543. <input type="checkbox"/>		
544. <input type="checkbox"/>		
545. <input type="checkbox"/>		
546. <input type="checkbox"/>		
547. <input type="checkbox"/>		
548. <input type="checkbox"/>		
549. <input type="checkbox"/>		
550. <input type="checkbox"/>		
551. <input type="checkbox"/>		
552. <input type="checkbox"/>		
553. <input type="checkbox"/>		
554. <input type="checkbox"/>		
555. <input type="checkbox"/>		
556. <input type="checkbox"/>		
557. <input type="checkbox"/>		
558. <input type="checkbox"/>		
559. <input type="checkbox"/>		
560. <input type="checkbox"/>		
561. <input type="checkbox"/>		
562. <input type="checkbox"/>		
563. <input type="checkbox"/>		
564. <input type="checkbox"/>		
565. <input type="checkbox"/>		
566. <input type="checkbox"/>		
567. <input type="checkbox"/>		
568. <input type="checkbox"/>		
569. <input type="checkbox"/>		
570. <input type="checkbox"/>		
571. <input type="checkbox"/>		
572. <input type="checkbox"/>		
573. <input type="checkbox"/>		
574. <input type="checkbox"/>		
575. <input type="checkbox"/>		
576. <input type="checkbox"/>		
577.		



DEPARTMENT OF THE ARMY  
HEADQUARTERS US ARMY AVIATION MATERIEL LABORATORIES  
FORT EUSTIS, VIRGINIA 23604

This report was prepared by the Goodyear Aerospace Corporation under the terms of Contract DAAJ02-68-C-0040. It consists of technical information developed as the basis for the contractor's design, and contains data on the results of flight tests of the 500-Pound Controlled Airdrop Cargo System.

The object of this contractual effort was to develop a flexible-wing delivery system for all-weather airdrop of 500 pounds of cargo to fulfill an approved Army requirement (QMR). This was done by testing, analyzing, and evaluating several configurations of flexible canopies. Prototypes of the best overall system were built, and full-scale flight tests conducted. As a result of these flight tests, a configuration was selected and fifteen systems have been produced for Army engineering and service tests.

The conclusions and recommendations contained herein are concurred in by this Command.

Project 1F164204D158  
Contract DAAJ02-68-C-0040  
USAAVLABS Technical Report 70-31  
September 1970

500-POUND CONTROLLED AIRDROP CARGO SYSTEM

Final Report

Engineering Research and Development Report

By

Robert G. Slayman  
Herbert Q. Bair  
Thomas W. Rathbun

Sponsored By

Advanced Research Projects Agency  
ARPA Order No. 294

Prepared By

Goodyear Aerospace Corporation  
Akron, Ohio

For

U. S. ARMY AVIATION MATERIEL LABORATORIES  
FORT EUSTIS, VIRGINIA

This document is subject to special export controls, and each transmittal to foreign governments or foreign nationals may be made only with prior approval of US Army Aviation Materiel Laboratories, Fort Eustis, Va. 23604.

This research was supported by the Advanced  
Research Projects Agency of the Department of the  
Defense and was monitored by U. S. Army Aviation  
Materiel Laboratories under Contract DAAJ02-68-C-0040.

### ABSTRACT

The purpose of this work was to develop and furnish to the Army (USAAVLABS) a flexible-wing delivery system for all-weather airdrop of 500 pounds of cargo with both automatic and command homing capability. These systems are for use in military engineering and service tests.

A detailed design analysis and trade-off was accomplished followed by a full-scale wind-tunnel test program and flight test evaluation effort, which resulted in the selection of a twin-keel catenary parawing, airborne control box, and suspension system. This final system was then tested for reliability and landing accuracy.

This report presents the results and findings of the work accomplished.

## FOREWORD

This report was prepared by Goodyear Aerospace Corporation (GAC), Akron, Ohio, under the authority of Contract DAAJO2-68-C-0040 (Project 1F164204D158). The work was performed under the direction of Mr. Everette Forehand and Mr. T. Barday Allardice, U. S. Army Aviation Materiel Laboratories, Fort Eustis, Virginia, who acted as the contract technical monitors and advisors.

The project staff was headed by Mr. Robert G. Slayman, who was assisted by Mr. Herbert Q. Bair, director of design and technology, and by Mr. Thomas W. Rathbun, director of field testing. The project team authored this report. Other contributing Goodyear personnel were Mr. Donald M. Marco, Systems Application Section Head in the Recovery Systems Engineering Department, Mr. Burton E. Sahli, Mr. Kenneth Easter, and Mr. Ralph E. Cuffman. The corporate internal document number for this report is GER-13801.

## TABLE OF CONTENTS

	<u>Page</u>
ABSTRACT . . . . .	iii
FOREWORD . . . . .	v
LIST OF ILLUSTRATIONS . . . . .	ix
LIST OF TABLES . . . . .	xiv
LIST OF SYMBOLS . . . . .	xvi
INTRODUCTION . . . . .	1
STATEMENT OF THE PROBLEM . . . . .	5
General . . . . .	5
Design Characteristics . . . . .	5
Performance Requirements . . . . .	5
Performance Objectives . . . . .	6
Operational Requirements . . . . .	6
Reliability and Environmental Requirements . . . . .	7
Maintainability Requirements . . . . .	7
APPROACH TO THE PROBLEM . . . . .	9
SYSTEM DESCRIPTION AND OPERATION . . . . .	11
General . . . . .	11
Deployable Wing . . . . .	11
Control Box . . . . .	13
System Operation . . . . .	24
TECHNICAL DISCUSSION . . . . .	26
General . . . . .	26
Aerodynamic Analysis . . . . .	26
Wind-Tunnel Tests . . . . .	27
Structural Analysis . . . . .	27
Guidance and Control Analysis . . . . .	29
DEVELOPMENT TEST . . . . .	35
General . . . . .	35
Antenna . . . . .	35
Control . . . . .	35

	<u>Page</u>
FLIGHT TEST . . . . .	37
General . . . . .	37
Preliminary Flight . . . . .	37
System Development Flight Test Plan . . . . .	40
Deployment Flight Tests . . . . .	41
Control System Evaluation Flight Test . . . . .	43
Performance and Reliability Flight Test . . . . .	44
ENVIRONMENTAL EVALUATION . . . . .	105
General . . . . .	105
Environmental Requirements . . . . .	105
Parawing Assembly . . . . .	106
Control Unit . . . . .	107
CONCLUSIONS . . . . .	116
RECOMMENDATIONS . . . . .	117
LITERATURE CITED . . . . .	118
APPENDIXES	
I. Aerodynamic Analysis . . . . .	119
II. Parawing Wind-Tunnel Tests . . . . .	140
III. Stress Analysis . . . . .	155
IV. Scale-Model Antenna Tests . . . . .	175
V. Full-Scale Antenna System Measurements . . . . .	189
VI. Instrumentation . . . . .	209
VII. Exempt Parts List . . . . .	234
DISTRIBUTION . . . . .	236



# LIST OF ILLUSTRATIONS

<u>Figure</u>		<u>Page</u>
1	Controlled Airdrop Cargo System . . . . .	3
2	System Approach Flow Chart . . . . .	10
3	Airborne CACS Equipment . . . . .	14
4	Sequence of Operation . . . . .	15
5	Flexible Wing . . . . .	16
6	Deployment Bag . . . . .	17
7	Bridle and Swivel . . . . .	18
8	Wing Planform Layout . . . . .	19
9	Installation of Wing on Control Box . . . . .	20
10	CACS Airborne Control Box and Ground-Based Transmitter . .	21
11	Controlled Airdrop Cargo System Control Box . . . . .	22
12	Parawing Configurations . . . . .	31
13	Deployment Velocity Versus Loading . . . . .	32
14	Antenna Directional Operation . . . . .	33
15	Homing Antenna RF Diagram . . . . .	33
16	Homing Antenna Signal Sensitivity . . . . .	33
17	Line Length Check and Preliminary Test Hardware Definition	46
18	Parawing Line Length Check . . . . .	47
19	Development Test Hardware Definition . . . . .	48
20	Flight Test Summary . . . . .	49
21	Control System Flight Ready Test - CACS . . . . .	50
22	Control System Flight Ready Test - CACS . . . . .	51
23	Effective L/D Definition . . . . .	52

<u>Figure</u>		<u>Page</u>
24	Parawing Performance Flight Test No. 326 L/D Performance Curve . . . . .	53
25	Parawing Performance Flight Test No. 327 L/D Performance Curve . . . . .	53
26	Vertical Descent Curves . . . . .	54
27	Environmental Test Antenna Hookup . . . . .	110
28	Control Cable Movement Measurement . . . . .	111
29	Environmental Test Setup . . . . .	112
30	Model of Parawing Having $\angle_0 = 45$ Degrees and $1/8 L_K$ Nose Cutoff . . . . .	122
31	Single-Keel Parawing Dimensions, 18-Foot Keel . . . . .	123
32	Resultant Velocity Versus Dynamic Pressure . . . . .	124
33	Wing Planform Area Versus Keel Length . . . . .	125
34	Wing Planform Area Versus Payload Weight Versus Wing Loading . . . . .	126
35	Payload Weight Versus Keel Length Versus Wing Loading . .	127
36	Payload Weight Versus Keel Length Versus Resultant Velocity	128
37	Velocity Versus L/D Versus Wing Loading . . . . .	129
38	Drag Coefficients . . . . .	130
39	Performance Characteristics-18-Foot Keel Length Parawing	131
40	18-Foot Single-Keel Parawing Performance . . . . .	132
41	Effect of Ground Wind on Glide Path . . . . .	133
42	Bank Angle Versus Control Line Retraction . . . . .	134
43	Radius of Turn Versus Control Line Retraction . . . . .	135
44	Control Line Displacement Versus Turn Time . . . . .	136
45	Control Line Displacement Versus Turning Radius . . . . .	136

<u>Figure</u>		<u>Page</u>
46	Turn Radii Versus Glide Velocities for Various Bank Angles	137
47	Turn Time Versus Glide Velocities for Various Bank Angles	138
48	Control Line Displacement Versus Loading . . . . .	139
49	Typical Configuration . . . . .	139
50	Wind-Tunnel Parawing Test . . . . .	142
51	Wind-Tunnel Test Setup . . . . .	143
52	Keel Rigging for Wind-Tunnel Tests . . . . .	144
53	L/D Versus $q$ for 18-Foot Single-Keel Parawings . . . . .	147
54	L/D Versus $q$ for 16-Foot Twin-Keel Parawings . . . . .	148
55	L/D Versus $q$ for 16-Foot High-Aspect-Ratio Twin-Catenary-Keel Parawing . . . . .	149
56	$C_L$ Versus $C_D$ Single-Keel Parawings . . . . .	150
57	$C_L$ Versus $C_D$ Twin-Keel Parawings . . . . .	151
58	Sketch of Inflated Single-Keel Wing and Sketch Plan View of Single-Keel Wing (Flat Pattern) . . . . .	156
59	Membrane Airload Distribution . . . . .	157
60	Plan View of Inflated Parawing . . . . .	157
61	Parawing Geometric Relationships . . . . .	160
62	Parawing System Coordinate Planform . . . . .	161
63	Load Distribution of Single-Keel Parawing . . . . .	167
64	Dimensional Layout of Suspension Line Loading . . . . .	170
65	Wing Load Distribution . . . . .	173
66	Antenna Pattern Coordinate System . . . . .	182
67	$f_{10}$ Azimuth Pattern (0-Degree Depression) . . . . .	193
68	$f_{10}$ Azimuth Pattern (15-Degree Depression) . . . . .	194
69	$f_{10}$ Azimuth Pattern (45-Degree Depression) . . . . .	195

<u>Figure</u>		<u>Page</u>
70	$f_{l0}$ Azimuth Pattern (60-Degree Depression) . . . . .	196
71	$f_0$ Azimuth Pattern (0-Degree Depression) . . . . .	197
72	$f_0$ Azimuth Pattern (15-Degree Depression) . . . . .	198
73	$f_0$ Azimuth Pattern (45-Degree Depression) . . . . .	199
74	$f_0$ Azimuth Pattern (60-Degree Depression) . . . . .	200
75	$f_{hi}$ Azimuth Pattern (0-Degree Depression) . . . . .	201
76	$f_{hi}$ Azimuth Pattern (15-Degree Depression) . . . . .	202
77	$f_{hi}$ Azimuth Pattern (45-Degree Depression) . . . . .	203
78	$f_{hi}$ Azimuth Pattern (60-Degree Depression) . . . . .	204
79	$f_{l0}$ Elevation Plane Pattern . . . . .	205
80	$f_0$ Elevation Plane Pattern . . . . .	206
81	Instrumentation Data Test 102 . . . . .	219
82	Instrumentation Data Test 102 . . . . .	220
83	Instrumentation Data Test 102 . . . . .	221
84	Instrumentation Data Test 108 . . . . .	222
85	Instrumentation Data Test 108 . . . . .	223
86	Instrumentation Data Test 108 . . . . .	224
87	Instrumentation Data Test 204 . . . . .	225
88	Instrumentation Data Test 208 . . . . .	226
89	Instrumentation Data Test 212 . . . . .	227
90	Instrumentation Data Test 217 . . . . .	228
91	Instrumentation Data Test 224 . . . . .	229
92	Instrumentation Data Test 225 . . . . .	230
93	Instrumentation Data Test 229 . . . . .	231

<u>Figure</u>		<u>Page</u>
94	Instrumentation Data Test 242 . . . . .	232
95	Instrumentation Data Test 242 . . . . .	233

## LIST OF TABLES

<u>Table</u>	<u>Page</u>
I Comparison of System Performance with Requirements . . .	4
II Nominal Line Lengths for Stable Flight . . . . .	23
III Deployment Sequence . . . . .	25
IV Systems Definition . . . . .	34
V Summary of Preliminary Flight Tests . . . . .	55
VI Summary of Preliminary Flight Tests . . . . .	58
VII Control Flight Summary . . . . .	61
VIII Performance Calculations - Parawing System With Drogue .	65
IX Reefing and Deployment Techniques . . . . .	66
X Control Systems Tests . . . . .	68
XI Reliability Tests . . . . .	74
XII Instrumentation Test Setups and Data Items . . . . .	76
XIII Flight Test Summary and Index . . . . .	77
XIV Deployment Tests Summary . . . . .	82
XV CACS Deployment Test Summary (3000-Ft Altitude) . . . .	87
XVI CACS Deployment Test Load Summary (3/4 Tuck - No Drogue)	89
XVII CACS Deployment Test Load Summary (3/4 Tuck - No Drogue)	90
XVIII Control System Test Summary . . . . .	92
XIX CEP Flight Data . . . . .	100
XX Reliability Flight Data . . . . .	102
XXI Voltage Measurements, High-Temperature Test 1 . . . .	113
XXII Cable Pull-in Measurements, High-Temperature Test 1 . .	113
XXIII Voltage Measurements, Low-Temperature Test 1 . . . .	114

<u>Table</u>	<u>Page</u>
XXIV Cable Pull-in Measurements, Low-Temperature Test 1 . . .	114
XXV Voltage Measurements, Low-Temperature Test 2 . . . . .	115
XXVI Cable Pull-in Measurements, Low-Temperature Test 2 . . .	115
XXVII Physical Characteristics of the Parawings Tested at the Wind Tunnel . . . . .	111
XXVIII Final Line Lengths (Wind Tunnel) . . . . .	152
XXIX Parawing Wind-Tunnel Flight Test Results . . . . .	153
XXX Coordinates of Suspension Line Attachment Points . . . .	164
XXXI Lengths and Direction Cosines of Suspension Lines . . .	166
XXXII Canopy Loads in Hoop Direction at Leading Edge . . . . .	168
XXXIII Canopy Loads in Hoop Direction at the Keels . . . . .	169
XXXIV Suspension Line Lengths and Load Under 1.0 g and 15.0 g	171
XXXV Azimuth Pattern Data . . . . .	183
XXXVI Azimuth Pattern Data . . . . .	184
XXXVII Azimuth Pattern Data . . . . .	186
XXXVIII Pitch Plane Pattern Data . . . . .	188
XXXIX Roll Plane Pattern Data . . . . .	188
XL Radiation Patterns . . . . .	192
XLI Radiation Pattern Data . . . . .	192
XLII Data Reduction (Sensitivity) . . . . .	218

### LIST OF SYMBOLS

$a$	ratio of the distance of the resultant air load from the theoretical nose to the theoretical keel length
$a'$	ratio of the distance of the peak air load from the theoretical nose to the theoretical keel length
$b_o$	parawing planform beam length, ft
$C_D$	drag coefficient
$C_L$	lift coefficient
$C_p$	ratio of distance of the center of pressure from the theoretical nose to theoretical keel length
$C_R$	shock factor
$D_o$	nominal diameter, in.
$F_{QB}$	minimum required canopy fabric breaking strength, lb /in.
$FS$	factor of safety
$g$	gravitational acceleration, ft/sec <sup>2</sup>
$h$	perpendicular distance between a plane thru the center of the control box parallel to the plane formed by the inflated parawing leading edges, in.
$L_C$	distance from theoretical nose to the center of the semi-circle formed by one side of the trailing edge of the inflated parawing, in.
$L_K$	theoretical keel length, in.
$MS$	margin of safety
$P$	total air load normal to the plane formed by the parawing leading edges, lb
$P_D$	total dynamic load, lb
$q$	dynamic pressure, lb/ft <sup>2</sup>
$q_o$	wing loading, lb/ft <sup>2</sup>
$q_o'$	maximum air load intensity normal to the plane formed by the keel and leading edges, lb/in.



$r$	radius formed by trailing edge of inflated parawing, in.
$R$	turn radius, ft
$R_H$	horizontal range, ft
$S_A$	surface area, ft <sup>2</sup>
$S_P$	planform surface area, ft <sup>2</sup>
$S_{REF}$	effective surface area, ft <sup>2</sup>
$t$	time, sec
$t_f$	inflation time, sec
$T$	minimum required suspension line tensile strength, lb
$T_F$	fabric tensile strength, lb/in.
$V_D$	deployment velocity, ft/sec
$V_F$	glide velocity in still air, ft/sec
$V_H$	horizontal velocity, ft/sec
$V_{HF}$	horizontal wing velocity in still air, ft/sec
$V_R$	resultant velocity, ft/sec
$V_V$	vertical velocity, ft/sec
$V_W$	wind velocity, ft/sec
$W_P$	payload weight, lb
$W_t$	total system weight, lb
$X_D$	X coordinate of left suspension line attachment point, in.
$X_E$	X coordinate of forward suspension line attachment point, in.
$X_F$	X coordinate of aft suspension line attachment point, in.
$x_i$	X coordinate of suspension line attachment point along the leading edge or keel, in.
$Y_D$	Y coordinate of left suspension line attachment point, in.
$Y_E$	Y coordinate of forward suspension line attachment point, in.

$Y_F$	Y coordinate of aft suspension line attachment point, in.
$Y_1$	Y coordinate of suspension line attachment point along the leading edge or keel, in.
$Z$	altitude, ft
$Z_D$	Z coordinate of left suspension line attachment point, in.
$Z_E$	Z coordinate of forward suspension line attachment point, in.
$Z_F$	Z coordinate of aft suspension line attachment point, in.
$z_1$	Z coordinate of suspension line attachment point along the leading edge or keel, in.
$\alpha$	angle of attack (the angle between the glide path and a plane formed by the parawing leading edges), deg
$\beta$	$\pi + 2\phi$ , deg
$\gamma$	the angle between the glide path and the horizontal, deg
$\phi$	1/2 the angle between the keel and leading edge of the inflated parawing, deg
$\lambda$	wave length, in.
$\tau$	the angle between the vertical and a plane formed by the parawing leading edges, deg
$\phi$	1/2 the angle between the vertical and the parawing leading edge at the widest point, deg
$\psi$	bank angle, deg
$\Lambda_0$	planform angle between keel and leading edge, deg

## INTRODUCTION

The Department of the Army has an approved Qualitative Material Requirement (QMR) for a simple, rugged system for accurate airdrop of supplies and equipment, 300 to 500 pounds, in areas where terrain, weather conditions, or tactical situation precludes the use of other means of resupply or techniques of airdrop.

Goodyear Aerospace Corporation (GAC), Akron, Ohio, was awarded contract DAAJ02-68-C-0040 by U. S. Army Aviation Materiel Laboratories (USAAVLABS), Fort Eustis, Virginia, to develop a system to meet the requirement and to deliver 15 such systems to the Army for engineering and service tests.

The controlled airdrop cargo system (CACS) (see Figure 1) as developed consists of a flexible wing canopy, a radio control system, a ground transmitter, and a bridle with swivel. The system is compatible with an A-21 or any standard single-point 500-pound cargo container with or without a standard ground release mechanism.

This flexible wing system is droppable from both fixed- and rotary-wing aircraft traveling at speeds of 0 to 150 knots IAS. The operational altitude range is from 500 to 30,000 feet, and it is capable of maintaining a range-to-altitude glide ratio (L/D) in excess of 1.9 in the automatic mode and up to 2.7 in the manual mode.

The control box subsystem is capable of both automatic and manual control by a compatible ground station. The system will impact within 100 feet of a desired target when being controlled manually in winds of up to 75 percent of the system's forward velocity. The circular error probability (CEP) during automatic homing is 180 feet with a 90-percent confidence level.

In the development of the equipment to meet the program requirements, several technical disciplines were employed, and wind-tunnel and extensive flight tests were conducted. Aerodynamic studies were made to size the wing, to estimate its stability and L/D characteristics as a function of angle of attack, and to determine control and control forces. In conjunction with this effort, full-scale wind-tunnel tests were conducted at NASA, Langley, Virginia, to determine correct suspension line lengths and to obtain wing characteristics. The results of the analysis and wind-tunnel tests were verified by flight tests conducted at Yuma Proving Ground, Yuma, Arizona. The flight test program was designed to evaluate the wing stress analysis, as well as the system antenna design, and to establish overall system performance. In addition to wind-tunnel and flight tests, antenna patterns and environmental tests were conducted where required.

As a result of the program conducted, a system which is the first major innovation in airdrop cargo delivery providing aircraft safety, all-weather

capability, and clandestine delivery potential with pinpoint accuracy is ready for Army use.

Table I summarizes the capability of the system and compares the results with the initial goals of the program.



Figure 1. Controlled Airdrop Cargo System.

TABLE I. COMPARISON OF SYSTEM PERFORMANCE WITH REQUIREMENTS

	Work Statement	System
L/D	1.8	1.9 to 2.1 (max. 3.1)
Descent Rate	25 ' /sec	17 ' /sec
Turn Radius	100'	100'
Impact		
Manual	100' radius	100' radius
Auto	-	Average 169.6'
Maximum g	-	12
Reliability	80% at 90%	93.3% at 90% 95.0% at 80%
Deployment	500' to 30,000'	500' to 24,000' demonstrated
Velocity	0 to 150 KIAS	0 to 150 KIAS
Reaction Time		
Preflight	15 min	15 min
Turnaround Time	125 min	45 min

## STATEMENT OF THE PROBLEM

### GENERAL

GAC, under Contract DAAJ02-68-C-0040, was to design, develop, and test a CACS having an all-weather capability. The system was to use a flexible type of canopy.

The system requirements as defined by the contract are presented in this section. In addition to the technical requirements set forth, a quality control program in accordance with MIL-Q-9858A was required.

### DESIGN CHARACTERISTICS

The design characteristics as defined in the subject contract are:

1. Wing shall be an all-flexible type canopy.
2. Suspension shall consist of those required lines, fittings, and straps which are used to connect or interrelate the wing and the control platform and shall be dimensionally stable.
3. Control platform shall house the guidance and control systems and any other system necessary for proper glider operation. The size shall be as small as possible. It shall be shaped to minimize aerodynamic drag, assist handling, and minimize hazards to the wing during deployment.
4. Payload - Attachment of the payload shall be designed to minimize CG variances. Automatic disconnect of the payload upon ground contact shall be studied. No shape or size of the payload is given, but standard airdrop-type containers shall be adaptable to the system (normally A21, A22, and A7).
5. Radio Control - The system shall be designed for use with the AN/ASN-95 radio. The equipment interfacing performance responsibility will reside with GAC, including the installation of program test recording capabilities in the test system to determine whether malfunctions or performance deviations are the result of GFE or contractor-developed hardware.

### PERFORMANCE REQUIREMENTS

1. Payload range of 300 to 500 pounds with no rigging changes (100 to 500 pounds desired).

2. Horizontal range to vertical height in still air 1.8 to 1 when operating in the automatic homing mode on straight track toward ground transmitter. Design objective shall be 2.4 to 1 for the same conditions.
3. Deployable from 500 to 30,000 feet.
4. Releasable from any type of aircraft at velocities of 0 to 150 KIAS.
5. Capable of a radius turn of 100 feet in either direction.
6. Command control from a ground station to a landing within 100 feet of the desired point in winds up to 75 percent of the glider forward airspeed.
7. Vertical rate of descent at impact of 25 fps or less.
8. Mission Duration - The airborne glider guidance and control system shall automatically activate after full deployment and have sufficient energy to insure 45 minutes of normal operation in automatic homing mode.

#### PERFORMANCE OBJECTIVES

1. Demonstrate automatic homing to a ground-based transmitter in winds up to 15 knots with 200-foot CEP or less to a confidence level of 90 percent.
2. Conduct adequate technical analyses of the design in areas of performance, stability and control, dynamics, loads, materials, stress, and weights to insure compliance with the performance requirements.
3. Prepare a test plan for flight testing of the system to demonstrate the ability of the system to meet the performance requirements and to identify its operational envelope.

#### OPERATIONAL REQUIREMENTS

1. Reaction Time - Time from the moment the operator decides to employ the equipment until the system makes final delivery of supplies or equipment at its ultimate destination. Sequence of employment from the moment a decision is made to employ the equipment is:



<u>Sequence of Employment</u>	<u>Reaction Time (Min.)</u>	
	<u>Required</u>	<u>Desired</u>
Preflight check	10	5
Attach system to cargo	15	2

2. Turnaround Time - Time required for the item to be returned to a condition for reuse.

<u>Sequence of Employment</u>	<u>Reaction Time (Min.)</u>	
	<u>Required</u>	<u>Desired</u>
Prepare for return to a using unit	10	5
Enroute	NA	NA
Inspection	25	10
Repacking	90	50

#### RELIABILITY AND ENVIRONMENTAL REQUIREMENTS

The flexible wing delivery system's operational reliability requirements under worldwide environments, assuming successful completion of preflight check, are:

1. Desired - 100 percent
2. Minimum required - 80 percent with 90 percent confidence

The equipment must be capable of employment in intermediate, hot-dry, warm-wet, cold, and extreme cold climates. The minimum environmental operational expressions required are specified in paragraph 7 of Change 1 to AR 705-15. For minimum storage and transit conditions, the equipment will incorporate the criteria specified in paragraph 7.1 of Change 1 to AR 705-15.

Sufficient testing of the equipment will be done to insure reliability. Number of samples tested will be in accordance with engineering judgment based on state-of-the-art knowledge or practice consistent with accepted statistical methods. MIL-R-27542 will be used as a reference for fulfillment of the reliability requirements. Contractor reliability plans and programs will fulfill the intent of MIL-R-27542.

#### MAINTAINABILITY REQUIREMENTS

Maintenance Concept - Operational readiness of the equipment is immediate. The equipment must be designed for minimum preventive and in-storage maintenance and for maximum interchangeability and use of standard parts and components. To satisfy this requirement, throwaway assemblies or modular design will be used whenever cost per assembly is under \$25 each

or when value analysis for higher cost items dictates. Maximum accessibility will be provided to high-mortality items that require adjustment or removal. No encumbrances will be placed around the components requiring field adjustment or repair. All components shall be removable with tools in the organizational mechanic's toolbox.

Quantification of Maintainability - The systems maintainability goal is to maintain a required combat readiness of 97 percent for expected utilization on a 24-hour-per-day operation. A comprehensive maintenance and skill analysis will be conducted during the contractor test program. MIL-M-26512 will be used as a reference for fulfillment of the maintainability requirement. Contractor maintainability plans and programs will fulfill the intent of MIL-M-26512.

Test and Checkout - Visual inspection at the organization maintenance level will be required to determine mechanical condition of the equipment. More comprehensive inspections will be accomplished at the higher levels of maintenance. Equipment will be calibrated and checked out with equipment currently in Army Standard Instrument and Electronic Repair Shops where possible.

Maintenance Personnel - Maintenance personnel will require skill levels similar to parachute riggers and electronics repairmen. No increase in maintenance personnel requirements is anticipated to operate and support the flexible wing delivery systems.

Human engineering principles shall be considered to insure that adequate consideration is given to the capabilities and limitations of man as a component of the flexible wing delivery systems. MIL-H-27894A (USAF) will be used as a reference for the application of Human Engineering principles.

### APPROACH TO THE PROBLEM

In general, the efforts necessary to develop a system having the desired flight characteristics, control functions, payload capability, and mission requirements were divided into two interrelated areas. The results were integrated into a final system which was then evaluated experimentally.

Simplicity of design compatible with the desired function and program schedule was a goal. Consideration was given to mission readiness, human factors, personnel consideration, maintenance, areas of operation, development, and final system cost. In some cases, in order to meet the schedule, hardware was selected early. In those cases, the approach was to satisfy the worst requirement.

Figure 2 is a flow chart showing how GAC's previous experience and the GFE were integrated into the overall approach. As stated, the program was accomplished by a definition of each major subsystem requirement, analysis, preliminary test, final design integration and evaluation, and reliability tests. The major subsystems are the wing and its associated hardware and the control box with the necessary Government-furnished hardware.

In the development of the wing subsystem, an aerodynamic sizing and configuration study was conducted to establish the wing size and shape as well as performance parameters. A theoretical analysis supplemented by wind-tunnel tests, component tests, free-flight experiments, and system evaluation was also conducted.

Parameters considered in the integration of the wing control box with the payload were that the control should be effected by the wing tips and that the wing directional rotation should be independent of the payload.

The initial philosophy for meeting the desired accuracy was that a proportional control would be required. This factor influenced the selection of hardware for converting the control signal to a mechanical motion, as well as the method of analyzing the incoming signal. A "bang-bang" control system was, however, used in the final design.

Based on component, subsystem, and total system experimental evaluation, necessary modifications and adjustments were made, and operational procedures were established. The final configuration was then tested for compliance with reliability, performance, and mission requirements. Fifteen systems of this configuration have been manufactured.

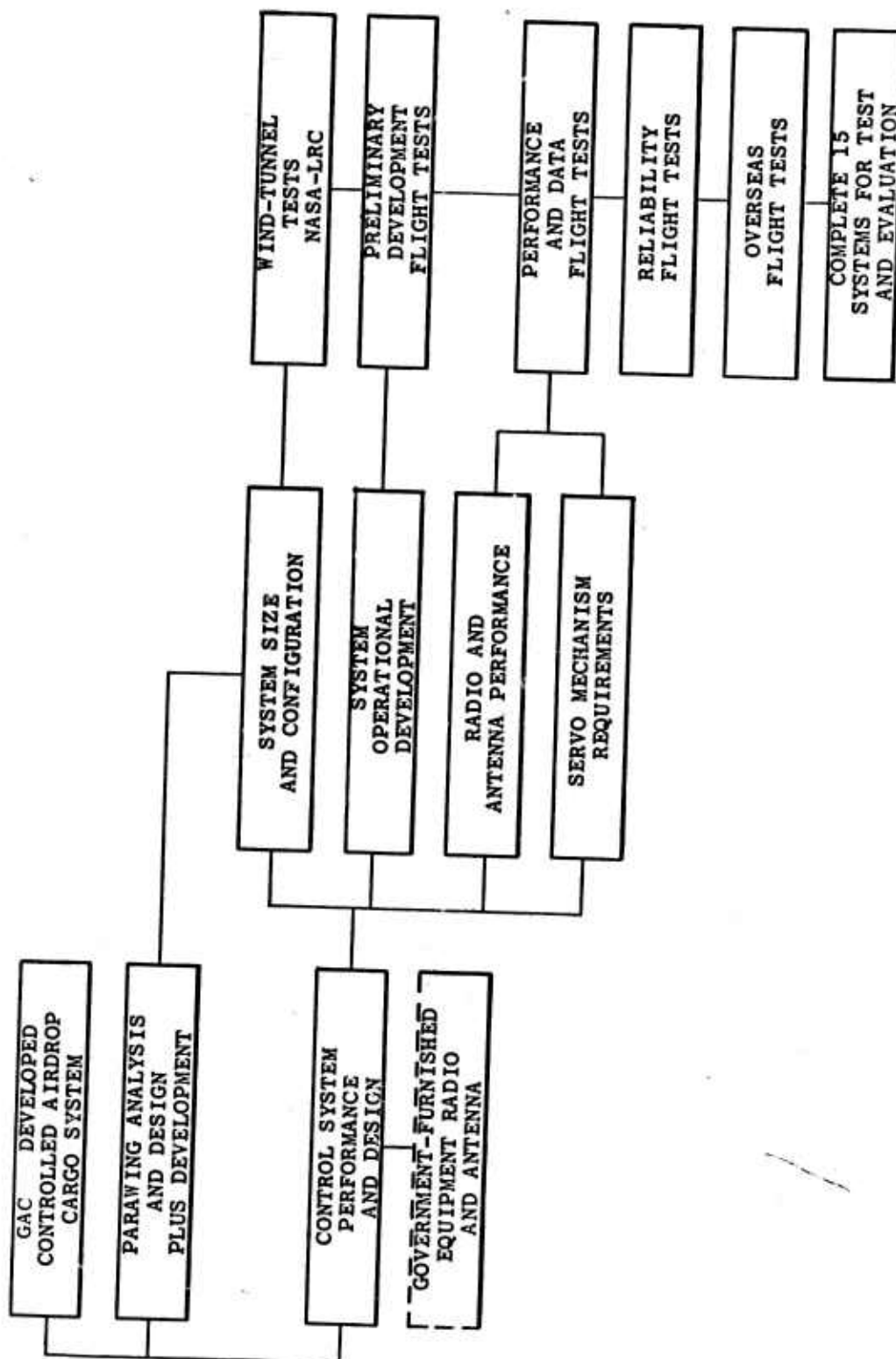


Figure 2. System Approach Flow Chart.

## SYSTEM DESCRIPTION AND OPERATION

### GENERAL

The CACS developed as a result of the work reported herein consists of a delta-shaped twin-keel catenary parawing, a control box, and a ground control unit. It is capable of being remotely guided to an accurate landing under a broad envelope of weather and tactical conditions. The hardware, receiver, and transmitter, which are the automatic homing and guidance ground-to-air link, were developed under the Army's direction and supplied as AN/ASN-95 system to GAC. The balance of the system was designed, developed, and built by GAC. As a design requirement, the system was made compatible with the AN/ASN-95 system and GFE hardware.

As shown in Figure 3, the operational system is composed of a deployable wing, a control platform, and a cargo container. The total system, less the ground-based transmitter and payload, weighs less than 100 pounds and occupies an envelope of less than 21 inches by 21 inches by 17 inches as installed upon a payload. The sequence of operation is shown in Figure 4.

### DEPLOYABLE WING

The deployable wing assembly consists of the wing suspension lines and risers (see Figure 5), the deployment bag (see Figure 6), and the bridle system including a swivel (see Figure 7).

The wing is made from calendered, rip-stop nylon cloth which has been coated with polyurethane. The porosity of the cloth is 7 CFM or less with a differential pressure of 1/2 inch of water. The planform is a modified delta of the twin-keel variety. It has a planform area of 270 square feet and a theoretical keel length of 16 feet. In the keel area, a catenary was added to increase lateral stability and to reduce the number of lines required. The use of the catenary results in a better load distribution into the wing; thus, a smoother contour and an aerodynamically cleaner wing is obtained.

Steering is effected by warping one outside wing lobe with respect to the other. This can be accomplished by adjusting the line lengths. The most efficient manner is by adjusting the length of the wing tip lines. In operation, a turn of sufficient radius to meet the contract requirements can be accomplished by a wing tip deflection of 2.75 and 2.25 inches for the manual and automatic modes of operation, respectively.

The line material is 2-in-1 stable braid. It is 1/4 inch in diameter and has a tensile strength of 1700 pounds. There are 24 lines, 6 attaching to each leading edge and 6 attaching to each catenary keel panel. The lines are terminated in a metal fitting having a heavy web for attachment to the control box and for securing the wing to the control box in the packaged

configuration. The actual line lengths are given in Table II, and a plan-form layout showing line location is given in Figure 8. In the rigging, the 6 lines from the right leading edge of the wing go to the right side of the control platform, and the 6 lines from the left leading edge of the wing go to the left side of the control platform. In order to assure that the control box and antenna axis are parallel with the wing, the odd keel lines are attached to the front attachment fitting of the control box and the even keel lines are attached to the aft attachment fitting. The control attachment fittings are located on lines 6 and 12 and are of the quick-connect variety.

Reefing of the parawing is accomplished during the packing operation by threading the zero-length reefing line through reefing rings attached to each line at a point 17 feet above the confluence fitting. The reefing line is also threaded through reefing rings attached to the four nose lines at a point three-fourths of the distance from the 17-foot ring to the edge of the canopy. A 4-second pyrotechnic time delay cutter is used to release the reefing line. This reefing method is referred to as "0" + 3/4 nose tuck reefing. A 4000-pound reefing line is required for the complete operational deployment range of altitude and velocity. For lesser requirements (under 125 knots and under 15,000 feet), a lighter reefing line (2000 pounds) is adequate.

The packing and deployment bag is made of nylon; when the wing is packed within the envelope, the wing in the bag is 18 inches by 18 inches by 10 inches high. In the package configuration, the attachment webs and control line attachment points are exposed for installation onto the control box. Once the wing has been packed, the unit can be stored in a parachute storage area.

The wing in the deployment bag is installed on top of the control box by four straps. A part of these attachment straps is the packaged wing restraint straps. The restraint straps are closed across the top of the packed wing and tied together, and a standard static line is attached (see Figure 9).

The bridle (see Figure 7) consists of two MIL-W-4088 Type I webs assembled in such a way as to allow four attachment legs to the control box and attachment of a Model GL-1850-1 swivel. The bridle is attached to the lower half of the fittings of the control box in such a manner as to be below the box during operation.

The weight of the wing, canopy, lines, confluence fittings, and attachment webs is about 29.75 pounds. The deployment bag is approximately 1.25 pounds, and the suspension system and bridle are about 3.5 pounds. It is estimated that the flexible part of the system weight is 34.5 pounds.

The details for rigging, folding, packing, and installing this equipment are presented in the instruction book<sup>1</sup>.

### CONTROL BOX

The control unit consists of a closed aluminum box (see Figures 10 and 11). The bottom of the box contains the erectable GFE antenna and the GFE antenna switching network. The top of the box contains the GFE radio receiver and power supply, the servo power supply, the servo actuator, the servo amplifier, the logic or junction box, the time delay, a press-to-test circuit, and the necessary wiring harnesses. In addition, the mechanical components necessary for routing the control cables from the servo actuator pulley out through the box and up to the wing are also located within the box. Exterior to the box are two spring-like sheaths for the control cables to pass through to maintain positive tension on the cables so that cable entanglement does not occur inside the control box. The control lines are terminated in large shock-absorbing springs which assure that loads beyond an allowable value are not transmitted into the servo mechanism. The control unit is approximately 21 inches by 21 inches by 7 inches and weighs 65 pounds.

The servo battery is a rechargeable nickel-cadmium battery having a nominal voltage of 28. It has a 4-ampere-hour capacity at a 5-hour rate.

The servo actuator and the servo amplifier are capable of producing an operational torque of 60 inch-pounds and stalls at 100 inch-pounds. Only 10 to 15 inch-pounds of torque is required in this application. The servo actuator is capable of 3-1/2 turns, which result in a possible control line travel of 10 inches based on drum diameter. Only 2-3/4-inch maximum movement is used in the application.

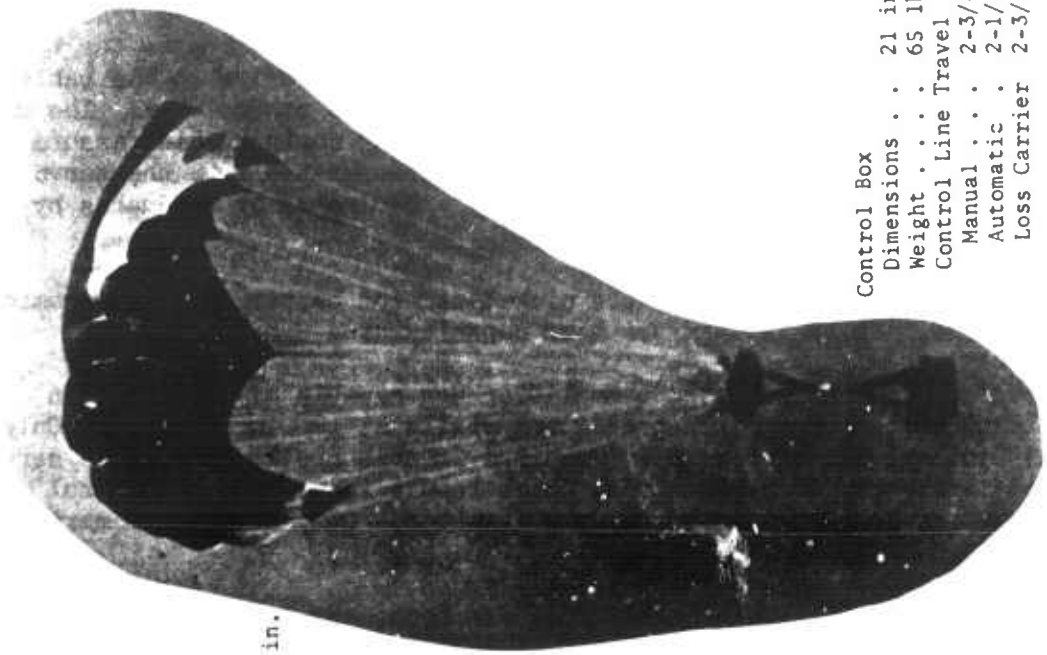
The balance circuits and the potentiometers necessary to adjust servo travel are located in the logic box. The adjustment of the pots allows from 0 to 10 inches of motion in either direction when a specific signal is received. The alignment of the circuits, the specific voltage values, and other parameters necessary for proper operation are presented in the instruction book.

In order to prevent excess loads in the control lines during deployment and disreefing, the system is neutralized during the checkout. By means of a time delay, the control system is not activated until the parawing is fully deployed.

Details for setup, adjustment, and checkout of the control unit are presented in the instruction book. Once the system has been checked out and made ready for flight, it can be stored in an electronics area with or without the batteries. Provisions have been made for the charging of the batteries while installed.

In addition, the hardware is equipped with a test button which, by lighting up two lights, indicates the condition of the servo and radio battery and certain elements of the circuits. Once checked out and placed on an external trickle charger, the equipment can be stored in a state of readiness.

Canopy  
 Keel Length . . . . . 14 ft (actual)  
                   16 ft (theoretical)  
 Span . . . . . 33.5 ft  
 Surface Area . . . . . 270 sq ft  
 Packed Dimensions . . . . . 18 in. x 18 in. x 10 in.  
 Weight . . . . . 29.75 lbs  
 Suspension System Weight . . . . . 3.5 lbs  
 Deployment Bag Weight . . . . . 1.25 lbs



Control Box  
 Dimensions . . . . . 21 in. x 21 in. x 7 in.  
 Weight . . . . . 65 lbs  
 Control Line Travel  
   Manual . . . . . 2-3/4 in.  
   Automatic . . . . . 2-1/4 in.  
 Loss Carrier 2-3/4 in.

Figure 3. Airborne CACS Equipment.



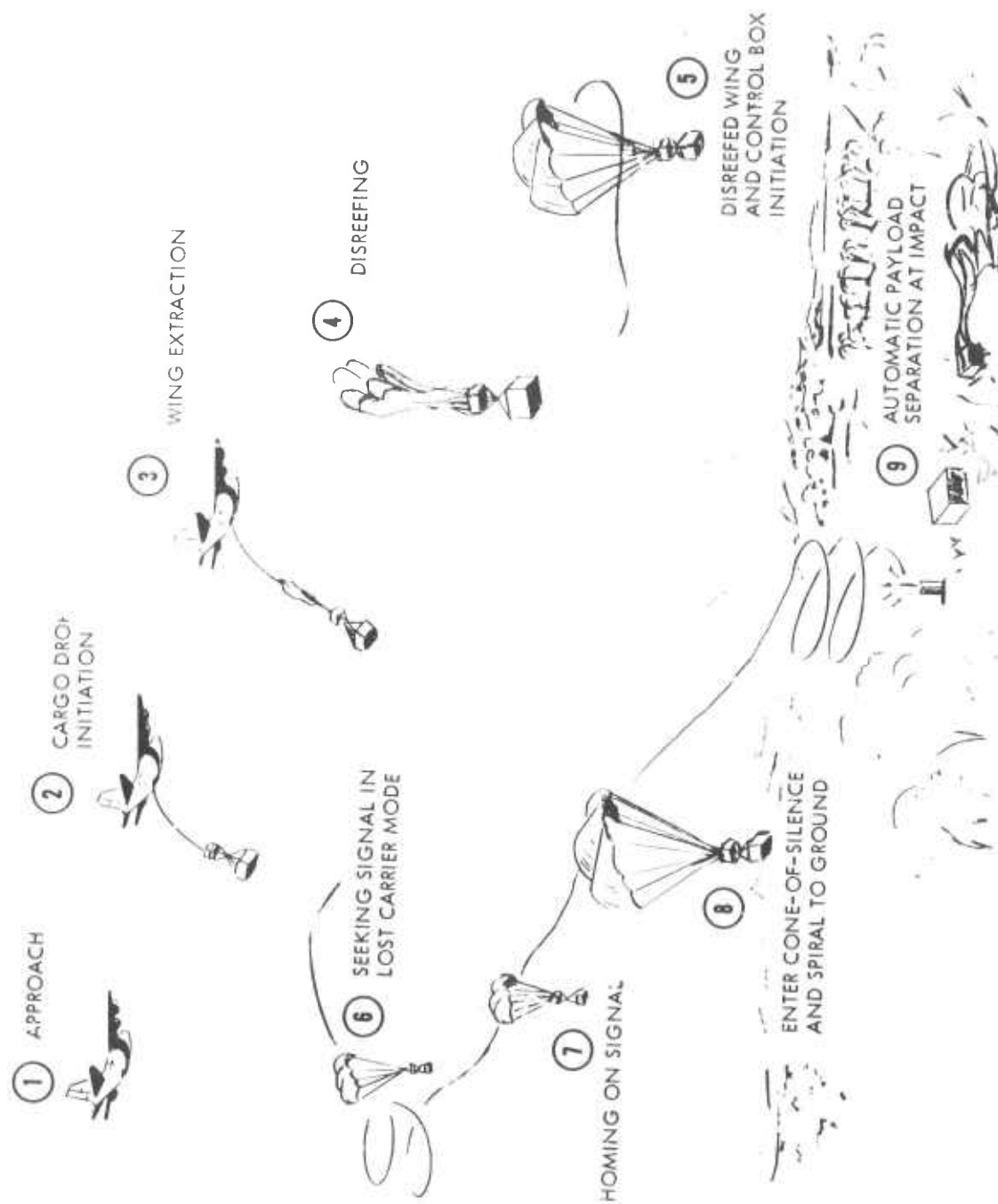


Figure 4. Sequence of Operation.

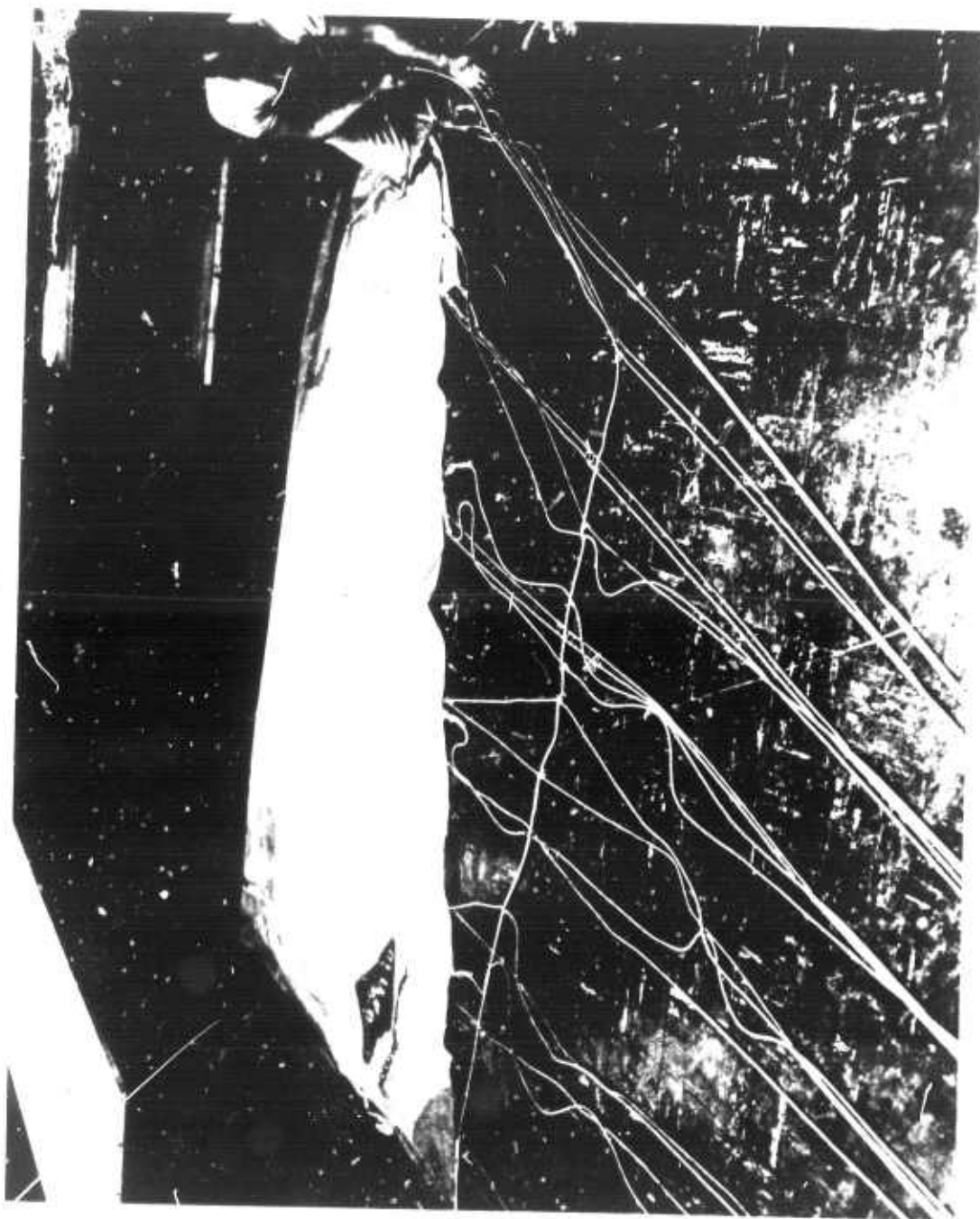


Figure 5. Flexible Wing.

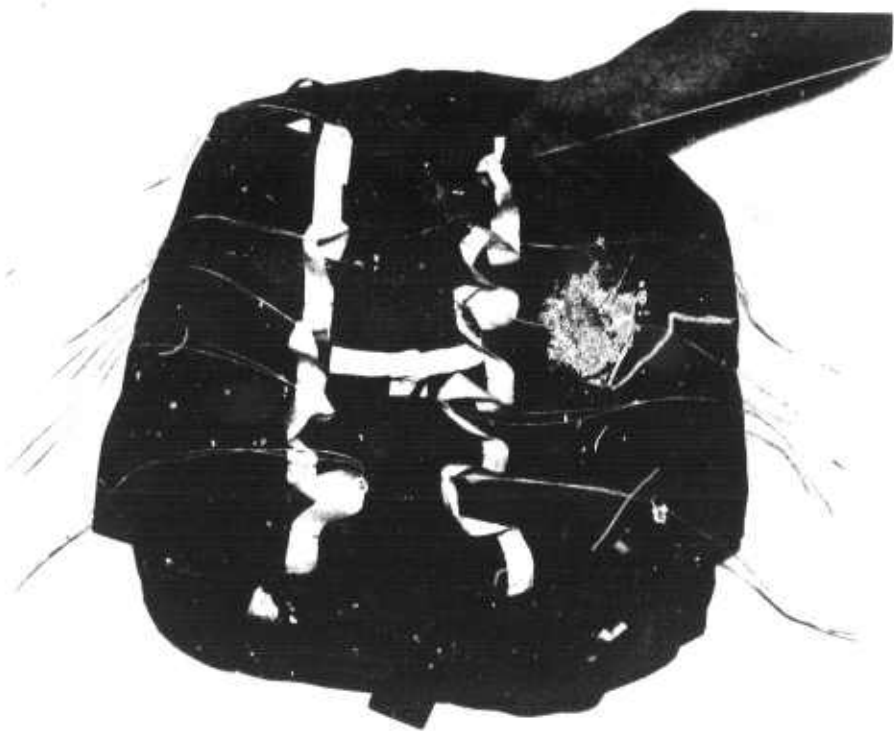
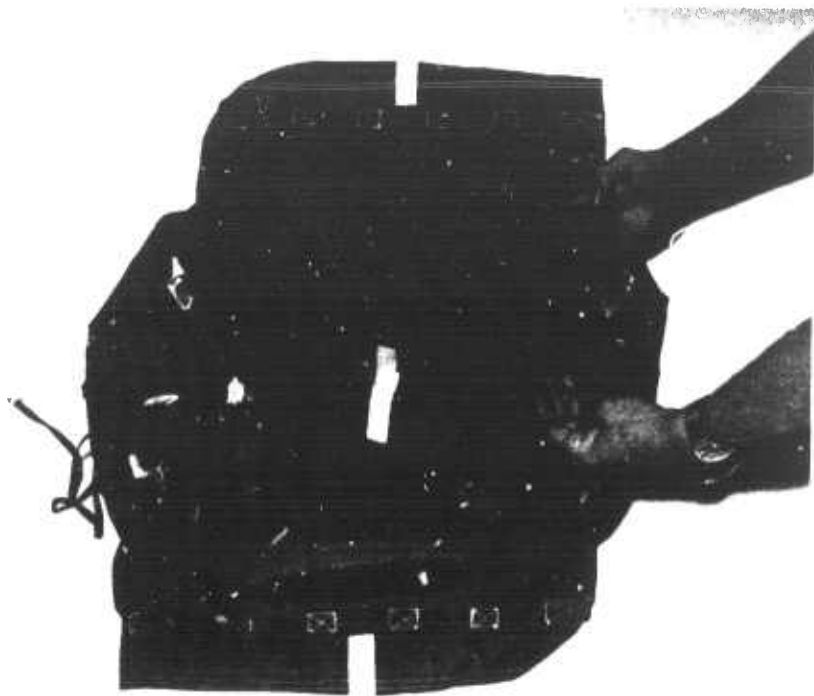


Figure 6. Deployment Bag.

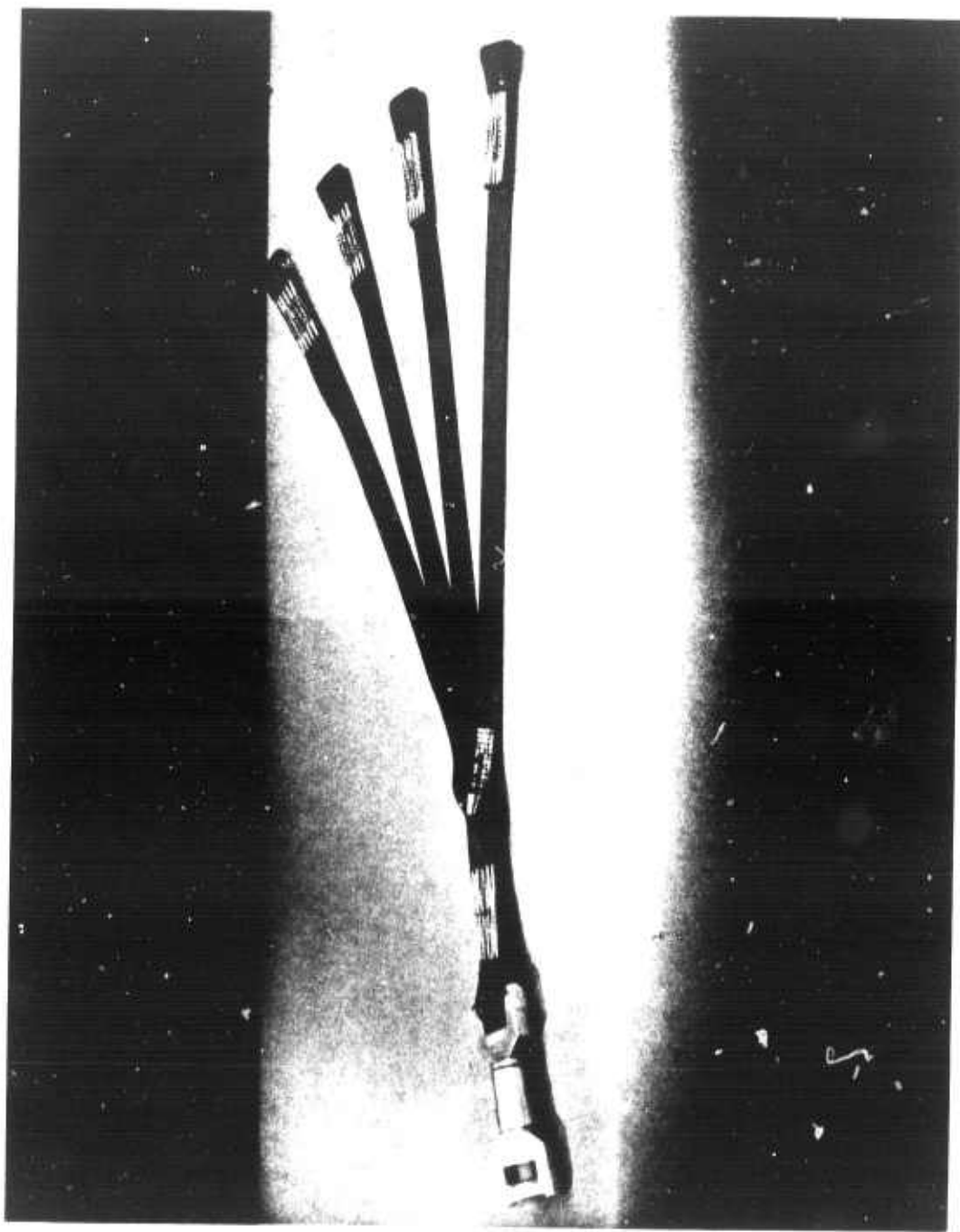


Figure 7. Bridle and Swivel.

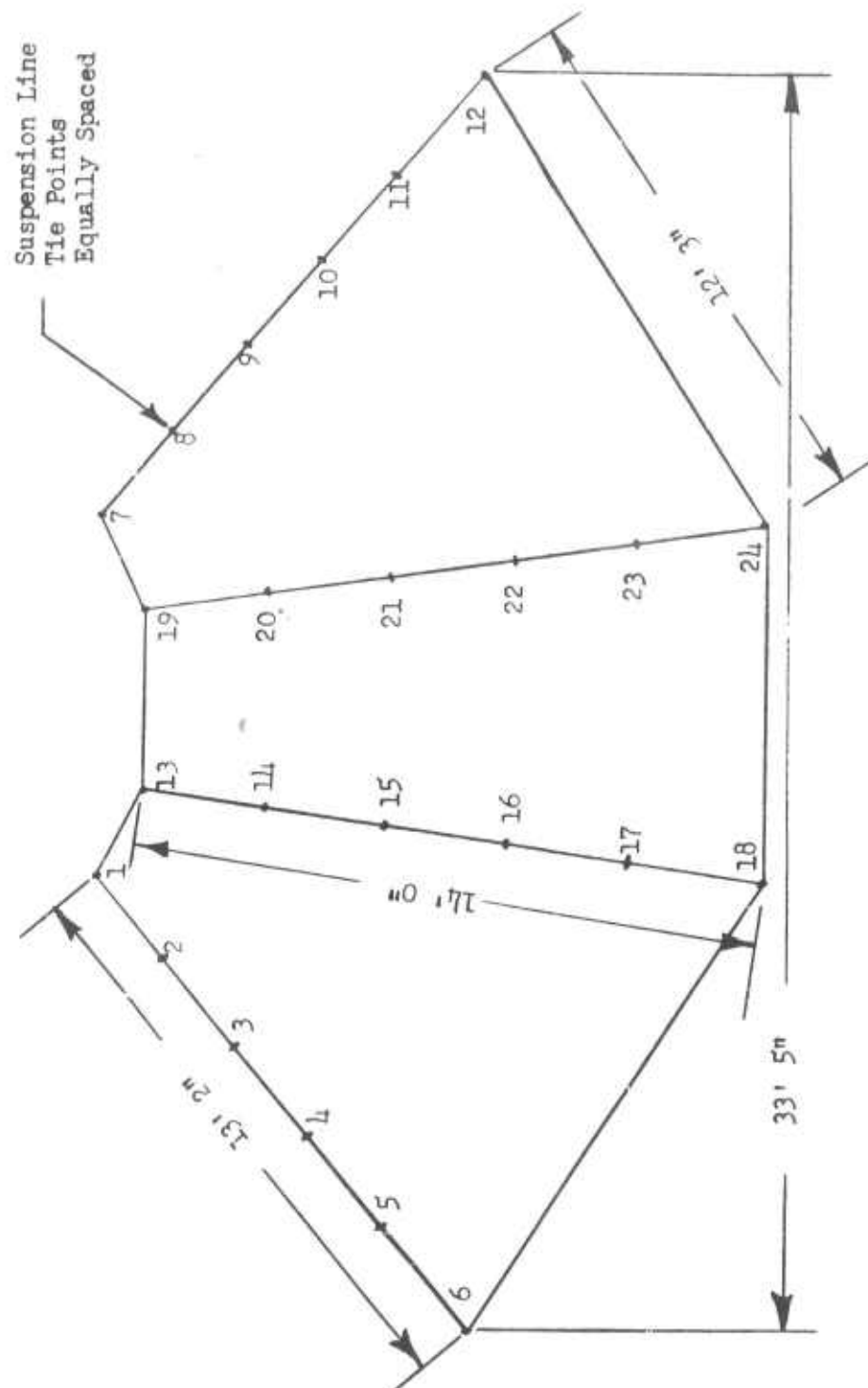


Figure 8. Wing Planform Layout •

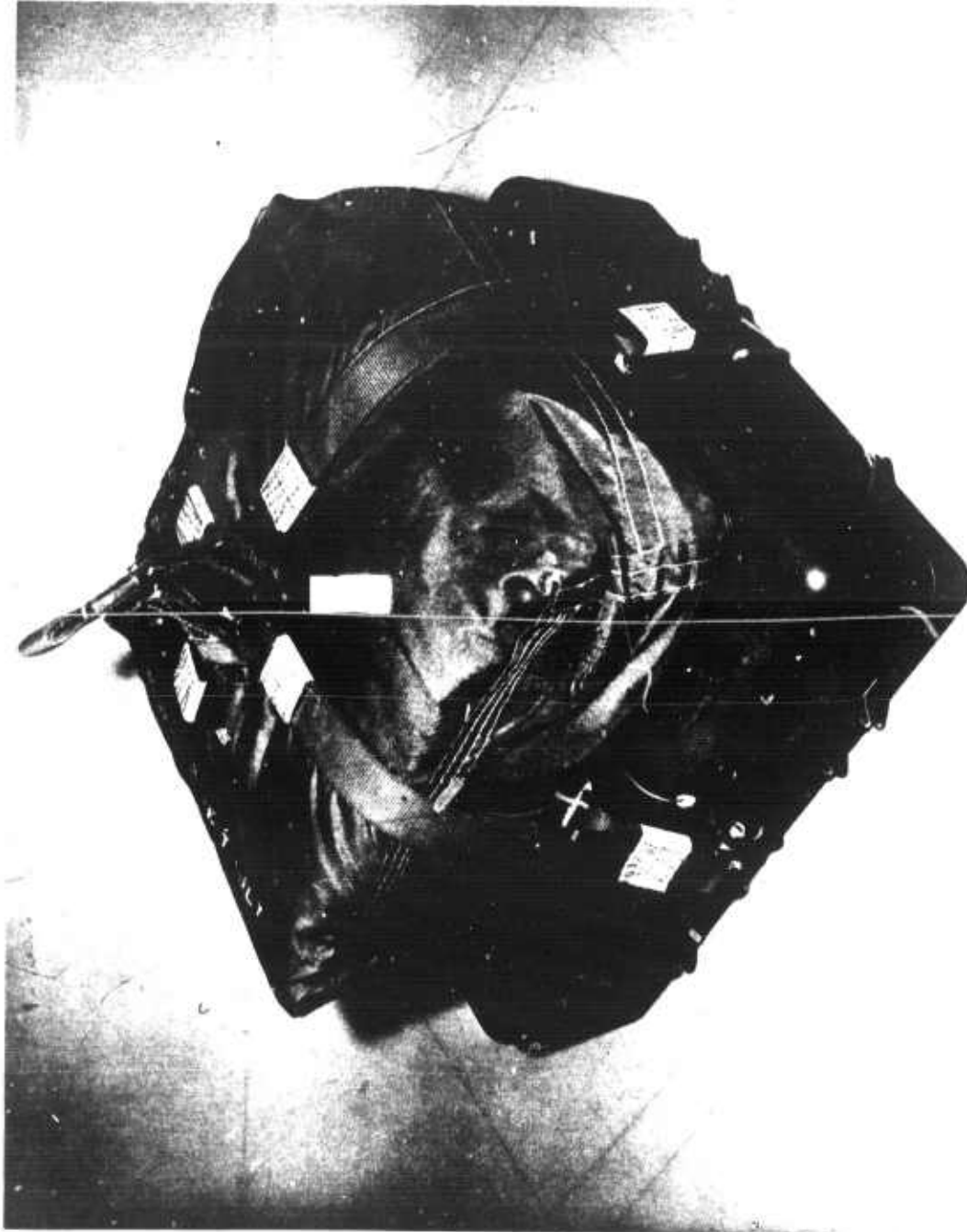
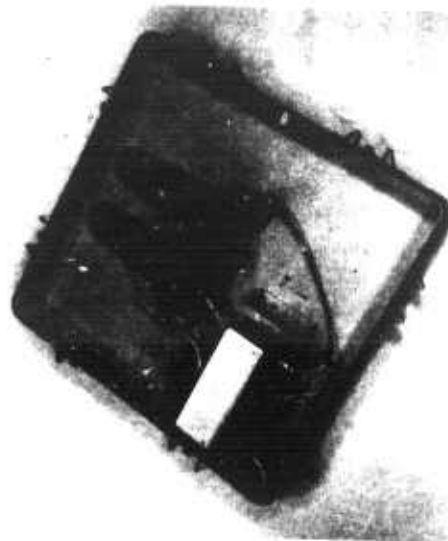


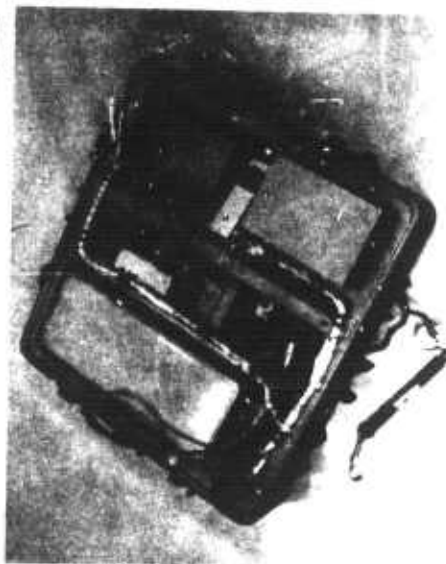
Figure 9. Installation of Wing on Control Box.



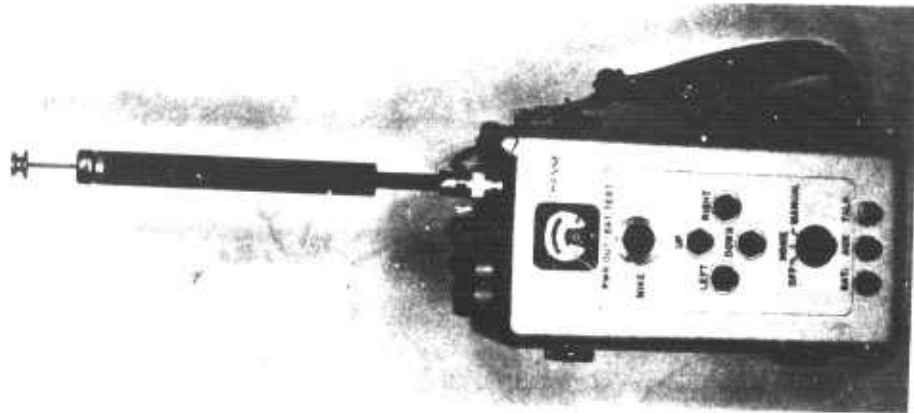
Two Antennas Protrude Vertically  
From Bottom of Control Box Housing



Inside Bottom



Inside Top



Radio Transmitter (GFE)

Figure 10. CACS Airborne Control Box and Ground-Based Transmitter.

1. RECEIVER, RADIO
2. SERVO AMPLIFIER
3. ANTENNA DEPLOYMENT RELEASE
4. LOGIC ASSEMBLY
5. COVER BONDING STRAP
6. SERVO-ACTUATOR
7. SERVO BATTERY PACK
8. TIME DELAY RELAY-K8
9. P3-ELECTRONIC SWITCH CONNECTION
10. P10-INITIATION SWITCH CONNECTION
11. ELECTRONIC SWITCH CONN. - #10067109-1

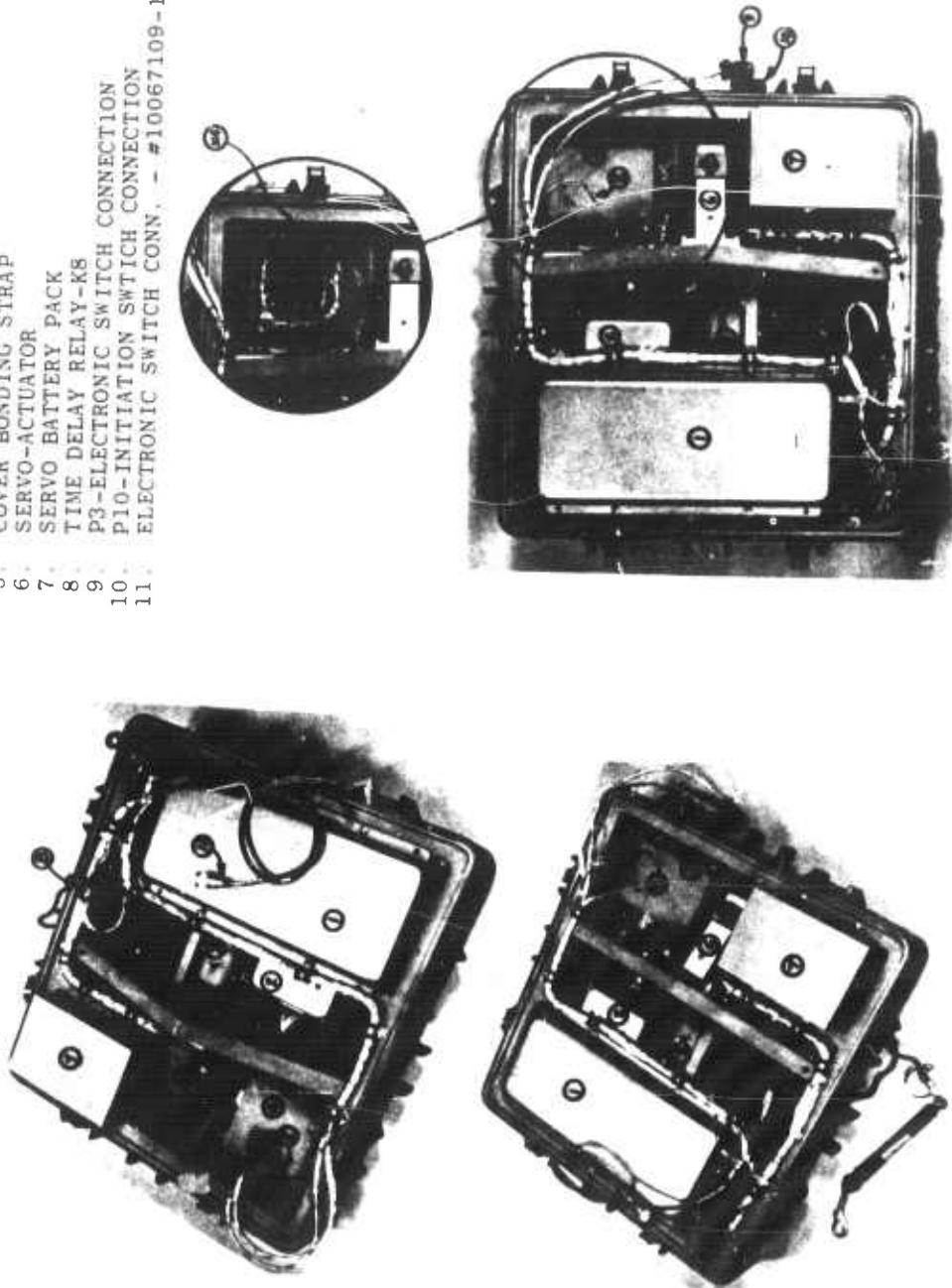


Figure 11. Controlled Airdrop Cargo System Control Box.



TABLE II. NOMINAL LINE LENGTHS FOR STABLE FLIGHT			
		Length	
Line Numbers (Ref. Figure 8)		(Ft)	(In.)
Leading Edge:	1 & 7	22	1
	2 & 8	22	1
	3 & 9	20	4
	4 & 10	20	4
	5 & 11	18	7
	6 & 12	17	0
Keel:	13 & 19	22	6 $\frac{1}{2}$
	14 & 20	21	$\frac{1}{2}$
	15 & 21	20	7
	16 & 22	20	2 $\frac{1}{2}$
	17 & 23	19	10
	18 & 24	19	4

## SYSTEM OPERATION

A schematic of the CACS in operation is shown in Figure 4. The total operation would consist of moving the packed wing and the control unit from their storage areas to an assembly area. The payload would be prepared in its area and moved to the assembly area. Any single-point suspension payload container holding 500 pounds of payload can be used.

The wing is installed on the control box, and the control lines are connected. A standard static line is attached to the wing deployment bag, and the bridle with the swivel is connected to the control box. The assembled system is then placed on the payload, and the proper attachment is made.

The complete assembly (wing, control box, and payload) is loaded on the aircraft, and the static line is attached to an adequate retaining ring. Once over the drop area, the signal from the ground-based transmitter is monitored by the aircraft. Upon receipt of the signal to assure that the radio is on and functioning and when within the operational envelope, the system is released from the aircraft.

As the system falls from the aircraft, the static line draws taut, breaking two loops of 80-pound cord tied through the retaining straps and allowing the bag to separate from the control box. The movement of the bag away from the control box allows the lanyard to the antenna release to function and the lines to pay out of the bag. At line stretch, the deployment bag holding the canopy is cut open, and the time delay pyrotechnic reefing line cutter is activated.

Upon erection of the antenna, power is applied to the time delay. This time delay (7 seconds) prevents any control function from occurring until after the reefing line has released the wing and the wing is completely inflated. When the time delay has closed, the complete control box including the receiver is turned on. At that point the system is ready for operation once the receiver has warmed up. The time and functions for deployment up to an operational system are presented in Table III.

Prior to system release from the aircraft, the transmitter is turned on. The ground personnel select either the automatic or the manual control mode. The mode can be changed during flight by the use of the selection switch only.

Assuming that the manual mode has been selected, the airborne system will orbit after 8 seconds in a loss carrier type of turn until the total system is operating, at which time the controls will neutralize, awaiting a command signal from the ground. As long as a command signal is received (either right or left), the system will remain in a turn. As soon as the command button is released on the transmitter, the system will neutralize and straightforward flight will be accomplished.

In the case in which the automatic mode has been selected, the unit will again spiral until an automatic signal is received. The received signal is

analyzed, and the correct control information is given to the servo actuator. The unit will continually correct itself, homing in on the ground-based unit. Should it pass over the transmitter and into the cone of silence (relatively low radiation energy), the loss carrier function will occur and the right-hand spiral will commence. The system will descend to an altitude and location such that a signal will once more be received, at which point the control box will make the necessary changes in directional control. It is possible that the system will orbit around the transmitter in still air and spiral all the way to the ground. In either case, the system is capable of automatic flight from the aircraft to the ground in the proximity of the transmitter in an automatic homing mode.

TABLE III. DEPLOYMENT SEQUENCE	
Total Time (sec)	Function
0.00	Drop
0.75	Lanyard taut
1.50	Deployment bag off <ul style="list-style-type: none"> <li>- antenna released and erected</li> <li>- control box power turned on</li> <li>- lines and wing stretched out</li> <li>- reefing line cutter activated</li> </ul>
2.00	Reefed parawing inflated
5.50	Reefing line cut
7.50	Parawing fully inflated
8.00	Control box turned on
17.00	System at full operation condition

## TECHNICAL DISCUSSION

### GENERAL

A technical program for the development of a flexible wing delivery system for all-weather airdrop of cargo with both automatic and command homing capabilities was developed by GAC. This system was intended for military engineering and service testing and is now representative of a final production item for tactical use. An aerodynamic study was made to determine the flexible wing configurations to be evaluated. As a result, five configurations were wind-tunnel tested to establish wing rigging dimensions. Limited L/D comparisons were made of the configurations during wind-tunnel testing to evaluate the wing performances. From the aerodynamic analysis, the wind-tunnel test results, a structural analysis, and the preliminary flight tests, a specific wing configuration was selected.

Additional flight testing resulted in the development and finalization of packing techniques, reefing method, and deployment method in order to develop a system capable of being dropped from 500 feet to 30,000 feet at velocities from 0 to 150 KIAS. A guidance and control study including antenna pattern investigation was conducted incorporating the GFE transmitters and receiver. The parawing and control box were then merged to evaluate the control system response and effect on wing performance through extensive flight testing. Finally, qualification tests were run, and the flight test data were evaluated to establish system reliability. An instrumentation system was designed to incorporate a GFE CEC recorder for the gathering of certain data for use in determining performance characteristics.

The program included generation of reliability, maintainability, and quality assurance plans as well as detailed test instructions and test plans and equipment as required for evaluation of system and equipment performance.

### AERODYNAMIC ANALYSIS

A preflight aerodynamic analysis was performed on a single-keel configuration of the all-flexible parawing to determine if it was feasible to meet the contract performance requirements. The single-keel configuration was used for the analysis because of the existence of more data on this configuration as opposed to a twin-keel or a twin-catenary-keel configuration.

The analysis defined performance characteristics such as maximum L/D attainable, vertical descent rates, effects of payload drag on L/D, and lateral control capabilities. Effects of the addition of a catenary-keel panel were also considered. The analysis was based primarily on the results of previous wind-tunnel data.

The analysis indicated that the performance requirements of (1) effective L/D greater than 1.8, (2) vertical descent rate at impact of less than 25 feet per second, and (3) 100-foot radius turn could be met and, in most cases, exceeded.

As a result of the aerodynamic analysis, which is included in Appendix I, five candidate wing configurations were selected for further examination and testing (see Figure 12):

1. Single Keel
2. Twin Keel
3. Single-Catenary Keel
4. Twin-Catenary Keel
5. High-Aspect-Ratio Twin-Catenary Keel

In addition to these five configurations, a twin-catenary keel reefed into a single-keel parawing was tested.

#### WIND-TUNNEL TESTS

GAC in conjunction with NASA-JRC personnel conducted a 4-day preliminary flight test program in the full-scale 30-foot-by-60-foot Langley wind tunnel. The purpose of the tests was to trim out the five parawing configurations selected as a result of the aerodynamic analysis. The configurations tested are shown in Figure 12.

These six configurations were trimmed, and rigging lengths were recorded. Due to the limited tunnel time available, optimization of L/D performance was not obtained. The wings were flown and trimmed, and data was taken at speeds of 35 to 60 feet per second. The data showed a good correlation with wind-tunnel data obtained by other experimenters. The rigging and suspension system geometry was used for the preliminary flight tests at Yuma Proving Ground, Yuma, Arizona.

The wind-tunnel test data is included in Appendix II.

The wind-tunnel tests indicated a 22-percent greater L/D for the twin-keel configurations as compared to the single keel.

#### STRUCTURAL ANALYSIS

A structural analysis of a single-keel parawing configuration was conducted to determine the structural requirements for the canopy and suspension system. The analysis was based on the assumption that the leading edges and keel are straight lines, and the angle of attack is the angle which the plane of the leading edges makes with the flight path. A brief analysis was also performed on the twin-keel parawing.

The single- and twin-keel parawing systems analyzed are defined in Table IV.

The structural analysis of the wings is given in Appendix III. A preliminary analysis was also done on the control box, bridle, swivel, and attachment fittings to define the requirements of the integrating hardware.

Deployment is a major consideration because the deployment condition is critical for most structural elements; therefore, the weight of the system is governed by deployment-stress requirements.

The parawing inflation time,  $t_f$ , may be predicted by

$$t_f = 2.5 L_K / V_D \quad (1)$$

where

2.5 = empirical constant

$L_K$  = keel length in feet

$V_D$  = deployment velocity in feet per second

The total dynamic load is given by

$$P_D = S_A q C_R \quad (2)$$

where

$S_A$  = wing area in square feet

$q$  = dynamic pressure in pounds per square foot

$C_R$  = shock opening factor

Preliminary tests showed  $C_R$  to be 3.0.

Figure 13 graphs the relationship between the deployment velocity, the wing loading, and the maximum g loading for systems without reefing. For example, with a payload weight of 500 pounds and a deployment velocity of 150 knots (253.5 feet per second), the resulting load is 38,000 pounds for an assumed wing loading of 3 psf, a load factor of 76 g.

This computation results in a high value because it was based on wind-tunnel test data and corresponds to an infinite payload mass. Figure 13 and the calculation are for the worst condition, that is, without reefing. Reefing techniques have reduced the opening shock by at least 75 percent.

## GUIDANCE AND CONTROL ANALYSIS

Two methods may be employed for guidance and control of parawing systems: (1) displacement of the suspension lines and (2) addition of a drag device. Most systems with all-flexible parawings use various forms of line-length adjustment. The CACS program currently is using the method developed at the outset of parawing development: that of adjusting the length of the rear leading-edge lines to afford directional control.

The guidance and control system is designed to operate as an integral part of CACS. It uses a radio receiver R-1593( )/ASN-95 as on-board equipment and a matching transmitter T-1110( )/ASN-95 as the ground homing station. If the radio frequency signal is lost, as when passing over the target transmitter, the system will automatically apply a control force to produce a preset turning rate. The vehicle will fly a helical path to the ground unless the signal is again received.

Although the system appears to be susceptible to a 180-degree ambiguity, no practical ambiguity exists. The system is designed to recognize which antenna is receiving the greater modulation signal and to turn toward the stronger signal. As Figure 14 illustrates, the system will fly toward the homing beacon regardless of initial heading.

The number of degrees of deviation from the 180-degree axis that is required to provide sufficient signal differences to be recognized by the control system depends upon factors such as transmitter and receiver antenna patterns, receiver sensitivity, roll attitude, differential amplifier resolution, and resolution of the comparison circuits. The sum of the above factors could exceed  $\pm 15$  degrees; however, preliminary testing indicates that the system resolution is within  $\pm 5$  degrees from the rear and the front.

The control cables are required to deliver a maximum force of 30 pounds for the twin-catenary-keel parawings. With a 1-inch-diameter wrap drum, the torque on the output shaft of the gearbox would be  $30 \times 1/2$ , or 15 inch-pounds. The servo system is capable of maximum control-line travel of 10 inches (present setting is  $2-3/4$  inches maximum left or right).

An antenna system has been designed to provide the best comparison between directivity and receiving sensitivity (see Figure 15). The antennas consist of the two quarter-wave elements on the mounting plate and connectors. The quarter-wave electrical loop and the RF switch, matching networks, and cables are also shown at the inputs to the RF switch (see Figure 15).

At the switching rate, the antenna pattern is essentially a cardioid homing pattern directed to the right or left side of the perpendicular line joining the antennas in the horizontal plane. The homing signal sensitivity, assuming a cardioid pattern as shown in Figure 16, is proportional to the sine ( $\pi S/\lambda$ ), where  $S/\lambda$  is the space between the two antenna elements in wavelengths.

The electrical length, in wavelengths, of the loop termination between the two antennas is equal to the space dimension,  $S$ . The RF switch supplies a single-ended output for the receiver and eliminates the need for two RF amplifiers. A spacing of  $S = 0.25$  seems to provide an ideal design compromise in sensitivity by giving an output differential signal change of 2.5 db for a 10-degree pointing error.

To operate at frequencies sufficiently high to remove interference from the ground, a one-to-three scale-model version of the antennas and the payload box was designed and fabricated. Pattern measurements were made on the antenna range at GAC's Wingfoot Lake facility. Both vertical and horizontal patterns were taken, including tests for voltage standing wave ratio (VSWR), impedance match, and equal gain at the boresight position for right- and left-hand patterns.

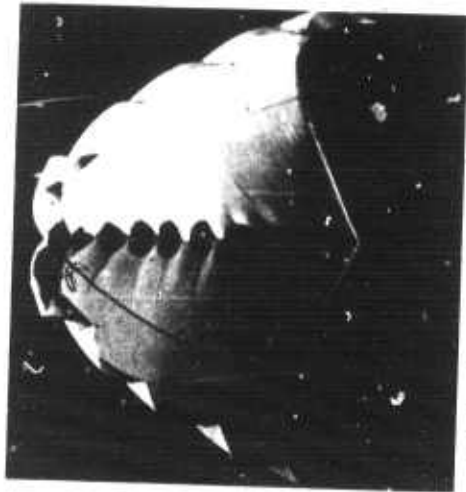
The approach to the mechanical development of a suitable control system for the parawing was to use as much of the knowledge and as many system components as possible from the list of those already developed and qualified. It was hoped that this approach would prevent redundant efforts and provide the most rapid means of achieving a qualified parawing system. The system was to use the radio receiver and transmitter system supplied as GFE. To complete the system, a servo system and a standard aluminum box were selected for the system. The initial units were designed around the larger interim-model receiver and battery. The necessary interface circuitry, instrumentation circuitry, and power distribution circuitry were designed. Servo system power requirements were determined, and a suitable nickel-cadmium battery pack was selected. The entire system was then adapted to the standard aluminum box.

The interim-model receiver was a lower frequency system and did not have the proportional homing capability but was modified by GAC to incorporate this feature for the early test phase.

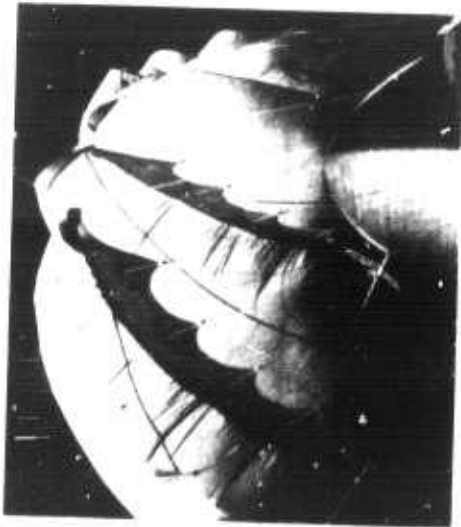
As stated previously, in order to analyze and evaluate the antenna system, a scale model was fabricated and tested. Antenna radiation patterns were measured at six different element spacings to optimize antenna placement. Effects of pitch and roll on radiation patterns for the optimum spacing and payload effects were also investigated. From these investigations, antenna placement and ground plane predictions were made for the low-frequency interim-model receiver. Indications were that a ground plane extension should be used for automatic homing with this system. As a result of this, and the fact that the final receiver system was to be ready early in the program, the interim radio was used in the manual mode only. The scale model antenna analysis also resulted in initial predictions for the higher frequency final receiver antenna system. For details of this scale model antenna system analysis, see Appendix IV.

An analysis was also made of the instrumentation requirements, and the necessary circuitry was designed to obtain this information using the GFE CEC recorder. The original instrumentation system is described in Appendix VI, and the instrumentation data obtained is summarized in Appendix VI.

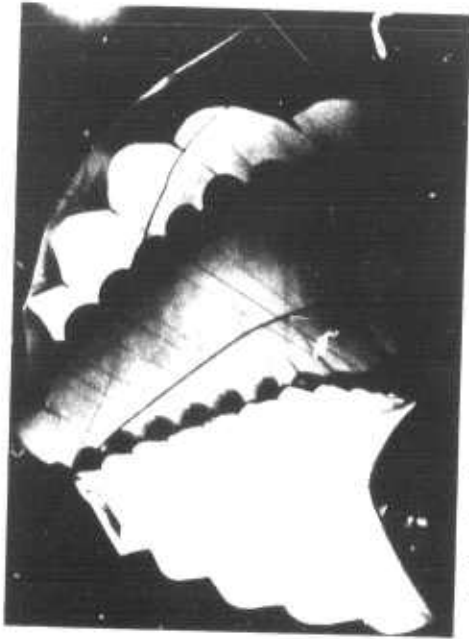




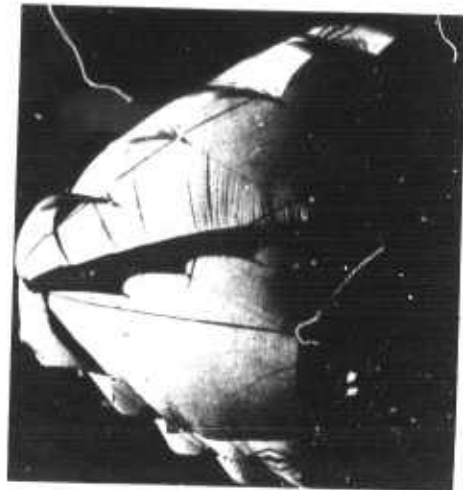
Single keel



Twin catenary keel



Twin keel



Single catenary keel



High aspect ratio, twin catenary keel

Figure 12. Parawing Configurations.

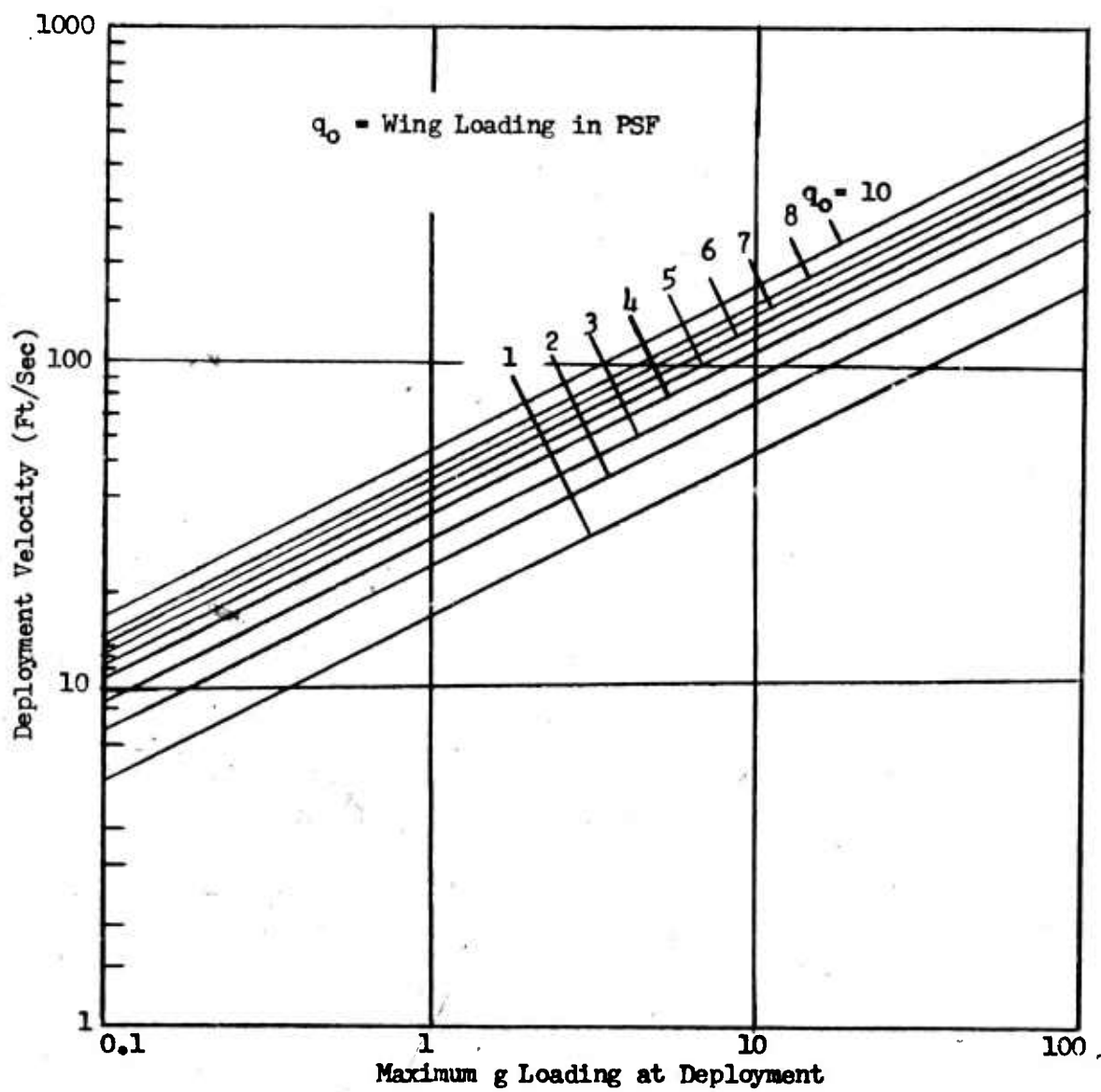


Figure 13. Deployment Velocity Versus Loading.

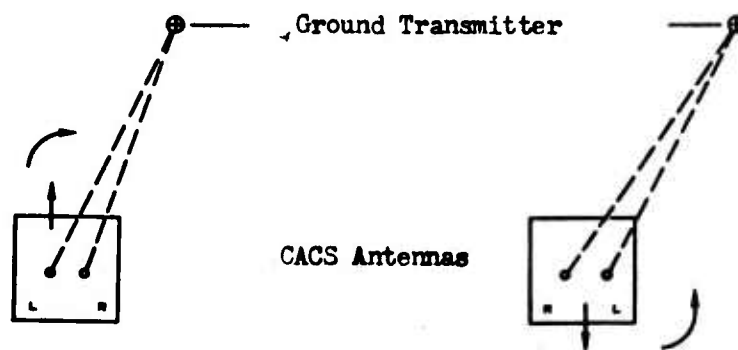


Figure 14. Antenna Directional Operation.

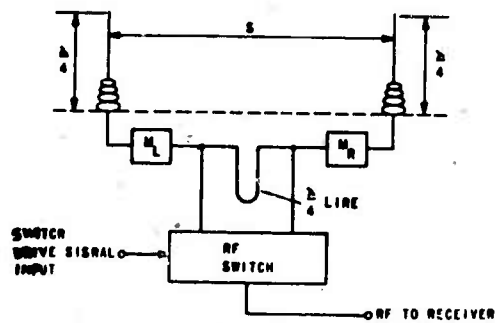


Figure 15. Homing Antenna RF Diagram.

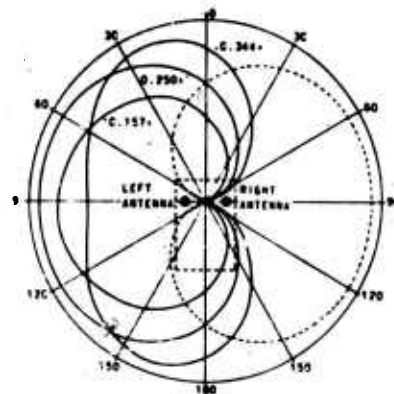


Figure 16. Homing Antenna Signal Sensitivity.

TABLE IV. SYSTEMS DEFINITION		
Item	Single Keel	Twin Keel
Wing planform area	220 sq ft	275 sq ft
Theoretical keel length	18 ft	16 ft
Maximum wing loading	2.7 psf	2.7 psf
Fabric tensile strength required, warp and fill	135 #/in.	120 #/in.
Minimum strip tensile with a factor of safety = 3/1. $T_F = 7.19 \times 10^{-5} L_K F_S V_D^2$ where $T_F$ is the tensile strength of fabric, $L_K$ is the theoretical keel length, $F_S$ is the factor of safety, and $V_D$ is the deployment velocity.		
Resultant velocity of system in flight	48.75 fps	43.75 fps
Vertical descent rate with L/D = 2	21.8 fps	-
Vertical descent rate with L/D = 3	-	15.4 fps

## DEVELOPMENT TEST

### GENERAL

The development tests were to include the evaluation of independent components of their assembly into a unit through a complete system. However, many of the system development tests were done in actual free flight and have been included under flight test. Also, part of the parawing development effort was accomplished in the wind tunnel and is presented as part of the technical discussion. Because of the nature of this program and the approach used, that is, the assembly of developed and qualified hardware, the development test area was limited to antenna performance and location evaluation and the detail examination of the subassemblies in the control unit. The objective of the control system test was twofold: (1) to assure that the total system would function as desired and that the independent components or assemblies would function properly, and (2) to establish the acceptance test procedures, Development Test Instruction (DTI), in accordance with the quality requirements of this program.

### ANTENNA

The preflight or development testing of the antenna system for the final receiver consisted of determination of optimum antenna spacing, design, and fabrication of the antenna erection mechanism, and testing of the full-scale antenna system.

The impedance of the individual antenna elements was taken, loss measurements were made through the RF switch, and radiation patterns were taken on the overall antenna system. For these tests, the actual antenna installation on the control box cover was used with full-scale mockups of the control box and payload. The detailed test results and antenna patterns obtained are given in Appendix V.

### CONTROL SYSTEM

Control system design and fabrication techniques were finalized, and DTI's were written for preinstallation tests of the following purchased and GFE items:

1. Proportional Servo System
2. Servo Battery Pack
3. Control System Time Delay Relay
4. Interim Model Radio Receiver and Transmitter System
5. AN/ASN-95 Navigation Set

In addition, test procedures were written for the logic box assembly and the complete control system. Calibration test instructions were also

written for the GFE receiver test set. Test setups were designed and fabricated as required for the DTI's. A complete set of DTI's can be found in the reliability and maintainability report.<sup>2</sup>

Each of the components was thoroughly tested, and their characteristics were noted for final integration into the control system.

The first two control systems were fabricated using the early model receiver, and they were delivered for field test. These two units were flown successfully, but only the manual control mode was used because the scale-model antenna tests indicated the need for a ground plane extension for the antennas for automatic homing. The manual control flights were useful for preliminary determination of such factors as control line pull-in versus turn rate, etc.

The R-1593( )/ASN-95 receivers were incorporated into the next systems. The preliminary tests of the final system in the proportional homing mode indicated that the system was very sensitive. The error angle required for full cable pull-in would result in what would amount to a "bang-bang" system. The system sensitivity was such that hunting of the servo system resulted. The tests showed the need for a more comprehensive investigation and optimization of the system with respect to receiver sensitivity, servo system sensitivity, servo dead band, noise levels, antenna patterns, desirable error angles, and antenna boresight errors. In the interest of cost and time, GAC elected to use the "bang-bang" steering for field test. The "bang-bang" system was found to satisfy the contract requirements and was incorporated into the system.

## FLIGHT TEST

### GENERAL

Because of the nature of the program and its ultimate objective, the aerodynamic and flight tests were the most significant tests that were conducted. The wind-tunnel tests and their results have been presented under technical discussion and in Appendix II. The objective of the flight test program was to evaluate the wing performance, deployment system, control box-wing integration, reefing and system performance, and reliability evaluation. The flight test evaluation was divided into four areas: preliminary flight tests, deployment tests, control flights, and performance and reliability evaluation.

During this task, the major system integration was accomplished by obtaining the best performance characteristics of each subsystem when combined with the balance of the hardware.

The results of the flight test program are presented in this section. Appendix VI presents the onboard flight instrumentation data.

### PRELIMINARY FLIGHT

The objective of this phase of the flight test program was the selection of the wing configuration for more complete evaluation.

The preliminary flight tests were conducted during two separate efforts. The first was from 8 July to 9 August 1968 at Yuma Proving Ground. The second series of flights occurred 10 September to 1 November 1968. During the first series of tests, 108 flights were conducted. They consisted of 6 dummy man drops for trim, 49 live man drops to evaluate deployment and control, 42 cargo drops without control box for deployment and trim evaluation, and 11 control drops for manual model considerations and the evaluation of certain mechanical features. The objective of this series of tests was to verify and adjust the rigging line lengths and material established by the wind-tunnel effort and structural analysis as well as wing configuration. In addition, the effect of various reefing and deployment techniques was investigated, and the control characteristics of the wing were to be determined by means of personnel and manual control drops.

The variables investigated for these series of tests were:

1. Line Material
  - a. Steel
  - b. Nylon - Polypropylene 2-in-1 stable braid

- c. Nylon tubular
- d. Nylon braid
- e. Dacron - Polypropylene 2-in-1 stable braid
- f. Dacron twisted

## 2. Canopy Configuration

- a. 220 ft<sup>2</sup> planform area - Single Keel (SK)
- b. 220 ft<sup>2</sup> planform area - Single-Catenary Keel (SCK)
- c. 270 ft<sup>2</sup> planform area - Twin Keel (TK)
- d. 270 ft<sup>2</sup> planform area - Twin-Catenary Keel (TCK)
- d. 360 ft<sup>2</sup> planform area - High-Aspect-Ratio Twin-Catenary Keel

## 3. Reefing Techniques

- a. Standard reefing line rings on the periphery of the parawing with line lengths from 50 to 80 percent of the parawing keel length
- b. Daisy chaining the keels together with the aft opening first
- c. Daisy chaining the trailing edges closed
- d. Combinations of a, b, and c
- e. Snyder reefer in lengths from 48 to 84 inches

## 4. Packing Techniques

- a. Simple sleeve with line stowage provision
- b. Stock bags with line stowage provision
- e. Disposable bags
- f. Commercial design sleeve

The test conditions were a suspended weight of 65 to 565 pounds (live man drops, approximately 180 pounds), a drop altitude of 1000 to 7000 feet, and a velocity of 5 to 150 KIAS.

The objective of the personnel tests was to make preliminary measurements and judgments, which would be difficult to obtain without a very sophisticated



on-board and ground instrumentation system. The indication was that the man's descent rate on the 270-foot<sup>2</sup> twin-catenary-keel parawing was 8 to 10 feet per second. Also, for the twin-catenary keel, a 6-inch pull on the control line with a man payload required 16 to 18 pounds of pull. This produced a 6- to 7-second 360-degree turn with a turning radius estimated at less than 50 feet. The parawings with a catenary keel could be flown in turns estimated to be 20- to 30-foot radius with no apparent sideslip or loss of control.

Based on personnel and cargo flights and observation only, it appeared that the wings with catenaries performed better than those without. It was also determined by observation and comments by the jump personnel that the twin-catenary keel performed the best.

As stated above, various line materials were investigated; as a result, Dacron polypropylene 2-in-1 stable braid was selected. With respect to the reefing techniques, it was determined that the approach in which only the lines are restrained would be used. The exact method was not determined; only the approach was considered.

Two flights in this series were instrumented, and the data is given in Appendix VI.

As a general result of this series of flight tests, it was determined that a twin-catenary-keel parawing with Dacron polypropylene 2-in-1 stable braid was the canopy and line configuration that should be used. Based on the use of the interim-model receiver and transmitter equipment, it was determined that manual control was possible. The use of the swivel was proven, and adequate control response was obtained. The indications were that the parawing system could meet the desired requirements. The specific deployment and packing technique was not worked out; however, the general folding arrangement for the parawing was established. Areas in which control box improvements could be effected with respect to the mechanical design were determined. Since the major objectives of this effort were accomplished, this part of the test program was concluded. A summary of the test phase is presented in Table V.

The preliminary flight tests, part two, were initiated at Yuma Proving Ground. The objectives of these tests were to investigate deployment and reefing techniques and the control system capability using the final receiver and transmitter in both the automatic homing and the manual control modes.

During this test sequence, 82 flights were made. They consisted of 36 dummy cargo "trim" flights and deployment tests and 46 flights for control tests. It was determined during this test series that the wrap-type reefing technique such as the Snyder reefs would not perform over the altitude-velocity envelope requirement, and a special package and deployment container was necessary for the unit. After several significant failures, this effort was terminated, and the information obtained was reviewed in detail prior to initiation of the deployment test phase. Table VI is a general summary

of this flight series, and Table VII is a summary of the flights in which a control unit was used.

It was determined that once good deployment had been accomplished and opening shock kept down, the system would function well. Based on this and the reefing line and packaging information, a detailed deployment test series with specially designed and fabricated hardware was planned, designed, and performed.

#### SYSTEM DEVELOPMENT FLIGHT TEST PLAN

An analysis of the data obtained on the preliminary program and an extensive review of the test movies were used to prepare a test plan. As stated in the requirements, the system must be deployable from a 500-foot altitude to 30,000 feet. Consideration was given to two general approaches. The first used a drogue, and the second was lanyard extraction of the wing.

The two general concepts were investigated. It was assumed that the drogue approach might encounter problems at the low-altitude limit and the lanyard would produce the maximum load. An analysis using the drogue concept assuming a 68-inch  $D_0$  flat circular pilot chute was performed and is summarized in Table VIII. It indicates that this concept should be investigated experimentally.

In evaluating the lanyard approach, it was assumed that the deployment velocity was 150 knots; a sea level air density was used, and an opening shock factor of 2 was assumed for the 30,000-foot condition. Based on these assumptions and a reefed mode, the peak load was calculated to be 6840 pounds. (The maximum load measured with proper reefing during the flight test was 6100 pounds.) The total capability of the lines (24 lines at 1700 pounds per line) is 40,800 pounds, resulting in a safety factor in excess of 3. In examining the 500-foot case, it was determined that a 4-second time delay should be used. This factor was also used in obtaining the above loads. Based on the above and the tolerances accumulated, such as reefing delay time and simplicity of system, the lanyard appeared to be somewhat better than the drogue concept. However, it was determined that an experimental evaluation would be required for final selection.

As stated, one of the conclusions from the preliminary flight test program was the requirement of a packing and deployment unit designed particularly for the parawing. This unit is to encompass the handling as well as operational requirements. Two concepts were investigated: a bag and a sleeve. In both cases, provisions were made so that a drogue or lanyard could be attached to the bag or sleeve.

As a result of the preceding test program, it was determined that the wing and rigging configurations were satisfactory, and the mechanism of the control box and the "bang-bang" control, instead of the proportional control, would be adequate to meet the contract requirements. Also, the final bridle length was determined.

It was determined that the balance of the tests should be to establish the best method for extracting and deploying the wing, establish the reefing method, determine the control adjustments and attachment requirements, and evaluate the performance and system reliability. In order to accomplish these objectives in the most expeditious manner, a test program was designed which had a series of tests each having a primary objective. However, they were integrated such that secondary objectives could be accomplished; i.e., a flight having deployment evaluation as its primary objective could have a secondary objective of control response. An order of preference was established, and most of the data for a particular factor was accumulated before the next series of tests was started. It should also be pointed out that the total test was changed when the data so indicated; however, a test series was always completed to assure the total availability of data. The program developed, as a result of the above, is presented in Tables IX through XII.

During the generation of the test program and the plan and review of hardware requirements, a system for recording and reporting test conditions and data was established. The specific forms are presented in Figures 17 through 22. (Note that Figure 17 was replaced by Figures 18 and 19 during the course of the program.) The forms were completed after each flight. The objective of these forms was to reduce the possible variations to a minimum and to record as much of the same data from each flight for comparison evaluation.

Upon completion of the test plan, forms, and approach, and a review with the cognizant Army personnel, the next phase of the flight test and evaluation program was initiated.

Because of the results of the flight test program, changes in the tests were made. Table XIII lists all the tests conducted beyond the preliminary tests. It shows the flight number, the deployment altitude, the deployment velocity, and the type of test.

#### DEPLOYMENT FLIGHT TESTS

The specific objective of the deployment test series was to finalize a system capable of being deployed from 500 to 30,000 feet at velocities from 0 to 150 knots indicated airspeed. In order to accomplish this objective, two reefing arrangements, two packing systems, and four extractions were experimentally evaluated at Yuma Proving Ground. One additional reefing arrangement was also examined experimentally.

A zero-length reefing line located at the length of the No. 6 line (17 feet from the fitting) on all the lines was the basic configuration. The variation evaluated was the distance that the nose was drawn down from its full-up position toward the 17-foot dimension. The four nose lines were pulled down either one-half or three-fourths of that distance. For one test the nose was drawn down to a point coincident with the 17-foot reefing line attachment point.

The packing configurations were a deployment bag and a deployment sleeve. The wing was extracted by means of a lanyard attached directly to the pack or to a drogue which then extracted the wing. The time delay is 4 seconds for the reefing line cutter when the lanyard approach is used. When a drogue is used, 2 seconds is expended on the drogue and 2 seconds for the disreefing of the wing. A 68-inch D<sub>0</sub> flat circular parachute was used as the drogue.

A summary of all the deployment flight tests is presented in Table XIV. The eight configurations tested were:

1. Bag with drogue and 0 + 1/2 nose tuck reefing
2. Bag without drogue and 0 + 1/2 nose tuck reefing
3. Bag with drogue and 0 + 3/4 nose tuck reefing
4. Bag without drogue and 0 + 3/4 nose tuck reefing
5. Sleeve with drogue and 0 + 1/2 nose tuck reefing
6. Sleeve without drogue and 0 + 1/2 nose tuck reefing
7. Sleeve with drogue and 0 + 3/4 nose tuck reefing
8. Sleeve without drogue and 0 + 3/4 nose tuck reefing

Each of the eight configurations was dropped from 3000 feet at deployment velocities of 40, 80, and 120 KIAS. Maximum shock loads were recorded by means of a Brinell block measuring device between the payload and the dummy control box. In several cases, the instrumentation unit was used to confirm the Brinell data. This series of tests consisted of flights 201 through 229. The results of these tests and a comparison are presented in Table XV. It can be seen that the 3/4 nose tuck gave the most consistent low deployment load.

The 3/4 tuck lanyard deployed in both the bag and sleeve was selected for the next series of tests. The two configurations were tested at 120 knots and deployment altitudes of 5000, 10,000, and 15,000 feet. These are flights 230 through 235 and are presented in Table XVI. The final configuration selected based on the data obtained was a deployment bag, without a drogue chute, with zero-length reefing line, and with a 3/4 nose tuck. Flights 237, 238, and 239 are of this configuration for indicated airspeeds of 150 knots and 5000-, 10,000-, and 15,000-foot altitudes (see Table XVI). The results of these flights verified the selection.

The reefing line was sized from the preceding flights and selected tests through flight 324. The flights used to size the reefing line and the results are presented in Table XVII. It was concluded that a 4000-pound line would allow the system to function over the complete range of condition and that a 1700-pound reefing line would limit the performance

envelope to 10,000 feet and 120 KIAS.

In summary, the deployment tests resulted in the selection of a bag, zero reefing line, 3/4 nose tuck, 4000-pound reefing line system. Sufficient data was obtained to establish insured performance over the required spectrum of conditions.

Upon completion of these tests, a preliminary series of control flights was made. They were flights 240 through 249 in which inconsistent results were obtained. It was determined upon examination of the flight hardware that excessive loading had been experienced during the deployment tests; therefore, new equipment should be used for the control tests.

#### CONTROL SYSTEM EVALUATION FLIGHT TEST

The objective of this part of the flight test program was to evaluate the effect of control system response on the wing performance and to establish the type and amount of control required. The flight tests necessary to obtain data to accomplish the objective of these tests were conducted at Yuma Proving Ground.

The general requirements of the total system including the control box were as presented in Statement of the Problem. It appeared from the data obtained on flights 201 through 239 that the wing was more than capable of meeting the objectives. The wing performance would be degraded by the addition of the control box. Because of this, a series of tests was conducted to evaluate the attachment point of the control line to the control cable and the amount of control line movement for each mode of operation. This series of tests was divided into two efforts. The first was to insure that the wing was in trim and performed properly, and the second consisted of controlled flights with the trimmed wing. There were 42 deployment and trim drops and 44 control flights for a total of 86 tests.

A summary of the control flights conducted is presented in Table XVIII.

The effect of the control box on the performance of the wing for the most part was based on visual observation, motion pictures, and stopwatch-type data. Several attempts were made to obtain adequate data using a variety of instrumentation systems. However, it was determined that cinetheodolite coverage would be required in the last analysis to determine specific performance parameters.

One of the items to be determined was effective L/D of the system. Figure 23 is a definition of effective L/D. It is the glide angle once the system is flying and heading toward the transmitter in a no-wind condition. Should it pass over the transmitter and enter the loss carrier mode of operation, that portion of flight is not considered for the effective L/D evaluation.

The cinetheodolite data was obtained on flights 326 and 327. A reduction of the data is presented in Figures 24 and 25. The L/D obtained for flights 326 and 327 was 1.9 and 2.1, respectively. Figure 25 shows that an effective L/D as high as 3.1 was achieved during the early part of that flight. All of the values obtained were well in excess of the required 1.8.

A second requirement was a vertical impact velocity of less than 25 feet per second. The results from both cinetheodolite flights are presented in Figure 26. The impact velocity was 20 feet per second and 17 feet per second. Both of these values are below the requirement set for impact velocity; that is, not to exceed 25 feet per second.

It was also required that the system be capable of a 100-foot turn radius. The data obtained shows that the 100-foot turn radius requirement was achieved.

The cinetheodolite data obtained from these two flights confirms the rough data obtained on the balance of the flights. Therefore, it can be concluded that the system performance with respect to the parameters discussed above are equal to or better than that necessary to meet the requirements.

As a result of this effort, it was concluded that for automatic operational mode, control would be accomplished by deflecting the wing tip 2-1/4 inches for the automatic homing mode and 2-3/4 inches for the manual and loss carrier modes. It was concluded that effective L/D could be obtained and that an average turn radius of 100 feet was achieved with the above wing tip deflection values. It was also concluded that impact within 100 feet of the target during manual operation could be achieved.

Although additional flights were not conducted, the data was reviewed for performance CEP and reliability predictions. This review is presented in the following section.

#### PERFORMANCE AND RELIABILITY FLIGHT TEST

A detailed analysis of the performance, turnaround time, reliability, and CEP is presented in the Reliability and Maintainability report<sup>2</sup>. Therefore, only the data used and conclusions are presented here.

Sufficient data was to be obtained to evaluate the CEP of the system in a 15-knot wind. A specific CEP was not a requirement; however, a goal of 200 feet was considered. The data applicable to this determination is presented in Table XIX. The average impact distance was 169.6 feet; a CEP of 180 feet with a 90-percent confidence level of 200 feet with a 91-percent confidence level was obtained.

The reliability predictions were based on the data presented in Table XX. It was determined that the system's reliability was 93.3 percent with a 90-percent confidence level or 95 percent with an 85-percent confidence level.

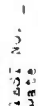
The reaction time objectives were preflight of 15 minutes and turnaround time of 125 minutes. The time achieved was 15 minutes and 45 minutes, respectively.

Results of testing show that the system meets all of the performance requirements as defined in the contract Statement of Work.

CORPORATION  
 ABBOTT, OHIO 44211

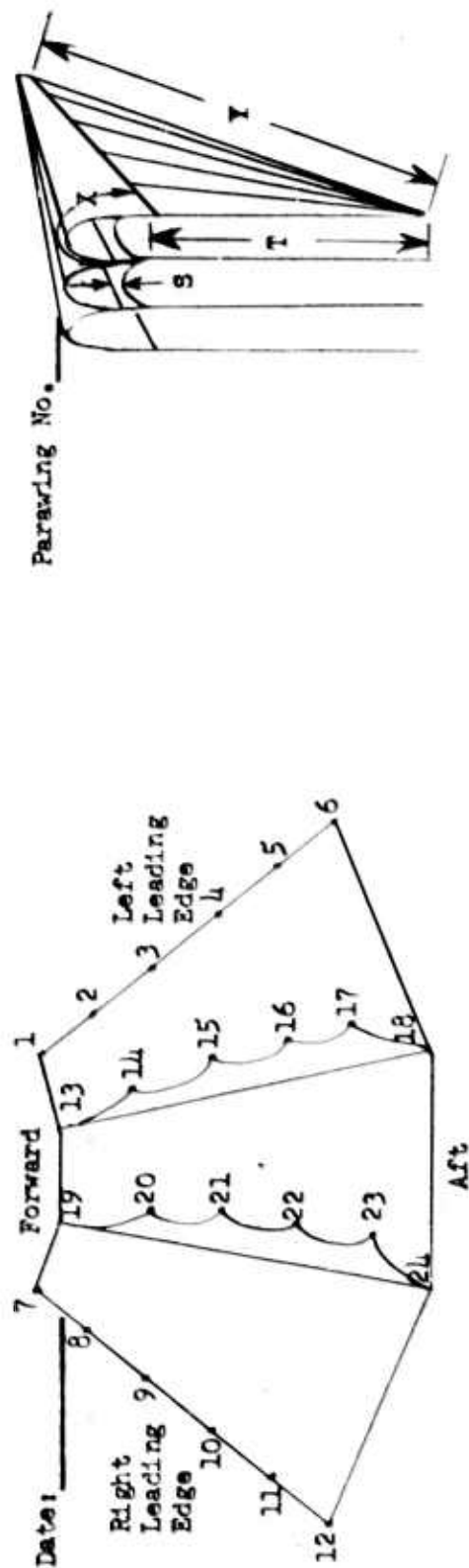
[illegible]

12.000



46





LINE NO.	ESTABLISHED LENGTH			LENGTH BEFORE TEST					LENGTH AFTER TEST						
	X	Y	X+Y	LINE NO.	X	Y	X+Y	LINE NO.	X	Y	X+Y	LINE NO.	X	Y	X+Y
LEADING EDGE															
1-7	2' 1"	22' 1"	24' 2"	1				7				7			
2-8	2' 2"	22' 1"	24' 3"	2				8				8			
3-9	6' 2 1/2"	23' 5"	29' 7 1/2"	3				9				9			
4-10	8' 3"	20' 4"	28' 7"	4				10				10			
5-11	10' 5 1/2"	18' 7"	28' 12 1/2"	5				11				11			
6-12	12' 4"	17' 0"	29' 4"	6				12				12			
FEEL	E	T	B+T												
1-19	0'	22' 6 1/2"	22' 6 1/2"												
2-20	1' 10 1/2"	21' 1 1/2"	22' 11 1/2"	13				19				19			
3-21	1' 10 1/2"	21' 7"	22' 17"	14				20				20			
4-22	1' 10 1/2"	20' 2 1/2"	21' 12 1/2"	15				21				21			
5-23	1' 10 1/2"	19' 10"	20' 10"	16				22				22			
6-24	0'	19' 8"	19' 8"	17				23				23			
				18				24				24			

Figure 18. Parawing Line Length Check.

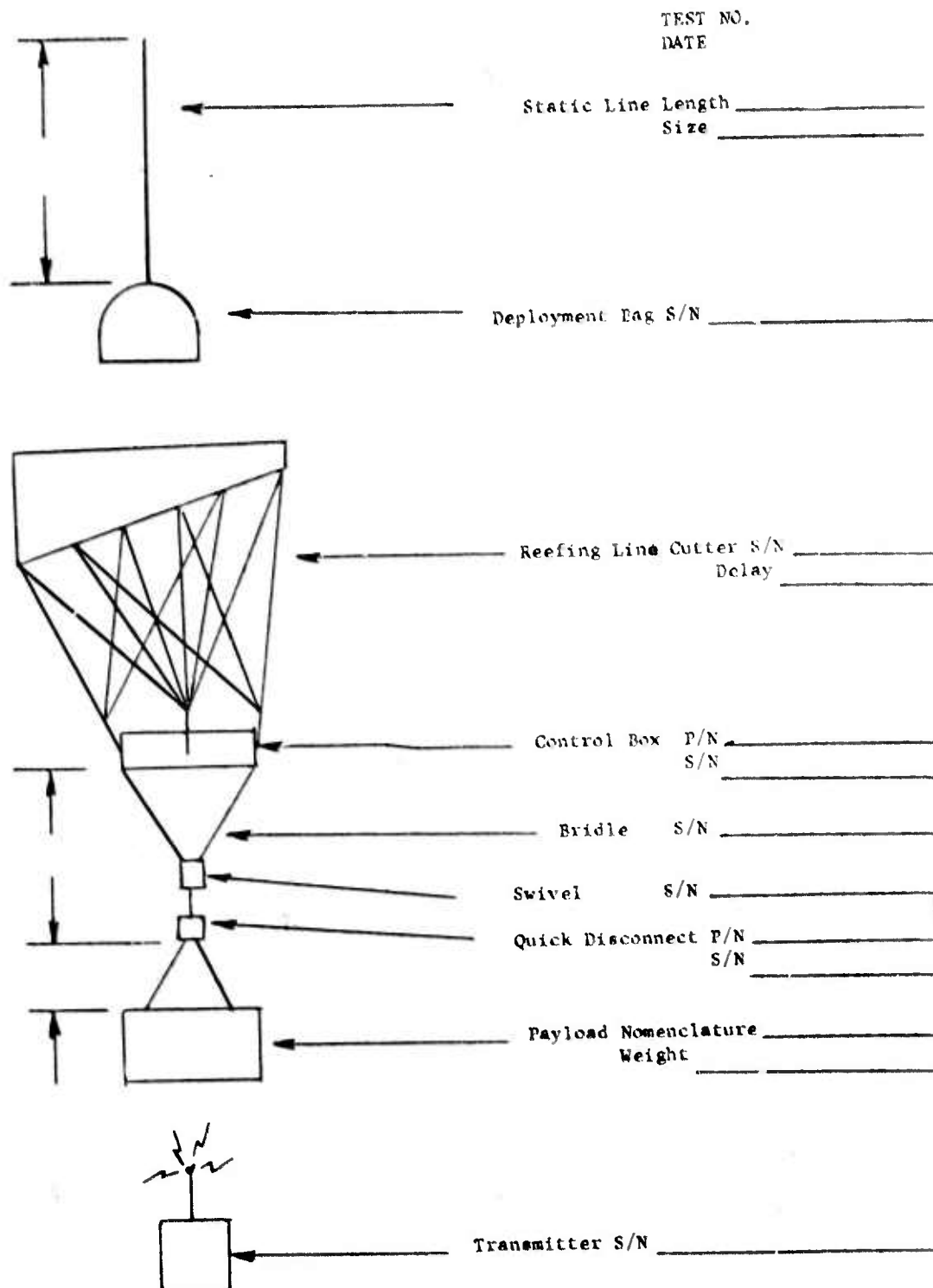


Figure 19. Development Test Hardware Definition

FLIGHT TEST SUMMARY

Date: \_\_\_\_\_ Time: \_\_\_\_\_ Test Number: \_\_\_\_\_

Aircraft: \_\_\_\_\_ Depl. Vel. \_\_\_\_\_ Altitude: \_\_\_\_\_

Parawing: \_\_\_\_\_ Contr. Syst: \_\_\_\_\_ Payload Weight: \_\_\_\_\_

Payload Weight: \_\_\_\_\_ Documentation: \_\_\_\_\_

Flight Type: \_\_\_\_\_

\_\_\_\_\_

\_\_\_\_\_

Flight Detail: \_\_\_\_\_

\_\_\_\_\_

\_\_\_\_\_

\_\_\_\_\_

\_\_\_\_\_

\_\_\_\_\_

\_\_\_\_\_

\_\_\_\_\_

\_\_\_\_\_

\_\_\_\_\_

\_\_\_\_\_

\_\_\_\_\_

Atmospheric: \_\_\_\_\_

\_\_\_\_\_

Recorder & Witnesses: \_\_\_\_\_

\_\_\_\_\_

\_\_\_\_\_

Figure 20. Flight Test Summary

CONTROL SYSTEM FLIGHT READY TEST - PPADS

Test Date \_\_\_\_\_

System Serial Number \_\_\_\_\_

Flight No. \_\_\_\_\_

Component List      Serial Number

Servo Amplifier \_\_\_\_\_

Servo Actuator \_\_\_\_\_

Time Decay Relay \_\_\_\_\_

Receiver \_\_\_\_\_

Component List      Serial Number

Battery Receiver \_\_\_\_\_

Battery Servo \_\_\_\_\_

Logic Box \_\_\_\_\_

Electronic Switch \_\_\_\_\_

<u>Battery Voltage</u>	<u>Servo</u>	<u>Battery</u>	<u>Receiver Battery</u>
No Load	32 $\pm$ 2V	No Load	28 $\pm$ 2 Volts
10 ohm	28 $\pm$ 2V	30 ohm	25 $\pm$ 2 Volts

Time Delay

Close Deployment Switch note between Deploy indicator out and Power (T + 9) indicator on.

\_\_\_\_\_ seconds (nominal 9 seconds)

Voltage Regulator

With Servo Battery  
Battery Voltage

Regulator Output

\_\_\_\_\_ 30 Volts Nominal \_\_\_\_\_

Flight Notes: \_\_\_\_\_

\_\_\_\_\_

\_\_\_\_\_

\_\_\_\_\_

\_\_\_\_\_

\_\_\_\_\_

\_\_\_\_\_

\_\_\_\_\_

\_\_\_\_\_

\_\_\_\_\_

\_\_\_\_\_

Figure 21. Control System Flight Ready Test - CACS

Adjust Potentiometers and operate control indicated, measure cable travel and voltages:

Function	Potentiometer Adjust	Control	Cable Travel	HiLever Preset	Feedback
Manual Left	R4	K2			
Manual Right	R5	K1			
Loss Carrier	R6	K3			
Home Left	R2	K6			
Home Right	R3	K7			

Measure an equal length of control cable in center position of actuator \_\_\_\_\_

Antennas checked for shorts and grounds. \_\_\_\_\_

#### Assembly Package

Note connectors are properly secured, hardware complete and bolts secured. \_\_\_\_\_

Loss Carrier jumper disconnected \_\_\_\_\_ Connected \_\_\_\_\_

Note irregularity \_\_\_\_\_

#### Final Check

With system completely assembled, operate the control box by releasing the antenna.

Operate the transmitter for the following actuator operation. (NOTE: Transmitter should be a minimum of 10 feet from the control box.)

#### Manual Control

Right \_\_\_\_\_  
Left \_\_\_\_\_

Transmitter Off

Home (Transmitter Position)

Right \_\_\_\_\_  
Left \_\_\_\_\_

#### Control Cable Pull In

Right \_\_\_\_\_  
Left \_\_\_\_\_

Right Left

Right \_\_\_\_\_  
Left \_\_\_\_\_

Return to actuator center position - note any deviation from position marked.

Tested by \_\_\_\_\_ Date \_\_\_\_\_ -57-

Figure 22. Control System Flight Ready Test - CACS

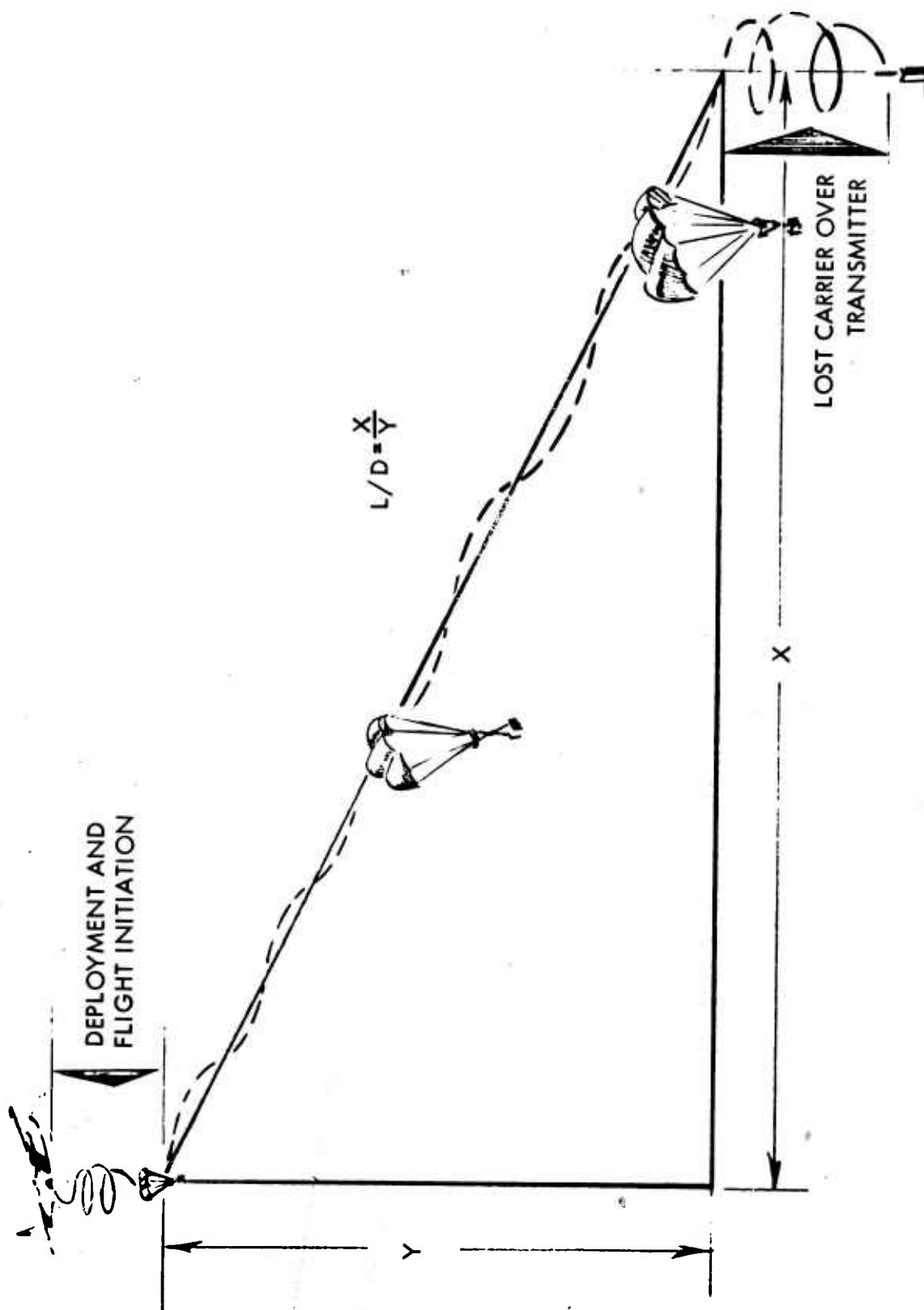


Figure 23. Effective L/D Definition

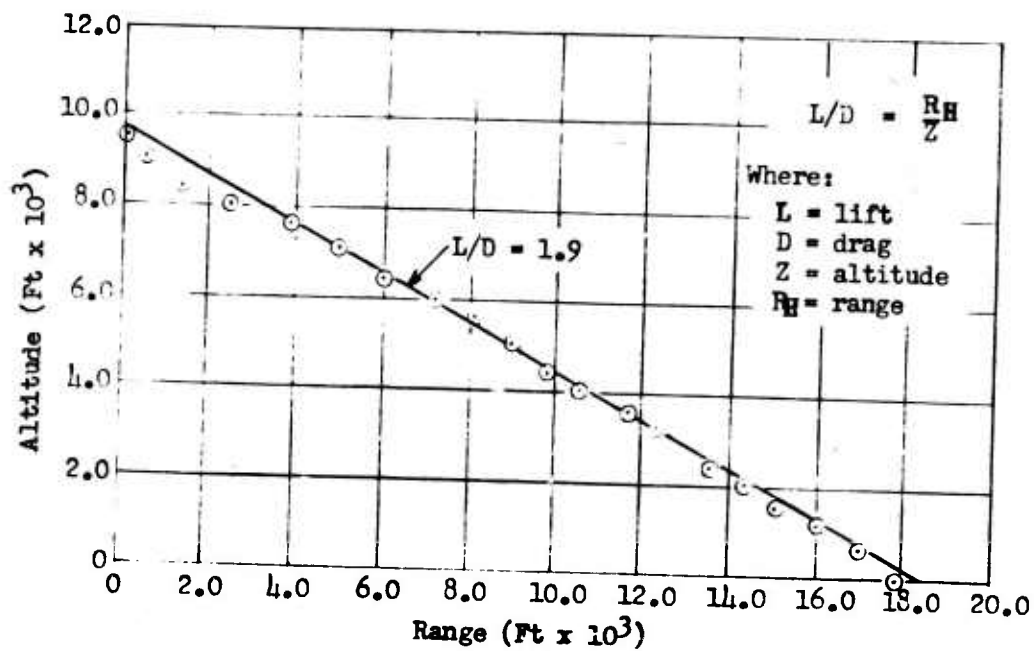


Figure 24. Parawing Performance Flight Test No. 326 L/D Performance Curve.

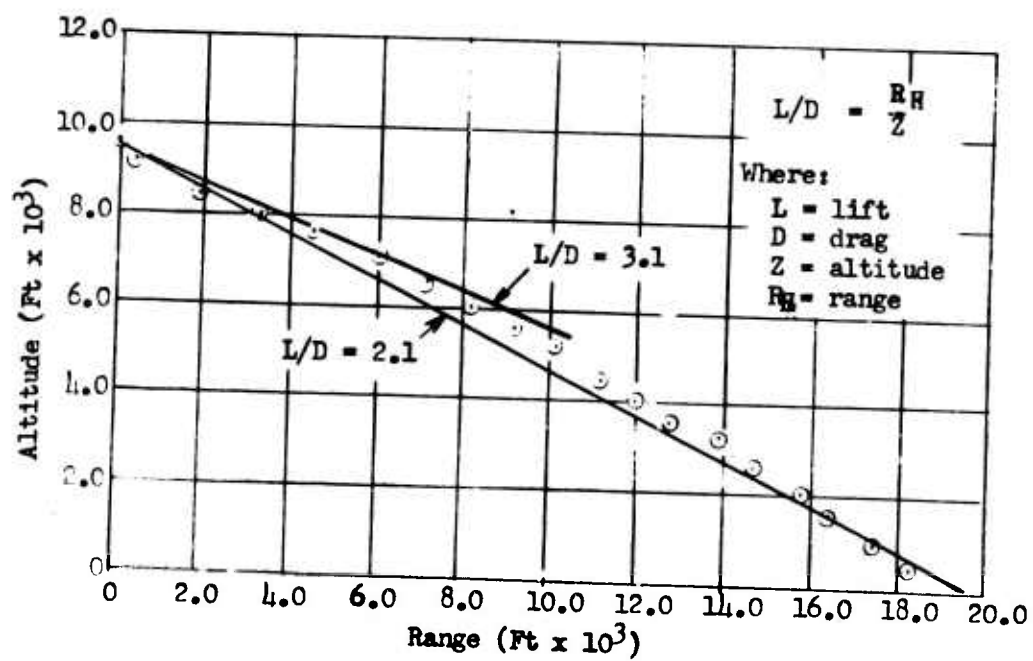
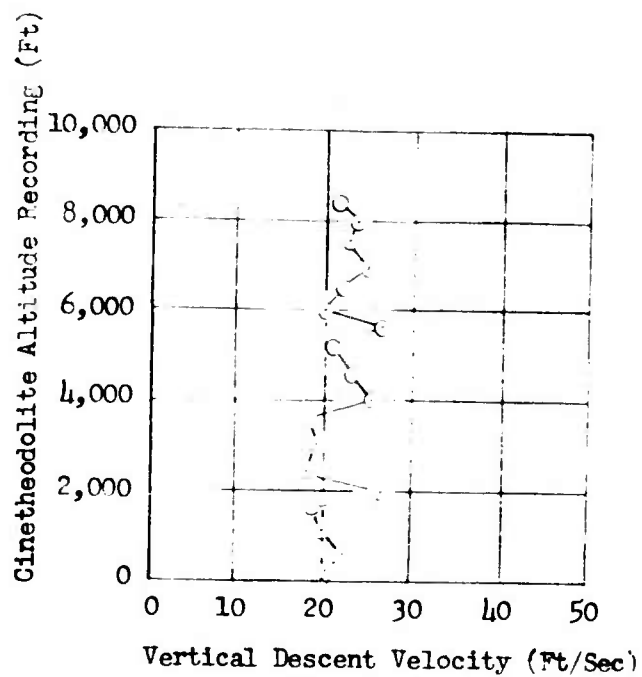
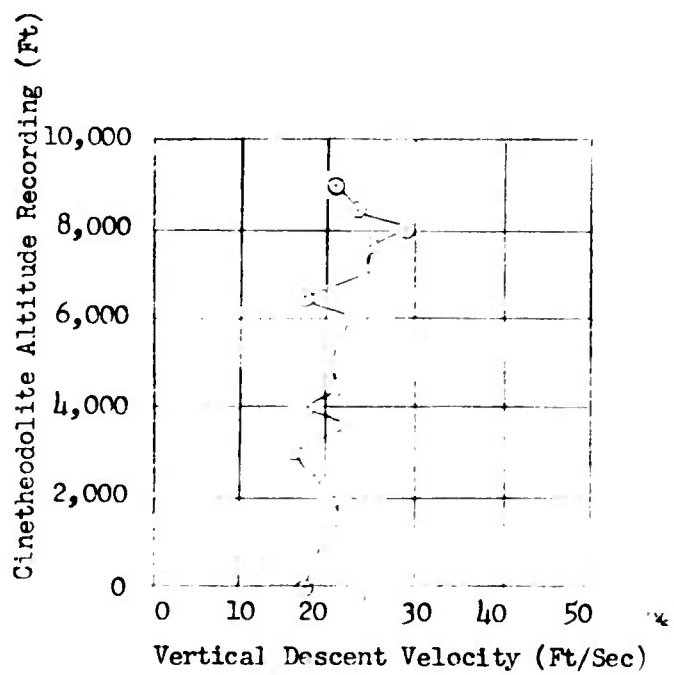


Figure 25. Parawing Performance Flight Test No. 327 L/D Performance Curve.



No. 326



No. 327

Figure 26. Vertical Descent Curves.



TABLE V. SUMMARY OF PRELIMINARY FLIGHT TESTS  
(8 JULY TO 9 AUGUST 1968)

No.	Flight	Parawing Type	Reefing	Notes
1	Trim	TCK <sup>a</sup>	Keels together	400# steel lines
2	Trim	SCK <sup>b</sup>	-	400# steel lines
3	Trim	HAR <sup>c</sup>	Keels together	480# steel lines
4	Trim	TCK	-	480# steel lines
5	Trim	SCK	-	480# steel lines
6	Trim	SCK	-	400# steel lines
7	Trim	TCK	-	480# steel lines
8	Trim	TCK	80% reefing line	Dummy, reefing delay failed
9	Trim	TCK	54" Snyder	Dummy, deployment good
10	Man	TCK	-	-
11	Man	TCK	-	-
12	Trim	TCK	4 sec aft 6-sec keels	500#
13	Trim	TCK	54" Snyder	Dummy
14	Trim	TCK	-	500#
15	Trim	TCK	-	Dummy
16	Trim	TK <sup>d</sup>	-	540#
17	Trim	SCK	-	Dummy
18	Man	TCK	-	-
19	Man	TCK	-	-
20	Trim	SCK	-	Dummy
21	Man	TCK	-	-
22	Man	TCK	-	-
23	Man	TCK	-	-
24	Man	SCK	-	-
25	Man	TCK	-	-
26	Man	TCK	-	-
27	Man	TCK	64" Snyder	10-15 sec disreef
28	Man	TCK	64" Snyder	7-10 sec disreef
29	Man	TCK	None	-
30	Man	SCK	64" Snyder	Less than 5 sec disreef
31	Man	TCK	64" Snyder	-
32	Man	TCK	54" Snyder	Less than 5 sec disreef
33	Man	TCK	-	-

<sup>a</sup> Twin-Catenary Keel  
<sup>b</sup> Single-Catenary Keel  
<sup>c</sup> High Aspect Ratio  
<sup>d</sup> Twin Keel

TABLE V - Continued

No.	Flight	Parawing Type	Reefing	Notes
34	Man	TCK	-	-
35	Man	TCK	-	-
36	Man	TCK	-	-
37	Man	TCK	-	-
38	Man	TCK	-	-
39	Man	SCK	-	-
40	Man	TCK	-	-
41	Man	SCK	-	-
42	Man	TCK	-	-
43	Man	TCK	-	-
44	Deploy	SCK	-	110 kn, steel lines
45	Deploy	TCK	Keels together	110 kn, steel lines, wing tore, static line
46	Deploy	TCK	Keels together	110 kn, steel lines, wing tore, static line
47	Man	TCK	64" Snyder	-
48	Man	TCK	64" Snyder	-
49	Man	TCK	-	-
50	Man	SCK	-	-
51	Deploy	TCK	Snyder + 6 sec	480#
52	Deploy	TCK	6 & 4	480#
53	Deploy	SCK	Snyder	400#, steel lines, payload strap broke
54	Man	TCK	-	-
55	Man	TCK	-	-
56	Man	SCK	Snyder	-
57	Man	TCK	-	-
58	Man	TCK	-	-
59	Man	SCK	-	-
60	Man	TCK	-	-
61	Man	TCK	-	-
62	Man	TCK	-	11 sec delay
63	Man	TCK	Hop & pop	-
64	Deploy	TCK	6 sec	110 kn, 500#
65	Deploy	TCK	6 sec	110 kn, 500#
66	Deploy	TCK	6 sec	110 kn, 300#
67	Deploy	SCK	-	30 kn
68	Deploy	SCK	-	30 kn, 500#
69	Deploy	TCK	-	30 kn, 500#, 10 sec to disreef
70	Deploy	SCK	-	30 kn, 500#, 6 sec to disreef
71	Deploy	-	-	30 kn, 500#
72	Deploy	TCK	-	110 kn, 600#, lost pay- load (release)

TABLE V - Continued

No.	Flight	Parawing Type	Reefing	Notes
73	Deploy	SCK	-	110 kn, 500#
74	Man	SCK	-	60 kn
75	Man	TCK	Snyder	60 kn
76	Deploy	SCK	-	130 kn, 500#
77	Deploy	TCK	-	130 kn, 500#
78	Man	SCK	-	-
79	Man	TCK	-	-
80	Deploy	SCK	-	150 kn, 300#
81	Deploy	TCK	-	150 kn, 300#
82	Deploy	TCK	2 sec	150 kn, 500#
83	Deploy	TCK	6 sec	150 kn, 500#
84	Man	TCK	-	-
85	Deploy	TCK	-	500#
86	Manual	TCK	-	160# lost payload (release failed)
87	Trim	TCK	-	100#
88	Manual	TCK	-	165#
89	-	-	-	No test
90	Manual	TCK	6 sec	360# control okay
91	Deploy	TCK	-	300#
92	Manual	TCK	-	360# rt control cable tangled
93	Deploy	TCK	-	300#
94	Manual	TCK	-	360# lt control cable tangled
95	Deploy	TCK	-	150 kn, 500#
96	Deploy	TCK	-	150 kn, 500#
97	Manual	TCK	-	60 kn, 360# control okay
98	Manual	TCK	-	60 kn, 360# control okay
99	Manual	TCK	-	-
100	Deploy	TCK	6 sec + 2 sec	150 kn, 500#
101	Deploy	TCK	6 + 2	500#, 150 kn
102	Manual	-	-	Inst. 165# 40 kn lt control cable tangled
103	Deploy	TCK	6 + 2	500#, 150 kn
104	Manual	TCK	6 + 2	500#, 150 kn lost pay- load (bolt sheared)
105	Man	-	-	-
106	Man	-	-	-
107	Man	-	-	-
108	Manual	-	Nose tuck	Inst. 165# 60 kn con- trol okay

TABLE VI. SUMMARY OF PRELIMINARY FLIGHT TESTS  
(10 SEPTEMBER TO 1 NOVEMBER 1968)

No.	Flight	Velocity (Kn)	Altitude (Ft)	Payload (Lbs)	Notes
101	Trim	40	2,000	300	-
102	Trim	40	2,000	-	Line tangled
103	Man	40	4,000	160	-
104	Manual Control	60	5,000	-	Lost payload
105	Trim	40	2,000	-	-
106	Manual Control	40	10,000	-	Violent drop from aircraft
107	Trim	-	2,000	300	-
108	Manual & Homing	-	5,500	500	50' from target
109	Trim	-	2,000	300	-
110	Homing	-	5,000	-	-
111	Trim	-	2,000	500	-
112	Homing	-	5,000	300	35' from target
113	Homing	-	7,000	500	Receiver battery dead
114	Homing	40	10,000	300	Line tangled
115	Trim	150	2,000	500	-
116	Homing	-	7,000	300	Antenna short - okay manual
117	Homing	-	7,000	300	300' from target
118	Homing	120	10,000	300	39' from target
119	Manual & Homing	120	10,000	500	70' from target on manual
120	Man	-	3,000	160	Reefing broke loose
121	Homing	-	7,500	300	417' from target
122	Homing	-	7,500	500	183' from target
123	Homing	40	7,000	-	Incomplete deployment
124	-	-	-	-	-
125	Homing	40	7,000	500	360' from target, rt turn cable broken
126	-	-	-	-	-
127	Homing	60	9,500	300	110' from target, 2-1/2 mi offset
128	-	-	-	-	No test
129	Manual & Homing	-	10,000	500	120' from target, manual (antenna open)
130	Homing	40	7,400	300	110' from target, lost payload
131	Homing	-	7,400	500	600', did not get fully back, lost payload
132	Homing	-	10,000	500	345'
133	Homing	-	7,000	500	54' (11,000' offset)
134	Homing	-	7,000	500	Lost payload

TABLE VI - Continued					
No.	Flight	Velocity (Kn)	Altitude (Ft)	Payload (Lbs)	Notes
135	Manual Control	-	7,000	500	58'
136	Manual Control	-	7,000	500	150'
137	Homing	120	15,000	-	Lost payload, strap broke
138	Homing	110	15,000	-	Lost payload
139	Homing	40	6,500	-	126'
140	Homing	-	10,000	500	Lost payload
141	Homing	120	10,000	-	Tore parawing, control box destroyed
142	Homing	-	8,000	500	Lost payload, damaged control box
143	Trim	70	2,500	-	Lost payload
144	Trim	80	2,500	-	-
145	Trim	150	2,500	-	-
146	Trim	150	2,500	-	-
147	Homing	120	3,000	-	Lost payload
148	Homing	40	6,500	-	120'
149	Homing	40	6,500	-	Tore wing
150	Trim	70	2,500	-	-
151	Trim	70	2,500	-	-
152	Trim	70	2,500	-	-
153	Trim	150	3,000	-	Line twisted
154	Homing	120	10,000	-	700' from target, 3-1/2 mi
155	Homing	120	10,000	-	450' from target
156	Trim	150	3,000	-	-
157	Homing	150	10,000	-	Antenna not open, line tangled
157a	Trim	150	3,000	-	Deployment malfunction
158	Trim	-	3,000	-	Tore deployment bag
158a	Homing	120	10,000	-	200' from target
159	Homing	120	10,000	-	No disreef
160	Homing	120	10,000	-	Dropped 6 mi away, landed 1-1/2 mi
161	Trim	150	15,000	-	Blew wing panel, 35 kn winds
162	Homing	120	10,000	-	No. 6 leading edge line broke, reefer tore
163	Homing	120	5,000	-	Slack control lines
164	Trim	40	2,500	-	-
165	Trim	40	2,500	-	-
166	Trim	40	2,500	500	-
167	Homing	40	7,000	-	Wing blew up
168	Trim	150	15,000	-	Okay
169	Trim	150	-	-	Okay

TABLE VI - Continued					
No.	Flight	Velocity (Kn)	Altitude (Ft)	Payload (Lbs)	Notes
170	Trim	150	3,000	-	Pilot chute broke loose
171	Homing	150	15,000	300	300' from 3 miles in cross wind
172	Homing	150	15,000	-	Pilot chute & wing broke
173	Homing	150	15,000	-	Manual control, one antenna gone
174	Reefing	75	5,000	-	Snyder + nose tuck, okay
175	Reefing	150	4,000	-	Snyder + nose tuck, okay
176	Reefing	150	4,500	-	Snyder + nose tuck, okay
177	Reefing	150	15,000	-	Snyder + nose tuck, okay
178	Homing	150	15,000	-	Control box destroyed tangled lines
179	Reefing	40	4,500	-	Snyder + nose tuck, 1950# shock load
180	Reefing	40	4,500	-	Snyder + nose tuck, 2200# shock load
181	Reefing	40	4,500	-	Snyder + nose tuck, 2400# shock load
182	Reefing	50	3,500	-	Zero reefing line, 3300# shock load

TABLE VII. CONTROL FLIGHT SUMMARY		
Date	Flight	Remarks
9-11-68	104 (5-1) *	Payload lost at deployment due to failure to bridle at the D ring
9-13-68	106 (5-2)	Deployment chute hangup on payload
9-16-68	108 (5-3)	Automatic home-to-target switched to manual to protect control box; wing out of trim; landing within 50' of target
9-17-68	110 (5-4)	Wing not quite in trim; 6" pull considered too great
9-17-68	112 (5-5)	Good flight within 35' of transmitter; automatic homing all the way; descent rate approximately 19 fps with 300# payload
9-18-68	113 (4-1)	Automatic homing good to approximately 1000' of target, then turned away from target; post flight check showed receiver battery low, 18.2 volts; descent rate 18 fps with 500# payload
9-18-68	114 (5-6)	Line tangled; system fell off backward in tight twist
9-18-68	116 (4-2)	Automatic homing did not function; manual control good; right antenna shorted to case
9-19-68	117 (4-3)	Automatic homing to 300' of target
9-19-68	118 (4-4)	Automatic homing to within 39' of transmitter, with 300# payload; descent rate 16 fps
9-18-68	119 (5-7)	Right turn in automatic mode, manual control to 70' of transmitter; flight 15 min from 10,000'; 12 fps descent rate, 300# payload
9-20-68	121 (4-5)	Good flight; 400' from target, 25 kn winds, 300# payload
9-20-68	122 (5-8)	Good flight; 180' from target
9-25-68	123 (4-6)	Instrumentation, right turn stall

TABLE VII - Continued		
Date	Flight	Remarks
9-25-68	125 (5-9)	Static line deployment from H-34; long and violent deployment; system homed well without right control, line broken; approximately 360' from target
9-26-68	127 (5-10)	Good flight to 110' from an altitude of 9500' and 13,000' up wind; descent rate approximately 20 fps
9-26-68	129 (4-7)	System did not automatically home, antenna open; manual control to 120' of target
9-26-68	130 (4-8)	Lost payload at deployment, homed to target with only the control box; landed within 110'; descent rate 6-7 fps
9-27-68	131 (5-11)	Automatic homing to within 600' of the target; lost payload, high cross winds
9-27-68	134 (5-12)	Payload strap broke and wrapped around the control lines
9-30-68	(4-9)	-
9-30-68	133 (4-10)	Homed to 54'; Fairchild 11,000' offset at 7,000'
9-30-68	135 (4-11)	Manual flight for Fairchild 58' from transmitter, 500# payload
9-30-68	136 (4-12)	Manual flight for Fairchild 150' from transmitter, 500# payload; displayed good wind penetration
10-01-68	137 (4-13)	Automatic home to 250'
10-01-68	138 (5-13)	Lost payload, bridle tangled control line
10-01-68	139 (4-14)	Automatic home to 126'
10-02-68	140 (4-15)	Quick release malfunction, homes with control box
10-03-68	141 (4-16)	Destroyed control box



TABLE VII - Continued		
Date	Flight	Remarks
10-03-68	142 (5-14)	Damaged control box
10-08-68	147 (4a-17)	Lost payload, homes with just control box
10-08-68	148 (5-15)	Automatic home, 120'
10-08-68	149 (5-15)	Field repack; wing ripped in half; descent rate 72 fps
10-11-68	154 (4a-18)	Dropped at 20,000'; offset at 10,000' altitude
10-10-68	155 (5a-16)	Deployed at 10,000' and 120 kn, 4 mi up wind from target, a few right turns at deployment; the homing alignment was within an angle of +15°; packaged loss carrier disconnected, came straight to target; when within 200' of target at approximately 1000', it went into a right turn stall; package damaged upon impact
10-11-68	157 (5a-17)	Line tangled during deployment, could not control
10-15-68	158 (4a-20)	Deployed 10,000' at 120 kn, 4-1/2 mi from target; homed to target, passed over the XMTR turn at approximately 250' and made a gentle turn into wind; load landing was very gentle upon release of load; control package damaged upon landing
10-16-68	159 (4a-21)	Parawing did not deploy; deployment reefer tied off with 550# cord
10-16-68	160 (5a-21)	Parawing flew well as reported by helicopter crew; C-130 drop at least 8 mi from target or 3 mi beyond the selected release point at 10,000'; package fell 1.5 mi short of target
10-17-68	162 (4a-22)	Wing torn apart; tape held the antenna closed
10-18-68	163 (4-23)	Slack control lines; lost carrier could not overcome slack; good deployment and stable flight

TABLE VII - Continued

Date	Flight	Remarks
10-22-68	167 (4a-24)	The wing was destroyed at deployment; the control system was a total loss
10-24-68	171 (5a-19)	Deployed at 15,000' at 150 kn with 300# payload, 3 mi from target and cross wind; good flight; came over the target and landed within 300'; attempt was made to measure turning radius for 2-1/2" pull-in with T.V. coverage
10-25-68	172 (3-1)	Deployed at 15,000' at 150 kn; the deployment chute separated without retracting the deployment bag; wing worked its way out of the bag at approximately 5000'; the wing tore up, the streamer and sandy area saved the package
10-25-68	173 (5a-20)	Deployed at 15,000' at 150 kn; no automatic control, package found with one antenna missing; assumed lost at deployment; wing operated with a built-in left turn; it appeared that the degree of left turn could be controlled manually
10-30-68	178 (3-2)	Retainer strap used to hold the parawing to the control box was tangled in the control lines; control box was destroyed
<p>*(5-1): The first number is the control system S/N; the second number is the flight number on that control box.</p> <p>Example: (4-3) indicates third flight with control box S/N 4.</p>		

TABLE VIII. PERFORMANCE CALCULATIONS - PARAWING SYSTEM WITH DROGUE		
Time (Sec)	Altitude Loss	Total Altitude Loss (Ft)
0	Launch 20' free fall, drogue riser pays out	
1.12	Drogue Inflated 124' drogue operation	20
3.12	Deploy Parawing 79' wing line stretch	144
3.60	Wing Reefed 210'	223
5.6	Initiate Disreefing 77'	433
7.0	Wing at Terminal Velocity	510

TABLE IX. REEFING AND DEPLOYMENT TECHNIQUES					
Test No.	Altitude (Ft)	Velocity (Kn)	Configuration *	Aircraft	Notes
1	3,000	40	A	Helicopter	Instrumentation: Brinell block, T.V., film  Objective: Determine desired fixed turn radius; evaluate packaging, reefing, and deployment techniques
2	3,000	40	B	Helicopter	
3	3,000	40	C	Helicopter	
4	3,000	40	D	Helicopter	
5	3,000	40	E	Helicopter	
6	3,000	40	F	Helicopter	
7	3,000	40	G	Helicopter	
8	3,000	40	H	Helicopter	
9	3,000	80	A	Helicopter	Instrumentation: Brinell block, instrumentation unit, T.V., film  Objective: Verify rigging and packaging configuration; determine calibration correlation between Brinell block and instrumentation; determine accuracy of load predictions; evaluate packaging, reefing, and deployment techniques
10	3,000	80	B	Helicopter	
11	3,000	80	C	Helicopter	
12	3,000	80	D	Helicopter	
13	3,000	80	E	Helicopter	
14	3,000	80	F	Helicopter	
15	3,000	80	G	Helicopter	
16	3,000	80	H	Helicopter	
17	3,000	120	A	C-130	Instrumentation: Brinell block, T.V., film  Objective: Evaluate packaging, reefing, and deployment techniques; determine accuracy of predictions
18	3,000	120	B	C-130	
19	3,000	120	C	C-130	
20	3,000	120	D	C-130	
21	3,000	120	E	C-130	
22	3,000	120	F	C-130	
23	3,000	120	G	C-130	
24	3,000	120	H	C-130	

TABLE IX - Continued

Test No.	Altitude (Ft)	Velocity (Kn)	Configuration*	Aircraft	Notes
25	5,000	120	A	C-130	Objective: Confirm selected configurations
26	10,000	120	A	C-130	
27	15,000	120	A	C-130	
28	5,000	120	B	C-130	
29	10,000	120	B	C-130	
30	15,000	120	B	C-130	
* Configurations A, B, C, D, E, F, G, and H are each one of eight possible combinations of the following: Deployment Bag, Deployment Sleeve, Drogue Chute, No-Drogue Chute, Reefing Method No. 1, and Reefing Method No. 2.					

TABLE X. CONTROL SYSTEM TESTS									
Test No.	Altitude (K Ft)	Velocity (Kn)	Payload Weight (Lbs)	Total Suspension Weight (Lbs)	Control Cable Pull-In			Flight Plan and Objectives	
					Auto Homing	Manual	Loss Carrier		
31	0.5	150	500	565	Dummy Control System			Launch over drop area with built-in 1" turn	
32	0.5	150	300	365	Dummy Control System			Launch over drop area with built-in 1" turn	Objectives: 3,4
33	10	50	A21 100	165	1.5	1.5	None	Launch 3 mi up wind; auto home for 3 min; command 720° right and left turn; command homing to impact	Objectives: 3,4
34	10	100	A21 300	365	1.5	1.5	None	Launch 3 mi up wind; auto home for 3 min; command 720° right and left turn; auto home to impact	Objectives: a,c,h,l; 1,2,3,6,9
								Launch 3 mi up wind; auto home for 3 min; command 720° right and left turn; auto home to impact	Objectives: a,c,h,m; 1,2,3,9,10

TABLE X - Continued									
Test No.	Altitude (K Ft)	Velocity (Kn)	Payload Weight (Lbs)	Total Suspension Weight (Lbs)	Control Cable Pull-In			Flight Plan and Objectives	
					Auto Homing	Manual	Loss Carrier		
35	10	50	A21 420	565	1.5	1.5	1.5	Launch 3 mi up wind; auto home for 3 min; command 720° right and left turn; auto home to impact	
36	10	150	A21 100	165	3.0	3.0	None	Objectives: a,b,c,d,e,f,h, j,m; 1,2,3,9,10 Launch 3 mi up wind; auto home for 3 min; command 720° right and left turn; auto home to impact	
37	10	100	A21 300	365	3.0	3.0	None	Objectives: a,c,h,m; 1,2,3, 7,9,10 Launch 3 mi up wind; auto home for 3 min; command 720° right and left turn; command home to impact	
38	10	50	A21 420	565	3.0	3.0	3.0	Objectives: a,c,h,l; 1,2,3, 6,7,9 Launch 3 mi up wind; auto home for 3 min; command 720° right and left turn; auto home to impact	

TABLE X - Continued

TABLE X - Continued								
Test No.	Altitude (K Ft)	Velocity (Kn)	Payload Weight (Lbs)	Total Suspension Weight (Lbs)	Control Cable Pull-In			Flight Plan and Objectives
					Auto Homing	Manual	Loss Carrier	
ESTIMATED VALUE - Pullin to be Determined from above Tests								
39	10	50	A21 20	165	4.0 2.25	4.0 2.25	4.0 2.25	Objectives: a,b,c,d,e,f,h, j,m; 1,2,3,7,9,10  Launch 3 mi up wind; auto home for 3 min; command 720° right and left turn; auto home to impact
40	10	50	A21 220	365	4.0 2.25	4.0 2.25	4.0 2.25	Objectives: a,b,c,d,e,f,h, j,m; 1,2,3,5,7,9,10  Launch 3 mi up wind; auto home for 3 min; command 720° right and left turn; auto home to impact
41	10	50	A21 120	565	4.0 2.25	4.0 2.25	4.0 2.25	Objectives: a,b,c,d,e,f,h, j,m; 1,2,3,5,7,9,10  Launch 3 mi up wind; auto home for 3 min; command 720° right and left turn; command home to impact
								Objectives: a,b,c,d,e,h,i, j,l; 1,2,3,5,6,7,9



TABLE X - Continued							
Test No.	Altitude (Y Ft)	Velocity (Kts)	Payload Weight (Lbs)	Suspension Weight (Lbs)	Control Cable Pull-In		Flight Plan and Objectives
					Auto Homing	Loss Carrier	
Review data and establish firm control cable pull-in settings							
42	5	50	420	565	Use established values		Launch directly over or near target transmitter, command, and auto home to impact; pass over transmitter many times
							Objectives: b,g,f,i,j,k; 3, 6,7,9
43	10	100	300	365	Use established values		Launch 4 mi up wind; auto home to impact
							Objectives: f,m; 3,4,8,10
44	10	100	420	565	Use established values		Launch 1 mi down wind; auto home to impact
							Objectives: b,c,d,e,f,m; 3,4,8,9,10
45	10	150	420	565	Use established values		Launch 1 mi down wind; manual home to impact
							Objectives: b,g,k,l; 3,4, 6,8,6,8
Note: Manual control may be used as necessary for final landing during any test in order to land the system up wind.							

## CACS TEST OBJECTIVES FOR TABLES X AND XI

### Performance Data Oriented Test Objectives

- a. Turn rate, roll angle, and turn diameter versus control cable pull-in and total suspended weight
- b. Determine control line forces versus control cable pull-in and total suspended weight
- c. Automatic homing turn angle versus control cable pull-in and total suspended weight
- d. Automatic homing duty cycle versus control cable pull-in and total suspended weight
- e. Proportional homing capability - Measure the receiver proportional outputs differential signal versus time to determine the system improvement and proportional time constants
- f. Determine time constants of lost subcarrier to automatic homing turns
- g. Determine time constants of lost subcarrier to command turns
- h. Determine the effects of payload size
- i. Determine characteristics of transmitter cone of silence
- j. Determine the effects of depression angles (26 to 90 degrees)
- k. Evaluate the apparent constant right turn over target
- l. Determine command homing capability
- m. Determine automatic homing capability

### Contract Performance Oriented Test Objectives

1. 300- and 500-pound payload with no rigging changes (100 to 500 design goal)
2. L/D of 1.8 to 1 (2.4 to 1 design goal)
3. 500- to 30,000-foot operation
4. 0- to 150-knot operation
5. 100-foot turn radius capability

6. 100-foot radius landing with command control
7. Vertical descent rate at impact of 25 feet per second or less
8. Mission duration
9. Automatic homing battery life of 45 minutes
10. Design goal of 200 feet CEP with 15-knot wind in the automatic homing mode

TABLE XI. RELIABILITY TESTS

Test No.	Altitude (K Ft)	Velocity (Kn)	Payload Weight (lbs)	Total Suspension Weight (lbs)	Data	Flight Plan and Objectives (See CACS Test Objectives)
46	0.5	50	300	365	Film	Launch over target transmitter; auto home to impact  Objectives: 1,2,3,4,8,9,10
47	0.5	50	300	565	Film	Launch over target transmitter; auto home to impact  Objectives: 1,2,3,4,7,8,9,10
48	5	100	500	565	Film	Launch 1 mi up wind; command home to target  Objectives: 1,3,4,5,6,7
49	5	150	300	365	Film	Launch 2 mi up wind; command home to target  Objectives: 1,3,4,5,6
50	5	150	420	565	Instrumentation No. 2, Film	Launch 1 mi down wind; auto home to impact  Objectives: 1,2,3,4,7,8,9,10
51	10	100	500	565	Film	Launch 3 mi up wind; auto home to impact  Objectives: 1,2,3,4,7,8,9,10

TABLE XI - Continued

Test No.	Altitude (K Ft)	Velocity (Kn)	Weight (Lbs)	Total Suspension Weight (Lbs)	Data	Flight Plan and Objectives (See CACS Test Objectives)
52	10	150	300	365	Film	Launch 3 mi up wind; command home to impact  Objectives: 1,3,4,5,6
53	10	150	500	565	Film	Launch over target; command to 1 mi from target; auto home to impact  Objectives: 1,2,3,4,5,7
54	15	150	300	365	Film	Launch 2 mi down wind; auto home to impact  Objectives: 1,2,3,4,7,8,9,10
55	15	150	500	565	Film	Launch 6 mi up wind; command home to impact  Objectives: 1,3,4,5,6
56	15	150	420	565	Instrumentation No. 2, Film	Launch 6 mi up wind; auto home to impact  Objectives: 1,2,3,4,7,8,9,10

Note: Control cable pull-in established in tests conducted in Table I.

TABLE XII. INSTRUMENTATION TEST SETUPS AND DATA ITEMS		
	Channel	Data
Test Setup No. 1	1	Front suspension tie point load
	3	Aft suspension tie point load
	5	Left suspension tie point load
	7	Right suspension tie point load
	9	Vertical axis acceleration
Test Setup No. 2	1	Servo amplifier input signal
	3	Servo actuator feedback signal
	5	Left control line loading
	7	Right control line loading
	9	Receiver proportional differential signal
	13	Receiver AGC voltage
	11	PAM (Pulse Amplitude Modulation - sampled signals)
	1	Command right turn relay K1
	2	Command left turn relay K2
	3	Lost subcarrier relay K3
	4	Receiver battery voltage
	5	Servo battery voltage
	6	Regulated power voltage (22 VDC)
	7	Accelerometer (either axis)
	8	Spare
	9	Lost subcarrier relay K3
	10	Suspension load
	11	Suspension load
	12	Suspension load
	13	Suspension load
	14	Spare
	15	Lost subcarrier relay K3
	16	Instrumentation regulated power voltage (5 VDC)
		Marker instrumentation battery voltage

TABLE XIII. FLIGHT TEST SUMMARY AND INDEX						
Flight No.	Deployment Altitude (Ft)	Deployment Velocity (KIAS)	Type of Test			CEP
			Trim	Deployment	Control	
201	3,000	40		x		
202	3,000	40		x		
203	3,000	40		x		
204	3,000	80		x		
205	3,000	40		x		
206	3,000	40		x		
207	3,000	40		x		
208	3,000	80		x		
209	3,000	40		x		
210	3,000	120		x		
211	3,000	40		x		
212	3,000	80		x		
213	3,000	60		x		
214	3,000	80		x		
215	3,000	120		x		
216	3,000	120		x		
217	3,000	80		x		
218	3,000	120		x		
219	3,000	120		x		
220	3,000	120		x		
221	3,000	120		x		
222	3,000	120		x		
223	3,000	120		x		
224	3,000	80		x		
225	3,000	80		x		
226	3,000	80		x		
227	3,000	80		x		
228	3,000	40		x		
229	3,000	80		x		

TABLE XIII - Continued

Flight No.	Deployment Altitude (Ft)	Deployment Velocity (KIAS)	Type of Test			
			Trim	Deployment	Control	Reliability CEP
230	5,000	120		x		
231	5,000	120		x		
232	10,000	120		x		
233	10,000	120		x		
234	15,000	120		x		
235	15,000	120		x		
236	500	0		x		
237	5,000	150		x		
238	10,000	150		x		
239	15,000	150		x		
240	10,000	50		x		
241	10,000	50			x	
242	10,000	50			x	
243	10,000	50			x	
244	10,000	50			x	
245	10,000	50			x	
246	10,000	50			x	
247	10,000	50			x	
248	10,000	50			x	
249	10,000	50			x	
250	2,500	50			x	
251	2,500	50	x			
252	2,500	60	x			
253	2,500	80	x			
254	9,500	50				x
255	2,500	80	x		x	
256	2,500	80	x			
257	2,500	80	x			
258	2,500	80	x			
259	2,500	80	x			



TABLE XIII - Continued						
Flight No.	Deployment Altitude (ft)	Deployment Velocity (KIAS)	Type of Test			CEP
			Trim	Deployment	Control	Reliability
260	7,500	50			x	x
261	7,500	50			x	x
262	2,500	80				
263	2,500	80	x			
264	2,500	80	x			
265	2,500	80	x			
266	1,000	150				
267	2,500	80	x		x	x
268	2,500	80	x			
269	2,500	80	x			
270	2,500	80	x			
271	2,500	80	x			
272	2,500	80	x			
273	2,500	80	x			
274	2,500	80	x			
275	2,500	90	x			
276	2,500	80	x			
277	2,500	80	x			
278	2,500	80	x			
279	2,500	80	x			
280	2,500	80	x			
281	10,000	150				
282	10,000	150			x	x
283	10,000	120			x	x
284	2,500	80			x	x
285	2,500	80	x			
286	10,000	80	x			
287	10,000	80			x	x
288	2,500	80			x	x
289	2,500	80	x			

TABLE XIII - Continued						
Flight No.	Deployment Altitude (ft)	Deployment Velocity (KIAS)	Type of Test			
			Trim	Deployment	Control	Reliability CEP
290	2,500	80				
291	10,000	120	x			
292	7,500	80				
293	2,500	80			x x	
294	10,000	80	x			
295	10,000	120			x x	
296	2,500	80				
297	7,500	80	x			
298	7,500	80				
299	10,000	80			x x	
300	10,000	80			x x	
301	7,500	80			x x	
302	7,500	80			x x	
303	7,500	80			x x	
304	15,000	150			x x	x x x x x x x
305	15,000	150			x x	
306	15,000	150			x x	
307	7,500	80			x x	
308	15,000	150			x x	
309	5,000	80				
310	5,000	80			x x	
311	2,500	80				
312	15,000	150				
313	15,000	150				
314	2,500	80				
315	7,500	80				
316	7,500	80				
317	15,000	150			x x	
318	15,000	150				
319	15,000	150				

TABLE XIII - Continued						
Flight No.	Deployment Altitude (Ft)	Deployment Velocity (KIAS)	Type of Test			
			Trim	Deployment	Control	Reliability CEP
320	15,000	150		x	x	x
321	20,000	150		x	x	x
322	24,000	150		x	x	x
323	15,000	150			x	x
324	15,000	150			x	x
325	7,500	80			x	x
326	10,000	80			x	x
327	10,000	80			x	x
328	7,500	80			x	x
329	12,000	150			x	x
330	9,700	150			x	x
331	15,000	150			x	x
332	15,000	150			x	x
333	15,000	150			x	x
334	15,000	150			x	x
335	15,000	150			x	x

TABLE XIV. DEPLOYMENT TESTS SUMMARY

Test No.	Altitude (Ft)	Velocity (KIAS)	Pack	Reefing Line (Lbs)	Nose Tuck	Wing Time Delay (Sec)	Drogue Time Delay (Sec)	Brinell Load (Lbs)	Comments
201	3,000	40	Sleeve	1,000	Full	4	-	3,700	Dummy control box
202	3,000	40	Sleeve	1,000	1/2	4	-	3,000	Dummy control box
203	3,000	40	Sleeve	1,000	3/4	4	-	2,250	Dummy control box
204	3,000	80	Sleeve	1,000	3/4	4	-	3,700	Instrumentation box
205	3,000	40	Bag	1,000	3/4	4	-	2,700	Dummy control box
206	3,000	40	Bag	1,000	1/2	4	-	1,500	Dummy control box; Brinell block had 1500- and 1600-lb depressions
207	3,000	40	Sleeve	1,000	1/2	2	2	3,200	Dummy control box
208	3,000	80	Bag	1,000	3/4	4	-	1,900	Instrumentation box
209	3,000	40	Bag	1,000	1/2	2	2	3,000	Dummy control box
210	3,000	120	Sleeve	1,000	3/4	4	-	3,700	Dummy control box
211	3,000	40	Bag	1,000	3/4	2	2	3,000	Dummy control box
212	3,000	80	Bag	1,000	1/2	2	2	3,300	Instrumentation box
213	3,000	60	Sleeve	1,000	3/4	2	2	3,700	Dummy control box

TABLE XIV - Continued

Test No.	Altitude (Ft)	Velocity (KIAS)	Pack	Reefing Line (Lbs)	Nose Tuck	Wing Time Delay (Sec)	Drogue Time Delay (Sec)	Brinell Load (Lbs)	Comments
214	3,000	80	Sleeve	1,000	3/4	2	2	4,200	Instrumentation box
215	3,000	120	Bag	1,000	3/4	4	-	2,700	Dummy control box
216	3,000	120	Sleeve	1,000	1/2	4	-	7,200	Dummy control box, reefing line broke
217	3,000	80	Sleeve	1,000	1/2	2	2	7,200	Instrumentation box, reefing line broke
218	3,000	120	Sleeve	1,000	1/2	2	2	7,000	Dummy control box, reefing line broke
219	3,000	120	Bag	1,000	1/2	4	-	8,400	Dummy control box, reefing line broke
220	3,000	120	Sleeve	2,000	3/4	2	2	5,800	Dummy control box
221	3,000	120	Bag	2,000	3/4	2	2	5,800	Dummy control box
222	3,000	120	Bag	2,000	1/2	2	2	4,400	Dummy control box
223	3,000	120	Sleeve	2,000	1/2	2	2	5,400	Dummy control box
224	3,000	80	Bag	2,000	1/2	4	-	3,600	Instrumentation box
225	3,000	80	Bag	2,000	1/2	2	2	3,000	Instrumentation box, drogue cutter failed

TABLE XIV - Continued									
Test No.	Altitude (Ft)	Velocity (KIAS)	Pack	Reefing Line (Lbs)	Nose Tuck	Wing Time Delay (Sec)	Drogue Time Delay (Sec)	Brinell Load (Lbs)	Comments
226	3,000	80	Bag	2,000	1/2	2	2	3,700	Instrumentation box
227	3,000	80	Sleeve	2,000	1/2	2	2	2,400	Dummy control box
228	3,000	40	Bag	2,000	1/2	4	-	2,700	Dummy control box
229	3,000	80	Bag	2,000	3/4	2	2	3,700	Instrumentation box
230	5,000	120	Bag	2,000	3/4	4	-	3,700	Dummy control box
231	5,000	120	Sleeve	2,000	3/4	4	-	4,000	Dummy control box
232	10,000	120	Bag	2,000	3/4	4	-	3,700	Dummy control box
233	10,000	120	Sleeve	2,000	3/4	4	-	5,000	Dummy control box
234	15,000	120	Bag	2,000	3/4	4	-	4,000	Dummy control box
235	15,000	120	Sleeve	2,000	3/4	4	-	3,000	Dummy control box
236	500	0	Bag	2,000	3/4	4	-	3,000	Dummy control box
237	5,000	150	Bag	2,000	3/4	4	-	3,700	Dummy control box
238	10,000	150	Bag	2,000	3/4	4	-	4,500	Dummy control box
239	15,000	150	Bag	2,000	3/4	4	-	3,000	Dummy control box
304	15,000	150	Bag	2,000	3/4	4	-	4,450	Control flight

TABLE XIV - Continued

Test No.	Altitude (Ft)	Velocity (KIAS)	Pack	Reefing Line (Lbs)	Nose Tuck	Wing Time Delay (Sec)	Drogue Time Delay (Sec)	Brinell Load (Lbs)	Comments
305	15,000	150	Bag	2,000	3/4	4	-	3,700	Control flight
306	15,000	150	Bag	2,000	3/4	4	-	7,200	Control flight - control box broke apart on wing opening; reefing line broke
308	15,000	150	Bag	2,000	3/4	4	-	5,000	Dummy control box
311	2,500	80	Bag	2,000	3/4	4	-	2,200	Dummy control box - reefing rings on canopy keel at trailing edge
312	15,000	150	Bag	2,000	3/4	4	-	8,600	Dummy control box - reefing line broke, rings on keel trailing edge tore off
313	15,000	150	Bag	4,000	3/4		-	6,100	Dummy control box - keel trailing edge rings broke
317	15,000	150	Bag	4,000	3/4		-	3,700	Dummy control box
318	15,000	150	Bag	4,000	3/4	6	-	5,700	Dummy control box
319	15,000	150	Bag	4,000	3/4	6	-	3,700	Dummy control box

TABLE XIV - Continued									
Test No.	Altitude (Ft)	Velocity (KIAS)	Pack	Reefing Line (Lbs)	Nose Tuck	Wing Time Delay (Sec)	Drogue Time Delay (Sec)	Brinell Load (Lbs)	Comments
20	15,000	150	Bag	4,000	3/4	6	-	6,100	Control flight, reliability
321	20,000	150	Bag	4,000	3/4	4	-	5,700	Control flight, reliability
322	24,000	150	Bag	4,000	3/4	4	-	6,100	Control flight



TABLE XV. CACS DEPLOYMENT TEST SUMMARY (3000-FT ALTITUDE)						
Test No.	Reefing Nose Tuck	Deployment System		Velocity (Kn)	Drogue	Remarks
		Bag (lbs)	Sleeve (lbs)			
201	Full	-	3700	40	No	-
203	3/4	-	2250	40	No	-
205	3/4	2700	-	40	Yes	-
211	3/4	3000	-	40	Yes	-
213	3/4	-	3700	80	No	Instrumentation 3700# at disreefing
204	3/4	1900	3700	80	No	Instrumentation 3700# at disreefing
208	3/4	-	-	80	Yes	-
214	3/4	3700	4200	120	No	-
229	3/4	-	3700	120	Yes	-
210	3/4	2700	3700	120	No	-
215	3/4	-	-	120	Yes	2000# reefing line
220	3/4	5800	5800	40	No	2000# reefing line
221	1/2	-	3000	40	No	-
202	1/2	2700	-	40	Yes	-
228	1/2	1500	-	40	Yes	Wing did not disreef
206	1/2	-	3200	80	No	Instrumentation
207	1/2	-	3000	80	No	Instrumentation
209	1/2	3600	3300	80	No	Instrumentation
212	1/2	-	-	80	No	Instrumentation
224	1/2	-	-	80	No	Instrumentation

TABLE XV - Continued

Test No.	Reefing Nose Tuck	Deployment System			Velocity (Kn)	Drogue	Remarks
		Bag (lbs)	Sleeve (lbs)				
227	1/2	-	2400		80	Yes	Instrumentation
217		-	7200				-
226		3700	-				-
216	1/2	-	7200		120	No	No. 6 keel line and 1000# reefing line broke
219		8400	-				-
223	1/2	-	5400		120	Yes	1000# reefing line broke
218		-	7000				-
222		4400	-				-

TABLE XVI. CACS DEPLOYMENT TEST LOAD SUMMARY  
(3/4 TUCK - NO DROGUE)

Test No.	Deployment System		Velocity (Kn)	Altitude (Ft)
	Bag (Lbs)	Sleeve (Lbs)		
210	-	3700	120	3,000
215	2700	-	120	3,000
231	-	4000	120	5,000
230	3700	-	120	5,000
233	-	5000	120	10,000
232	3700	-	120	10,000
235	-	3000	120	15,000
234	4000	-	120	15,000
237	3700	-	150	5,000
238	4500	-	150	10,000
239	3000	-	150	15,000

TABLE XVII. CACS DEPLOYMENT TEST LOAD SUMMARY  
(3/4 TUCK - NO DROQUE)

Test No.	Deployment System (Bag - Lbs)	Reefing Line (Size - Lbs)	Velocity (Kt)	Altitude (Ft)	Remarks
265	-	1900	150	10,000	-
281	-	1900	150	10,000	-
282	-	1900	150	10,000	Reefing line broke or failed, Nos. 23 and 24 lines broke
304	4450	1900	150	15,000	-
305	3650	1900	150	15,000	-
306	7200	1900	150	15,000	Reefing line broke or failed; No. 6 line broke
308	5300	1900	150	15,000	Line No. 18 broke
311	2200	1900	80	2,500	-
312	8600	1900	150	15,000	Reefing line broke
313	6100	4000	150	15,000	Reefing line not cut per test setup; No. 18 line broke
317	3700	4000	150	15,000	No cutter; everything ok
318	5700	4000	150	15,000	6-sec cutter
319	3700	4000	150	15,000	6-sec cutter

TABLE XVII - Continued					
Test No.	Deployment System (Bag - Lbs)	Reefing Line (Size - Lbs)	Velocity (Kn)	Altitude (Ft)	Remarks
320	6100	4000	150	15,000	6-sec cutter; control impact 180'
321	5700	4000	150	20,000	Impact 250'; 4-sec cutters
322	6100	4000	150	24,000	4-sec cutters
323	4400	4000	150	15,000	-
324	5300	4000	150	15,000	-

TABLE XVIII. CONTROL SYSTEM TEST SUMMARY						
Test No.	Drop Altitude (Ft)	Velocity (KIAS)	Drop Point (Mi)	Impact Point	Control Mode	Comments
240	10,000	50	-	1300' short	Auto & man.	Loss carrier 0", auto 1-l/2", man. 1-l/2", calm
241	10,000	50	-	2500' short	Auto & man.	Loss carrier 0", auto 3", man. 3"
242	10,000	50	-	1000' short	Auto & man.	Loss carrier, 1-l/2", auto 1-l/2", man. 1-l/2"; 15-20 kn surface wind
243	10,000	50	-	750' down wind	Auto & man.	Loss carrier 0", auto 3", man. 3"; 5-10 kn surface wind
244	10,000	50	-	2.5 mi	-	Loss carrier 3", auto 3", man. 3"; no control; reason unknown; right turn to impact
245	10,000	50	-	1300'	-	Loss carrier 0", auto 1-l/2", man. 1-l/2"; right control cable broken at deployment, payload/control box collision; no right control
246	10,000	50	-	1500'	Auto & man.	Loss carrier 1", auto 2-l/2", man. 2-l/2"; inducing man. right turn (3000') resulted in right turn spiral to impact, 20 kn surface
247	10,000	50	-	-	-	Loss carrier 1", auto 2-l/2", man. 2-l/2"; no control, antenna not released

TABLE XVIII - Continued						
Test No.	Drop Altitude (Ft)	Velocity (KIAS)	Drop Point (Mi)	Impact Point	Control Mode	Comments
248	10,000	50	-	-	Auto & man.	Loss carrier 1", auto 2-1/2", man. 2-1/2"; payload quick disconnect at deployment; all controls ok but unable to reach XMTR
249	10,000	50	-	-	-	Loss carrier 0", auto 2-1/2", man. 2-1/2"; right turn spiral to impact; no noticeable control in any mode
254	9,500	50	-	-	Auto & man.	Loss carrier 1", auto 2-1/4", man. 2-3/4"; all control functions good
260	7,500	50	-	-	Auto & man.	Loss carrier 1", auto 2-1/4", man. 2-3/4"; all controls ok; Fairchild run
261	7,500	50	-	-	Auto & man.	Loss carrier 1", auto 2-1/4", man. 2-3/4"; all controls ok; Fairchild run
265	10,000	150	1.5 up wind	150 yds down wind	Auto & man.	Loss carrier 1", auto 2-1/4", man. 2-3/4"; all controls ok; 24-kn wind at 2000'; 10-15-kn surface wind
281	10,000	150	-	-	-	Loss carrier 1", auto 2-1/4", man. 2-3/4"; deployment good and trim; good, but no control due to failure of new antenna release mechanism

TABLE XVIII - Continued						
Test No.	Drop Altitude (Ft)	Velocity (KIAS)	Drop Point (Mi)	Impact Point	Control Mode	Comments
282	10,000	150	-	-	-	Lines 23 and 24 broken at deployment due to premature disreefing
283	10,000	120	-	-	Auto	Good homing, swing angle = 40°; control lines 1-1/4" off on post flight check
286	10,000	80	4.0	100 yds	Auto	Loss carrier 1", auto 2-1/4", man. 2-3/4"; 8-10-kn surf wind, good wind penetration; accepted as reliability flight
287	10,000	80	3.5 up wind	-	Auto	Loss carrier 1", auto 2-1/4", man. 2-3/4"; good homing, but turns had too large a radius over XMTR at 3500'
291	10,000	120	3.5 up wind	200 yds	Auto	Loss carrier 1", auto 2-1/4", man. 2-3/4"; good homing, over at 3000'; turns not tight enough
292	7,500	90	2.5 up wind	60 yds	Auto	Loss carrier 2", auto 3", man. 3-1/2"; good homing flight
294	10,000	80	3 up wind	500' down wind	Auto & man	Loss carrier 1", auto 2-1/4", man. 2-3/4"; good homing; 360° right turn not timed, 360° left turn in 17 sec; turns not tight enough



TABLE XVIII - Continued						
Test No.	Drop Altitude (Ft)	Velocity (KTAS)	Drop Point (Mi)	Impact Point	Control Mode	Comments
295	10,000	120	-	0.2 mi down wind	Auto & man.	Loss carrier 1", auto 2-1/4", man. 2-3/4"; built-in left turn resulted in poor homing control; high winds at 2000-3000'
297	7,500	80	1.5 up wind	50' up wind	Auto	Loss carrier 1", auto 2-1/4", man. 2-3/4"; turns too tight, nearly 180° turns (left to right) during homing; good behavior near XWTR; wing forward velocity 44 fps
298	7,500	80	1 up wind	100'	Auto & man.	Loss carrier 1", auto 2-1/4", man. 2-3/4"; good homing; man. turns of 17-22 sec
299	10,000	80	2.5 cross wind	0.3 mi down wind	Auto	Loss carrier 1", auto 2-1/4", man. 2-3/4"; good homing; passed XWTR and could not penetrate wind, 15-20 kn surface
300	10,000	80	4 up wind	1 mi up wind	Auto	Loss carrier 2-3/4", auto 2-1/4", man. 2-3/4"; homed away from XWTR, could not make up altitude loss when homing well
301	7,500	80	1.5 up wind	100 yds down wind	Auto & man.	Loss carrier 2-3/4", auto 2-1/4", man. 2-3/4"; swing angle approximately 40° in auto; turned to man. mode to increase glide capability, then back to auto

TABLE XVIII - Continued						
Test No.	Drop Altitude (Ft)	Velocity (KIAS)	Drop Point (Mi)	Impact Point	Control Mode	Comments
302	7,500	80	1.5 down wind	20' left cross wind	Auto	Loss carrier 2-3/4", auto 2-1/4", man. 2-3/4"; good homing and behavior near XMTR, 15-20 km velocity (forward)
303	7,500	80	1.5 up wind	260' up wind	Auto	Loss carrier 2-3/4", auto 2-1/4", man. 2-3/4"; good homing and behavior near XMTR
304	15,000	150	1 up wind	360' cross wind	Auto	Loss carrier 2-3/4", auto 2-1/4", man. 2-3/4"; good homing, 15 sec, 360° loss carrier turn; deployment test
305	15,000	150	1.5 up wind	180'	Auto	Loss carrier 2-3/4", auto 2-1/4", man. 2-3/4"; good homing, deployment test
306	15,000	150	-	-	-	Loss carrier 2-3/4", auto 2-1/4", man. 2-3/4"; payload lost and control box torn open on deployment; reefing line broke
307	7,500	80	1.5 up wind	200' down wind	Auto	Loss carrier 2-3/4", auto 2-1/4", man. 2-3/4"; acceptance flight; good homing and behavior near XMTR
309	5,000	80	-	-	Auto & man.	Loss carrier 2-3/4", auto 2-1/4", man. 2-3/4"; Fairchild flight; cross wind spoiled flight path

TABLE XVIII - Continued

Test No.	Drop Altitude (ft)	Velocity (KIAS)	Drop Point (Mi)	Impact Point	Control Mode	Comments
310	5,000	80	-	-	-	Loss carrier 2-3/4", auto 2-1/4", man. 2-3/4"; weak antenna spring or bent antenna; prevented activation of control system (Fairchild)
315	7,500	80	-	-	-	No homing due to bad XMTR
316	7,500	80	-	80'	Auto	Loss carrier 2-3/4", auto 2-1/4", man. 2-3/4"; good homing
320	15,000	150	3 up wind	180'	Auto	Loss carrier 2-3/4", auto 2-1/4", man. 2-3/4"; reliability-deployment test; good homing
321	20,000	150	overhead	225'	Auto	Loss carrier 2-3/4", auto 2-1/4", man. 2-3/4"; reliability-deployment test; good homing
322	24,000	150	4 up wind	1.5 mi down wind	-	No homing; receiver battery clip came loose
323	15,000	150	unknown down wind	Short	Auto	Loss carrier 2-3/4", auto 2-1/4", man. 2-3/4"; good homing; drop aircraft too far downward
324	15,000	150	unknown down wind	Short	Auto	Loss carrier 2-3/4", auto 2-1/4", man. 2-3/4"; good homing; drop aircraft too far downward

TABLE XVIII - Continued					
Test No.	Drop Altitude (Ft)	Velocity (KIAS)	Drop Point (Mi)	Impact Point	Comments
325	7,500	80	-	-	Loss carrier 2-3/4", auto 2-1/4", man. 2-3/4"; L/D determination; homing to XMTR No. 1 then XMTR No. 2 good
326	10,000	80	2 up wind	110'	Auto & man. Loss carrier 2-3/4", auto 2-1/4", man. 2-3/4"; good homing, 360° right and left man turns; cinetheodolite flight 508
327	10,000	80	2 up wind	45'	Auto Loss carrier 2-3/4", auto 2-1/4", man. 2-3/4"; good homing; cinetheodolite flight 509
328	7,500	80	-	-	Auto Loss carrier 2-3/4", auto 2-1/4", man. 2-3/4"; good homing
329	12,300	150	3 up wind	500' down wind	Auto Loss carrier 2-3/4", auto 2-1/4", man. 2-3/4"; reliability test; good homing; 15-20-kn surface wind
330	9,700	150	3 up wind	400' down wind	Auto Loss carrier 2-3/4", auto 2-1/4", man. 2-3/4"; reliability test; good homing; 15-20-kn surface wind
331	15,000	150	3 cross wind	210' down wind	Auto Loss carrier 2-3/4", auto 2-1/4", man. 2-3/4"; reliability test; good homing

TABLE XVIII - Continued

Test No.	Drop Altitude (Ft)	Velocity (KIAS)	Drop Point (MI)	Impact Point	Control Mode	Comments
332	15,000	150	3 cross wind left	35' up wind	Auto	Loss carrier 2-3/4", auto 2-1/4", man 2-3/4"; reliability test; good homing
333	15,000	150	unknown down wind	Short	Auto	Loss carrier 2-3/4", auto 2-1/4", man 2-3/4"; good homing; reliability test; drop point too far down wind
334	15,000	150	-	-	-	Servo battery failed due to internal open (life exceeded)
335	15,000	150	-	-	-	Right section of wing torn on opening (life exceeded); control box shell damaged on impact

TABLE XIX. CEP FLIGHT DATA					
Flight No.	Altitude (Ft)	Deployment Velocity (KIAS)	Offset (MI)	Impact (Ft)	Comments
300	10,000	80	3 +	-	Offset too great; possible aircraft interference
301	7,500	80	1.5 "p wind	300 down wind	Surface wind 15 kn
302	7,500	80	1.5 up wind	20 cross wind	Surface wind 3 kn
303	7,500	80	1.5 up wind	260 up wind	Surface wind 3 kn
304	15,000	150	1.0	360 cross wind	Surface wind 3 kn
305	15,000	150	1.5	180	Surface wind 3 kn
306	15,000	150	-	-	Inadequate reefing line used; No. 6 line broke
307	7,500	80	1.5	200	-
309	5,000	80	-	-	L/D flight (man. & auto control)
310	5,000	80	-	-	Antenna release problem
315	7,500	80	-	-	XMTR malfunctioned
316	7,500	80	1.0	80	-
320	15,000	150	3.0 up wind	180	Surface calm
321	20,000	150	0	225 down wind	Surface 2 kn
322	24,000	150	4.0	-	Receiver battery circuit opened

TABLE XIX - Continued

Flight No.	Altitude (Ft)	Deployment Velocity (KIAS)	Offset (Mi)	Impact (Ft)	Comments
323	15,000	150	-	-	Drop aircraft out of position
324	15,000	150	-	-	Drop aircraft out of position
325	7,500	80	-	-	L/D flight (man. & auto control)
326	10,000	80	2.0 up wind	110 up wind	-
327	10,000	80	2.0 up wind	45 cross wind	-
328	7,500	80	-	-	L/D test (man. & auto control)
329	12,300	150	3.0 up wind	-	Excess wind velocity, 18-20 kn surface
330	9,700	150	3.0 up wind	-	Excess wind velocity, 18-20 kn surface
331	15,000	150	3.2 cross wind	210 down wind	Surface wind 8-10 kn
332	15,000	150	3.2 cross wind	35 up wind	Surface wind 8-10 kn
333	15,000	150	-	-	Drop aircraft out of position
334	15,000	150	-	-	Servo battery had an open circuit
335	15,000	150	-	-	Wing torn upon deployment
Average impact distance 169.6 feet; CEP 180 feet at 90-percent confidence level					

TABLE XX. RELIABILITY FLIGHT DATA						
Flight No.	Altitude (Ft)	Deployment		Offset (MI)	Impact (Ft)	No Test
		Velocity (KIAS)	Good			
254	9,500	50	X	-	-	-
260	7,500	50	-	-	-	Wing not trimmed; man. flight
261	7,500	50	X	-	-	-
265	10,000	150	-	-	450	Wing not trimmed
281	10,000	150	-	-	-	Antenna release design changed
282	10,000	150	-	-	-	Premature disreefing
283	10,000	120	X	-	-	-
286	10,000	80	X	3.8	300 down wind	-
287	10,000	80	X	3.5	-	-
291	10,000	120	X	4.0	-	-
292	7,500	80	X	2.8	180	-
294	10,000	120	X	3.0	500	-
295	10,000	120	X	-	1000 down wind	-
297	7,500	80	X	1.75	50	-
298	7,500	80	X	1.0	100	-
299	10,000	80	X	2.5	-	-



TABLE XX - Continued

Flight No.	Altitude (Ft)	Deployment Velocity (KIAS)	Good	Offset (Mi)	Impact (Ft)	No Test
300	10,000	80	-	3.5	-	May have had aircraft interference
301	7,500	80	X	1.5	300 down wind	-
302	7,500	80	X	1.5	-	-
303	7,500	80	X	1.5	260 up wind	-
304	15,000	150	X	1.0	360 cross wind	-
305	15,000	150	X	1.5	180	-
306	15,000	150	-	-	-	Deployment test with lightweight reefing line; line inadequate
307	7,500	80	X	1.5	-	-
309	5,000	80	X	-	-	-
310	5,000	80	-	-	-	Antenna did not deploy; check out flight after system rework
315	7,500	80	-	-	-	XMTR
316	7,500	80	X	-	80	-
320	15,000	150	X	3.0	180	-
321	20,000	150	X	0	225 down wind	-

TABLE XX - Continued						
Flight No.	Altitude (Ft)	Deployment Velocity (KIAS)	Good	Offset (Mi)	Impact (Ft)	No Test
322	24,000	150	-	4.0	-	Receiver battery clip off
323	15,000	150	X	-	-	-
324	15,000	150	X	-	-	-
325	7,500	80	X	-	-	-
326	10,000	80	X	2.0	110	-
327	10,000	80	X	2.0	45	-
328	7,500	80	X	-	-	-
329	12,300	150	X	3.0	-	-
330	9,700	150	X	3.0	-	-
331	15,000	150	X	3.2	210 down wind	-
332	15,000	150	X	3.2	35 up wind	-
333	15,000	150	X	3.2	-	-
334	15,000	150	-	-	-	Servo battery failed (life exceeded)
335	15,000	150	-	-	-	Wing torn (life exceeded)
Based on the above 33 flights without failure, system reliability is 93.3% at C.L. or 95% at 80% C.L.						

## ENVIRONMENTAL EVALUATION

### GENERAL

The CACS was to be designed to be compatible with the environmental requirements set forth in paragraph 7 of Change 1 to AR 705-15. The temperature limits for the environments specified are as described in AR 705-15, paragraph 7c.

Compliance with the requirement was accomplished by design and by the use of approved MS parts and processes. In areas in which such evidence was not directly available, compliance could be demonstrated either by actual test or by establishing similarity of hardware, materials, or processes to those that have demonstrated compliance with required environment. In addition to the above, the acceptability of certain component parts has been established by means of an exempt parts list (see Appendix VII), which was approved by the contracting officer. In those cases in which actual tests are required, the specific test shall be in accordance with MIL-STD-810.

It was assumed that if major subassemblies were acceptable, then the total integrated system was acceptable. In line with this approach, the CACS was divided into two major subassemblies: parawing and control unit. By definition, herein, the parawing subassembly consisted of all the textile material components. Thus, the subdivision results in similar materials being grouped together for investigation.

The following is the specific approach, discussion, and results of the investigation to verify the compatibility of the CACS design and equipment with AR 705-15, paragraph 7 of change 1, temperature requirements.

### ENVIRONMENTAL REQUIREMENTS

Because of the availability of the reference documents and the length of the description, the environmental requirements will not be presented in detail herein. The tests, by title, which would be used in MIL-STD-810 Category 5, Class 6, are:

1. Temperature and Pressure
  - Low Temperature
  - High Temperature
  - Low Pressure
  - Sunshine
2. Corrosion and Erosion
  - Sand and Dust
  - Rain
  - Humidity

Fungus  
Salt Fog

3. Mechanical  
Shock  
Vibration

The objective of investigating the CACS as a function of the above items was to assure that the system is capable of reliable operation under world-wide operational conditions.

PARAWING ASSEMBLY

The parawing is made from nylon or polyamide, Dacron or polyester, polypropylene, and polyurethane elastomer, which has been integrated into an engineering material or used by itself in the parawing fabrication. Both nylon and polyester have been used in a multitude of parachute programs in which the hardware has been qualified. Therefore, this complete subassembly has been qualified by similarity herein.

The parawing assembly consists of a canopy and lines (part No. 10068109-1), deployment bag (part No. 10068143-1), and attachment bridle (part No. 10068140-1).

As stated previously, a material and/or item that has been manufactured by, and certified to comply with, a military specification would be qualified for this program. Both the deployment bag and the attachment bridle are made from certified material. The process for assembling the units is in accordance with standard Government specification. Therefore, it can be assumed that these items will meet the environmental requirements specified for the CACS without detailed investigation.

The canopy is made from nylon coated with polyurethane elastomer. As stated previously, nylon is used extensively in the manufacturing of parachutes. However, its use as a substrate to polyurethane is not as well known. A laminate of polyester, nylon (polyamid), and polyurethane has undergone extensive evaluation as part of Air Force Contract AF30(602)-4084, "Extremely Lightweight Inflatable 'LF' Antenna." The tests were conducted in accordance with MIL-STD-810. They included high and low temperature, antenna pressure, bounce, shock, rain, humidity, fungus, sand and dust, sunshine, salt fog, wind load, electrical, and performance tests. The results of these tests are presented in GER-137373. The material as well as the resulting structure meets all of the requirements.

Polyurethane elastomer has been qualified for use in the Apollo program as a gas barrier for the uprighting bags. In this particular application, the elastomer is used with a woven Dacron substrate. Thus, its performance--since used on a woven material--should be the same, whether nylon or Dacron yarns are used. The qualification test consisted of acceptance test and inspection, humidity, vibration, vacuum and temperature, acceleration,

shock, submersion, proof pressure, operating life, burst strength verification, and mission simulation. The results and a description of these tests are presented in GA556D-35 (GER-139114), "Qualification Test Report Apollo Inflatable Flotation Bag Packs," July, 1968; and GA556D-33 (GER-13123), "Qualification Test Report Bag Pack, Inflatable Flotation," 16 March 1967. The units must be capable of sustaining the earth, space, and moon environments as well as launch and reentry.

The actual tests conducted were more severe than those required for the CACS. Therefore, it has been concluded that the canopy and its materials do comply with the environmental requirement because of its similarity to the material described above.

The lines are 2-in-1 stable braid. The braid is 1/4 inch in diameter and has a breaking strength of 1700 pounds. The line is fabricated from a polyester shield and a polypropylene core.

The outer braid is fabricated from a polyester material. The material used is the same as that in rope which qualifies to MIL-C-43256A, dated 25 May 1967. Thus, the exterior shield can be assumed to qualify because of its similarity to this material.

The polypropylene core has also been qualified to Mine Defense Laboratory Specification 2468-003A(MDL) dated 5 September 1969, entitled "Specification, Rope-Nylon Polypropylene," issued by the Naval Ship Research and Development Laboratory, Panama City, Florida. The core is the same as that used in the rope described by the above specification. Therefore, this material complies with the environmental requirement because it has been qualified to a Government specification.

In summary, all of the materials used in the parawing subassembly either are manufactured to a Government specification, are the same as material that has been qualified to a Government specification, or are similar to materials that have been tested to conditions equal to or worse than those required for the CACS. Therefore, it can be concluded that this subassembly complies with the environmental requirements.

#### CONTROL UNIT

The control unit subassembly consisted of all the mechanical and electrical components. The GFE items while contained in the control unit were not considered since their acceptability had been established by the Army and were supplied as qualified hardware. As stated previously, the detail parts list was examined, and Military Standard parts or those certified by the manufacturer to comply with the MIL STD were considered to be adequate. Again, a review of the components was made, and an exempt parts list was established. These parts were considered to qualify because of the reason for exemption.

An area of concern was the susceptibility of the assembly to salt fog requirements. In the design and fabrication of the hardware, the battery was sealed. The electrical components and connections in the logic box were coated with a monitor protective coating in accordance with approved processes (conformal coating). For the most part, the backs of the connectors and other electrical joints were potted. In addition, the complete system was located within an aluminum box, through which only the control cables passed. The antenna housing and installation area were protected by means of an elastomeric membrane. The only areas which could possibly be susceptible to salt fog were some of the readily changeable connectors. As stated, these were located within the aluminum box and would, under normal circumstances, not be exposed. Therefore, it was concluded that adequate protection from this environment had been offered the system in accordance with the requirements.

A random unit was selected and instrumented for the hot and cold temperature tests. The tests were to monitor specific voltages and cable travel at ambient temperature and at 105°F and -25°F.

It had been determined prior to the initiation of the program that the battery was not capable of operation in the -25°F environment. Therefore, a waiver had been established. However, in order to obtain some additional data, the battery was to be used as the power source. During the first experiment, the battery voltage dropped below a minimum (17 volts), resulting in an unstable electrical circuit, and the servo operated in the right turn direction until mechanically stopped. The battery was then recharged and the cold portion of the test repeated. The system functioned in accordance with the required cable travel at all temperatures.

The test data obtained and specific procedures used are as follows.

A random unit that was complete and ready for delivery was selected from the assembly area for the hot and cold temperature tests. Thermocouples were installed on the logic box, the servo amplifier, the servo actuator, and the servo battery. The unit was then placed in the ARC-WI temperature chamber and connected so that the amount of pull-in could be measured and so that the various voltages and thermocouples could be monitored. In order to facilitate operation in the automatic homing mode, the transmitter was connected through suitable attenuators directly to the antenna connectors on the control box so that a left or right error signal could be simulated for automatic homing. Figure 27 shows the box in the chamber during the test. For the pull-in measurement, a 10-pound weight was suspended from the control line, and the travel was measured by means of a fixed scale mounted behind the cable (see Figure 28). The thermocouples were monitored with a six-channel IC thermocouple readout. Figure 29 shows the test setup including the digital voltmeter used to measure the various voltages. For voltage monitoring purposes, a cable from J9 on the control unit was brought out of the chamber to a terminal strip.

The test proceeded as follows:

Ambient temperature (82°F) measurements of voltages and pull-in were recorded. The chamber temperature was then increased until the thermocouples indicated between 155°F and 160 F. This temperature was maintained for 4 hours. The chamber was then allowed to cool until the thermocouples indicated between 105°F and 110°F; this temperature was maintained for 1 hour. The control system was then operated, and the voltages and pull-in were measured and recorded. The chamber was allowed to return to ambient temperature, and the unit was inspected and operated at ambient temperature (80°F). The results of this test are given in Table XXI for the voltage measurements and in Table XXII for the cable travel measurements.

The unit was then removed from the chamber and thoroughly inspected. The batteries were recharged, and the unit was replaced in the chamber for the cold test.

The test setup and test plan were the same as those used for the high temperature test except that the chamber was held at -65°F for 4 hours and then raised to -25°F for 1 hour, and the control unit operated at -25°F. The measurements made are recorded in Tables XXIII and XXIV. The control system failed to operate at -25°F due to failure of the servo battery. The battery voltage dropped radically after the fourth operation of the servo actuator. The receiver battery voltage is also seen to be well below nominal at the cold temperature.

After the failure, the chamber was brought back to ambient temperature, and the control unit was removed and thoroughly tested with no discrepancies noted other than the battery. The unit was tested using external power, and it functioned normally. The same batteries were recharged, the unit was replaced in the chamber, and the cold-temperature test was repeated. An external power supply was kept on standby in case of a repeat of the battery failure, but the system functioned on the internal batteries for the second test. The results of this test are given in Tables XXV and XXVI.

Based on the initial approach of compliance by design, similarity, use of approved or MS parts and procedures, and experimental evaluation where required, it is concluded that the unit complies with paragraph 7 of change 1 to AR 705-15 within the intent of this program.

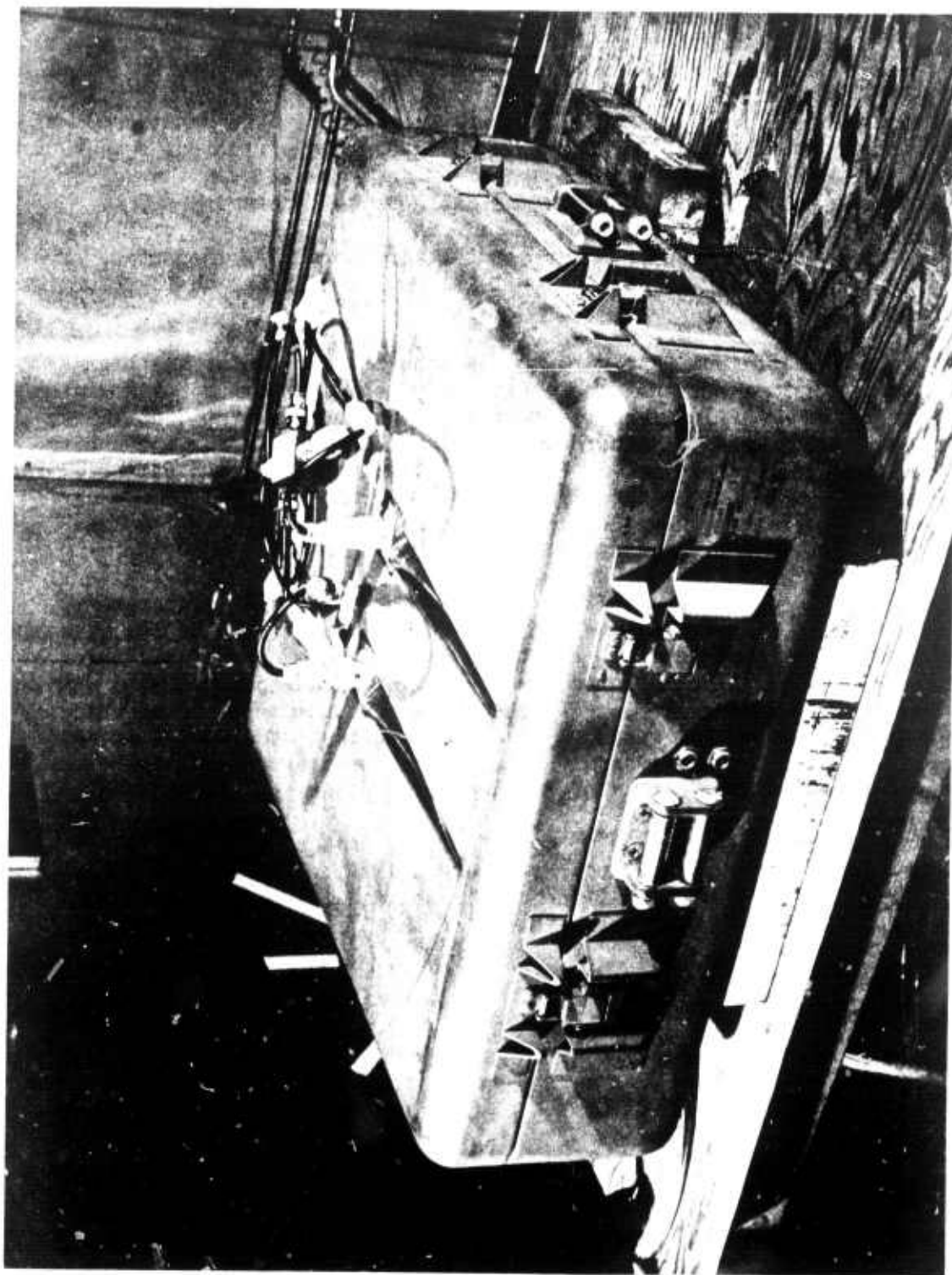


Figure 27. Environmental Test Antenna Hookup.



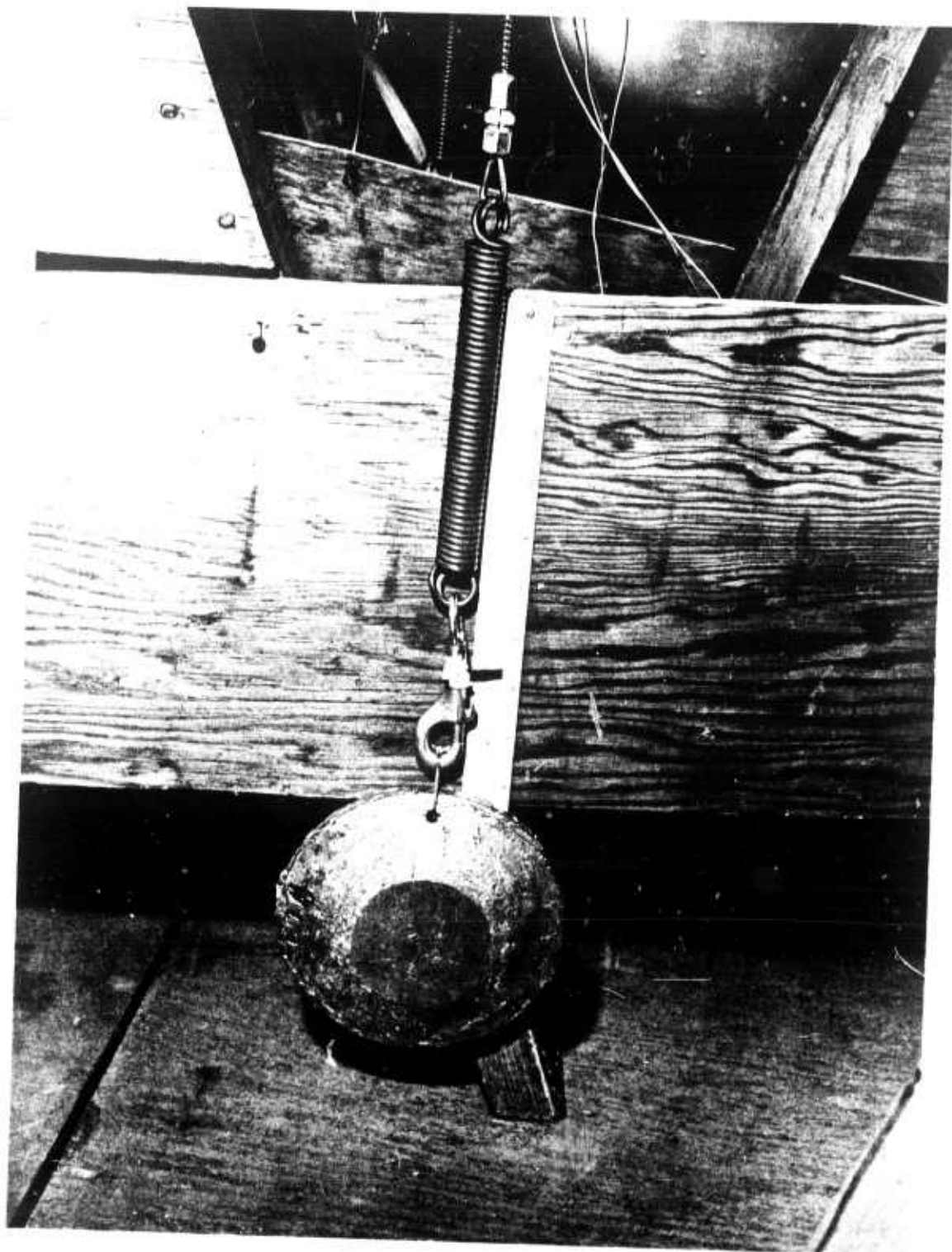


Figure 28. Control Cable Movement Measurement.

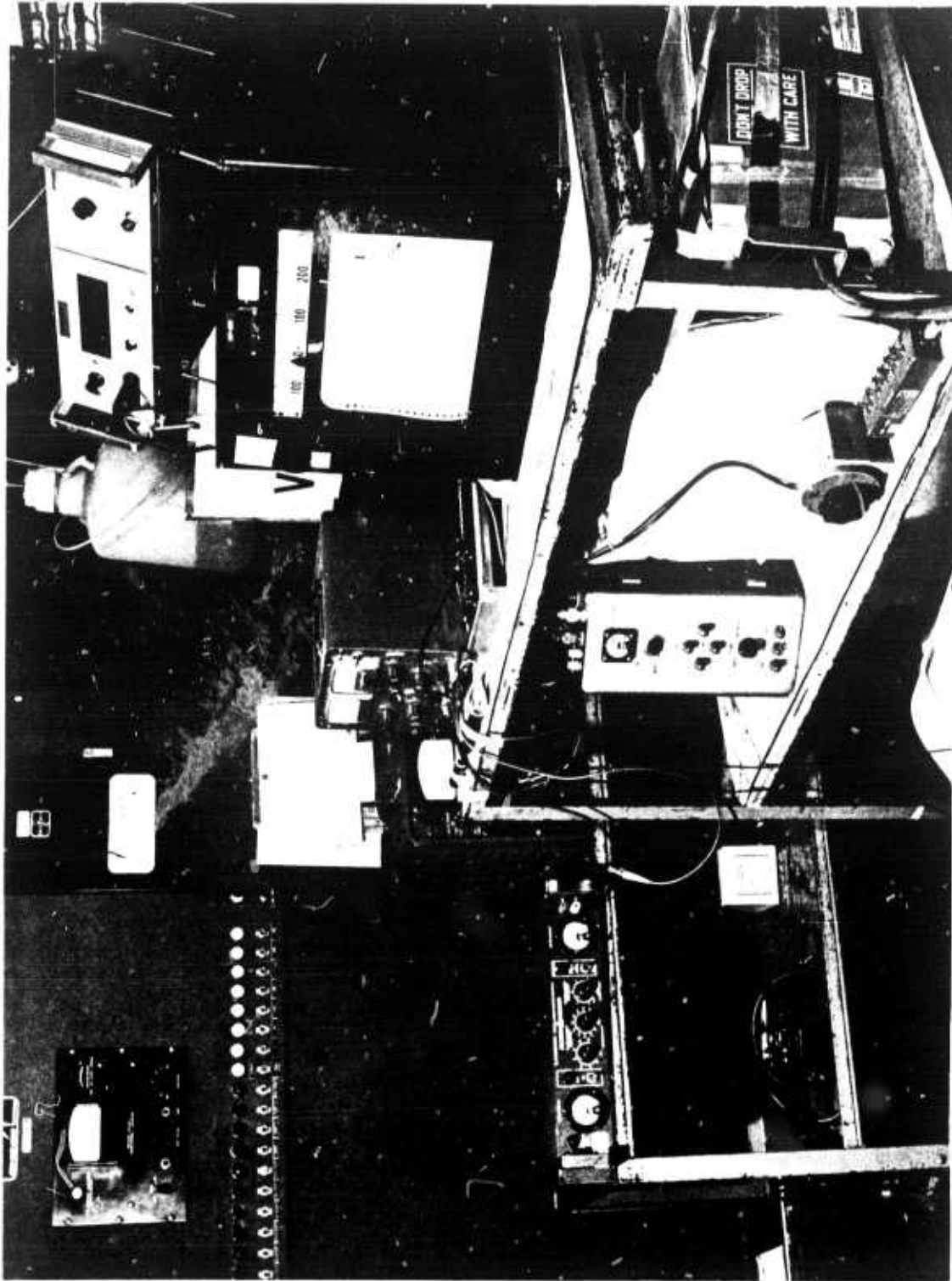


Figure 29. Environmental Test Setup.

TABLE XXI. VOLTAGE MEASUREMENTS, HIGH-TEMPERATURE TEST 1						
	Servo Battery	Receiver Battery	Regulated 22 VDC	Hi-Level Preset	Relay Common	Servo Feedback
<u>Pretest Ambient</u>						
Loss Carrier	30.54	27.00	21.64	8.18	26.72	13.31
Neutral	30.49	26.82	21.71	10.72	25.70	10.84
Man. Left	30.43	26.71	21.73	13.62	26.69	8.56
Man. Right	30.32	26.68	21.75	8.17	26.63	13.34
Auto Left	30.21	26.62	21.77	13.07	26.46	9.07
Auto Right	30.16	26.61	21.80	8.69	26.57	12.84
<u>105°F</u>						
Loss Carrier	28.91	25.4	21.75	8.19	25.29	13.28
Neutral	28.79	25.12	21.88	10.76	25.04	10.88
Man. Left	28.88	25.33	21.81	13.64	25.23	12.87
Man. Right	28.78	25.27	21.84	8.19	25.17	10.61
Auto Left	28.84	25.22	21.86	13.10	25.06	9.09
Auto Right	28.81	25.14	21.87	8.73	25.05	12.89
<u>Post-Test Ambient</u>						
Loss Carrier	28.64	24.82	21.61	8.14	24.74	13.18
Neutral	28.80	25.13	21.52	10.67	25.04	10.90
Man. Left	28.60	24.82	21.61	13.51	24.74	8.50
Man. Right	28.61	24.81	21.61	8.10	24.73	13.22
Auto Left	28.67	24.87	21.60	12.95	24.79	9.00
Auto Right	28.71	24.96	21.59	8.61	24.87	12.75

TABLE XXII. CABLE PULL-IN MEASUREMENTS, HIGH-TEMPERATURE TEST 1						
	Loss Carrier	Neutral	Manual Left	Manual Right	Auto Left	Auto Right
Pretest Ambient	2.80	0	2.90	2.83	2.28	2.23
105°F	2.74	-0.01	2.94	2.76	2.32	2.20
Post-Test Ambient	2.70	-0.05	2.96	2.74	2.35	2.18

TABLE XXIII. VOLTAGE MEASUREMENTS, LOW-TEMPERATURE TEST 1						
	Servo Battery	Receiver Battery	Regulated 22 VDC	Hi-Level Preset	Relay Common	Servo Feedback
<u>Pretest Ambient</u>						
Loss Carrier	30.55	26.48	21.62	8.15	26.34	13.13
Neutral	30.48	26.40	21.70	10.74	26.30	11.10
Man. Left	30.41	26.30	21.74	13.62	26.19	8.55
Man. Right	30.31	26.13	21.77	8.16	26.04	13.32
Auto Left	30.26	26.04	21.78	13.06	25.94	9.06
Auto Right	30.18	25.91	21.79	8.69	25.81	12.87
<u>-25°F</u>						
Loss Carrier	28.57	22.74	22.57	7.66	22.38	12.54
Neutral	28.16	22.38	20.38	10.10	22.31	10.60
Man. Left	27.90	22.28	20.42	12.78	22.18	8.18
Man. Right	27.79	22.17	20.44	7.67	22.10	12.60
Auto Left	13.30	22.00	12.51	4.98	21.92	5.55
Auto Right	Servo battery completely discharged; system stayed in hard right turn.					

TABLE XXIV. CABLE PULL-IN MEASUREMENTS, LOW-TEMPERATURE TEST 1						
	Loss Carrier	Neutral	Manual Left	Manual Right	Auto Left	Auto Right
Pretest Ambient	2.75	0	2.94	2.83	2.34	2.23
<u>-25°F</u>	2.76	-0.09	2.88	2.86	Failed, right cable into stop	
Post-Test Ambient (on ext. power)	2.72	-0.09	2.98	2.76	2.36	2.42

TABLE XXV. VOLTAGE MEASUREMENTS, LOW-TEMPERATURE TEST 2						
	Servo Battery	Receiver Battery	Regulated 22 VDC	Hi-Level Preset	Relay Common	Servo Feedback
<u>Pretest Ambient</u>						
Loss Carrier	28.78	25.01	21.64	8.19	24.93	13.24
Neutral	28.79	25.01	21.66	10.79	24.94	11.00
Man. Left	28.79	25.01	21.69	13.59	24.95	8.56
Man. Right	28.80	25.01	21.70	8.17	24.94	13.28
<u>-25°F</u>						
Loss Carrier	28.77	24.03	20.37	7.68	23.84	12.58
Neutral	28.41	23.72	20.47	10.15	23.64	10.49
Man. Left	28.26	23.55	20.49	12.82	23.47	8.19
Man. Right	28.08	23.34	20.50	7.70	23.27	12.63
Auto Left	27.95	23.21	20.49	12.28	23.14	8.67
Auto Right	27.75	23.01	20.49	8.18	22.94	12.20
<u>Post-Test Ambient</u>						
Loss Carrier	29.46	24.50	21.50	8.05	24.38	12.75
Neutral	29.20	24.12	21.52	10.63	24.04	10.09
Man. Left	28.62	24.04	21.49	13.38	23.96	8.57
Man. Right	28.56	24.50	21.46	8.06	23.92	13.17
Auto Left	28.67	23.90	21.49	12.88	23.82	8.94
Auto Right	29.27	24.20	21.50	8.58	23.12	12.60

TABLE XXVI. CABLE PULL-IN MEASUREMENTS, LOW-TEMPERATURE TEST 2						
	Loss Carrier	Neutral	Manual Left	Manual Right	Auto Left	Auto Right
Pretest Ambient	2.75	0	2.92	2.83	2.36	2.25
-25°F	2.78	-0.06	2.94	2.80	2.34	2.20
Post-Test Ambient	2.78	-0.09	2.93	2.84	2.31	2.24

## CONCLUSIONS

At the initiation of this effort, a requirement existed for a system which could deliver up to 500 pounds of payload, by air, to ground under all weather conditions, during any time of the day or night, and under a wide range of battlefield conditions with increased aircraft safety. It is concluded that the system developed and reported herein is ready for use by the Army; is the first major innovation in cargo delivery; provides aircraft safety, all-weather capability, and clandestine delivery with pinpoint accuracy.

It is concluded that significant technology advancements were made. It is also concluded that a well performing base-line vehicle is now available for the testing of new concepts and ideas by which future improvements or changes can be judged.

## RECOMMENDATIONS

Based on the experience gained during the program and in line with the Army requirements, it is recommended that a system be developed for the 1000- to 2000-pound payload range. In addition, it is recommended that a value engineering effort commence to reduce the cost of the total system as well as a review of the system requirements to establish the areas in which increased performance is not worth the increased equipment cost. The integration of the last two efforts would result in a system able to meet the major Army requirements at a very reasonable price.

As is always the case in the development of an initial system from a new technology, many areas for research become apparent. These areas of research are necessary for major advancement in the concept. Areas requiring investigation and in which it is recommended that work be conducted are wind-tunnel evaluation of wing shapes, dynamics of deployment, theory of reefing and reefing techniques, and method of stress analysis. Many more areas of technology can be examined for technology advancement; however, enough technology exists to advance to a 2000-pound system.

The major recommendation is to commence the 2000-pound system development to assure its availability to the Army in the least amount of time.

#### LITERATURE CITED

1. INSTRUCTION BOOK FOR CONTROLLED AIRDROP CARGO SYSTEM (500#), GER 14198, Goodyear Aerospace Corporation, Akron, Ohio June 1969.
2. RELIABILITY AND MAINTAINABILITY FOR CONTROLLED AIRDROP CARGO SYSTEM (500#), GER 14392, Goodyear Aerospace Corporation, Akron, Ohio, June 1969.
3. QUALIFICATION TEST OF EXTREMELY LIGHTWEIGHT INFLATABLE "LF" ANTENNA, GER 13737, Goodyear Aerospace Corporation, Akron, Ohio, February 1968.
4. Hoerner, Sighard, FLUID DYNAMIC DRAG, Second Edition published by the author, 1965, p. 3-17.
5. PARAGLIDER DEVELOPMENT PROGRAM, PHASE IIA, MID-TERM REPORT, GER 10640, Goodyear Aerospace Corporation, Akron, Ohio, April 1962.
6. Naeseth, R. L., and Fournier, P. G., LOW SPEED WIND-TUNNEL INVESTIGATION OF TENSION STRUCTURE PARAWINGS, Langley Working Paper (LWP) 310, NASA Langley Station, October 1966.



## APPENDIX I AERODYNAMIC ANALYSIS

### INTRODUCTION

A preflight aerodynamic analysis of the single-keel, all-flexible parawing cargo delivery system was made to define several performance characteristics of the all-flexible parawing as required by contract definition. They include maximum L/D attainable, effects of payload drag on L/D, vertical descent rate, and a lateral control capability. The analysis is based primarily on wind-tunnel data, due to the limited amount of flight test data available. A detailed planform diagram including the location of the keel and leading-edge lines is shown in Figure 30. Use of a catenary-keel panel will reduce the number of keel lines required from 11 to 6. For trim flight, the current method of rigging a single-keel cargo-carrying parawing has evolved from a series of test flights conducted by NASA-LMC, USAAVLABS at Fort Eustis, and Goodyear Aerospace Corporation during the past several years. The present single-keel parawing configuration with its line lengths and tension coefficients, as determined during these preliminary tests, is shown in Figure 31. Also shown is a preliminary estimate of the changes to be expected for the addition of a catenary-keel panel. Figures 32 through 37 are the parametric curves used to define an operational parawing cargo delivery system. These curves include the following parameters:

1. Resultant velocity versus dynamic pressure
2. Wing planform area versus keel length
3. Wing planform area versus payload weight versus wing loading
4. Payload weight versus keel length versus wing loading
5. Payload weight versus keel length versus resultant velocity
6. Velocity versus L/D versus wing loading

### L/D CHARACTERISTICS

While a maximum L/D for the parawing is the most desirable, this also produces a system with the maximum response sensitivity to control forces and movement. Several variables determine the highest L/D attainable by an all-flexible parawing system. These include line rigging, canopy planforms and inflated shapes, payload configuration, and system geometry. Canopy planforms and inflated shapes have been studied extensively in the wind tunnel, and an optimum layout having a sweep angle of 45 degrees with a 1/8 L<sub>k</sub> nose cutoff has been standardized (see Figure 31) for the single-keel parawing.

The next most important variable in designing a parawing system is the line rigging, which also affects the inflated shape.

The rigging which produced the maximum L/D during wind-tunnel tests was used as a baseline for the free-flight tests. The lines were then adjusted to obtain the best overall performance. The other important variable in determining best overall performance is the drag of the payload due to its shape. The wind-tunnel L/D does not include this. Size and shape of the payload will determine the final net L/D and the overall performance.

Wind-tunnel tests of the all-flexible single-keel parawings used in this program have shown that a maximum L/D of 2.7 is obtainable at dynamic pressures near 2.0 with no payload or control box included. The control box has been designed for a minimum drag using rounded edges and a minimum forward projected surface. All payload drag estimates have been based on standard shapes which can be fitted into an Army A21 canvas container. The payload shapes and their associated drag coefficients which were considered in this analysis are shown in Figure 38.

The estimated L/D characteristics of the single-keel parawing, including the drag addition from the control box and payload, are shown in Figures 39 and 40. Effective flight L/D based on the premise that the parawing system will move along an S-shaped trajectory along the horizontal plane with a maximum deviation from the target of +10 degrees reduces the L/D by 1.5 percent. These theoretical estimates indicate that the single-keel parawing system under development will exceed the contract performance effective L/D requirement and will approach the design objective of 2.4. The twin-keel parawing is expected to increase the L/D by at least 20 percent. For this parawing system with L/D between 2.3 and 2.7, the vertical descent rate will be approximately 20 feet per second.

The effect of wind on the glide path is shown in Figure 41. This figure is a plot of the horizontal-to-vertical velocity ratio ( $V_H/V_V$ ) versus the ratio of the wind velocity to the resultant glide velocity ( $V_W/V_R$ ) for various values of L/D. It is apparent from this figure that a high L/D and a high glide velocity are desirable to penetrate winds.

#### LATERAL CONTROL

Control of the all-flexible parawing delivery system is limited entirely to lateral control using the technique of controlling the length of the aft leading-edge lines. The amount of length adjustment required for the desired control varies greatly between wind-tunnel and free flight available data as shown in Figures 42 and 43.

Data obtained from the early flight tests at Fort Eustis is shown in Figures 44 and 45. These figures show control line displacement versus time for a 360-degree turn with a wing loading of 0.7. Figure 45 was used in determining the flight bank angle in conjunction with the following analytical technique.

The turning radius and time to turn 360 degrees may be computed from

$$R = \frac{V_R^2}{g \tan \psi} \quad (3)$$

where  $R$  = turning radius in feet

$V_R$  = velocity in feet per second

$g$  = acceleration due to gravity in feet per second per second

$\psi$  = bank angle

$$t = \frac{2 \pi R}{V_R} \quad (4)$$

where  $t$  = time to turn 360 degrees

The turning radius and the time to make a 360-degree turn are plotted in Figures 46 and 47 against glide velocities for various bank angles  $\psi$ . The maximum bank or roll angle is assumed to be 50 degrees at this time.

The maximum bank angle is desirable in order to obtain the minimum turning radius for a given configuration. Basically, the control line loads and change in length are required for the design of the control system but may also affect the configuration. Preliminary data on the control lines is given in Figure 48.

A typical configuration is shown in Figure 49. With the single-point suspension, it is necessary to spread at least some of the leading-edge lines apart a distance  $C$  to provide a counteracting torque on the control package to resist the torque produced by the unbalanced control forces.

In conclusion, the preliminary aerodynamic analysis performed has shown that the contract performance requirements of effective  $L/D$  greater than 1.8 with a goal of 2.4, vertical descent rate at impact of less than 25 fps, and 100-foot turn radius capability can be met and exceeded to the extent that the design requirements can be met.

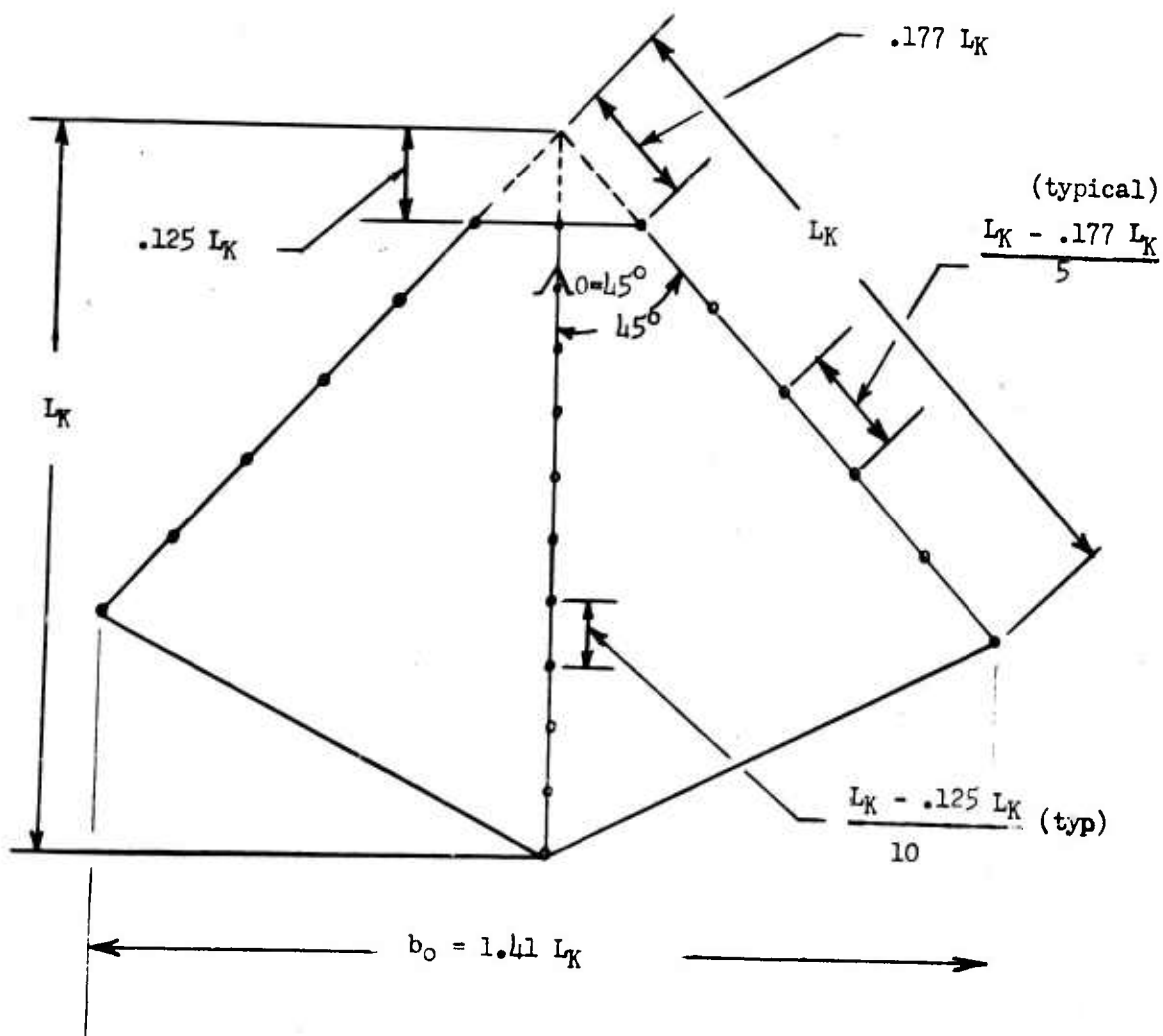
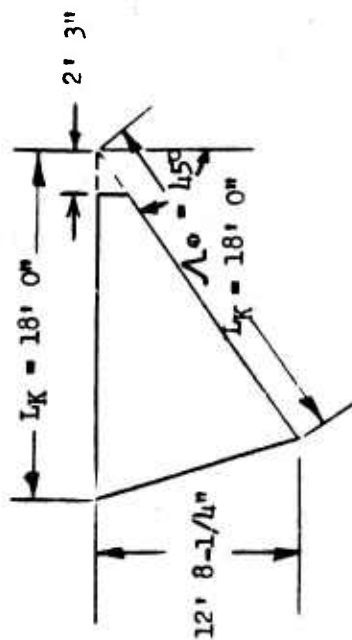


Figure 30. Model of Parawing Having  $\theta = 45^\circ$  and  $1/8 L_K$  Nose Cut off.



	Tension Coefficient (% of sys-tem weight)				Position From Apex (Ft) (In)				Line Lengths (In)				Tension Coefficient (% of sys-tem weight)				Position From Apex (Ft) (In)				Line Lengths (In)				Line Length Including Catenary Keel Panel (Ft) (In)				
	Position From Apex (Ft)	Line Lengths (Ft)	Line Lengths (In)	Tension Coefficient (% of sys-tem weight)	Position From Apex (Ft)	Line Lengths (In)	Line Lengths (Ft)	Line Lengths (In)	Tension Coefficient (% of sys-tem weight)	Position From Apex (Ft)	Line Lengths (In)	Line Lengths (Ft)	Line Lengths (In)	Tension Coefficient (% of sys-tem weight)	Position From Apex (Ft)	Line Lengths (In)	Line Lengths (Ft)	Line Lengths (In)	Tension Coefficient (% of sys-tem weight)	Position From Apex (Ft)	Line Lengths (In)	Line Lengths (Ft)	Line Lengths (In)	Tension Coefficient (% of sys-tem weight)	Position From Apex (Ft)	Line Lengths (In)	Line Lengths (Ft)	Line Lengths (In)	
Leading Edge	3	2-1/4	24	.011	3	2-1/4	24	-	.011	3	2-1/4	24	-	.011	3	2-1/4	24	-	.011	3	2-1/4	24	-	.011	3	2-1/4	24	-	.011
	6	-	23	.035	6	-	23	11/16	.035	6	-	23	11/16	.035	6	-	23	11/16	.035	6	-	23	11/16	.035	6	-	23	11/16	.035
	9	-	22	.072	9	-	22	3-3/8	.072	9	-	22	3-3/8	.072	9	-	22	3-3/8	.072	9	-	22	3-3/8	.072	9	-	22	3-3/8	.072
	12	-	21	.082	12	-	21	1/16	.082	12	-	21	1/16	.082	12	-	21	1/16	.082	12	-	21	1/16	.082	12	-	21	1/16	.082
	15	-	20	.055	15	-	20	1-11/16	.055	15	-	20	1-11/16	.055	15	-	20	1-11/16	.055	15	-	20	1-11/16	.055	15	-	20	1-11/16	.055
	18	-	18	.084	18	-	18	-	.084	18	-	18	-	.084	18	-	18	-	.084	18	-	18	-	.084	18	-	18	-	.084
Keel Lengths and Factors	2	3	23	.007	2	3	23	2-7/8	.007	2	3	23	2-7/8	.007	2	3	23	2-7/8	.007	2	3	23	2-7/8	.007	2	3	23	2-7/8	.007
	3	0	23	.023	3	0	23	8	.023	3	0	23	8	.023	3	0	23	8	.023	3	0	23	8	.023	3	0	23	8	.023
	5	3	23	.033	5	3	23	9-1/2	.033	5	3	23	9-1/2	.033	5	3	23	9-1/2	.033	5	3	23	9-1/2	.033	5	3	23	9-1/2	.033
	6	9	23	.057	6	9	23	5-3/16	.057	6	9	23	5-3/16	.057	6	9	23	5-3/16	.057	6	9	23	5-3/16	.057	6	9	23	5-3/16	.057
	8	3	23	.058	8	3	23	1/4	.058	8	3	23	1/4	.058	8	3	23	1/4	.058	8	3	23	1/4	.058	8	3	23	1/4	.058
	9	9	22	.069	9	9	22	9-5/8	.069	9	9	22	9-5/8	.069	9	9	22	9-5/8	.069	9	9	22	9-5/8	.069	9	9	22	9-5/8	.069
	11	7-1/2	22	.072	11	7-1/2	22	9-5/8	.072	11	7-1/2	22	9-5/8	.072	11	7-1/2	22	9-5/8	.072	11	7-1/2	22	9-5/8	.072	11	7-1/2	22	9-5/8	.072
	13	6	22	.061	13	6	22	9-5/8	.061	13	6	22	9-5/8	.061	13	6	22	9-5/8	.061	13	6	22	9-5/8	.061	13	6	22	9-5/8	.061
	15	-	22	.046	15	-	22	6-1/8	.046	15	-	22	6-1/8	.046	15	-	22	6-1/8	.046	15	-	22	6-1/8	.046	15	-	22	6-1/8	.046
	16	6	21	.030	16	6	21	2-7/8	.030	16	6	21	2-7/8	.030	16	6	21	2-7/8	.030	16	6	21	2-7/8	.030	16	6	21	2-7/8	.030
	18	-	19	.058	18	-	19	8-5/16	.058	18	-	19	8-5/16	.058	18	-	19	8-5/16	.058	18	-	19	8-5/16	.058	18	-	19	8-5/16	.058
																	Catenary Keel Parawing												

Figure 31. Single-Keel Parawing Dimensions, 18-Foot Keel.

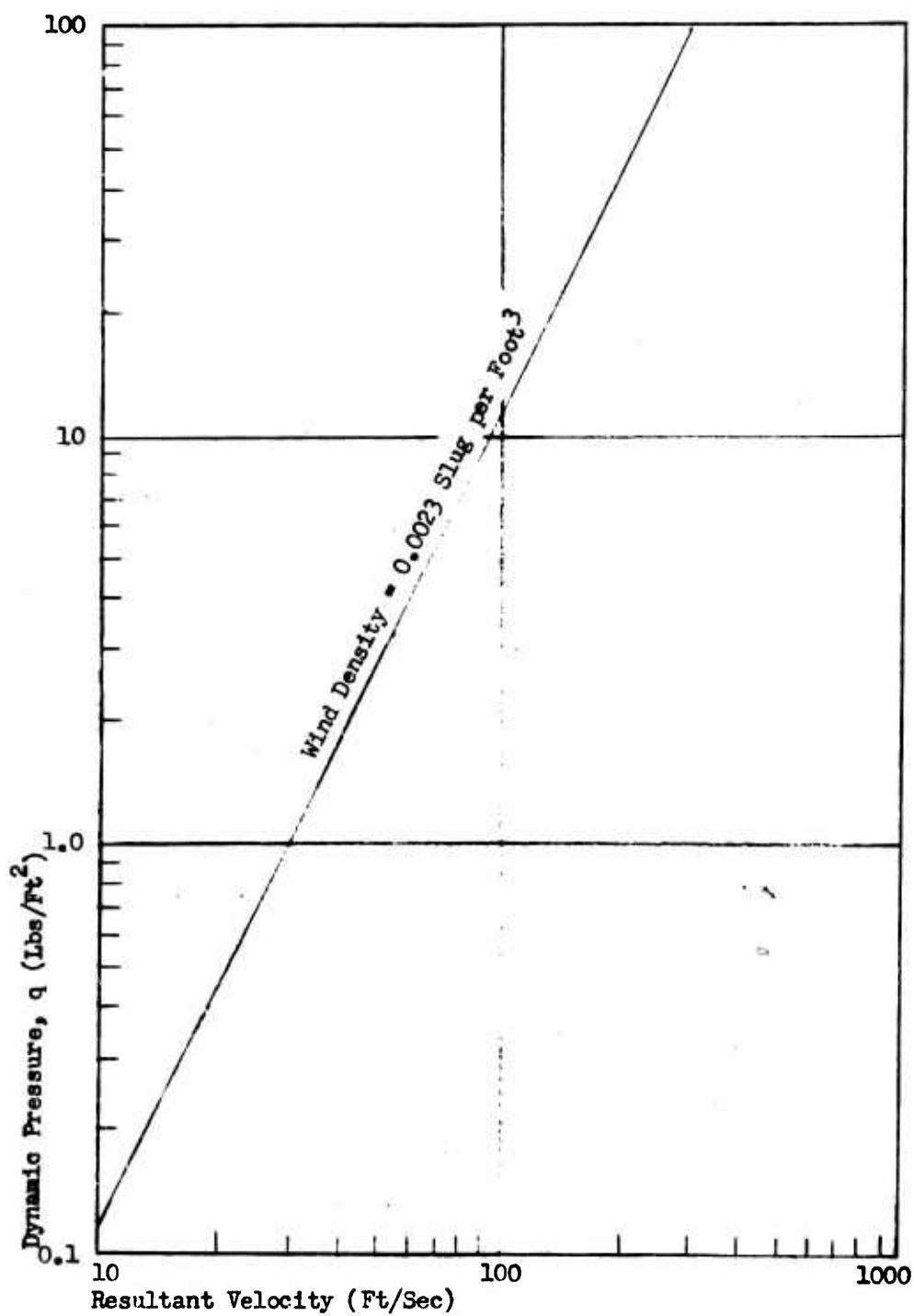


Figure 32. Resultant Velocity Versus Dynamic Pressure.

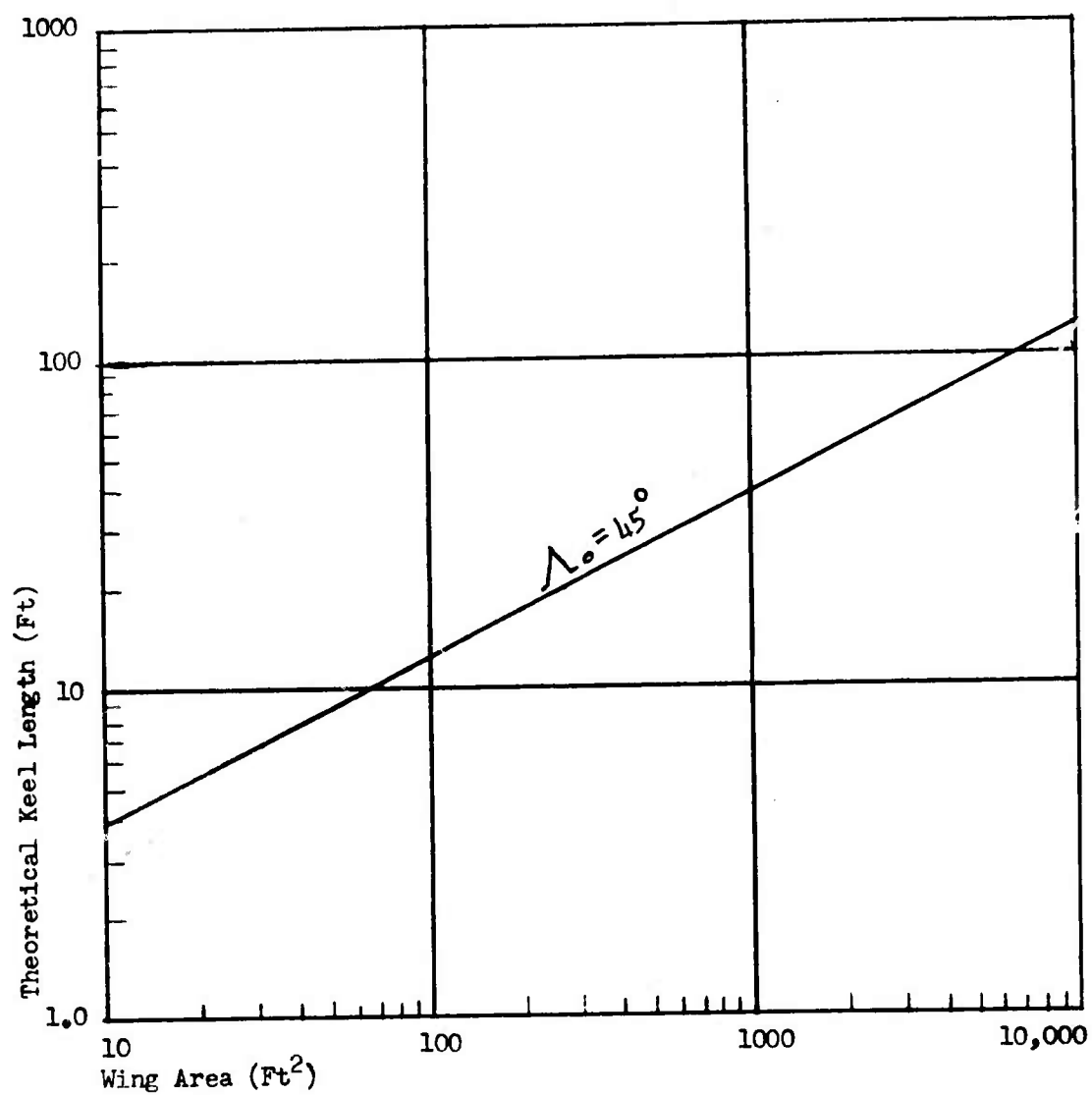


Figure 33. Wing Planform Area Versus Keel Length.

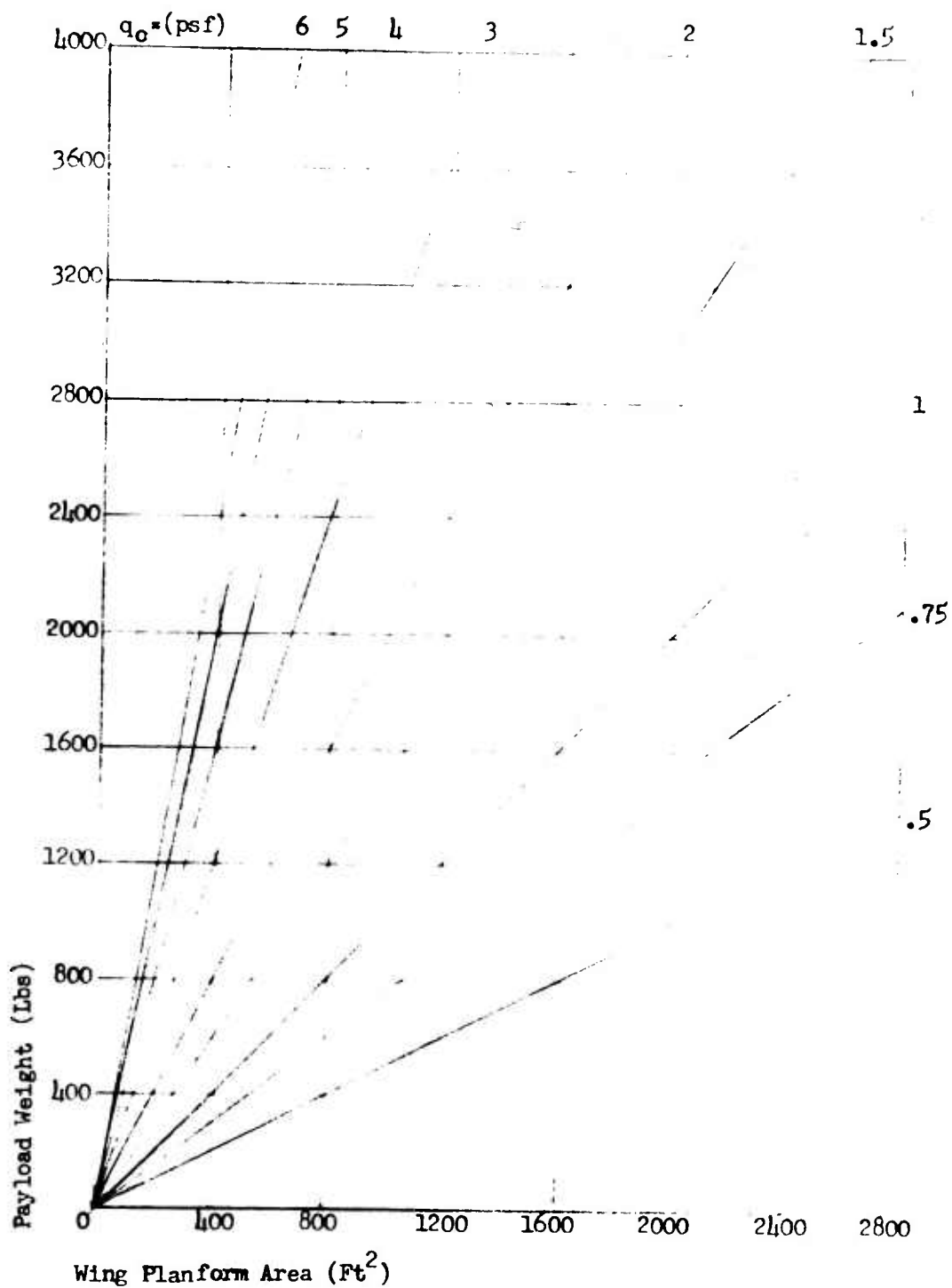


Figure 34. Wing Planform Area Versus Payload Weight Versus Wing Loading.



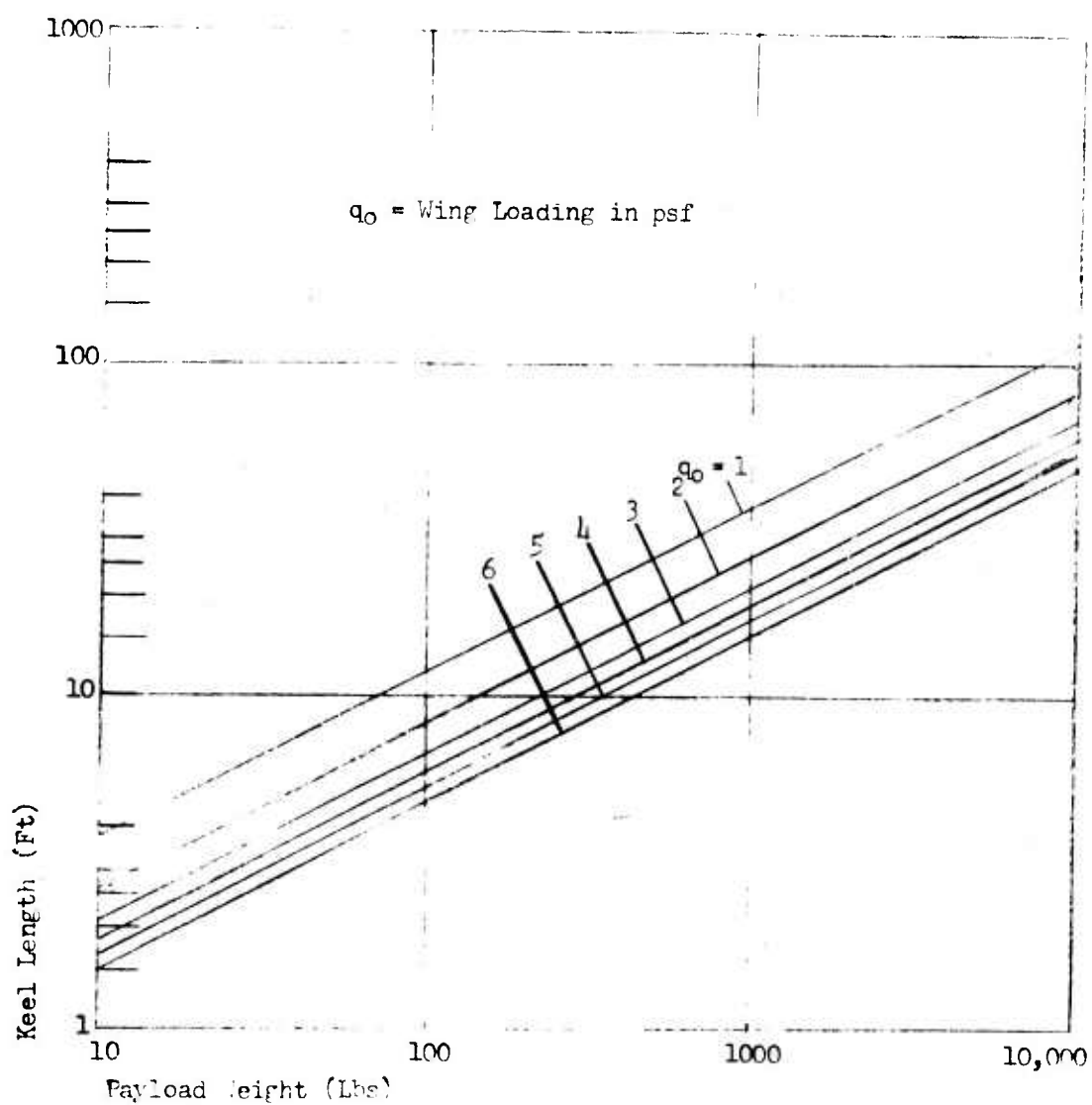


Figure 35. Payload Weight Versus Keel Length Versus Wing Loading.

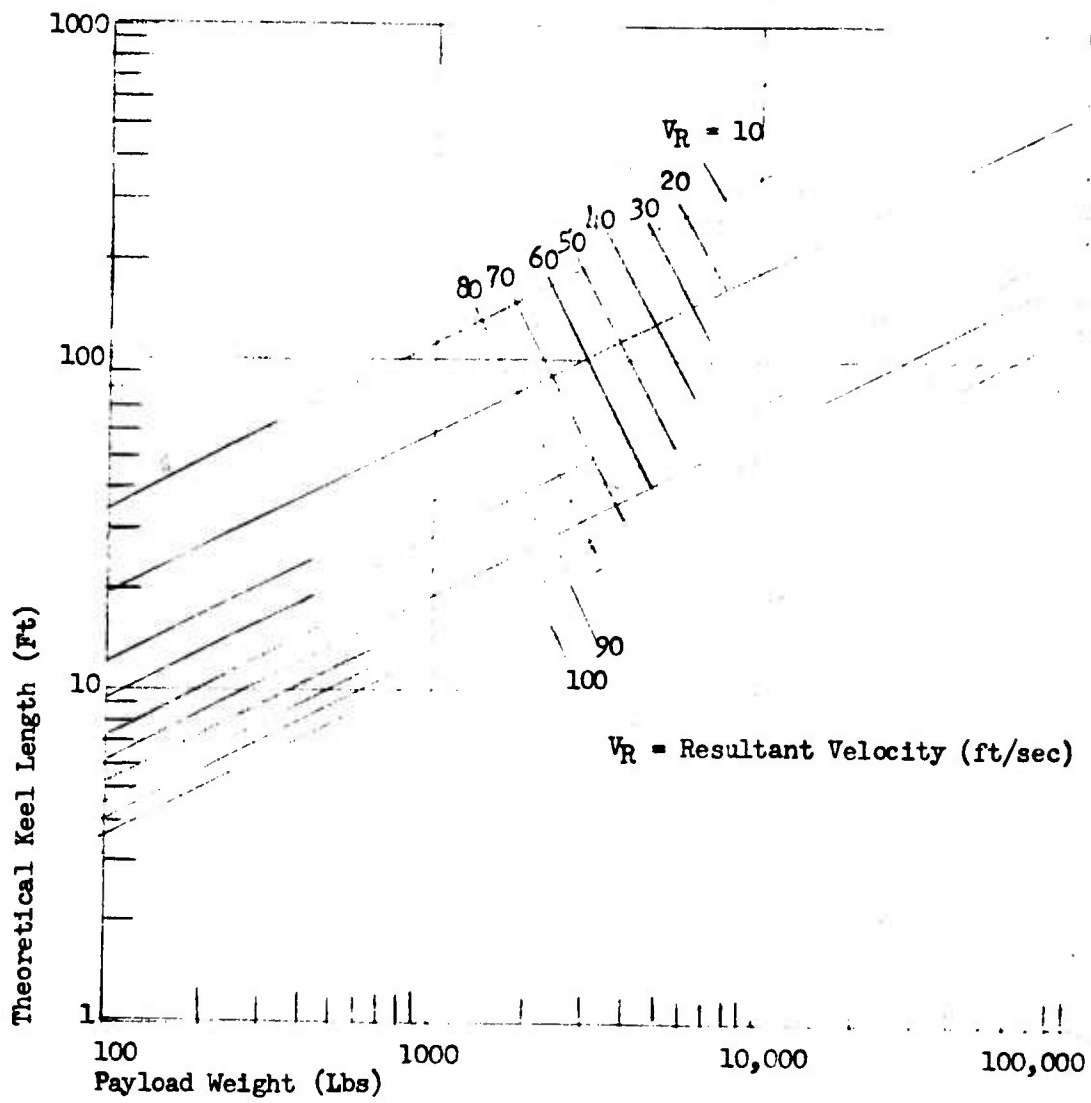


Figure 36. Payload Weight Versus Keel Length Versus Resultant Velocity.

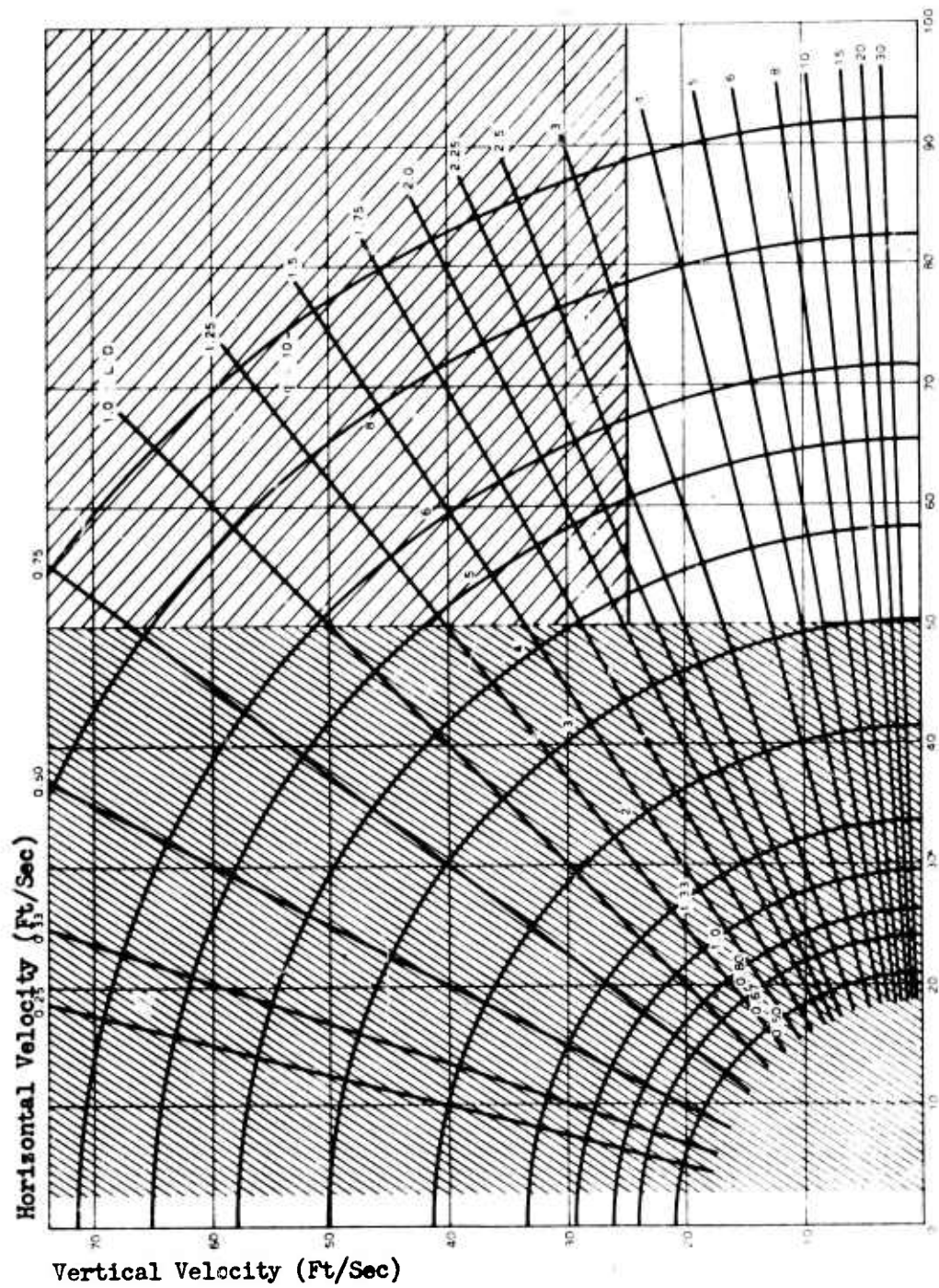
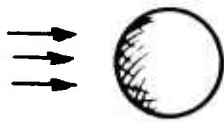
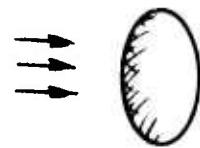
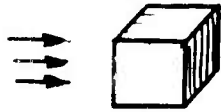
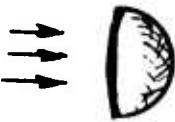

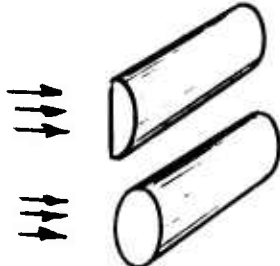
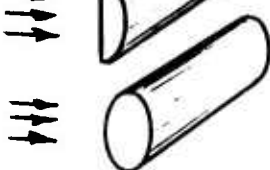


Figure 37. Velocity Versus L/D Versus Wing Loading.

Payload	$C_{D_0}$
	0.47
	0.59
	1.05
	1.17
	0.8
	1.17
	0.875

$S_{REF}$  = Frontal Area Exposed to Flow

Figure 38. Drag Coefficients.

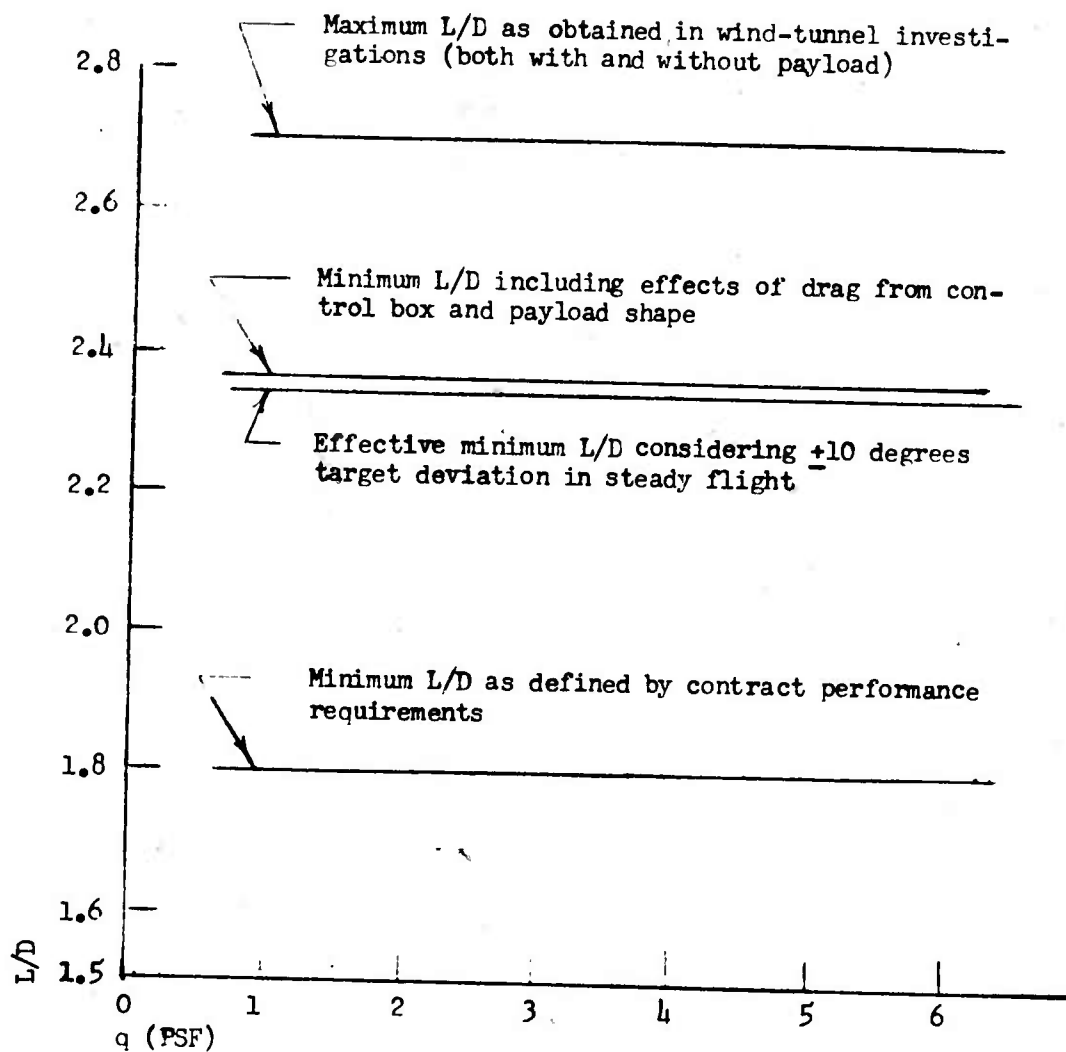
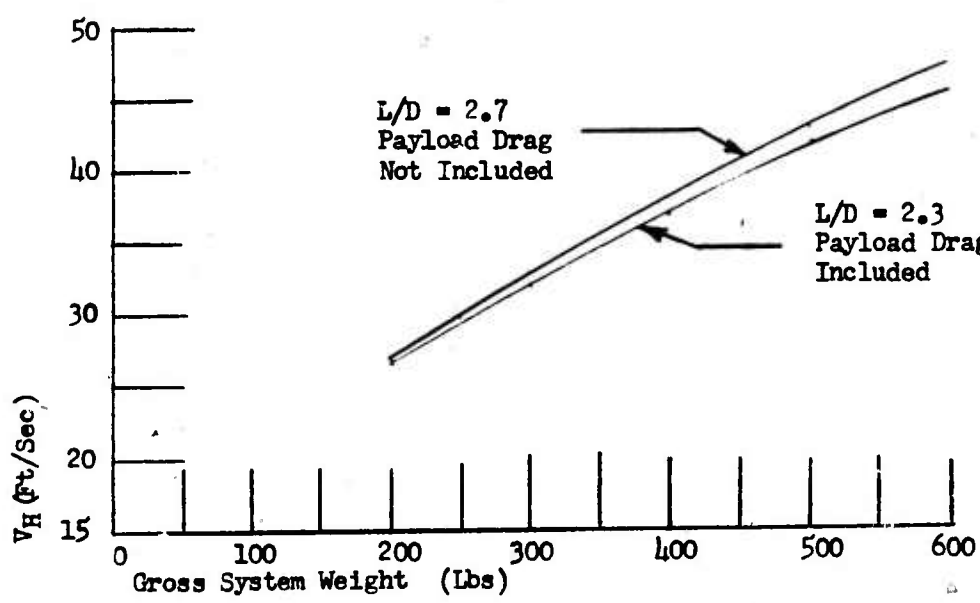


Figure 39. Performance Characteristics -  
18-Foot Keel Length Parawing.

18-Foot Single-Keel Parawing  
Horizontal Velocity Versus System Weight



18-Foot Single-Keel Parawing Vertical  
Descent Rate Versus System Weight

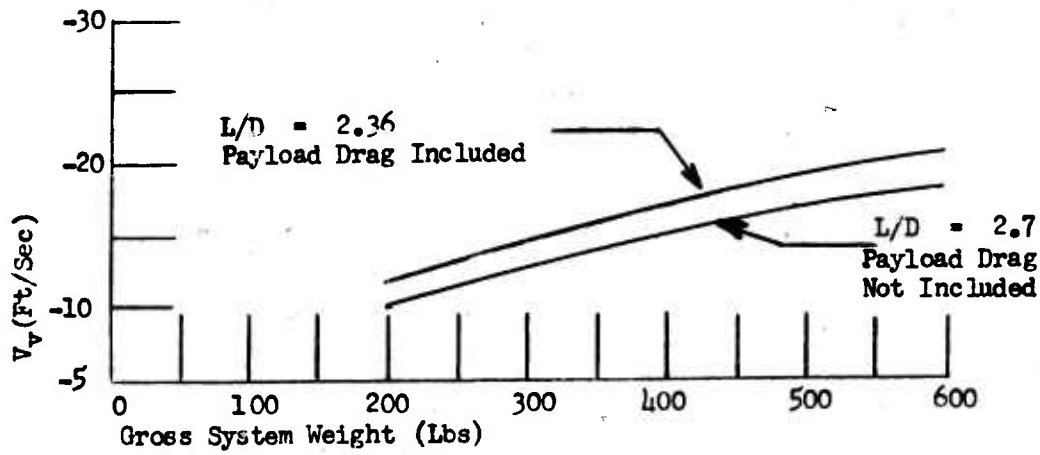


Figure 40. 18-Foot Single Keel Parawing Performance.

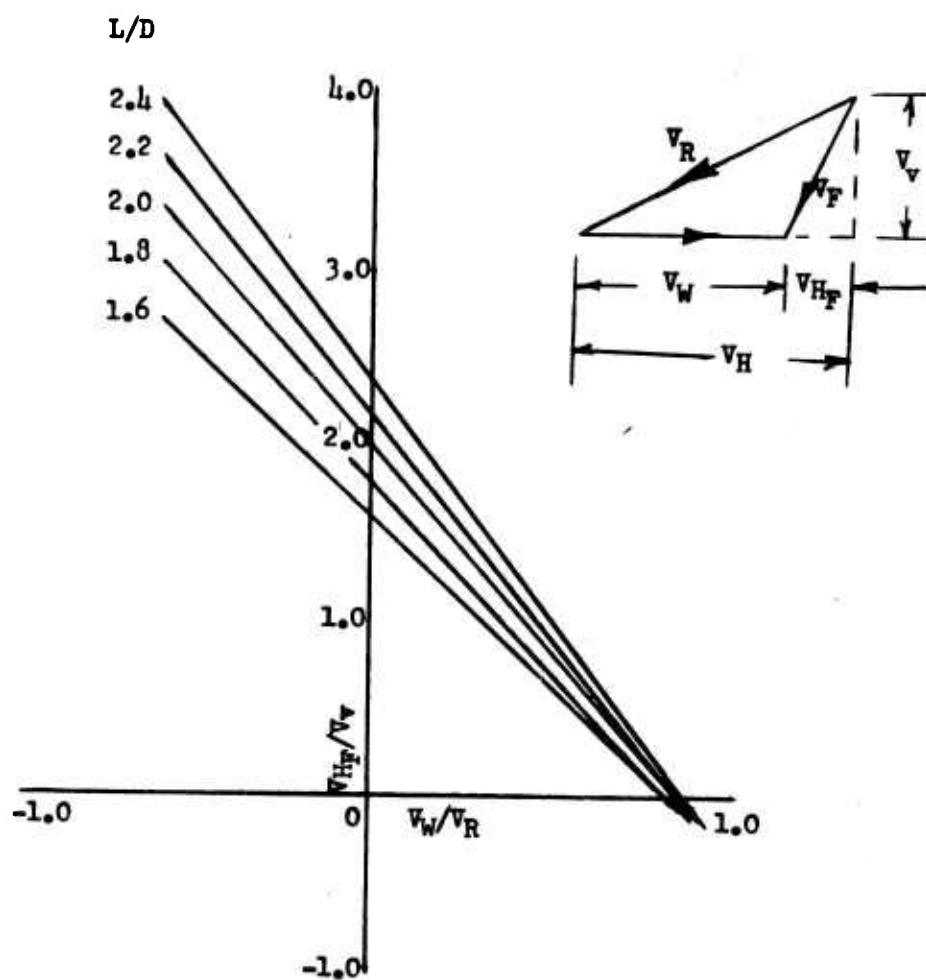


Figure 41. Effect of Ground Wind on Glide Path.

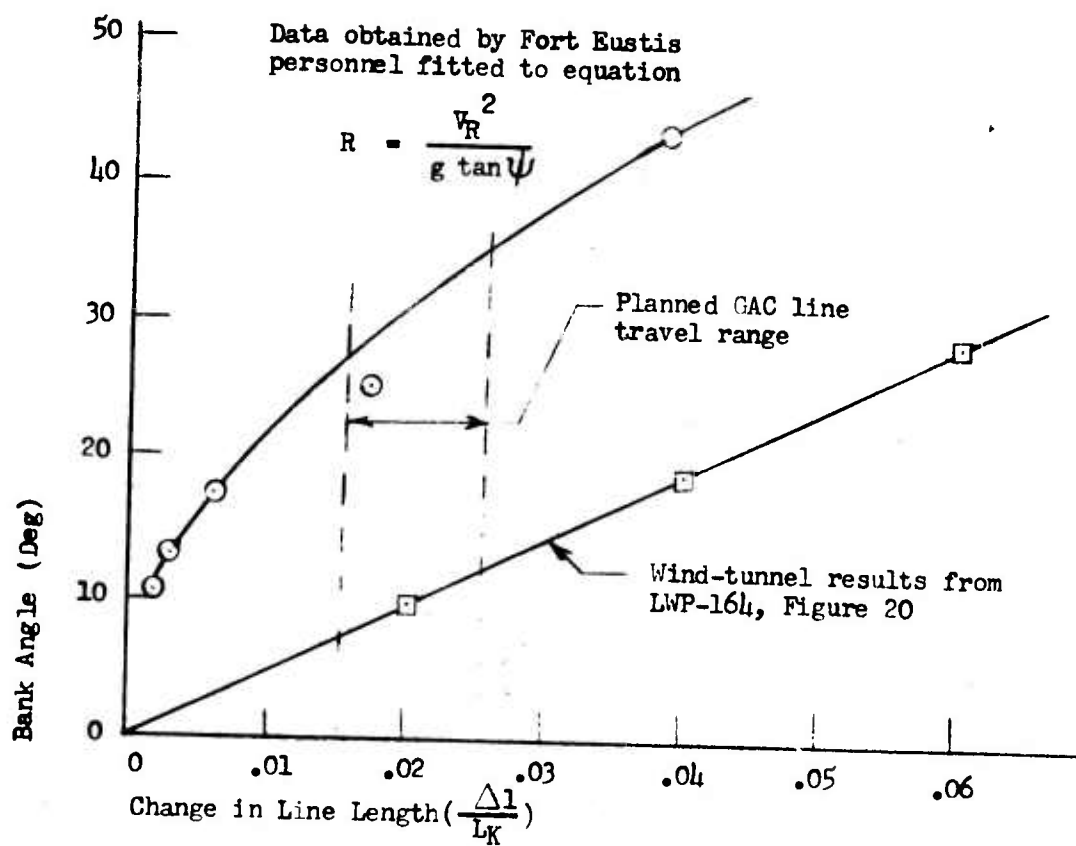
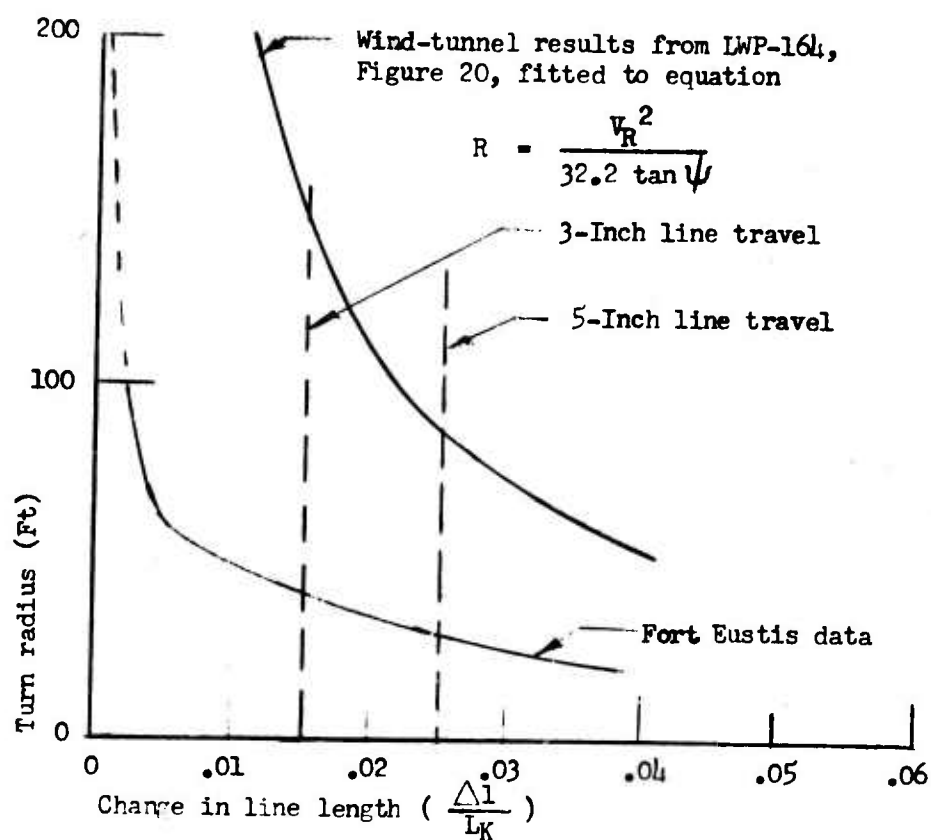


Figure 42. Bank Angle Versus Control Line Retraction.





(Note: All data is for a glide velocity of 24 feet per second and an  $L/D = 2.0$ .)

Figure 43. Radius of Turn Versus Control Line Retraction.

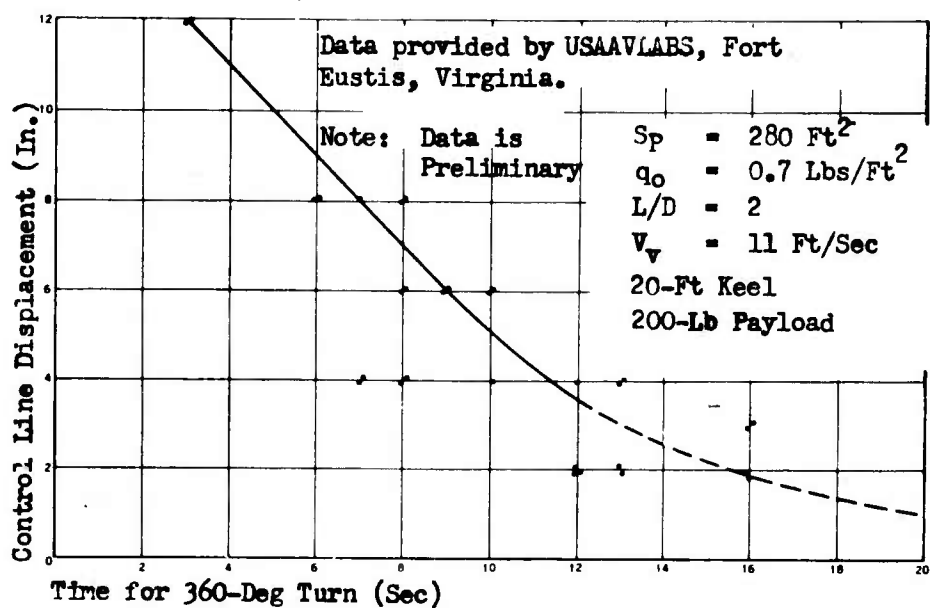


Figure 44. Control Line Displacement Versus Turn Time.

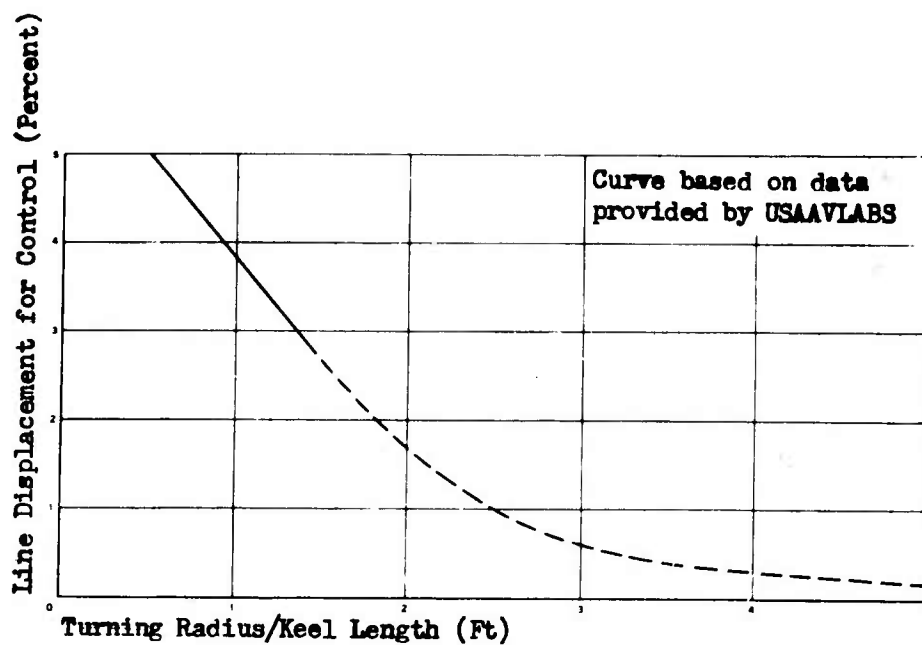


Figure 45. Control Line Displacement Versus Turning Radius.

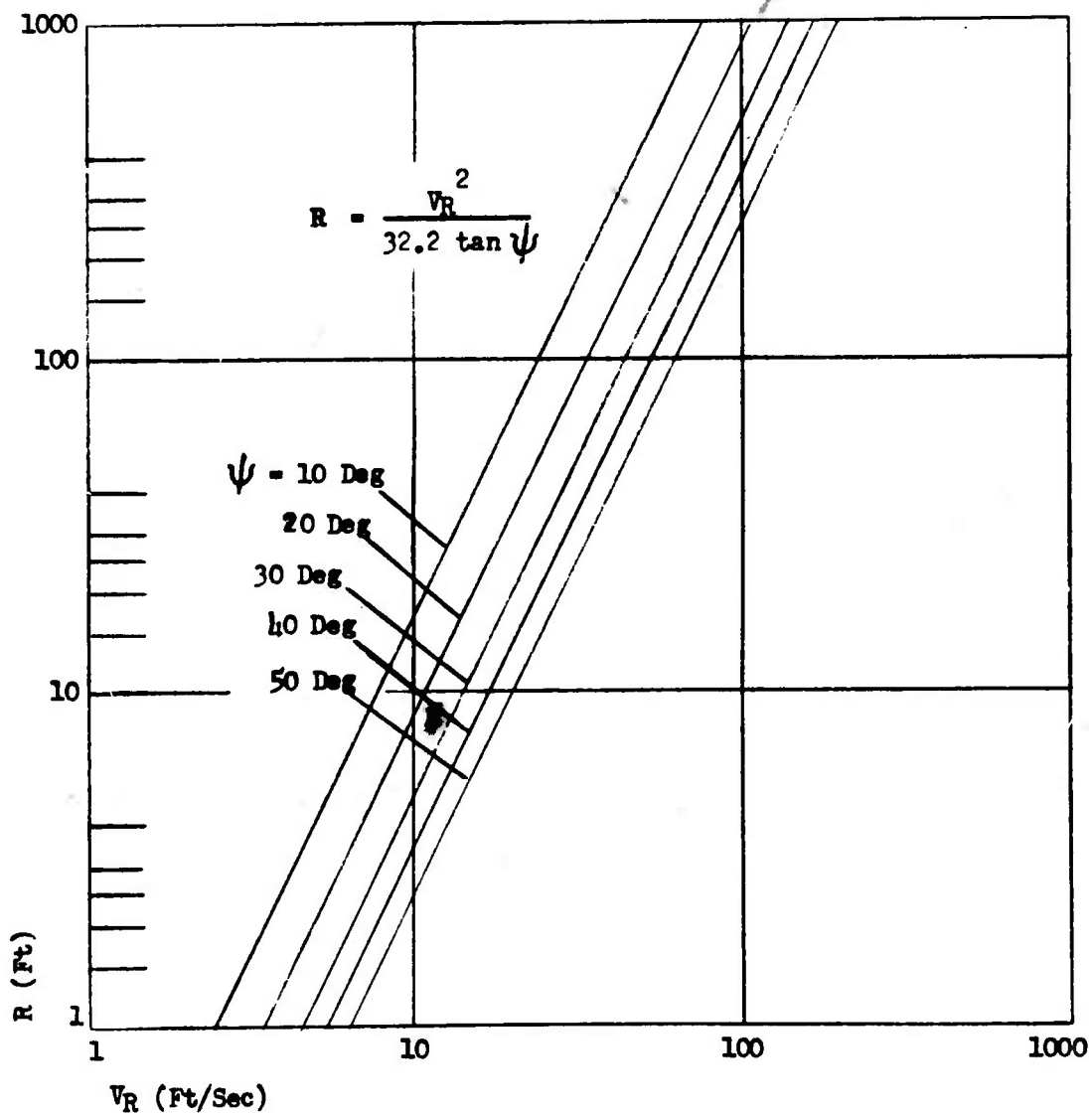


Figure 46. Turning Radii Versus Glide Velocities for Various Bank Angles.

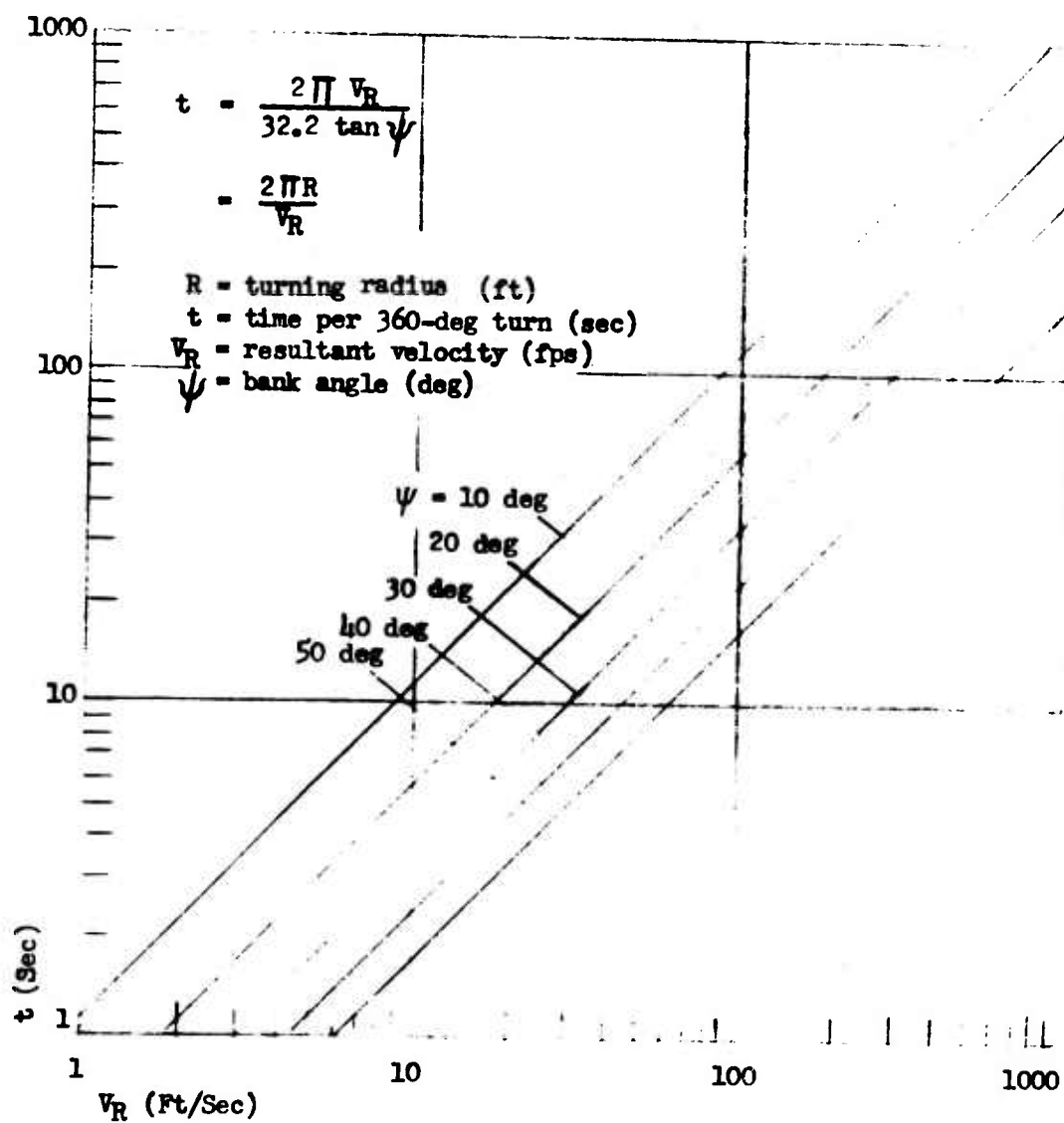


Figure 47. Turning Time Versus Glide Velocities for Various Bank Angles.

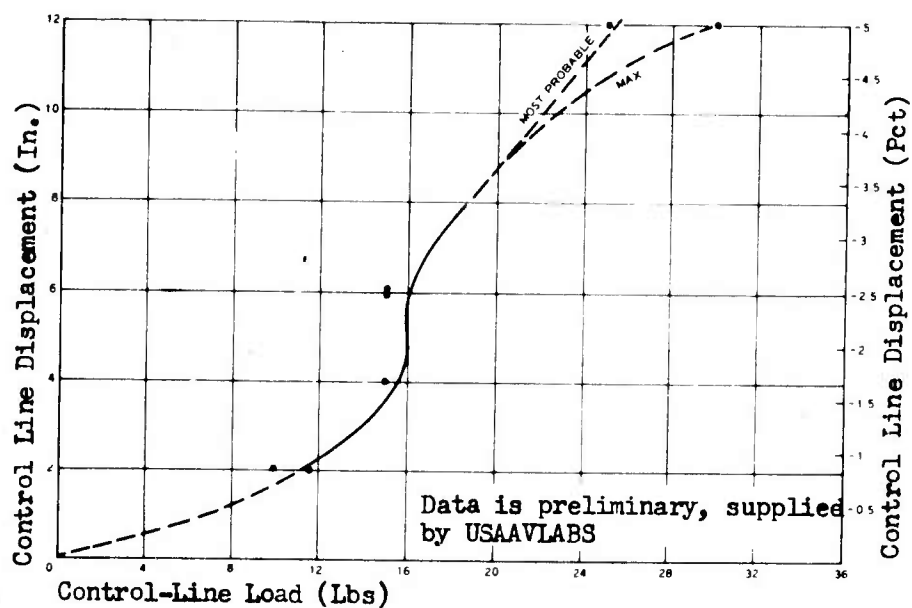


Figure 48. Control Line Displacement Versus Loading.

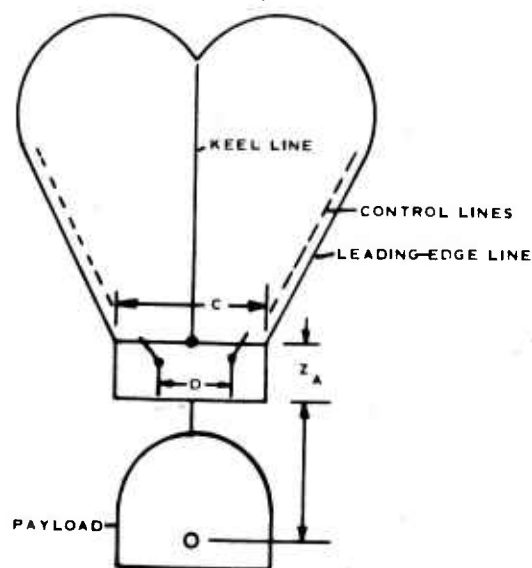


Figure 49. Typical Configuration.

## APPENDIX II PARAWING WIND-TUNNEL TESTS

### SUMMARY

GAC, in conjunction with NASA-LRC personnel, conducted a 4-day preliminary flight test program in the 30' x 60' full-scale tunnel.

The purpose of this program was to trim out, for flight, five variations of parawings. These included one each of the following items:

1. Standard single-keel parawing
2. Single-catenary-keel parawing
3. Twin-keel parawing - center area =  $1/3$  total area
4. Twin-catenary-keel parawing - center area =  $1/3$  total area
5. Twin-catenary-keel parawing - center area =  $1/2$  total area

Due to the limited time available, optimization of L/D performance was not attained. All five parawings were flown and trimmed out with data taken at wind speeds from 35-60 feet per second. (Wing loadings from 1.4 to 4.05 pounds per foot<sup>2</sup> were displayed.) The data obtained fits the pattern of previously published data obtained in this wind tunnel. In addition, two systems of rigging the parawing to the payload were tested with no apparent difference. The rigging established was very close to the line lengths shown on the preliminary drawings used to fabricate these first parawings.

### INTRODUCTION

GAC conducted a 4-day preliminary flight test program in the Langley full-scale 30' x 60' wind tunnel on several all-flexible parawing configurations. The purpose of this flight test program was to study comparative performance of several parawing configurations and to evaluate various payload rigging techniques. The results of this program were used in the initial phase of the GACS flight test program.

Both single- and twin-keel, full-scale parawings were tested, with and without catenary-keel panels. All configurations were trimmed out, and a minor effort was made to optimize the L/D due to the limited duration of the test program.

This appendix documents the results of the parawing test program conducted by GAC and NASA personnel during the period 6-11 June 1968. Included are descriptions of the test, plots of the reduced data, and GAC's interpretations of the test program results.

### TEST PROCEDURE

All tests were conducted in the open throat section of the Langley full-scale 30' x 60' wind tunnel. A tunnel speed of 35 feet per second was required to fly the parawings and to overcome the weight of the canopy material and steel suspension lines (approximately 50 pounds). Once the parawing was inflated, the line lengths were adjusted until a stable trim condition existed. Initial line length adjustments were made manually, while final changes were accomplished using turnbuckles. Some manual assistance was required in stabilizing the parawing until a trimmed condition was obtained.

All initial test runs were conducted at a tunnel speed of 35 feet per second. Additional runs were made at tunnel speeds of 40, 45, 50, 55, and 60 feet per second. If the nose would tend to buckle under at higher velocities, the tests were stopped, and additional rigging changes were attempted. Flow dynamic pressures of 1.4 up to 4.05 were obtained during the test runs. During all tests, lift and drag data was obtained for later reduction. Tares were obtained before and after each set of runs to insure data accuracy. At the conclusion of the test program, a dynamic pressure survey of the test section was made to determine any adverse effects due to the open section on the tunnel floor. No flow field variations were found; thus, the tunnel flow was assumed to be horizontal.

### DESCRIPTION OF PARAWINGS TESTED

Six parawing configurations, including three single and three twin keel, were tested, including five actual parawings. Figure 50 shows the canopy shapes obtained during the test program. Figure 51 is the twin-catenary-keel parawing showing the test setup.

A summary of the important physical features of the parawings tested is presented in Table XXVII.

TABLE XXVII. PHYSICAL CHARACTERISTICS OF THE PARAWINGS TESTED AT THE WIND TUNNEL				
Type	Catenary	$L_K$	$S_{REF}$	No. of Suspension Lines
Single	No	18	220	23
Single	Yes	18	220	18
Single	Yes	16	180	18
Twin	Yes	16	270	24
Twin	No	16	270	34
Twin	Yes	16	370	24

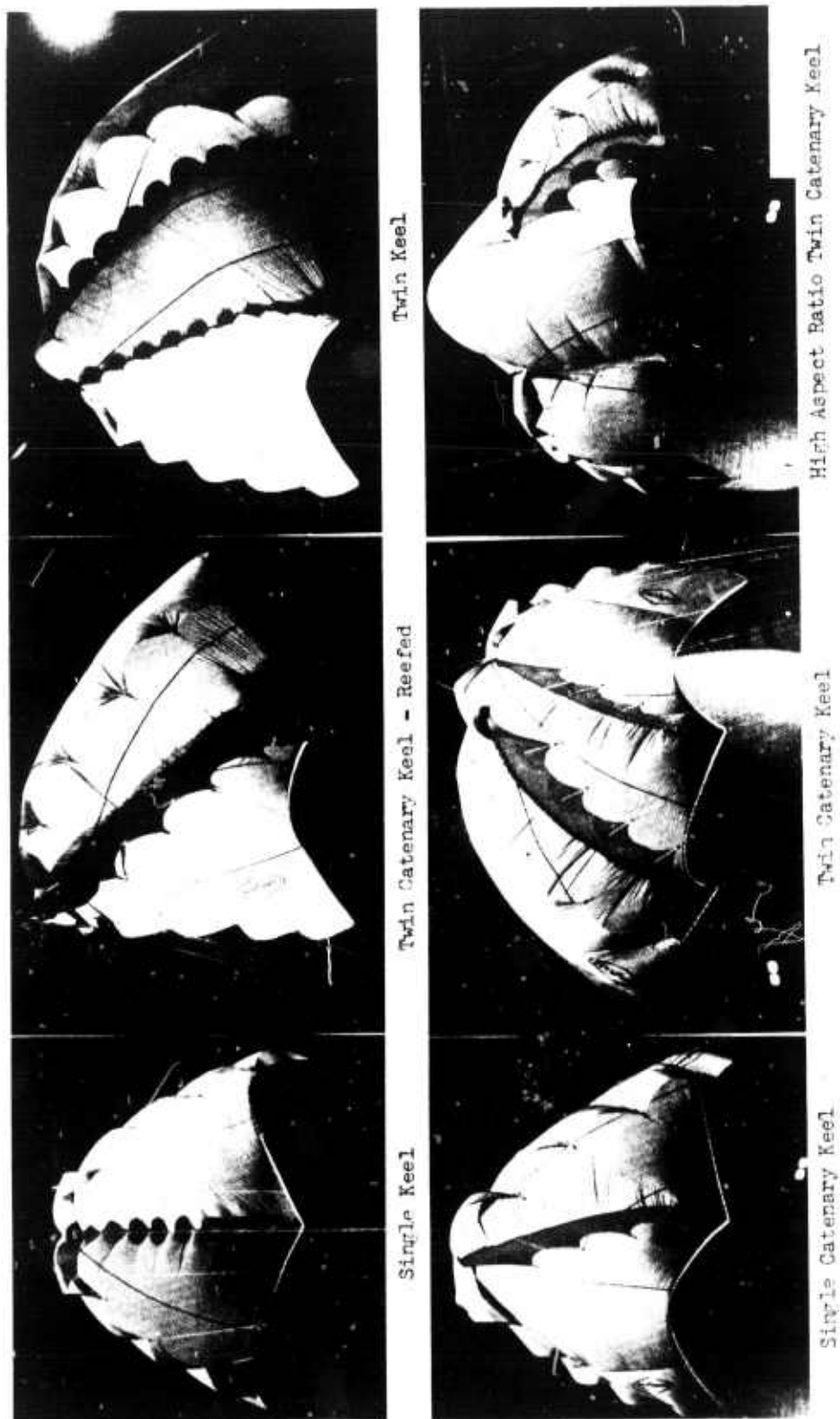


Figure 50. Wind-Tunnel Parawing Test



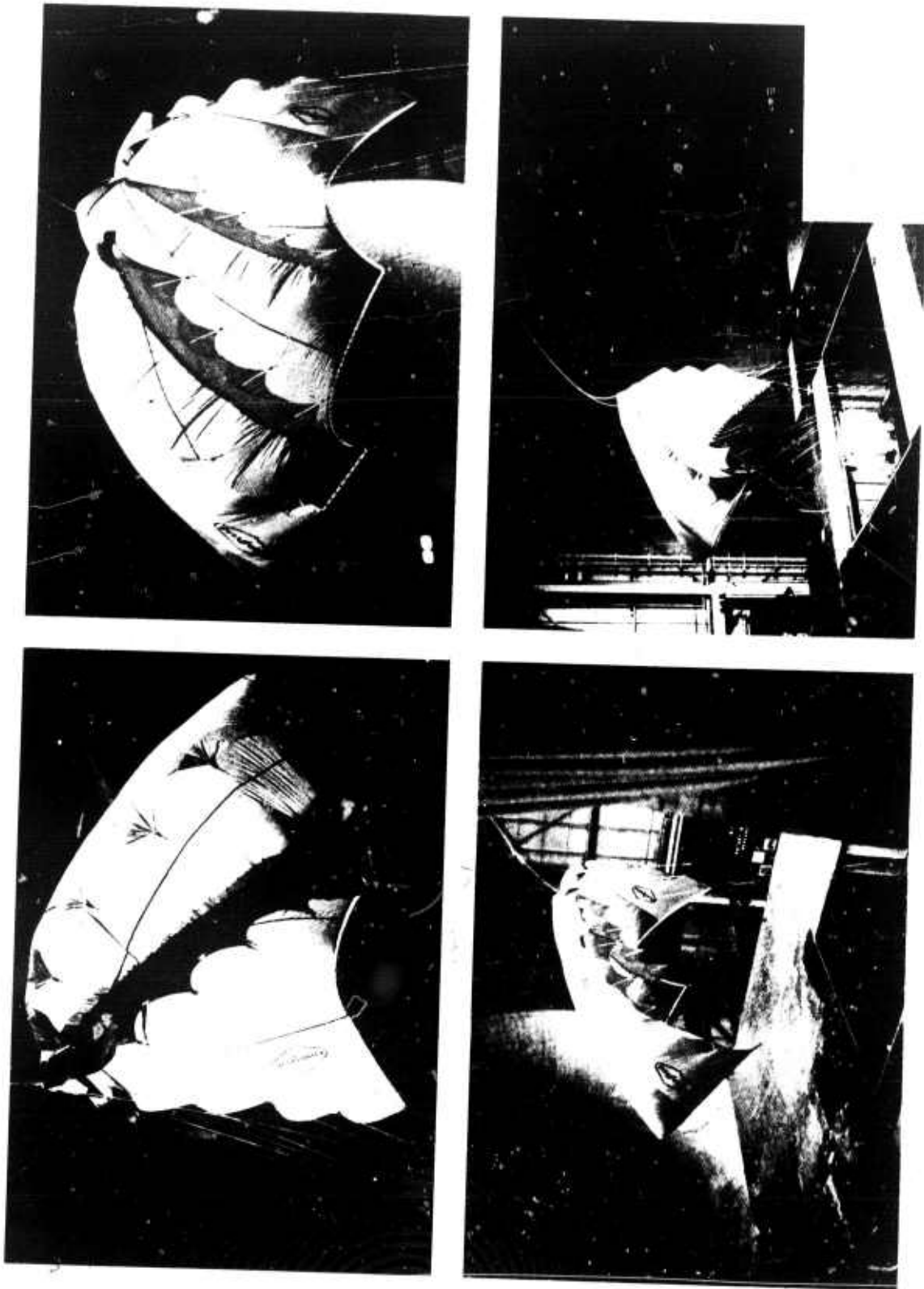


Figure 51. Wind-Tunnel Test Setup

All parawings were rigged to a model of the actual flight control box. Leading-edge lines were suspended from the sides of the control box while the keel line suspension was changed. Two methods of rigging the keel lines were used with no apparent effect on the performance of the parawings. The first attached the keel lines alternately from the front and rear suspension points, while the second added an additional No. 4 keel line to allow for rigid forward and aft rigging as shown in Figure 52.

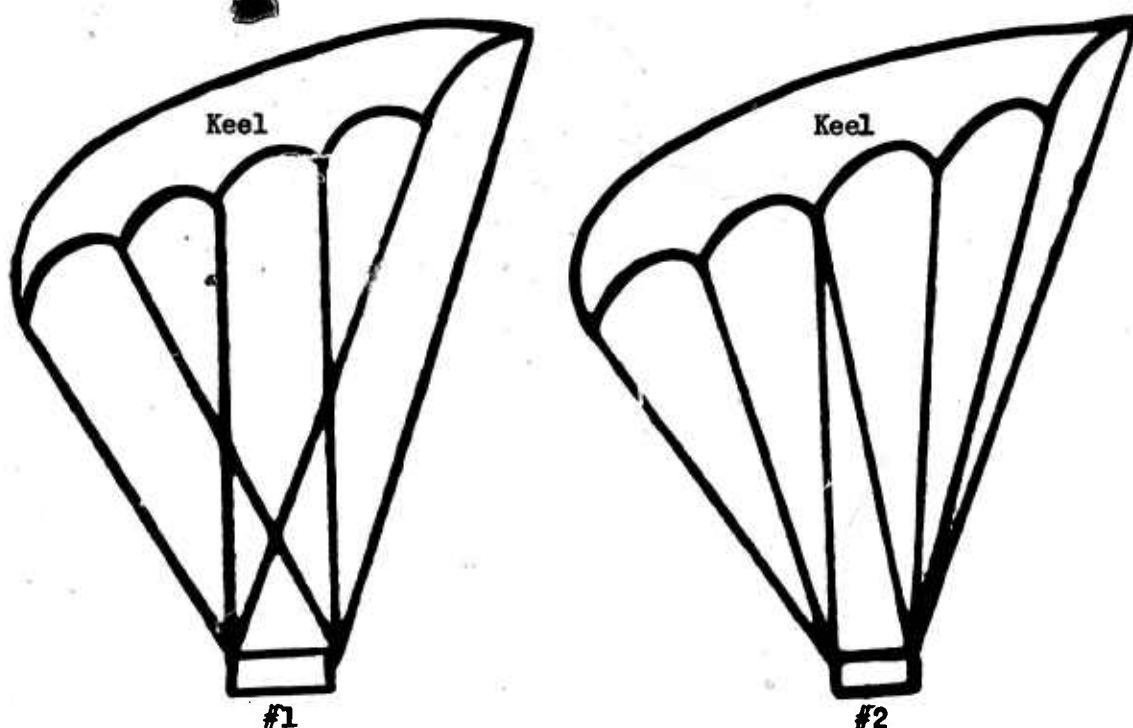


Figure 52. Keel Rigging for Wind-Tunnel Tests

All suspension lines were of 1/8-inch-diameter steel cable to eliminate the line stretch as one variable in the tests.

#### PRESENTATION OF DATA

The reduced data, which includes lift-to-drag ratio ( $L/D$ ), lift coefficient ( $C_L$ ), and drag coefficient ( $C_D$ ), is presented in Figures 53 through 57. Lift-to-drag ratio is shown in Figures 53, 54, and 55 as a function of dynamic pressure for each configuration tested. Lift and drag coefficients in the drag polar form are presented in Figures 56 and 57 for both the single- and twin-keel parawings tested. Line lengths which correspond to the best trimmed condition obtained for each configuration are listed in Table XXVIII.

## DISCUSSION OF TEST RESULTS

The parawing wind-tunnel test results have established that the performance characteristics of the parawings tested compared favorably with those obtained by Northrop Ventura on their 15-foot keel length models. These facts were established with the assistance of NASA wind-tunnel personnel during the test program. Due to the short duration of the test program, no significant attempt was made to vary the lengths of the keel and aft lines in a systematic process to optimize L/D. Therefore, major emphasis was placed on the adjustment of line lengths to obtain a trimmed configuration with a smooth canopy surface. The results presented then are not representative of optimum performance.

Figures 53, 54, and 55 show L/D characteristics obtained for each single- and twin-keel parawing tested. Shown in Figures 53, 54, and 55 is the relative comparison between the single-keel parawing with and without a catenary. No significant differences are evident in the performance characteristics between the two wings; however, an examination of Table XXVIII, which lists the line lengths of the two wings, has shown that a 2-percent shortening of the tip lines on the catenary-keel parawing was made. Previous wind-tunnel results have shown that a shortening of the tip lines would increase L/D approximately 10 percent. If this rule is adhered to, then, based on the data presented, it is concluded that the catenary-keel panel will slightly degrade performance. This could occur because of the added drag on the catenary-keel panel and a change in the flow characteristics over the nose region. Figure 53 also shows that the weight of the steel lines in the nose was detrimental in that the lightly loaded nose tips were pulled down, thus degrading performance. It was concluded that lightweight nylon lines should be used in the nose region to obtain an improved trimmed configuration.

Also shown in Figure 53 is the effect of a modified rigging technique in which the keel lines were not alternately attached to the front and rear suspension points. The modified rigging had the Nos. 1, 2, 3, and 4 keel lines attached to the forward suspension point. The Nos. 4, 5, and 6 keel lines were attached to the rear or aft suspension point. No significant line length changes in the keel panel were required to trim out this configuration and no significant performance changes were noted. The slight reduction in L/D is within the data accuracy of the test.

Figures 56 and 57, which are drag polar curves of the aerodynamic coefficients  $C_L$  and  $C_D$ , show that the single-keel parawing test results did give consistent data. Comparison of this drag polar curve with other wind-tunnel data on single-keel parawings as furnished by NASA-Langley tunnel personnel during the test program showed that the data did compare favorably. This data showed that a true optimum L/D was not obtained. There appeared to be no reason why higher L/D's could not be obtained had the test program duration been longer.

The reduced data on the twin-keel parawing is presented in Figures 54, 55, and 57. L/D characteristics of the small twin-keel parawing (see Figure 54)

with and without a catenary-keel panel has indicated an opposite trend in performance to the single-keel configuration. A comparison of the line lengths of the two twin-keel parawings has revealed no major differences except that the aft keel line is approximately 3 percent shorter for the catenary-keel version. Previous wind-tunnel studies have shown that a shortening of the aft keel line decreased L/D by 10 percent. The data showed only about a 5-percent reduction in L/D, which indicated that the catenary-keel panel did not degrade performance but instead improved performance on the twin-keel parawing. The L/D data on the high-aspect-ratio twin-keel parawing was the highest obtained during the test program. Figure 57, which is a drag polar of the twin-keel configurations, was compared to that of other twin-keel configurations tested in the wind tunnel, with no significant differences being noted.

The effect of dynamic pressure on L/D is not clearly defined. A general trend toward higher L/D's with increasing dynamic pressure was evident from the test results. Reasons for some runs decreasing with L/D are not apparent but could be due to the nose tucking under and the subsequent tendency of the wing to stall.

Table XXIX presents a summary of the data obtained during the wind-tunnel effort.

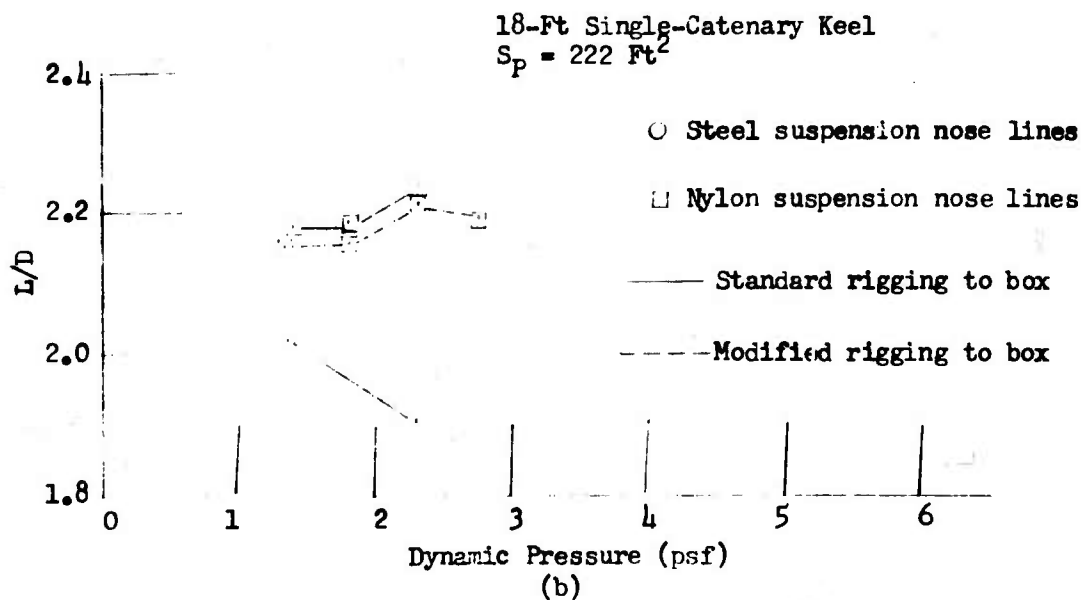
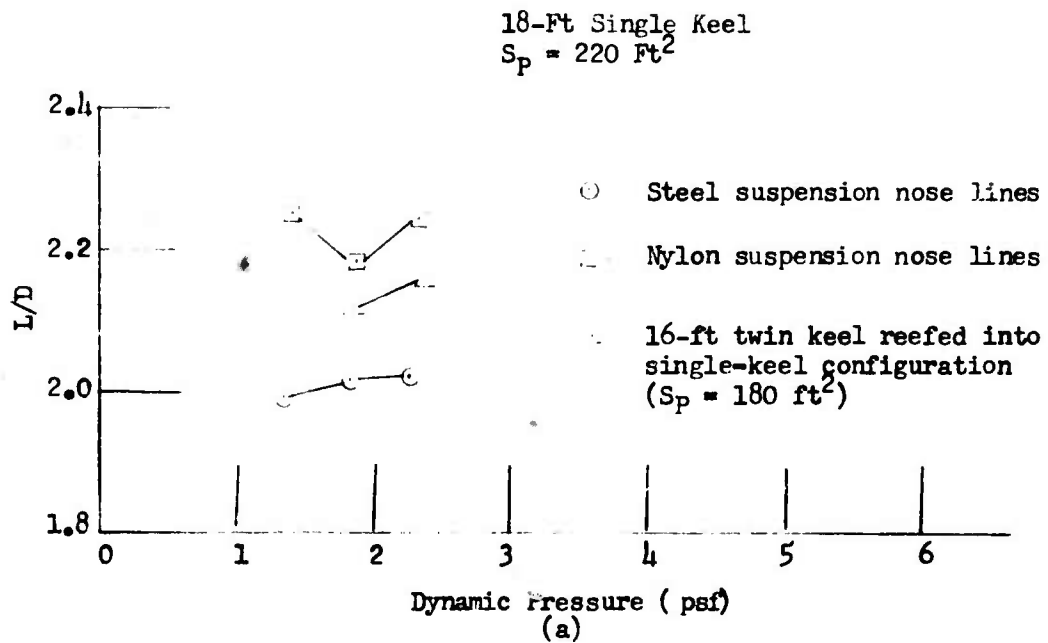


Figure 53. L/D Versus  $q$  for 18-Ft Single-Keel Parawings.

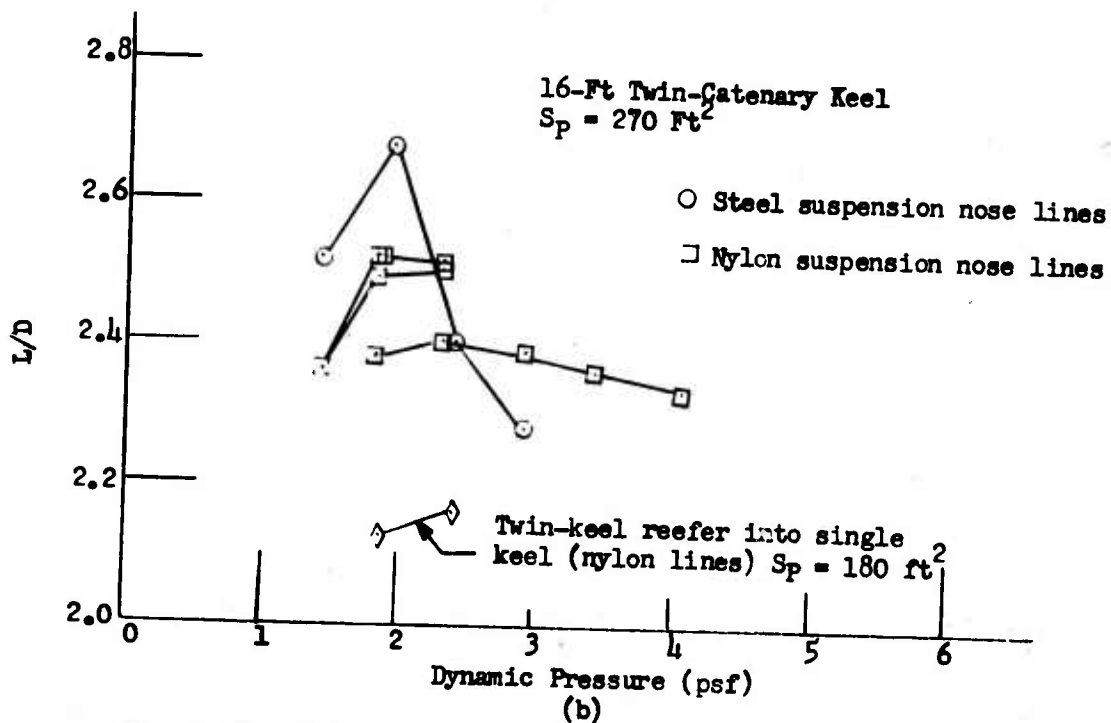
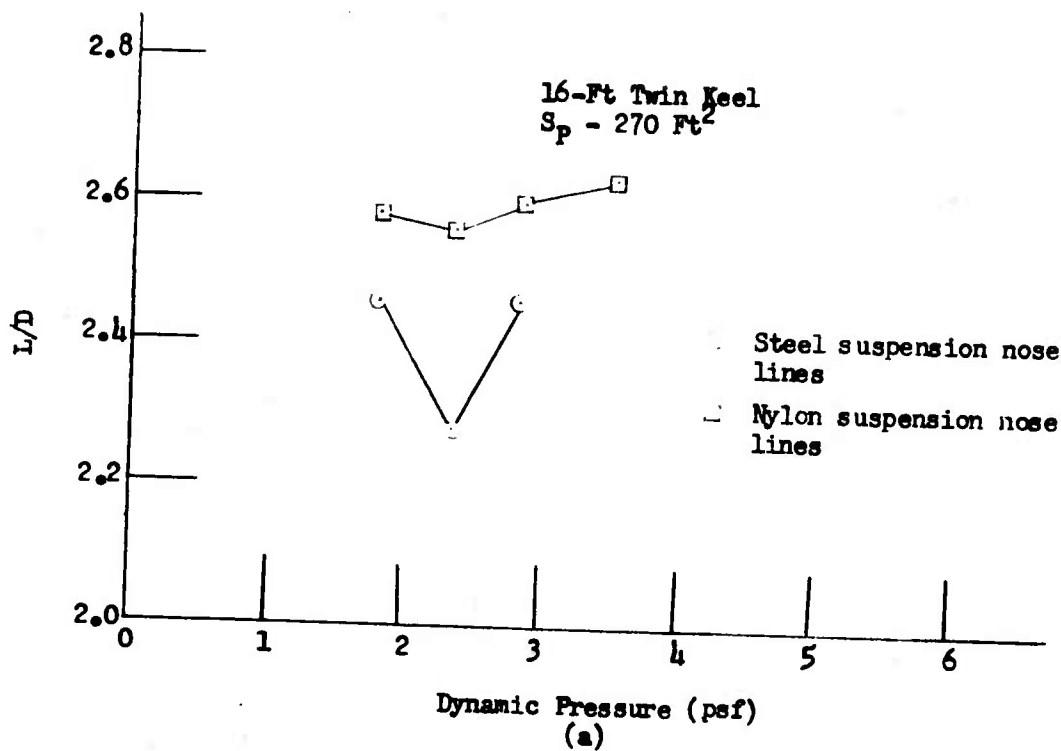


Figure 54.  $L/D$  Versus  $q$  for 16-Ft Twin-Keel Parawings.

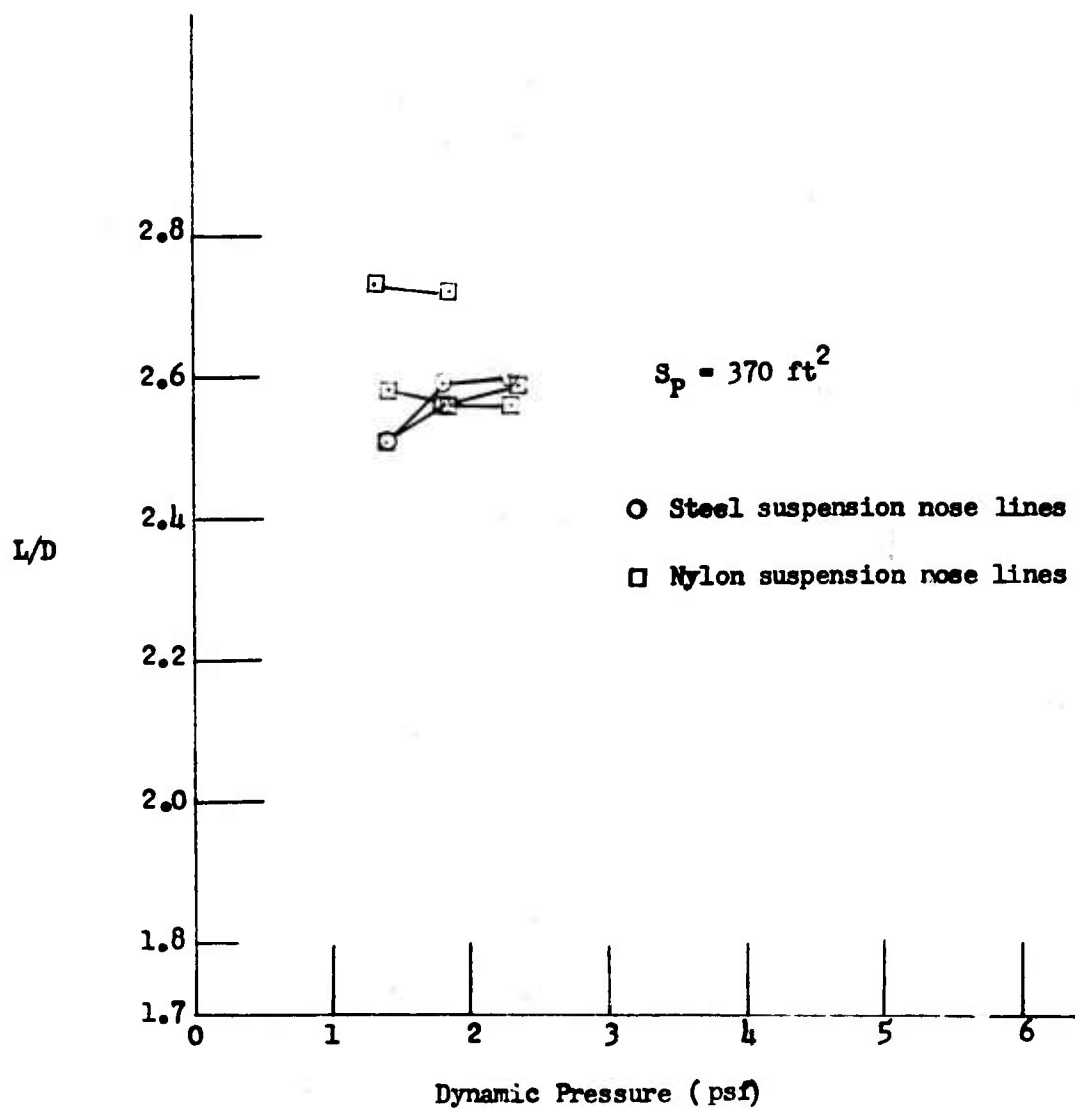


Figure 55.  $L/D$  Versus  $q$  for 16-Ft High-Aspect-Ratio Twin-Catenary Keel Parawing.

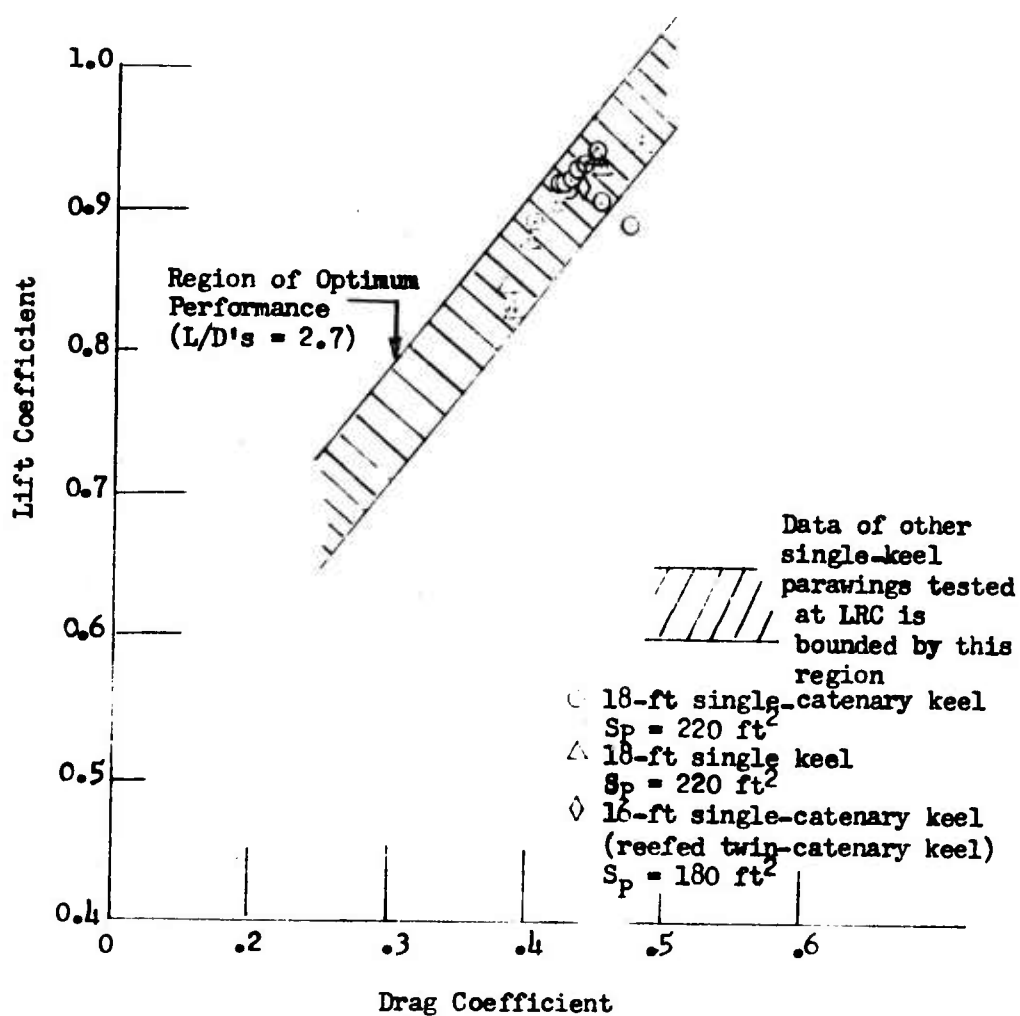


Figure 56.  $C_L$  Versus  $C_D$ , Single-Keel Parawing.



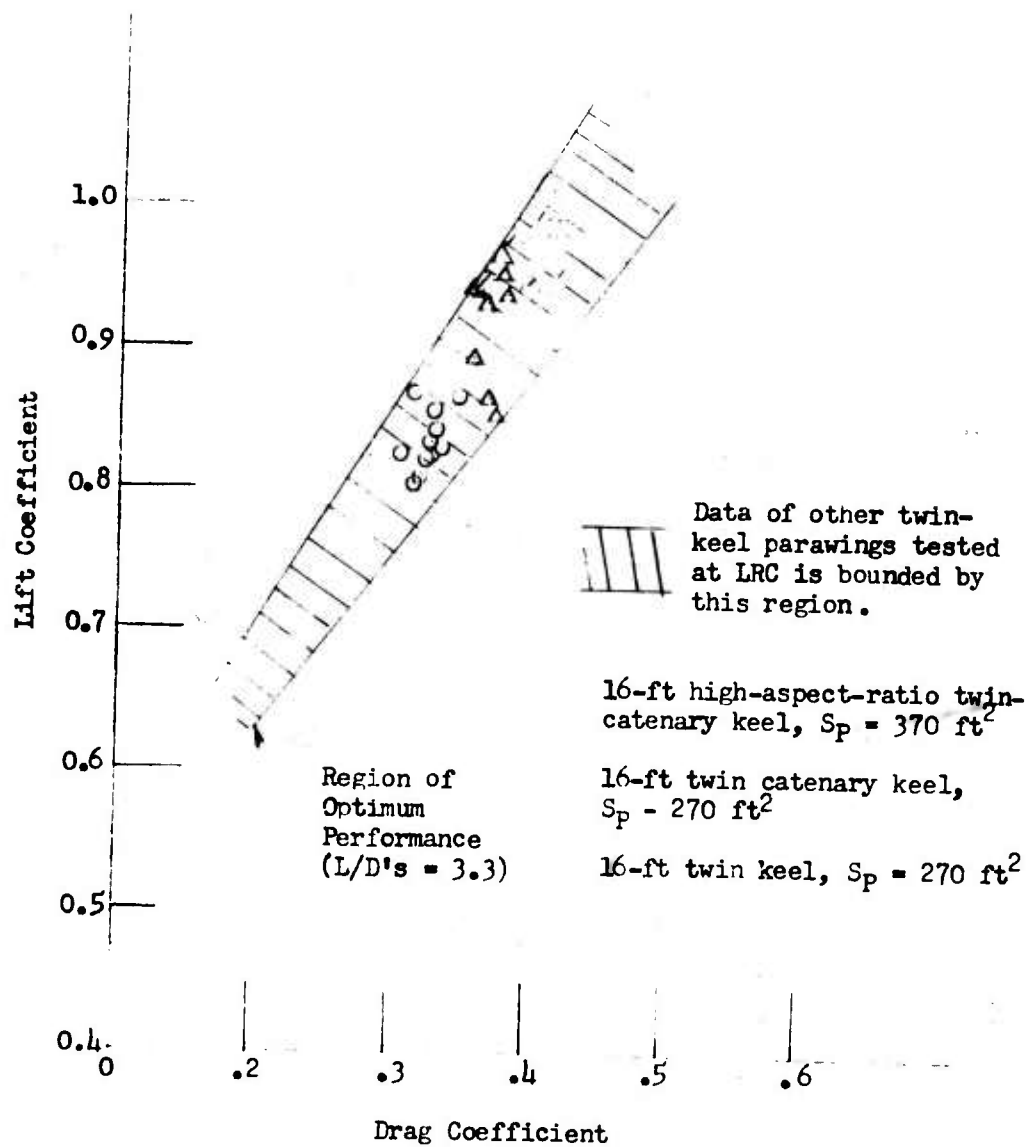


Figure 57.  $C_L$  Versus  $C_D$  Twin-Keel Parawings.

TABLE XXVIII. FINAL LINE LENGTHS (WIND TUNNEL)											
Position	No. of Lines	Single Keel		Single Keel		Twin Keel		Twin Keel		Large Twin Keel	
		Without Catenary (Ft)	(In)	With Catenary (Ft)	(In)	Without Catenary (Ft)	(In)	With Catenary (Ft)	(In)	With Catenary (Ft)	(In)
Keel Lines	1	22	3	24	4	21	2-7/8	21	2-3/4	21	8-1/2
	2	23	1-1/4	22	9-3/4	21	4-1/4	21	5	20	5-1/8
	3	22	3-3/4	22	5/8	20	7	20	9-1/8	19	8-1/2
	4	21	1-1/8	20	11	19	8-3/4	19	8-1/4	18	6-1/2
	5	19	10-5/8	19	7-3/4	18	-	18	3/8	16	9-3/8
	6	18	5-7/8	18	-	16	1/2	16	1-1/8	15	1/8
Leading-Edge Lines	1	22	8	23	4-1/4	21	9-1/4	-	-	20	6-1/2
	2	23	4-5/8	22	3-1/2	21	11-3/4	20	4-1/2	19	5
	3	24	-	22	1	22	5	19	10-3/4	19	5-1/2
	4	23	5	21	10-1/2	22	4	19	5-1/4	19	3-1/4
	5	23	8-3/4	21	2-3/4	22	4	18	11-1/8	18	5-1/2
	6	23	8-3/4	20	3	21	8	18	9-1/2	17	7-1/8
	7	23	8-3/4	-	-	21	8	-	-	-	-
	8	23	5-7/8	-	-	21	4-3/4	-	-	-	-
	9	23	6-1/8	-	-	21	-	-	-	-	-
	10	21	8	-	-	20	3-3/4	-	-	-	-
	11	20	3-1/2	-	-	19	3-1/2	-	-	-	-

TABLE XXIX. PARAWING WIND-TUNNEL FLIGHT TEST RESULTS						
Run No.	Configuration	Velocity (Ft/Sec)	q (PSF)	Lift (Lbs)	Drag (Lbs)	L/D
1	Reefed Twin-Catenary Keel (TCK) $S_p = 180 \text{ Ft}^2$	35	1.4	309	107	2.89
2	"	40	1.84	304	143	2.12
3	"	45	2.36	353	164	2.16
4	TCK $S_p = 270 \text{ Ft}^2$	35	1.43	344.5	137	2.52
5	"	40	1.91	487.5	182	2.68
6	"	45	2.4	562	237	2.38
7	"	50	2.89	665.5	292	2.28
8	"	40	1.8	479	201	2.38
9	"	45	2.29	614	256	2.4
10	"	50	2.89	744	313	2.38
11	"	55	3.41	901	382	2.36
12	"	60	4.02	1046	449	2.33
13	"	40	1.8	463	186	2.49
14	"	45	2.29	575	229	2.51
15	"	40	1.84	475	197	2.42
16	"	45	2.33	596	248	2.4
17	"	35	1.4	359	152	2.36
18	"	40	1.84	468	194	2.42
19	TK $S_p = 270 \text{ Ft}^2$	40	1.82	482	187	2.58
20	"	45	2.33	609	237	2.56
21	"	50	2.84	721	278	2.6
22	"	55	3.5	903	343	2.63
23	"	40	1.8	477	194	2.46
24	"	45	2.34	597	262	2.28
25	"	50	2.82	714	290	2.46
26	Single-Catenary Keel (SCK) $S_p = 220 \text{ Ft}^2$	35	1.36	276	127	2.18
27	"	40	1.8	359	178	2.02
28	"	45	2.29	449	237	1.9
29	"	35	1.38	283	130	2.18
30	"	40	1.8	363	167	2.18
31	"	45	2.29	449	201	2.24
32	SCK $S_p = 220 \text{ Ft}^2$	35	1.33	279	130	2.15
33	"	40	1.78	366	170	2.16
34	"	45	2.29	465	210	2.21
35	"	50	2.75	547	250	2.19
36	SK $S_p = 220 \text{ Ft}^2$	35	1.35	282	142	1.99
37	"	40	1.78	367	176	2.08
38	"	45	2.26	467	222	2.1
39	"	35	1.4	272	121	2.25
40	"	40	1.84	337	155	2.18
41	"	45	2.31	431	194	2.22

TABLE XXIX - Continued						
Run No.	Configuration	Velocity (Ft/Sec)	q (PSF)	Lift (Lbs)	Drag (Lbs)	L/D
42	High-Aspect-Ratio TCK $S_p = 370 \text{ Ft}^2$	35	1.36	436	174	2.51
43	"	40	1.8	564	218	2.59
44	"	45	2.29	727	279	2.6
45	"	35	1.36	431	158	2.73
46	"	40	1.78	544	200	2.72
47	"	35	1.36	419	167	2.51
48	"	40	1.8	547	214	2.56
49	"	45	2.29	685	268	2.56
50	"	35	1.36	418	162	2.58
51	"	40	1.78	546	213	2.56
52	"	45	2.33	695	268	2.59

## APPENDIX III STRESS ANALYSIS

### INTRODUCTION

With the aid of the previous testing performed by both Goodyear Aerospace and Langley Research Center, a stress analysis was done on the single-keel parawing. From this basic analysis, theoretical calculations were done for the twin-keel wing. The analysis was done for a single, theoretical keel length of 18 feet, having a total surface area,  $S_p$ , of 220 square feet. The single-keel parawing and suspension lines weighed 20 pounds, and the total system weight including the control box was 580 pounds. The twin keel had a surface area of 270 square feet with a theoretical keel length of 16 feet. Included are calculations for 1.0 g suspension line and canopy loading and 15.0 g suspension line loads.

### GENERAL

The present parawing is a flexible configuration, the geometry of which is dependent upon the aerodynamic load distribution. Consequently, for the wing shape during descent, one must primarily rely on experimental measurements. A simplified theoretical approach is required to handle the structural aspects of the parawing configuration when some parameters (such as the length of the suspension lines, the angle of attack, the dynamic wind pressure, etc.) are to be changed. The following analysis is based on the assumption that the leading edges and keel are straight lines, and that the angle of attack is the angle which this plane of the leading edges makes with the path along which the wing glides. With this assumption, the suspension line lengths have to be modified slightly to conform to other requirements of the problem. The canopy assumes a two-lobed shape, each lobe being a portion of a conical surface (see Figure 58).

### AIRLOAD DISTRIBUTION

The component of the airload normal to the parawing is assumed to be transmitted symmetrically in each lobe to the leading edges and keel. The load distribution in the membrane is assumed to be triangular in shape as shown in Figure 59.

The location,  $a'$ , of the peak airload,  $q'_0$ , is related to the location of the resultant,  $a$ , by

$$a' = 3a - 1 \quad (5)$$

The resultant load distribution is shown in Figure 60. It is apparent from symmetry that the relationship between the resultant load location and the aerodynamic center of pressure is

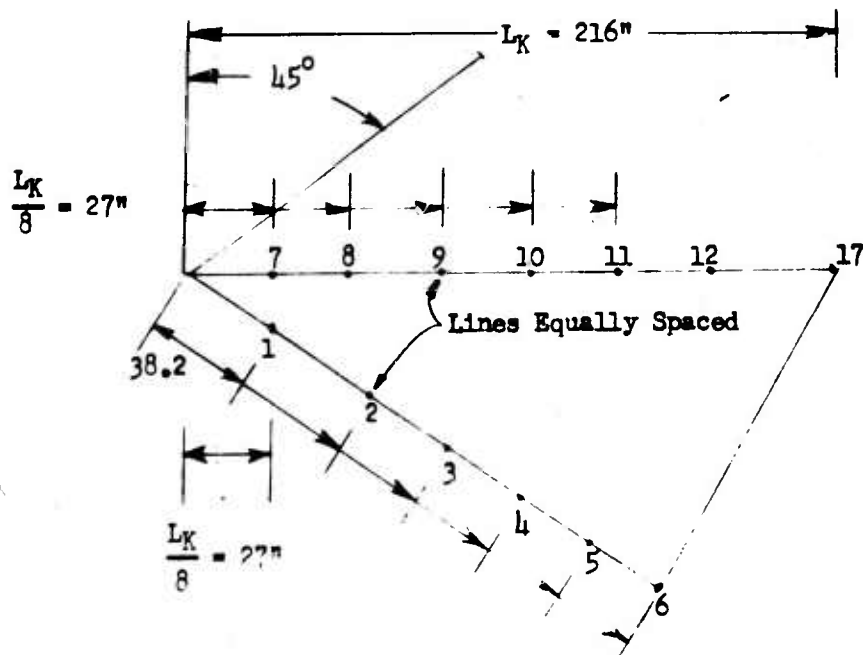
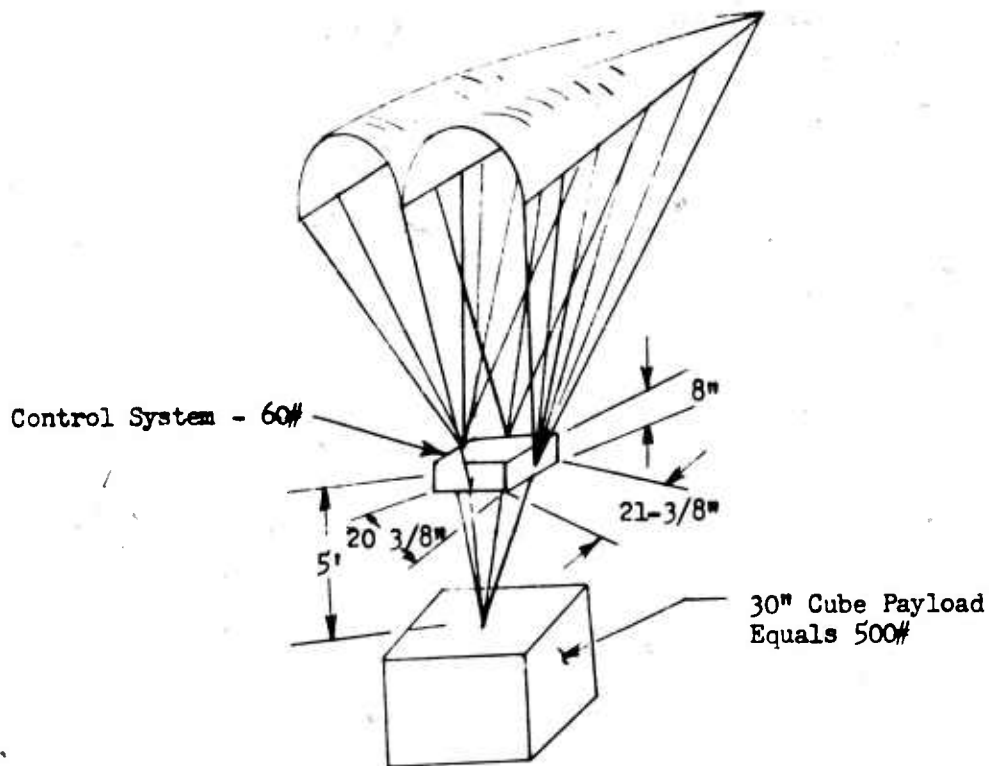


Figure 58. Sketch of Inflated Single-Keel Wing and Sketch Plan View of Single-Keel Wing (Flat Pattern).

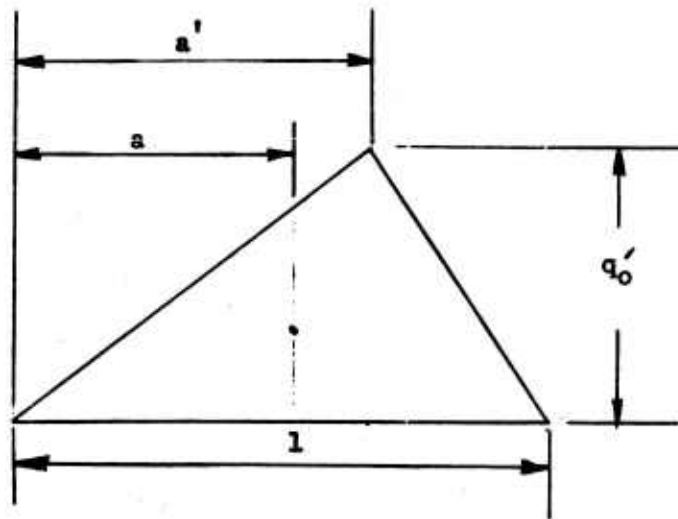


Figure 59. Membrane Airload Distribution.

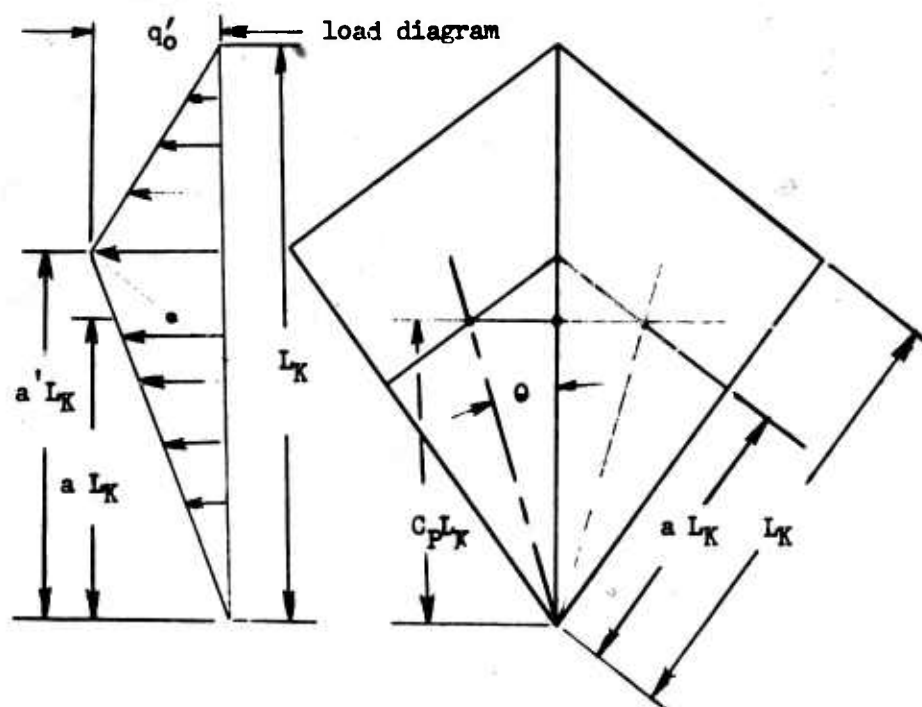


Figure 60. Plan View of Inflated Parawing.

$$a = \frac{C_p}{\cos^2 \theta} \quad (6)$$

where  $C_p$  is the ratio of the distance of the center of pressure from the apex to the keel length ( $L_K$ ).  $C_p$  is determined in terms of angle of attack as outlined in Reference 5 (pages 4-21).  $C_p$  is given as 0.574, 0.535, and 0.531 for angles of attack of 25, 35, and 40 degrees respectively. The  $C_p$  for an angle of attack ( $\alpha$ ) of 27.5 degrees is

$$C_p = 0.0002067\alpha^2 - 0.0163025\alpha + 0.85238 \quad (7)$$

$$C_p = 0.560 \quad (8)$$

Having assumed that each leading edge takes one-fourth the total airload, the maximum intensity  $q'_0$  may be found from the equation

$$1/2 q'_0 L_K = W_t/4 \quad (9)$$

$$q'_0 = W_t/2L_K \quad (10)$$

To simplify the statics, it is assumed with negligible significance that the weight of the parawing and suspension lines act at the c.g. of the control box. The system weight ( $W_t$ ) is made up of the following elements:

Payload	500 lbs
Control Box	60 lbs
Parawing & Suspension Lines	<u>20 lbs</u>
$W_t$	= 580 lbs

Then, from equation (10),

$$q'_0 = \frac{580}{2 \times 18 \times 12} \quad (11)$$

$$q'_0 = 1.3425 \text{ lb/in} \quad (12)$$



### PARAWING GEOMETRIC RELATIONSHIPS

To determine the structural loads in the parawing, certain geometric relationships of the fully inflated wing must first be established, and the suspension line lengths and direction cosines must be determined. Referring to Figure 61, the following relationships can be established:

$$\text{Arc ABC} = 2L_K \sin 22.5^\circ \quad (13)$$

$$\text{Arc ABC} = R (\pi + 2 \phi) \quad (14)$$

$$\tan \phi = r/h \quad (15)$$

$$\tan \theta = r/L_C \quad (16)$$

$$L_C = L_K \cos 22.5^\circ \quad (17)$$

Equating equations (13) and (14), we obtain

$$2 L_K \sin 22.5^\circ = R (\pi + 2 \phi) \quad (18)$$

Dividing equation (18) by equation (15), we obtain

$$\frac{2 L_K \sin 22.5^\circ}{\tan \phi} = h(\pi + 2 \phi) \quad (19)$$

Let

$$\beta = \pi + 2 \phi \quad (20)$$

Equation (19) yields

$$-\beta \cot \beta/2 = 2 L_K \sin 22.5^\circ / h \quad (21)$$

The above expressions can be further expanded if we consider that the parawing glide path angle is assumed to be such that an L/D of 2.4 is achieved. Also from wind-tunnel data<sup>6</sup>, the distance of the control box from the plane of the leading edges is assumed to be 1.245  $L_K$ . Further, noting that the center of gravity of the system must be on a vertical line, the system configuration can be established as shown in Figure 62.

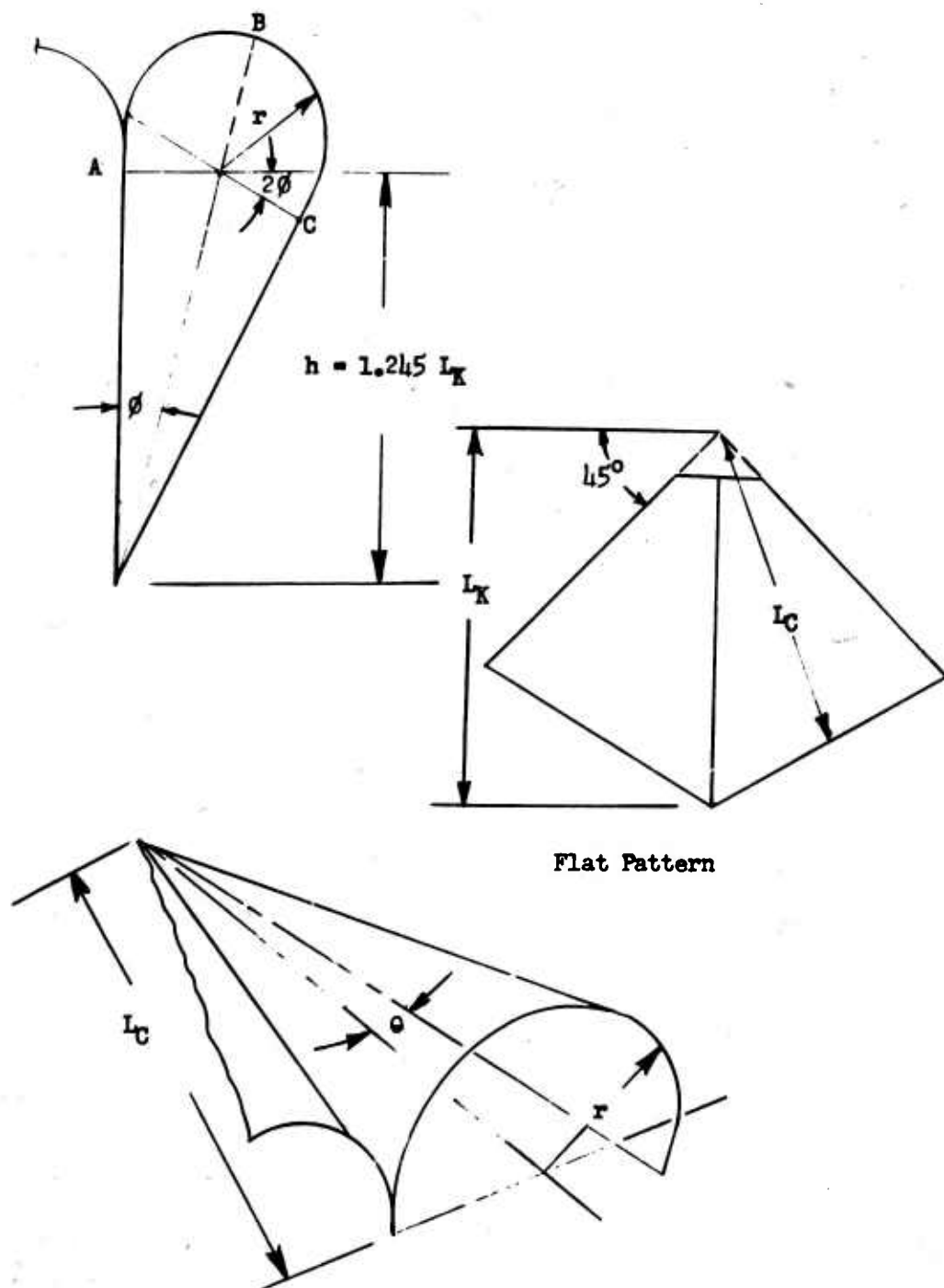


Figure 61. Parawing Geometric Relationships.

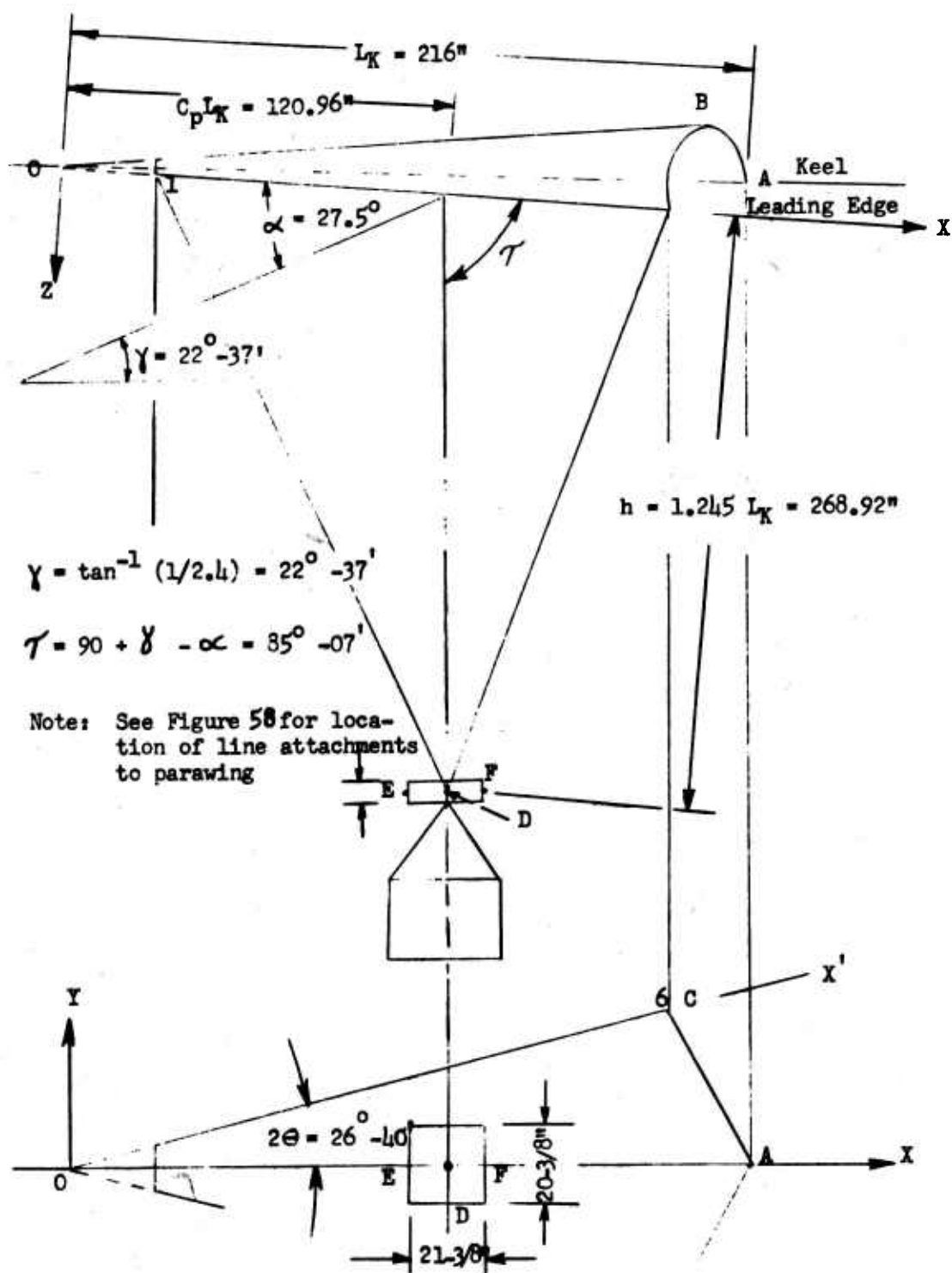


Figure 62. Parawing System Coordinate Planform.

Using the theoretical nose of the parawing as the origin of the coordinate system x, y, and z, as shown in Figure 62, the coordinates of cable attach points to both the parawing and the control box can be determined. From this data, suspension line direction cosines can be determined. The suspension lines are oriented such that the starboard leading-edge lines attach to the starboard side of the control box, and the port lines attach to the port side of the box. Keel line No. 7 attaches to the forward end of the control box, with each subsequent line alternating between attachment to the aft and forward end of the box.

From Figure 62 it will be noted that  $h = 1.245 L_K$ . Then from equation (21)

$$-\beta \cot \frac{\beta}{2} = \frac{2}{1.245} (0.38268) = 0.61175 \quad (22)$$

from which

$$\beta = 199^\circ - 59' \quad (23)$$

Then from equation (20),

$$\phi = \frac{(\beta - \pi)}{2} = 9^\circ - 59.5' \quad (24)$$

Using the values for  $\beta$  and  $\phi$  obtained in equations (23) and (24), values for  $R$ ,  $L_C$ ,  $\theta$ , and  $a$  can be determined from equations (15), (17), (16), and (6) respectively.

$$r = 1.245 L_K \tan 9^\circ - 59.5' = 47.38 \text{ in.} \quad (25)$$

$$L_C = 216 \times .92388 = 200 \text{ in.} \quad (26)$$

$$\theta = \tan^{-1} \left( \frac{24.7}{200} \right) = 13^\circ - 20' \quad (27)$$

$$a = \frac{.560}{(.97304)^2} = .591 \quad (28)$$

The coordinates for line attachment locations on the control box are determined as follows.

$$X_D = C_P L_K + 1.245 L_K \cot \mathcal{T} = 143.9 \text{ in.} \quad (29)$$

$$Y_D = 10.2 \text{ in.} \quad (30)$$

$$Z_D = 1.245 L_K = 268.9 \text{ in.} \quad (31)$$

$$X_E = 143.9 - 10 \frac{11}{16} \cos(\alpha - \gamma) = 133.3 \text{ in.} \quad (32)$$

$$Y_E = Y_F = 0 \quad (33)$$

$$Z_E = 268.9 + 10 \frac{11}{16} \sin(\alpha - \gamma) = 269.8 \text{ in.} \quad (34)$$

$$X_F = 143.9 + 10 \frac{11}{16} \cos(\alpha - \gamma) = 154.5 \text{ in.} \quad (35)$$

$$Z_F = 268.9 - 10 \frac{11}{16} \sin(\alpha - \gamma) = 269.0 \text{ in.} \quad (36)$$

The X coordinates (see Figure 62) for the suspension line attachment points along the leading edge are determined by the expression

$$x_i = x_i' \cos 2\theta \quad (37)$$

$$x_i = 0.8936 x_i' \quad (38)$$

where  $x_i'$  is the distance of the point under consideration from the apex of the narrowing measured along the leading edge.

The Y coordinates of the same points can be expressed as

$$Y_i = y_i' \sin 2\theta \quad (39)$$

$$Y_i = 0.4488 y_i' \quad (40)$$

The Z coordinates for all points along the leading edge are zero.

The X coordinates of the keel line attachment points can be expressed with an error of less than 1 percent as

$$X_i = x_i \quad (41)$$

where  $x_i$  is the distance of the keel attachment from the apex. The Y coordinates are zero. The Z coordinates can be expressed as (see Figure 62)

$$Z_i = -\frac{R x_i}{L_K} \sin 2\phi \quad (42)$$

$$Z_i = -.075 x_i \quad (43)$$

Table XXX summarizes these values.

TABLE XXX. COORDINATES OF SUSPENSION LINE ATTACHMENT POINTS				
Line Attachment Point		Coordinates of Attachment Point		
		X	Y	Z
Control Package	D	143.9	10.2	268.9
	E	133.3	0	269.8
	F	154.5	0	269.0
Leading Edge	1	34.1	12.1	0
	2	65.9	23.3	0
	3	97.7	34.7	0
	4	129.5	45.9	0
	5	161.2	57.2	0
	6	193.0	68.5	0
Keel	7	27.0	0	- 2.0
	8	45.9	0	- 3.4
	9	64.8	0	- 4.9
	10	83.7	0	- 6.3
	11	102.7	0	- 7.7
	12	121.5	0	- 9.1
	13	140.4	0	-10.5
	14	159.3	0	-11.9
	15	178.2	0	-13.4
	16	197.1	0	-14.8
	17	216.0	0	-16.2

Using the expressions for the determination of the suspension line coordinates, the line lengths and direction cosines can be determined. These values are summarized in Table XXXI.

#### CANOPY AND SUSPENSION LINE LOADS FOR 1.0 g LOADING

The load distribution shown in Figure 63 is distributed along the leading edge and keel. The load is then distributed to the line attachment points, and line loads and wing canopy loads are determined at these points. From equations (5) and (28).

$$a' = 3 \times .591 - 1 = .773 \quad (44)$$

and

$$q_0' = 1.3425 \text{ lb/in.} \quad (45)$$

from equation (12).

From the above equations, the area of the triangles and trapezoids (airloads) can be found and distributed equally at each attachment point (see Tables XXXII and XXXIII).

Of the forces in Tables XXXII and XXXIII, those applied at points on the keel are parallel to the unit vector (0,0,1), and those applied at points on the leading edge are parallel to the unit vector ( $\sin 2\theta \sin \theta$ ,  $-\sin 2\theta \cos \theta$ ,  $\cos 2\theta$ ) or (0.07881, -0.33657, 0.93979).

The tensions in the suspension lines may be found from the direction cosines of the lines and the loads of Tables XXXII and XXXIII and their direction as follows: let  $|\bar{a}|$  be the canopy load (pounds) taken by a certain line and  $\bar{X}$  be a vector (see Figure 64). Then for equilibrium along the line,

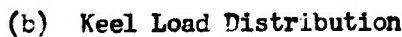
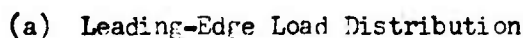
$$\bar{X} \cdot \bar{a} = |\bar{a}| \quad (46)$$

or

$$|\bar{X}| \cdot \bar{x} \cdot \bar{a} = |\bar{a}| \quad (47)$$

TABLE XXXI. LENGTHS AND DIRECTION COSINES OF SUSPENSION LINES							
Suspension Lines	Coordinates of Suspension Lines as Vectors			Line Length (In)	Direction Cosines of Suspension Lines		
	X	Y	Z		X	Y	Z
1-D	109.8	- 1.9	268.9	290.46	.3779	-.0065	.9256
2-D	78.0	-13.1	268.9	280.29	.2783	-.0467	.9594
3-D	46.2	-24.5	268.9	273.94	.1686	-.0894	.9815
4-D	14.4	-35.7	268.9	271.64	.0530	-.1314	.9898
5-D	-17.3	-47.0	268.9	273.52	-.0633	-.1720	.9842
6-D	-49.1	-58.3	268.9	279.49	-.1757	-.2086	.9621
7-E	106.3	0	271.8	291.85	.3642	0	.9312
8-F	108.6	0	272.4	293.25	.3703	0	.9289
9-E	68.5	0	274.7	283.11	.2420	0	.9703
10-F	70.8	0	275.3	284.26	.2491	0	.9685
11-E	30.6	0	277.5	279.18	.1096	0	.9940
12-F	33.0	0	278.1	280.05	.1178	0	.9930
13-E	- 7.1	0	280.3	280.39	-.0253	0	.9997
14-F	- 4.8	0	280.9	280.94	-.0171	0	.9999
15-E	-44.9	0	283.2	286.74	-.1566	0	.9877
16-F	-42.6	0	283.8	286.98	-.1484	0	.9889
17-E	-32.7	0	286.0	297.72	-.2778	0	.9506





167

TABLE XXXII. CANOPY LOADS IN HOOP DIRECTION  
AT LEADING EDGE (REF. FIGURE 63)

Load Point	$q_1$ (Lbs/In.)	$x_1$	$P'$	$P_1$
0	0			0
1	.3071	38.19	5.86*	13.86
2	.5929	35.55	16.00	21.08
3	.8788	35.55	26.16	31.24
4	1.1647	35.55	36.32	39.81
4a	1.3425	22.12	27.73**	-
5	.9746	13.43	15.56	30.32
6	0	35.60	17.35	8.68
Total				144.99
* Distributed entirely to attachment point 1				
** Distributed equally to attachment points 4 and 5				

TABLE XXXIII. CANOPY LOADS IN HOOP DIRECTION  
AT THE KEELS (REF. FIGURE 63)

Load Point	$q_1$ (Lbs/In)	$x_1$	$P'$	$P_1$
0	0			0
7	.4342	27.00	5.86*	11.40
		18.9	11.08	
8	.7381			13.95
		18.9	16.82	
9	1.0420			19.70
		18.9	22.57	
10	1.3460			25.44
		18.9	28.31	
11	1.6499			31.12
		18.9	34.05	
12	1.9538			36.93
		18.9	39.80	
13	2.2578			42.67
		18.9	45.54	
14	2.5617			44.93
		7.67	20.12**	
14a	2.685			-
		11.23	24.19**	
15	2.070			36.83
		18.9	29.34	
16	2.0350			19.56
		18.9	9.78	
17	0			4.89

\* Distributed entirely to attachment point 7

\*\* Distributed equally to attachment points 14 and 15

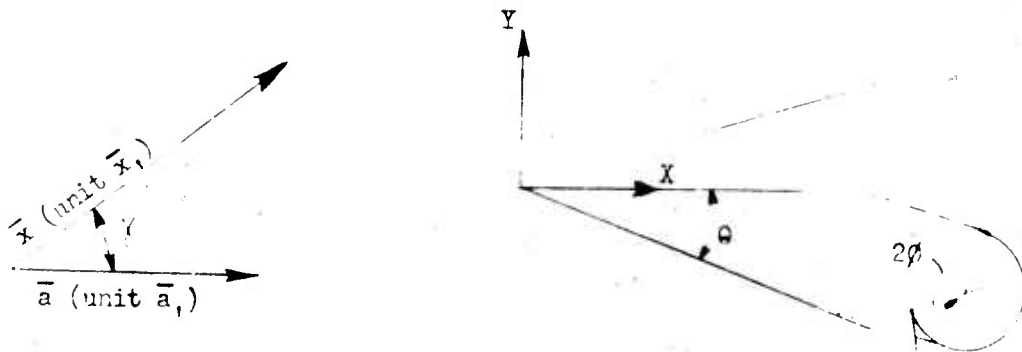


Figure 64 . Dimensional Layout of Suspension Line Loading  
from which

$$\frac{|\bar{x}|}{\bar{x}_i \cdot \bar{a}_i} = \frac{|\bar{a}|}{\cos \gamma} \quad (48)$$

where  $\gamma$  is the angle between the line under consideration and the corresponding unit vector—either (0,0,1) for keel points or (0.07881, -0.33657, 0.93979) for L. E. points.

Using the loads of Tables XXXII and XXXIII and the direction cosines from Table XXI, the axial loads in the lines may be found as follows:

Loads in suspension lines under 1.0 g:

1	13.86 + [(0.3779)(0.078814) + (.33657)(.0065) + (.9256)(.93979)]	= 12.50
2	21.08 + [(0.2783)(0.078814) + (.33657)(.0467) + (.9594)(.93979)]	= 19.80
3	31.24 + [(0.1686)(0.078814) + (.33657)(.0894) + (.9815)(.93979)]	= 30.17
4	39.81 + [(0.0530)(0.078814) + (.33657)(.1314) + (.9893)(.93979)]	= 38.98
5	30.32 + [-(0.0633)(0.078814) + (.33657)(.1720) + (.9842)(.93979)]	= 29.68
6	8.68 + [-(0.1757)(0.078814) + (.33657)(.2086) + (.9621)(.93979)]	= 8.24
7	11.40 + .9312	= 12.24
8	13.95 + .9289	= 15.02
9	19.70 + .9703	= 20.30
10	25.44 + .9685	= 26.27
11	31.12 + .9940	= 31.31
12	36.93 + .9930	= 37.19
13	42.67 + .9997	= 42.68
14	48.93 + .9990	= 49.93
15	36.83 + .9877	= 37.29
16	19.56 + .9839	= 19.78
17	4.89 + .9606	= 5.09

From the above line loads, the tension coefficients may be found by dividing each line load by the total weight of 580 pounds.

In Table XXXIV, theoretical lengths and tensions are given for all 17 lines of the parawing under 1.0 g condition.

TABLE XXXIV. SUSPENSION LINE LENGTHS AND LOAD UNDER 1.0 g AND 15.0 g				
Landing Edge	Line No.	Theoretical Length (In)	Theoretical Line Tension Under 1.0 g (Lbs)	Theoretical Line Tension Under Dynamic Opening (15.0 g's) (Lbs)
			Total Weight	
	1	290.46	12.50	187.5
	2	280.29	19.80	297.0
	3	273.94	30.17	452.6
	4	271.64	38.98	584.7
	5	273.52	29.68	445.2
	6	279.40	8.34	125.1
keel	7	291.35	12.24	183.6
	8	293.25	15.04	225.6
	9	283.11	20.30	304.5
	10	284.26	26.27	394.1
	11	279.13	31.31	460.7
	12	280.05	37.19	557.9
	13	280.39	42.68	639.2
	14	280.94	44.93	674.0
	15	286.74	37.29	559.4
	16	296.98	19.78	296.7
	17	297.72	5.09	70.4

## MAXIMUM CANOPY STRESS AND LINE TENSION UNDER 15 g'S DYNAMIC OPENING

### Canopy

The maximum canopy stress occurs at a point .773  $L_K$  distance from the apex. Its value under 1.0 g is 1.34 pounds per inch. Hence, under 15.0 g's  $f = 20.1$  pounds per inch. Using a factor of safety of 1.5, the required fabric should have a quick break strength of

$$F_{QB} = 1.5 \times 20.1 = 30 \text{ lbs/in.} \quad (49)$$

The fabric used in the flight hardware has a ravel strip breaking strength of 150 pounds per inch. Therefore, the margin of safety of the canopy is:

$$MS = \frac{150}{30} - 1 = +4.0 \quad (50)$$

### Suspension Lines

The maximum load under 15.0 g's is carried by keel line No. 14. This load is 674 pounds (see Table XXXIV). For a safety factor of 1.5, the required line strength is

$$T = 1.5 \times 674 = 1011 \text{ lbs} \quad (51)$$

The suspension line material used in the flight hardware is 1/4-inch-diameter, 2-in-1 Dacron polypropylene stable braid having a minimum strength of 1700 pounds. Reducing this by 80 percent for knot efficiency, a design strength of 1360 pounds results. Therefore, the margin of safety for the suspension lines is seen to be

$$MS = \frac{1360}{1011} - 1 = +0.35 \quad (52)$$

### Twin-Catenary-Keel Parawing

A rationale showing the structural adequacy of the twin-catenary-keel parawing can be presented when related to the structural analysis of the single-keel parawing. Although the results are qualitative in nature, the high structural margins shown on the single-keel wing do not warrant a more discrete analysis.

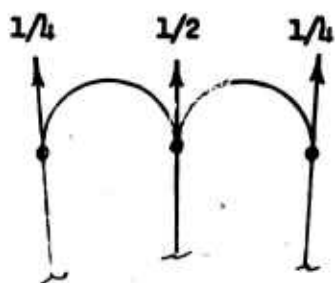
The canopy planform as used for a twin-catenary-keel parawing consists of a standard single-keel parawing with an added center section which increases the total planform area 50 percent. The finally configured twin-keel parawing, shown in planform in Figure 9, has a theoretical keel length of 16 feet. The planform area is 270 square feet as compared to 220 square feet for the single-keel parawing. Therefore, for the same payload weight and assuming a symmetrical load distribution on the wing, the maximum wing loading is

$$q_0 = 2.685 \times \frac{220}{270} \times \frac{.33}{.5} = \quad (53)$$

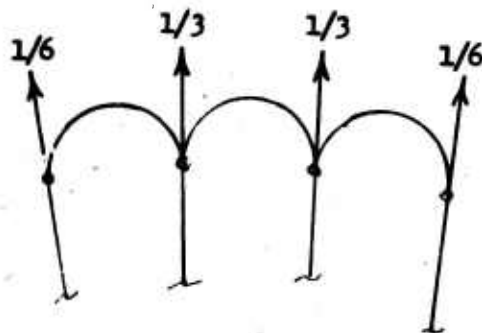
$$q_0 = 1.44 \text{ lb/in.} \quad (54)$$

The lower wing loading, coupled with smaller inflated wing radius, due to the twin-keel shorter trailing-edge length, will result in a margin of safety greater than 4.00 as obtained in equation (50) for the single keel.

The twin-keel leading edge lines will carry a smaller proportion of the total load in the ratio of 1/6 to 1/4 or 67 percent by virtue of the symmetrical load distribution. Figure 65 shows the relative load distribution schematically.



(a) Single Keel



(b) Twin Keel

Figure 65. Wing Load Distribution.

The twin-catenary-keel wing has one more keel line than the single-keel wing. Ignoring this fact, the keel line loads in the twin-keel wing will increase in the ratio of 1/3 to 1/4, or 33 percent. Assuming the same relative line load distribution and using line 14 (Ref. Table XXXIV) as

the maximum loaded line, the maximum required line strength for the twin-keel wing under 15 g's is

$$T = 44.93 \times 1.33 \times 15 \quad (55)$$

$$T = 900 \text{ lbs} \quad (56)$$

The margin of safety for the lines is

$$MS = \frac{1360}{900 \times 1.5} - 1 = +0.01 \quad (57)$$



APPENDIX IV  
SCALE-MODEL ANTENNA TESTS

GENERAL

Preliminary testing and evaluation of the CACS antenna array were performed on a scale-model system as follows:

1. A mockup of the control box, antennas, and payload was fabricated.
2. An antenna test range was instrumented and checked out.
3. The impedance of the individual antenna elements and the impedance of the elements coupled through a hybrid were measured. The antenna lengths were adjusted for a good impedance match.
4. The antenna radiation patterns were measured at six different element spacings to determine the radiation characteristics with antenna placement. Effects of pitch and roll attitudes of the control box on the radiation patterns were measured for the optimum spacing. The effects of the payload were determined qualitatively from the radiation patterns.
5. Antenna placement and ground plane predictions were made for the Ryan low-frequency system.

The radiation patterns were investigated using only the largest size payload, a scaled version of a 3-foot by 3-foot by 3-foot container. The payload is located several wavelengths below the control box and should not affect the radiation patterns appreciably until high depression angles are reached where the payload is physically between the control box and the transmitting antenna. Therefore, a smaller payload would only reduce the angular area over which the patterns were degraded. In addition, the radiation patterns of the homing antennas would have a null area or very little radiation downward; and the radiation pattern would be degraded considerably without the payload.

The azimuth radiation patterns of the antenna system were taken at 0-, 15-, 30-, 45-, 60-, 75-, and 82.5-degree depression angles for the various antenna spacings investigated. Depression angle is defined as the angle between the line of sight to the transmitter and a plane horizontal through the center of the control box. The patterns then describe the response of the antenna system over 360-degree azimuth for the given depression angle. The box is rotated around a vertical axis; thus, the radiation in the lower hemisphere is fully described. In addition, the box was pitched or rolled with respect to the vertical axis of rotation to describe the azimuth pattern for a given depression angle when the wing is turning. Again, the lower hemisphere of radiation is described for each pitch or roll attitude investigated. The nomenclature used here is somewhat

different from that originally requested. The original request calls for investigation of  $\pm 75$ -degree pitch and roll. The maximum pitch was later defined as  $\pm 15$  degrees; radiation patterns were taken to  $\pm 30$  degrees in 10-degree increments. The maximum calculated roll was defined as  $\pm 50$  degrees, with photographs indicating only  $\pm 15$  degrees actually attained. Radiation patterns were taken in 10-degree increments to  $\pm 50$ -degree roll.

#### TESTING ACCOMPLISHED

Two monopole antennas were mounted in the mockup of the control box. They were initially spaced 2 inches apart on a line through the center of the box and parallel to the front edge. The antennas were placed symmetrically about the center and perpendicular to the bottom surface of the box. The antenna lengths were adjusted to 1-15/16 inches for good impedance match. The VSWR of the individual elements was 1.3:1 or less at the test frequency (1440 MHz).

The elements were then connected to a FXR C-145 hybrid to combine the two antenna outputs in phase quadrature to provide the homing cardioid pattern. Switching between the input ports of the hybrid changes the phase relationship of the two antenna elements and thus provides a right- or left-hand cardioid pattern. The VSWR into the hybrid ports measured 1.65:1 with the antennas connected and in the mockup. Subsequent radiation patterns indicated that a 1-inch spacing provided more desirable antenna performance. The individual antenna element VSWR was 1.75:1, and the input to the hybrid was 2.2:1 at this spacing. The antennas were again symmetrically located on the box. The symmetrical mounting is used to provide as nearly omnidirectional radiation patterns as possible from each antenna element; thus, symmetrical radiation patterns are right and left or fore and aft when the antennas are combined in the hybrid.

The coordinate system used for the radiation patterns is shown in Figure 66. For azimuth radiation patterns, the mockup is rotated around the vertical axis, and the patterns are recorded at the various depression angles (for 0-degree depression angle, the incident energy is perpendicular to the axis, and for 90-degree depression, the incident energy is parallel to the axis). For azimuth patterns investigating pitch or roll, the box is tilted with respect to the vertical axis, and the radiation patterns are again recorded for the various depression angles. The model was also rotated about the pitch or roll axis of rotation to obtain pitch plane patterns at various roll positions and roll plane patterns at various pitch angles. This method of model azimuth rotation provides radiation patterns which show the antenna response for all headings of the box with respect to a ground transmitter for horizontal and pitch and roll attitudes of the box. The various depression angles simulate the position of the center of the box (regardless of attitude) with respect to the horizontal and vertical distance from the ground transmitter.

The initial sequences of radiation patterns did not consider roll and pitch attitudes but only horizontal flight of the box at various depression angles.

The azimuth patterns were measured at 0-, 15-, 30-, 45-, 60-, 75-, and 82.5-degree depression angles for 1-, 1-1/2-, 1-3/4-, 2-, 2-1/2-, and 3-inch spacings of the elements at 1140 MHz to determine the change of radiation characteristics with spacing. Neglecting ground plane and mutual coupling effects, the radiation pattern should have a very low side-lobe level when the spacing between model elements is 2 inches or 1/4 wavelength. Side-lobe level of radiation is defined here as the radiation to the right side of the box when the maximum of the radiation pattern is on the left side (or vice versa). If the side-lobe level is not considerably below the maximum radiation, the signal received broadside to the box could be misinterpreted as a homing signal, and the control system could cause the wing to fly a circle about the transmitter at some undetermined range. The error signal for 5- and 12-degree course errors from electrical boresight (right and left cardioid pattern crossover point) and the side-lobe level in db down from the maximum radiation level are shown in Table XXXIV for various antenna spacings and depression angles.

The error signal is the difference (in db) between the signal level received for the right-hand cardioid and left-hand cardioid patterns for a given number of degree course error. Five- and twelve-degree errors were arbitrarily chosen to compare performance at different antenna spacings and depression angles.

In general, the sequences of radiation patterns show that for a given depression angle, the error signal does not change rapidly with a change of spacing. The error signal increases slightly between 0- and 15-degree depressions and decreases from 15 to 82.5 degrees. Therefore, for a given spacing, a particular value of error signal will represent a slightly different course error depending on the depression angle. The side-lobe level is shown to change considerably with spacing. The lowest side-lobe levels (maximum number of db down) were obtained at a 1-inch spacing over the range of depression angles. The higher spacings provided much higher side lobes, especially at low depression angles. Since the error signal did not vary appreciably with spacing and the side lobes were low at 1-inch spacing, the radiation patterns with pitch and roll attitudes were investigated for this spacing with the thought that the side lobes would be maintained at a low level.

Table XXXVI contains data taken from azimuth radiation patterns for all combinations of the 0- through 82.5-degree depression angle increments and 0- through 30-degree up and down pitch. The error signals at 10- and 20-degree up-down pitch are seen to be approximately the same values as those with no pitch angle. The side-lobe levels are also approximately the same. However, at 30-degree up-pitch and high depression angles, the pattern shape and side-lobe level are degraded to the point that the pattern is not usable. There is no crossover point in the pattern, or the right and left pattern amplitude levels have reversed; this would lead to inaccurate error signals or a complete reversal of error signal sense. For example, the antenna system would indicate a right course error when the error was really left. This occurs when the sum of the pitch angle and depression angle is near or greater than 90 degrees, and operation is in the null area of the control box radiation pattern. At 30-degree up-pitch and 75-degree

depression, the angle of incident radiation is really toward the rear of the box and, thus, the reversal of error signal. At the lower depression angles and 30-degree up-pitch, the patterns still have the right error sense, but the error signal is reduced somewhat. No reversal in pattern is seen for the 30-degree down-pitch because the pitch angle is subtracted from the depression angle, and incident radiation is toward the front of the box.

Table XXXVII contains data taken from azimuth patterns at all combinations of the depression angle increments and 10, 20, 30, 40, and 50 degrees right and left roll of the control box. The error signal is approximately the same as for a 0-degree roll attitude for the low depression angles, and the side-lobe levels are maintained considerably below the maximum radiation. Again, as in the case of pitch angles, when the sum of the roll angle and depression angle is near or greater than 90 degrees, the radiation patterns reverse right for left, and inaccurate or wrong sense course errors result. Thus, as the roll angle increases, the radiation patterns reverse at lower depression angles until at 50 degrees roll only 0 through 30 degrees depression is usable. This data pertains to roll angles away from the ground station where the sum of depression and roll angles causes operation in the null area or opposite side of the box. If the box rolls toward the ground station, which is located at a high depression angle and near broadside to the box, the error will be of the correct sense. In all cases, either right or left roll, the crossover point in the forward direction is destroyed; in fact, several crossovers may occur. Large error or complete reversal of sense will result. This characteristic of the radiation patterns becomes especially important near the cone of silence.

Table XXXVIII contains data taken from pitch plane patterns of the antenna system at 0 through 50 degrees roll in 10-degree increments. The depth of the null in the radiation pattern perpendicular to the bottom of the box and the width of this null at 20 db down from maximum radiation level are shown. The null is always located perpendicular to the box in the pitch plane; thus, the null area would fall on different points on the ground, depending on the pitch attitude of the box. This data was taken to determine performance near the cone of silence.

Table XXXIX contains data taken from roll plane patterns at 0 through 30 degrees pitch. The null depth with respect to peak radiation, the width of the null at 20 db down from peak radiation, and the position of the null with respect to the perpendicular to the box are tabulated. This data was also taken to determine performance near the cone of silence.

Due to the large number of patterns recorded, the pertinent data is presented in Tables XXXV through XXXIX, and copies of the patterns are not presented with this report.

## DISCUSSION

The optimum spacing of antenna elements considering side-lobe level was found to be 1 inch for the scale model for the GAC high-frequency system. Theoretical calculations indicate that the spacing should be 2 inches, but these do not include ground plane and mutual coupling effects. Since the ground plane is small in wavelengths, the amplitude and phasing of RF energy received by the two antenna elements is unbalanced, and a reduction of spacing is required to produce a low side lobe to the left of the right-hand cardioid pattern.

The reversal of radiation pattern sense at high depression angles with pitch and roll could cause erratic maneuvering of the wing near the cone of silence. The error signals will be inaccurate or in the wrong direction when the sum of the pitch or roll angle and depression angle is near 90 degrees. Little or nothing can be done to the antenna system to correct this situation.

One possibility of erratic maneuvering is seen in the following example. If the wing were approaching the ground station at a high depression angle and slightly to the right side of the station when the cone of silence was entered, signal would be lost and the wing would commence a right turn, causing the control box to roll right. Signal might then be received again because rolling has taken the ground station out of the null area of the control box pattern. At high depression angles and roll away from the station, the pattern sense is reversed; the wing would continue a right turn when a left turn would provide the shortest route to the ground station. This should be considered in system analysis.

The cone of silence, where signal between the ground station and control box is lost, is determined by many factors. These include transmitter power, receiver sensitivity, control box radiation patterns, ground station radiation pattern, attitude of the control box, and flight characteristics of the wing. Transmitter power and receiver sensitivity will determine the range (horizontal and vertical) at which it is possible to enter the cone of silence. Reduced power or sensitivity would effectively increase the cone size. In addition, the pitch and roll attitudes of the control box will change the effective size of the cone. Therefore, the angular limits of the cone of silence will vary considerably. A thorough review of the system performance characteristics and antenna patterns would be required to define the flight performance of the wing. This is also true for areas outside the cone of silence.

Based on the radiation patterns obtained for the scale model, the ground plane size, antenna spacing, and antenna length would have to be an exact scale for the low-frequency system to obtain the same performance characteristics. This does not preclude the fact that a low-frequency system with no ground plane extensions may provide adequate radiation patterns, but experimental measurements to verify this were not included in the work statement. The effects of the payload are not seen until very high depression angles are reached, and the antenna pattern itself is deteriorating.

The low-frequency patterns would be approximately the same shape for a scaled ground plane; therefore, payload effects would not be significant. The high-frequency system (and scale model) uses a hybrid to combine the radiation received by the two antenna elements in phase quadrature. This approach is defined as an active system. The null to one side of the box and the maximum radiation to the other are obtained by balancing the amplitude and phase of the two antennas to cancel one another in one case and to reinforce on the opposite side. Exact amplitude and a 180-degree phase between antennas is required to produce a null or a very low side-lobe level. On the low-frequency system, a passive approach is used where one element acts as a parasitic element to receive and reradiate energy to the element connected to the receiver. It is difficult to obtain low side-lobe levels with this approach because an amplitude balance cannot be obtained between elements. Therefore, it is anticipated that the cabling arrangement between the antennas must be changed to an active type system to obtain side-lobe levels comparable with the scale model patterns of the high-frequency system. If flights with the low-frequency system are limited to manual control, a single antenna element or a modified version of the high-frequency system could be used with no ground plane extensions to provide radiation pattern coverage.

The radiation patterns show that for a given spacing, the error signal varies somewhat with depression, pitch, and roll angles. A given error signal does not always represent exactly the same number of degree course error. This effect must be considered in system performance.

#### RECOMMENDATIONS

The following recommendations are based on the results of the scale model measurements and general performance requirements of a homing system. Since exact receiver and control system signal requirements and wing flight characteristics are not defined, a final determination of pattern adequacy cannot be made. It is anticipated that exact tailoring of radiation patterns with respect to the error signal (db error/degree course error) could not be obtained without additional measurements or possible degradation of the side-lobe level. The recommendations on this basis are:

1. The antenna element spacing should be  $\lambda/8$  inch. The location is  $\lambda/16$  inch on each side of the center of the box with the antennas at equal distances from the front and rear edges of the box.
2. The antenna element length should be near  $\lambda/4$  inch, but exact length will change due to antenna construction. Impedance measurements will be made on the full-scale model.
3. Since the antenna patterns show a reversal of sense at high depression, pitch, and roll angles, a method of turning toward the direction of last course error before the loss of signal should be investigated. This should reduce erratic maneuvers of the wing.

4. Operation near the cone of silence should be investigated and pattern data correlated with specific control system performance to determine possible problem areas.
5. If the low-frequency system is used for homing, the radiation patterns should be measured, and the cabling of the feed network should be modified to an active system. A single antenna or modification to a high-frequency system would be satisfactory for manual control.
6. Flight characteristics of the wing should be such that minimum pitch and roll of the control box is obtained consistent with flight performance requirements. High pitch and roll may cause wrong turns and reduce range of wing delivery capabilities.
7. With the anticipated receiver output characteristics, a small course error signal (2 to 3 db) will command a maximum turn rate for small course errors, usually less than 12 degrees. In addition, changes of course error signal for a given number of degrees course error with depression, pitch, and roll angles of the box will cause the maximum turn rate to occur at varying values of course error. This could cause undue maneuvering of the wing, overshoot on steering, and loss of delivery range. It is suggested that the receiver and control system remain a proportional system but that the range of course errors for proportionality be extended and that the db/degree course error be increased. This will increase the accuracy of direction finding and smooth the flight path. Pitch and roll angles should be decreased and the possibility of erroneous error signals reduced.

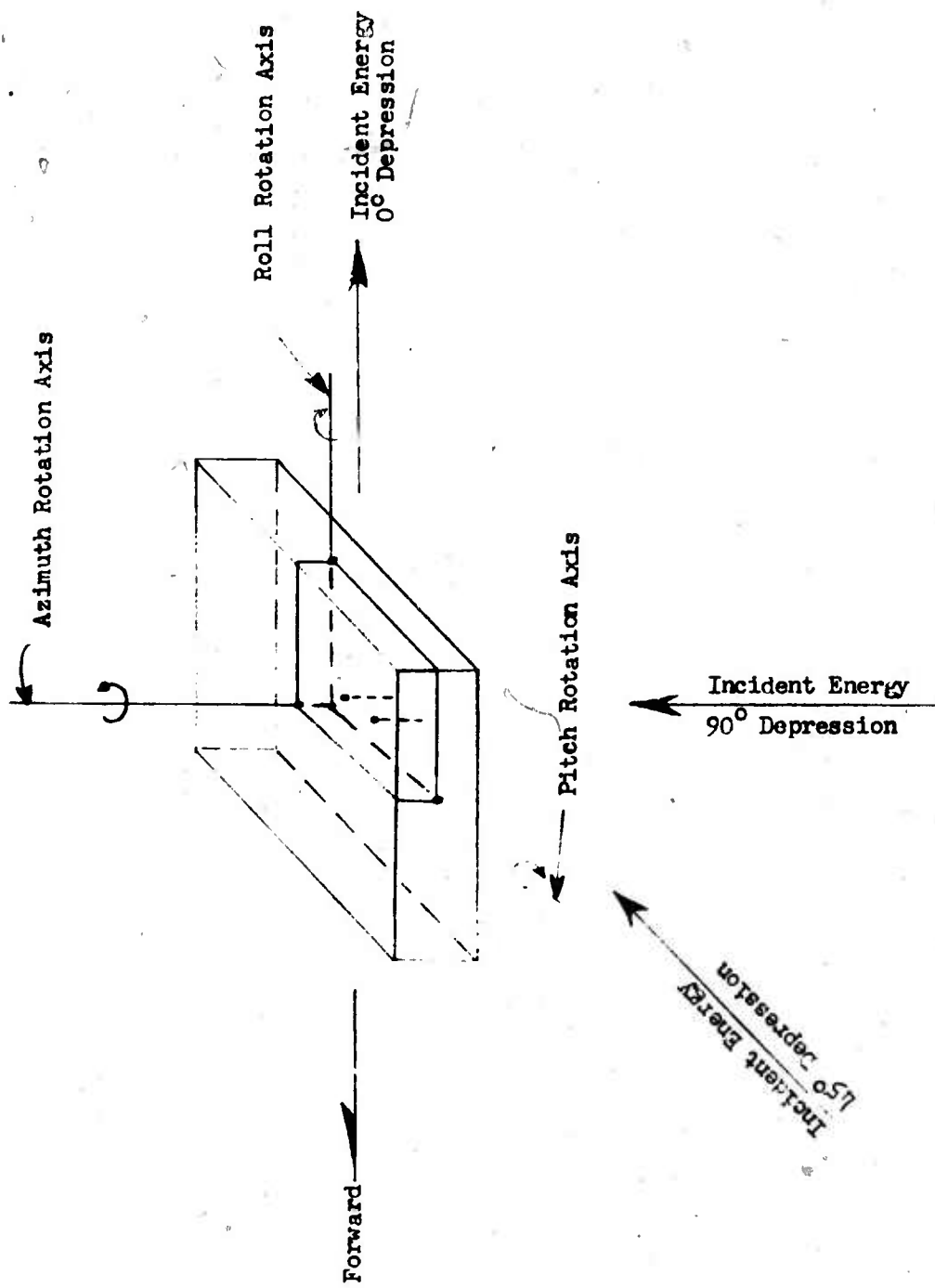


Figure 66. Antenna Pattern Coordinate System.



TABLE XXXV. AZIMUTH PATTERN DATA

Frequency, 1440 MHz  
Mockup Attitude, 0° Pitch, 0° Roll

Depression Angle (Deg)	Antenna Spacing (In)				
	1.0	1.5	2.0	2.5	3.0
Error Signal at 5° from Electrical Boresight (db)					
0	1.1	1.4	1.7	1.2	1.3
15	1.4	1.7	1.7	1.8	1.8
30	1.2	1.3	1.3	1.5	1.4
45	1.2	1.4	1.8	1.7	1.7
60	0.9	1.5	1.5	1.4	1.7
75	0.6	0.6	0.8	0.6	0.8
82.5	1.0				0.5
Error Signal at 12° from Electrical Boresight (db)					
0	2.5	3.2	4.1	3.2	3.7
15	3.0	4.7	4.5	3.4	4.1
30	2.4	3.3	3.0	3.8	3.4
45	3.0	3.6	4.0	3.9	3.9
60	2.5	3.6	4.0	3.5	4.1
75	1.2	1.6	1.7	1.2	1.6
82.5	1.9				1.0
Minimum Side-Lobe Level (db)					
0	27.0	13.7	7.7	6.3	3.4
15	26.0	12.5	6.4	4.0	2.5
30	14.0	9.0	5.5	4.9	3.4
45	12.3	8.5	6.2	5.3	4.9
60	14.0	18.2	11.0	10.8	10.0
75	5.7	5.0	4.3	1.5	6.0
82.5	6.5				0.5

TABLE XXXVI. AZIMUTH PATTERN DATA

Frequency, 1440 MHz  
 1.0-Inch Antenna Spacing  
 Mockup Attitude, 0° Roll, Pitch Variable

Depression Angle (Deg)	Pitch Angle (Deg)	Error Signal (db) at 5° From Elec. Boresight	Error Signal (db) at 12° From Elec. Boresight	Minimum Side-Lobe Level (db)
0	10 up	1.1	2.5	23.0
15		1.1	2.4	23.0
30		1.0	2.4	13.0
45		1.1	3.0	12.0
60		0.9	2.1	14.5
75		0.8	2.2	6.5
82.5	10 up	reversal	reversal	6.7
0	10 down	1.0	2.3	23.0
15		0.8	2.3	23.0
30		1.0	2.2	13.0
45		1.1	2.3	12.0
60		1.0	2.1	14.5
75		0.7	1.4	6.5
82.5	10 down	0.6	1.2	6.7
0	20 up	1.0	2.5	26.0
15		1.0	2.5	30.0
30		1.4	3.3	13.0
45		1.3	2.7	9.5
60		1.0	2.2	17.5
75		0.4	0.9	12.0
82.5	20 up	0.4 reversal	0.8 reversal	13.0
0	20 down	1.8	4.0	26.0
15		1.2	2.8	30.0
30		1.1	2.5	13.0
45		1.0	2.4	9.5
60		0.8	1.7	17.5
75		0.6	1.7	12.0
82.5	20 down	0.6	1.3	13.0

TABLE XXXVI - Continued

Frequency, 1440 MHz  
 1.0-Inch Antenna Spacing  
 Mockup Attitude, 0° Roll, Pitch Variable

Depression Angle (Deg)	Pitch Angle (Deg)	Error Signal (db) at 5° From Elec. Boresight	Error Signal (db) at 12° From Elec. Boresight	Minimum Side-Lobe Level (db)
0	30 up	1.3	3.0	20.0
15		1.4	3.3	27.0
30		2.2	5.8	14.0
45		0.9	2.5	8.5
60		no crossover	no crossover	10.0
75	30 up	no crossover	no crossover	no side lobe
80.5		reversal	reversal	no side lobe
0	30 down	1.6	4.0	20.0
15		1.0	3.4	27.0
30		1.1	2.7	14.0
45		1.0	2.4	8.5
60		0.7	1.8	10.0
75	30 down	0.5	1.2	no side lobe
82.5		0.6	1.5	no side lobe

TABLE XXXVII. AZIMUTH PATTERN DATA

Frequency, 1440 MHz  
 1.0-Inch Antenna Spacing  
 Mockup Attitude, 0° Pitch, Roll Variable

Depression Angle (Deg)	Roll Angle (Deg)	Error Signal (db) at 5° From Elec. Boresight	Error Signal (db) at 12° From Elec. Boresight	Minimum Side-Lobe Level (db)
0	10 left	1.5	3.5	24.0
15		1.2	3.1	29.0
30		1.0	2.5	16.5
45		1.0	2.6	14.0
60		1.0	2.6	8.4
75		0.8	1.6	7.5
82.5	10 left	no good reversal	no good reversal	-
0	10 right	1.5	3.5	24.0
15		1.3	3.0	29.0
30		1.0	2.5	16.5
45		1.0	2.5	14.0
60		1.3	2.9	8.4
75		0.6	1.6	7.5
82.5	10 right	no good reversal	no good reversal	-
0	20 left	1.0	2.5	14.2
15		1.2	2.9	26.3
30		1.0	2.3	17.8
45		0.8	2.1	13.0
60		1.0	2.4	12.5
75		no good reversal	no good reversal	-
82.5	20 left	no good reversal	no good reversal	-
0	20 right	1.0	2.6	14.2
15		1.3	3.1	26.3
30		0.9	2.2	17.8
45		1.0	2.3	13.0
60		0.8	2.1	12.5
75		no good reversal	no good reversal	-
82.5	20 right	no good reversal	no good reversal	-
0	30 left	0.6	1.6	13.0
15		0.9	2.0	25.0
30		1.1	2.4	24.2
45	30 left	0.9	1.5	18.0

TABLE XXVII - Continued

Depression Angle (Deg)	Roll Angle (Deg)	Error Signal (db) at 5° From Elec. Boresight	Error Signal (db) at 12° From Elec. Boresight	Minimum Side-Lobe Level (db)
60	30 left	1.0	2.6	11.8
75		no good reversal	no good reversal	-
82.5	30 left	no good reversal	no good reversal	-
0	30 right	0.8	2.1	13.0
15		1.5	3.4	25.0
30		0.9	2.1	24.2
45		1.1	2.5	18.0
60		1.5	3.4	11.8
75		no good reversal	no good reversal	-
82.5	30 right	no good reversal	no good reversal	-
0	40 left	1.6	3.4	20.0
15		0.9	2.3	11.0
30		1.4	3.0	15.6
45		0.9	1.8	16.0
60		no good reversal	no good reversal	-
75		no good reversal	no good reversal	-
82.5	40 left	no good reversal	no good reversal	-
0	40 right	0.5	1.5	20.0
15		1.4	2.3	11.0
30		1.3	3.2	15.6
45		1.2	2.6	16.0
60		no good reversal	no good reversal	-
75		no good reversal	no good reversal	-
82.5	40 right	no good reversal	no good reversal	-
0	50 left	1.6	2.9	15.5
15		0.8	2.0	11.0
30		1.2	2.6	15.0
45		no good reversal	no good reversal	-
60		no good reversal	no good reversal	-
75		no good reversal	no good reversal	-
82.5	50 left	no pattern	-	-
0	50 right	1.7	3.4	15.5
15		1.2	2.3	11.0
30		1.4	3.0	15.0
45		no good reversal	no good reversal	-
60		no good reversal	no good reversal	-
75		no good reversal	no good reversal	-
82.5	50 right	no pattern	-	-

TABLE XXXVIII. PITCH PLANE PATTERN DATA				
Roll Variable Frequency, 1440 MHz 1.0-Inch Antenna Spacing				
Roll Angle (Deg) Rt or Lt	Null* Depth (db) Down From Peak		Null Width (Deg) 20 db Down From Peak	
	Rt Patt Port #1	Lt Patt Port #2	Rt Patt Port #1	Lt Patt Port #2
0	22.6+	22.6+	5.0	5.0
10	27.0+	28.0+	7.5	6.0
20	25.3+	26.0+	6.0	11.0
30	24.0+	24.6+	17.0	7.0
40	24.3+	23.0+	14.0	8.0
50	24.0+	21.4+	33.0	14.0
*Null is always perpendicular to box.				

TABLE XXXIX. ROLL PLANE PATTERN DATA						
Pitch Variable Frequency, 1440 MHz 1.0-Inch Antenna Spacing						
Pitch Angle (Deg) Up or Down	Null Depth (db) Down From Peak		Null Width (Deg) 20 db Down From Peak		Null Position (Deg) From Perpendicular to Box	
	Rt Patt Port #1	Lt Patt Port #2	Rt Patt Port #1	Lt Patt Port #2	Rt Patt Port #1	Lt Patt Port #2
10	22.9	28.1	10	10	5	4
20	31.4+	31.6	15	17	5	2
30	31.4+	31.6+	31	36	13	5

APPENDIX V  
FULL-SCALE ANTENNA SYSTEM MEASUREMENTS

GENERAL

The following antenna system measurements were made on the full-scale antenna array for the CACS.

1. The impedance of the individual antenna elements was measured. These measurements were taken on the antennas as received from Ryan, with the antennas shortened, and with the antennas shortened and recessed into the holding assembly.
2. Loss measurements on the RF switch between the antenna ports and the output port to the receiver were made.
3. Radiation patterns were taken for several depression angles at the low, center, and high frequencies of the desired frequency band.
4. A draft of the test plan was prepared.

IMPEDANCE MEASUREMENTS

Impedance measurements were made on the individual antenna elements, associated cables, and the RF switching circuitry by standard UHF bridge techniques.

The cables between the antennas and RF switch were checked for equal length by a short-circuit impedance method. The cable length difference was found to be .006 wavelength or 2.16 degrees difference in phase shift. This small value will have negligible effect on the radiation patterns.

The impedance of the individual elements, as received from Ryan, was then measured. The measurements included the antenna's associated cable. The opposite antenna was removed during the measurement to reduce the effects of mutual coupling. The impedance of the antennas was as follows at  $f_0$  (center frequency):

Antenna #1	$50\Omega \angle + 5.4^\circ$	VSWR = 1.12
Antenna #2	$48\Omega \angle + 4.7^\circ$	VSWR = 1.10

The impedance of the RF switch was then measured looking into the input ports (J1 and J2) with the output port (J3) loaded with a  $50\Omega$  resistive load. The RF switch biasing voltage was first applied to connect J1 to output jack J3 and then to connect J2 directly to the output. The impedance at  $f_0$  was as follows:

Impedance in J1 (J1 on)	52 $\Omega$	$\angle + 3.6^\circ$	VSWR = 1.08
Impedance in J1 (J2 on)	52 $\Omega$	$\angle + 3.6^\circ$	VSWR = 1.08
Impedance in J2 (J2 on)	53 $\Omega$	$\angle + 3.6^\circ$	VSWR = 1.09
Impedance in J2 (J1 on)	53 $\Omega$	$\angle + 3.6^\circ$	VSWR = 1.09

The No. 2 antenna length was shortened 5/16 inch since the antenna length as received from Ryan was too long to fit into the control box's recessed cutout. This 5/16-inch shortening along with a 1/4-inch recessing of the antenna connectors in the mounting bar would give adequate clearance. The impedance of the No. 2 antenna shortened but not recessed at the connector was:

Antenna #2	40 $\Omega$	$\angle - 10.5^\circ$	VSWR = 1.32
------------	-------------	-----------------------	-------------

The No. 1 antenna was shortened the same amount, and both antenna connectors were recessed 1/4 inch. The impedances were measured at three frequencies throughout the desired band:

$f_{lo}$	Antenna #1	106 $\Omega$	$\angle - 14.1^\circ$	VSWR = 2.22
	Antenna #2	111 $\Omega$	$\angle - 17.5^\circ$	VSWR = 2.36
$f_o$	Antenna #1	37 $\Omega$	$\angle - 14.5^\circ$	VSWR = 1.50
	Antenna #2	36 $\Omega$	$\angle - 14.5^\circ$	VSWR = 1.52
$f_{hi}$	Antenna #1	54 $\Omega$	$\angle + 7.5^\circ$	VSWR = 1.18
	Antenna #2	54 $\Omega$	$\angle + 6.8^\circ$	VSWR = 1.16

The antenna impedance has been degraded somewhat by shortening the elements and by recessing the connectors, but the antennas are still reasonably well matched to the transmission lines and RF switch. The system sensitivity at  $f_o$  would be reduced by less than 0.2 db due to mismatched loss. It was not desirable to recess the connectors 1/4 inch even though the antennas would not recess into the control box. In this case, the antenna VSWR is 1.32 at  $f_o$ , and the mismatch loss would be less than 0.1 db. The loss at  $f_{lo}$  would be approximately 0.3 db.

The final antenna length was 7-21/32 inches including the connectors.

#### SWITCH LOSS MEASUREMENTS

RF loss measurements were made by applying RF power to J1 and J2 (the antenna input ports) and by measuring the power level out J3 of the RF switch assembly. The output power is referenced to the level at the input ports. It should be noted that with power applied to either input port, there will be signal out J3 irrespective of the switch bias condition (either J1 or J2 energized). This results from the fact that power applied to either input port is split in the hybrid, and an output from the hybrid at both J5 and J6 will exist. Thus, one of these signals will have a path to the output no matter which way the RF switch is biased. The measured losses for the various conditions are shown as follows:



Power in J1 (J1 on)	-4.0 db out J3
Power in J1 (J2 on)	-4.6 db out J3
Power in J2 (J2 on)	-4.0 db out J3
Power in J2 (J1 on)	-4.5 db out J3

These measurements show that the RF switch introduces an additional signal loss of 1.0 to 1.6 db (depending on path) over the theoretical value of the hybrid alone. This loss may be attributed to the input cables, the output cables, and the switch losses. These losses are considered to be reasonable. The element measurements also show that the signal amplitude from each antenna element will be slightly unbalanced due to 0.5 to 0.6 db additional loss through the -90-degree phase lag port of the hybrid. This characteristic of the hybrid may cause some change in the side-lobe level of the radiation patterns.

#### RADIATION PATTERN MEASUREMENTS

Radiation pattern measurements of the CACS antenna system were made at the Point Receiving Site. Unit No. 3 control box cover was mounted on a mockup of the control box and payload, and the complete assembly was mounted on the roof-top azimuth rotator. The control box was mounted in a horizontal position and rotated in azimuth, while the radiation patterns were continuously recorded. The transmitter consisted of a Hewlett-Packard 608C signal generator connected to a log-periodic transmitting antenna. The transmit antenna was located at different orientations with respect to the control box to simulate the radiation patterns at various depression angles. The receiving system consisted of a Scientific Atlanta Polar Recorder and 402 Series Wideband Receiver.

Radiation patterns were recorded for both the right-hand and the left-hand cardioid patterns at several frequencies and several depression angles. Table XL lists the radiation patterns taken.

It should be noted that the radiation patterns at 45- and 60-degree depressions may be somewhat in error since the transmit antenna was placed relatively close to the control box, and the control box/payload combination was not in the far field of the transmit antenna. The true pattern shape may be slightly different due to payload reflections.

The right-hand cardioid pattern was recorded and then the RF switch state changed to record the left-hand cardioid pattern on the same piece of paper. In addition to the data recorded, the boresight error was determined by reading angular information from a selsyn readout on the rotator control panel. The selsyn reading was noted at the point where the right and left patterns had equal amplitudes. This value was compared to the mechanical boresight to determine the homing course error. Data taken from the radiation patterns is tabulated in Table XLI. This data includes frequency, depression angle, boresight error, course error signal at 5 degrees from electrical boresight (average of right and left side), course

error signal at 12 degrees from electrical boresight and minimum sidelobe level below the pattern peak. Figures 67 through 80 are the radiation patterns taken.

TABLE XL. RADIATION PATTERNS		
Pattern No.	Frequency	Depression Angle (Deg)
1	$f_{lo}$	0
2	$f_{lo}$	15
3	$f_{lo}$	45
4	$f_{lo}$	60
5	$f_o$	0
6	$f_o$	15
7	$f_o$	45
8	$f_o$	60
9	$f_{hi}$	0
10	$f_{hi}$	15
11	$f_{hi}$	45
12	$f_{hi}$	60
13	$f_{lo}$	elevation pattern right to left
14	$f_o$	elevation pattern right to left

TABLE XLI. RADIATION PATTERN DATA					
Frequency	Depression Angle (Deg)	Boresight Error (Deg)	Error Signal at 5 Deg (DB)	Error Signal at 12 Deg (DB)	Minimum Side-Lobe Level (-DB)
$f_{lo}$	0	5.3L	1.7	3.5	13.5
$f_{lo}$	15	4.0R	1.0	2.3	12.3
$f_{lo}$	45	0.0	1.0	2.2	8.5
$f_{lo}$	60	3.5L	0.9	2.1	8.5
$f_o$	0	0.5L	1.4	3.0	10.0
$f_o$	15	4.0R	1.1	2.4	12.8
$f_o$	45	1.2R	1.1	2.5	9.6
$f_o$	60	2.3R	1.1	2.4	11.3
$f_{hi}$	0	5.1R	1.0	2.7	9.0
$f_{hi}$	15	1.3R	1.2	2.9	14.5
$f_{hi}$	45	4.0R	1.2	2.9	11.8
$f_{hi}$	60	1.7R	1.1	3.0	12.2R

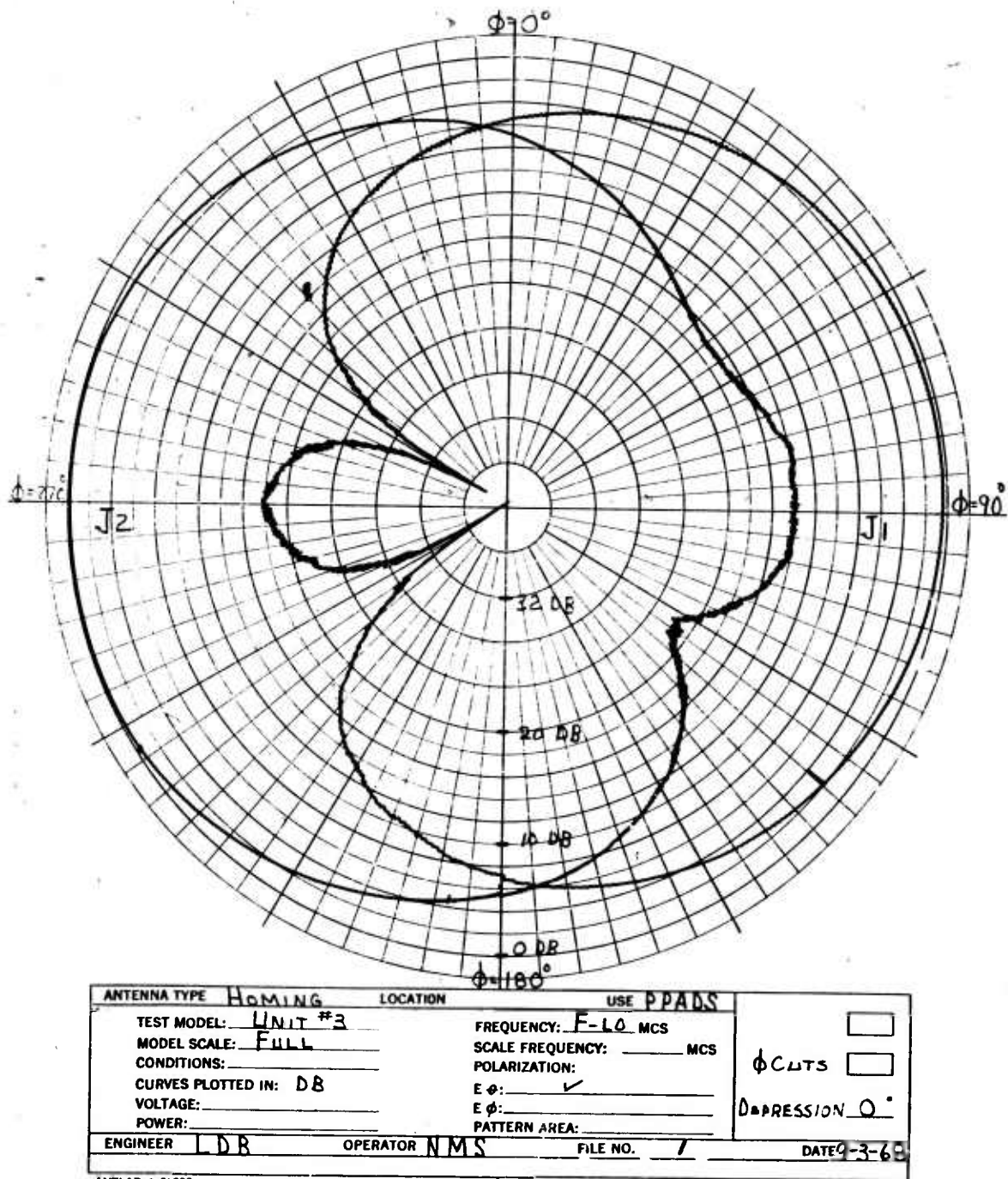
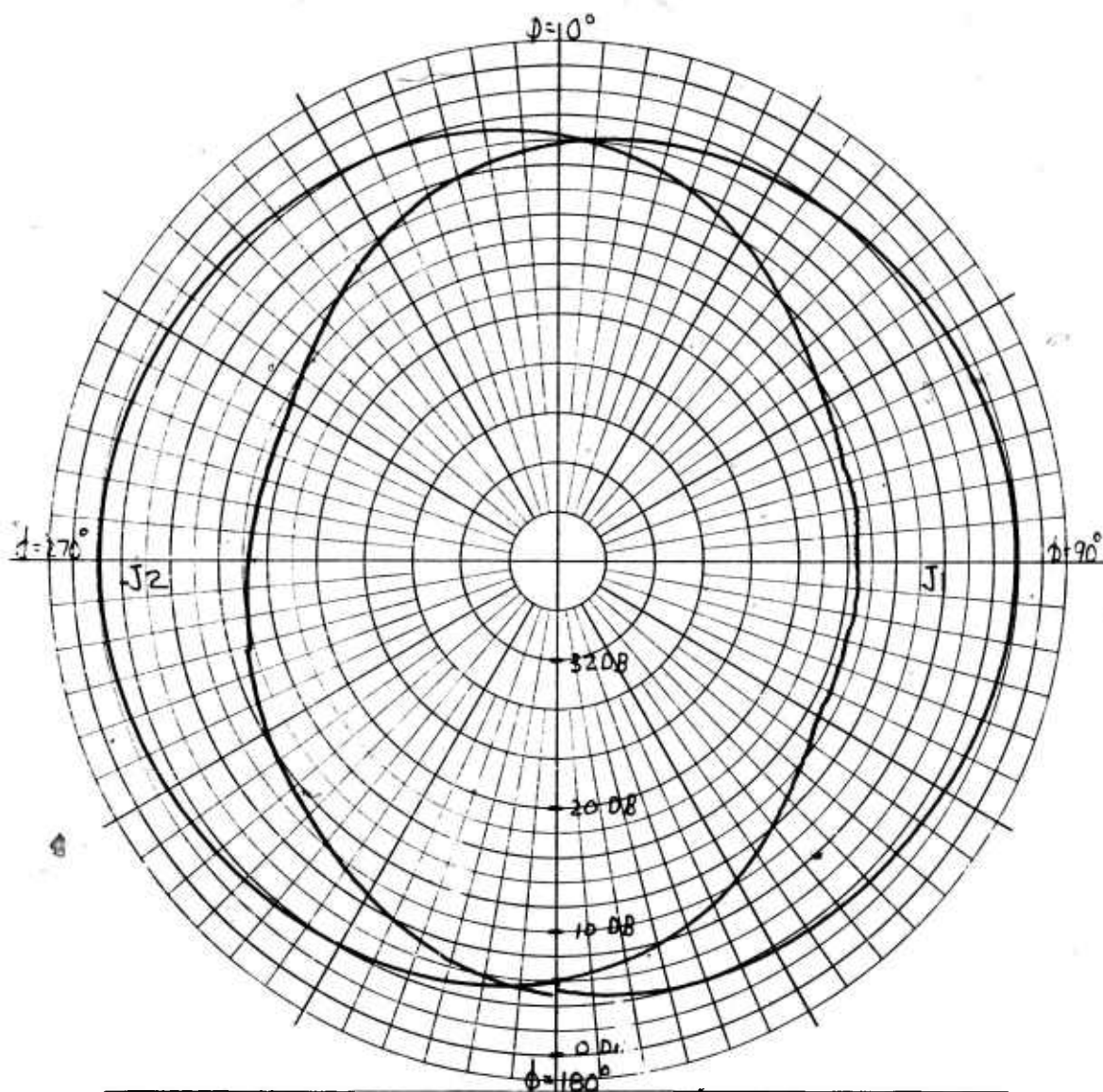


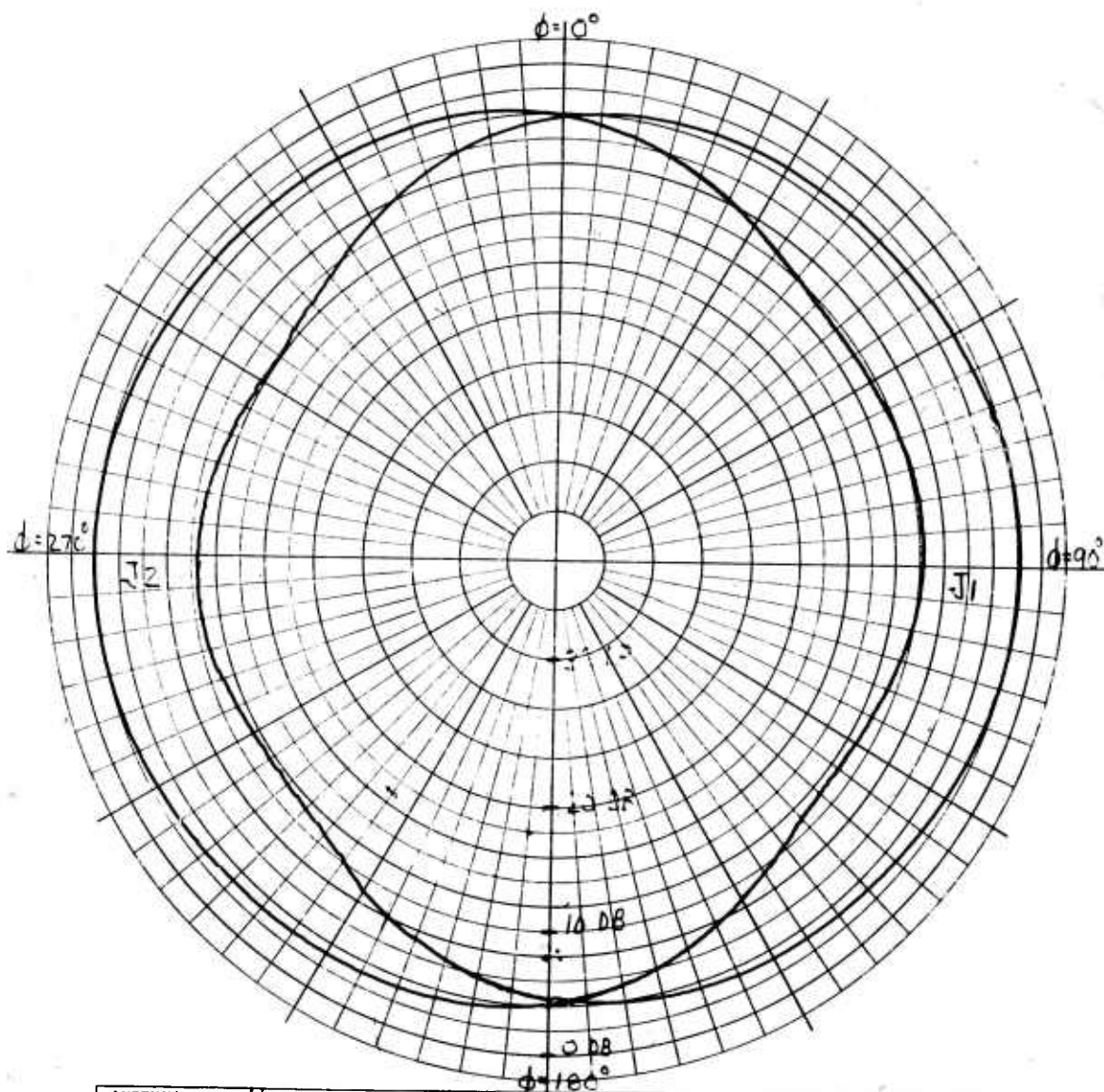
Figure 67.  $f_{10}$  Azimuth Pattern (0-Degree Depression)



ANTENNA TYPE <u>HOMING</u>	LOCATION	USE <u>PPADS</u>	<input type="checkbox"/> $\phi$ CUTS <input type="checkbox"/> DEPRESSION <u>15°</u>
TEST MODEL: <u>UNIT #3</u>	FREQUENCY: <u>F-10</u> MCS	SCALE FREQUENCY: _____ MCS	
MODEL SCALE: <u>FULL</u>	POLARIZATION:	E $\phi$ : <input checked="" type="checkbox"/>	
CONDITIONS: _____	E $\phi$ : _____	PATTERN AREA: _____	
CURVES PLOTTED IN: <u>DB</u>	VOLTAGE: _____	POWER: _____	
ENGINEER <u>LDB</u>	OPERATOR <u>NMS</u>	FILE NO. <u>2</u>	DATE <u>8-29-68</u>

ANTLAB # 36330

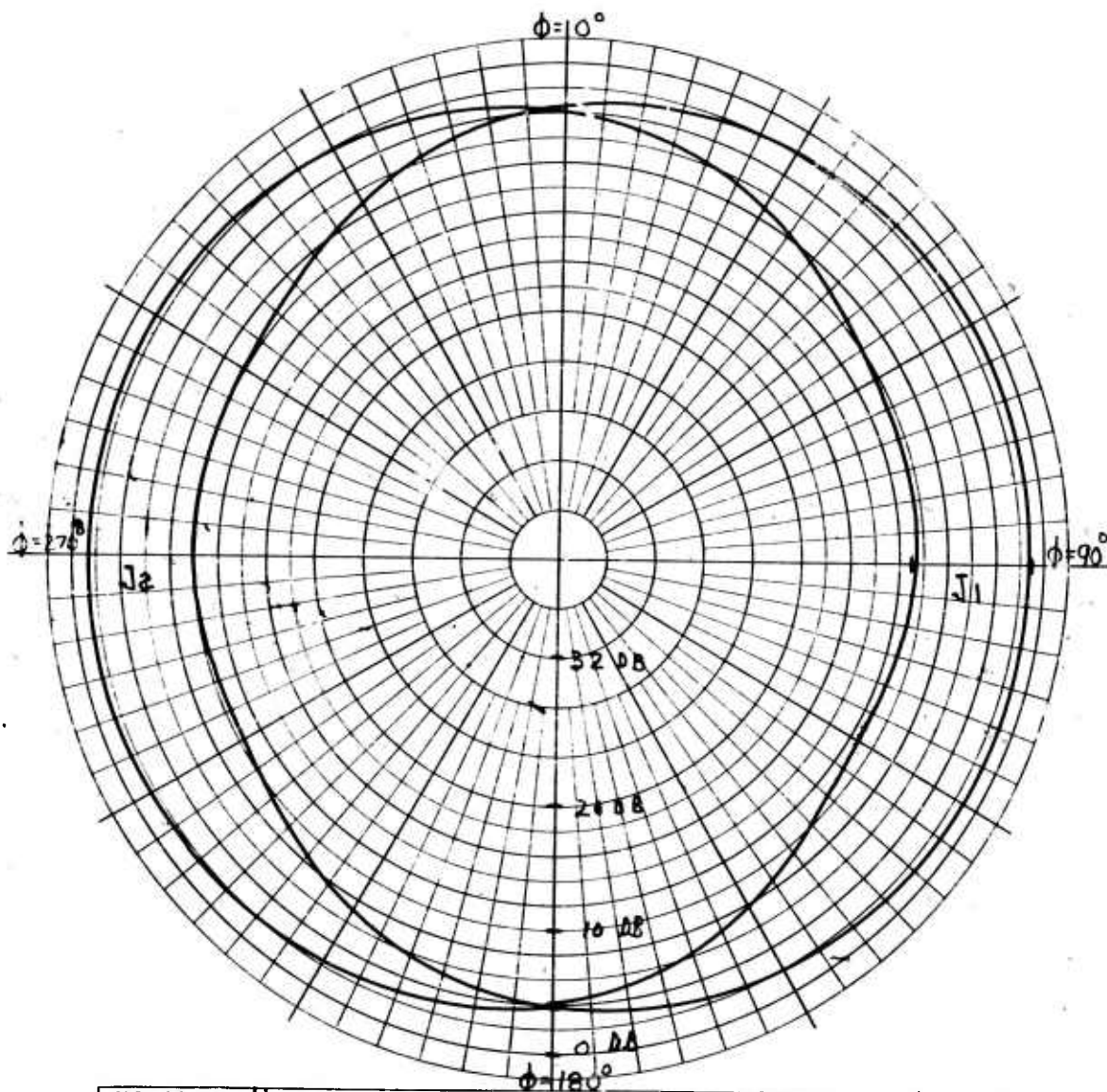
Figure 68.  $f_{10}$  Azimuth Pattern (15-Degree Depression)



ANTENNA TYPE	HCMING	LOCATION	USE	EPADS
TEST MODEL:	UNIT #3	FREQUENCY:	F-LD	MCS
MODEL SCALE:	FULL	SCALE FREQUENCY:		MCS
CONDITIONS:		POLARIZATION:		
CURVES PLOTTED IN:	DB	E φ:	✓	
VOLTAGE:		E φ:		
POWER:		PATTERN AREA:		
ENGINEER	LDB	OPERATOR	NMS	FILE NO. 3
			DATE	8-30-68

ANTLAB # 36330

Figure 69.  $f_{10}$  Azimuth Pattern (45-Degree Depression)

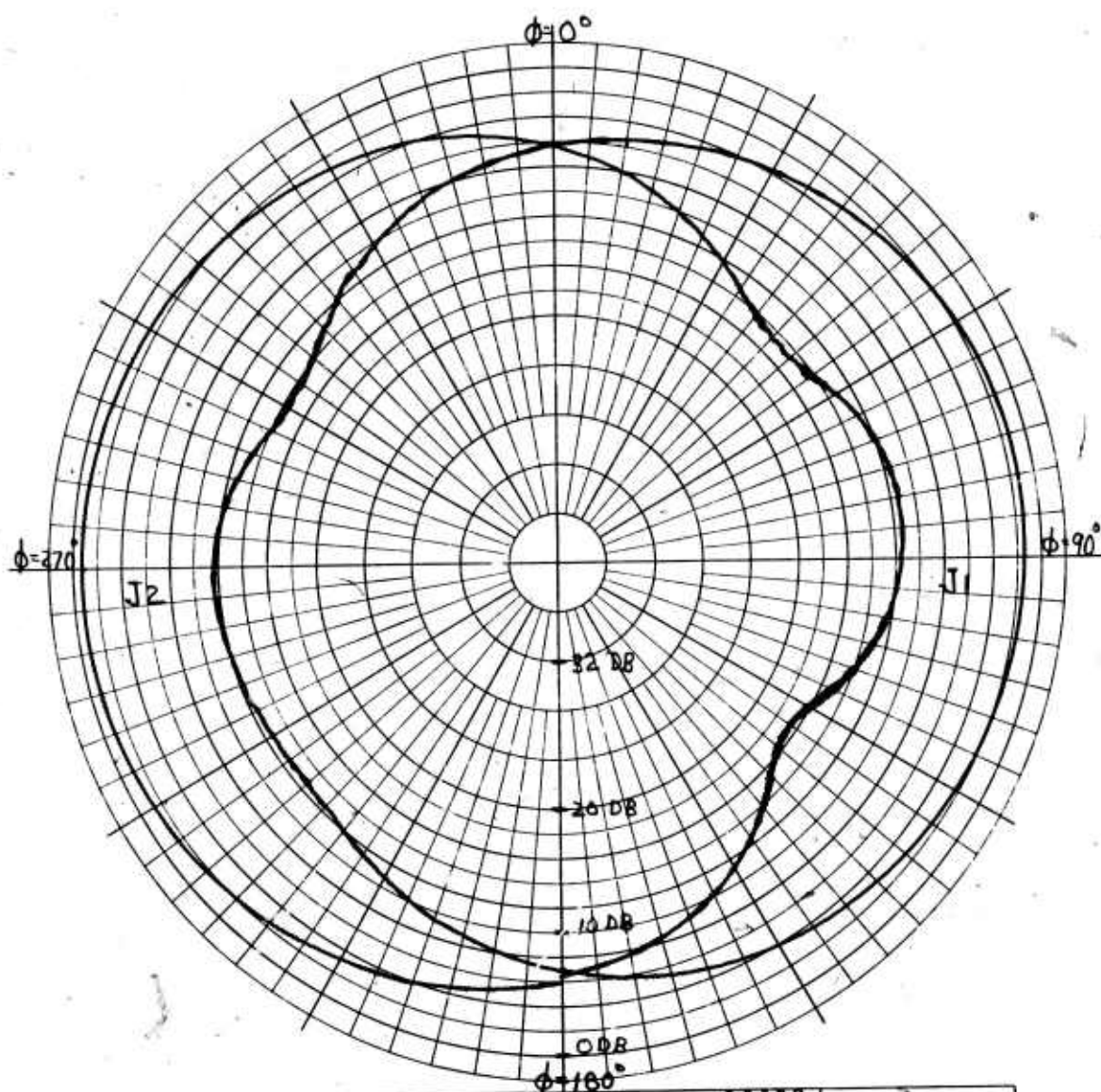


ANTENNA TYPE	HCMING	LOCATION	USE PPADS
TEST MODEL:	UNIT #3	FREQUENCY:	F-10 MCS
MODEL SCALE:	FULL	SCALE FREQUENCY:	MCS
CONDITIONS:		POLARIZATION:	
CURVES PLOTTED IN:	DB	E φ:	✓
VOLTAGE:		E φ:	
POWER:		PATTERN AREA:	
ENGINEER	LDB	OPERATOR	NMS
FILE NO.	4	DATE	9-3-68

ANTLAB # 36330

Figure 70.  $f_{10}$  Azimuth Pattern (60-Degree Depression)



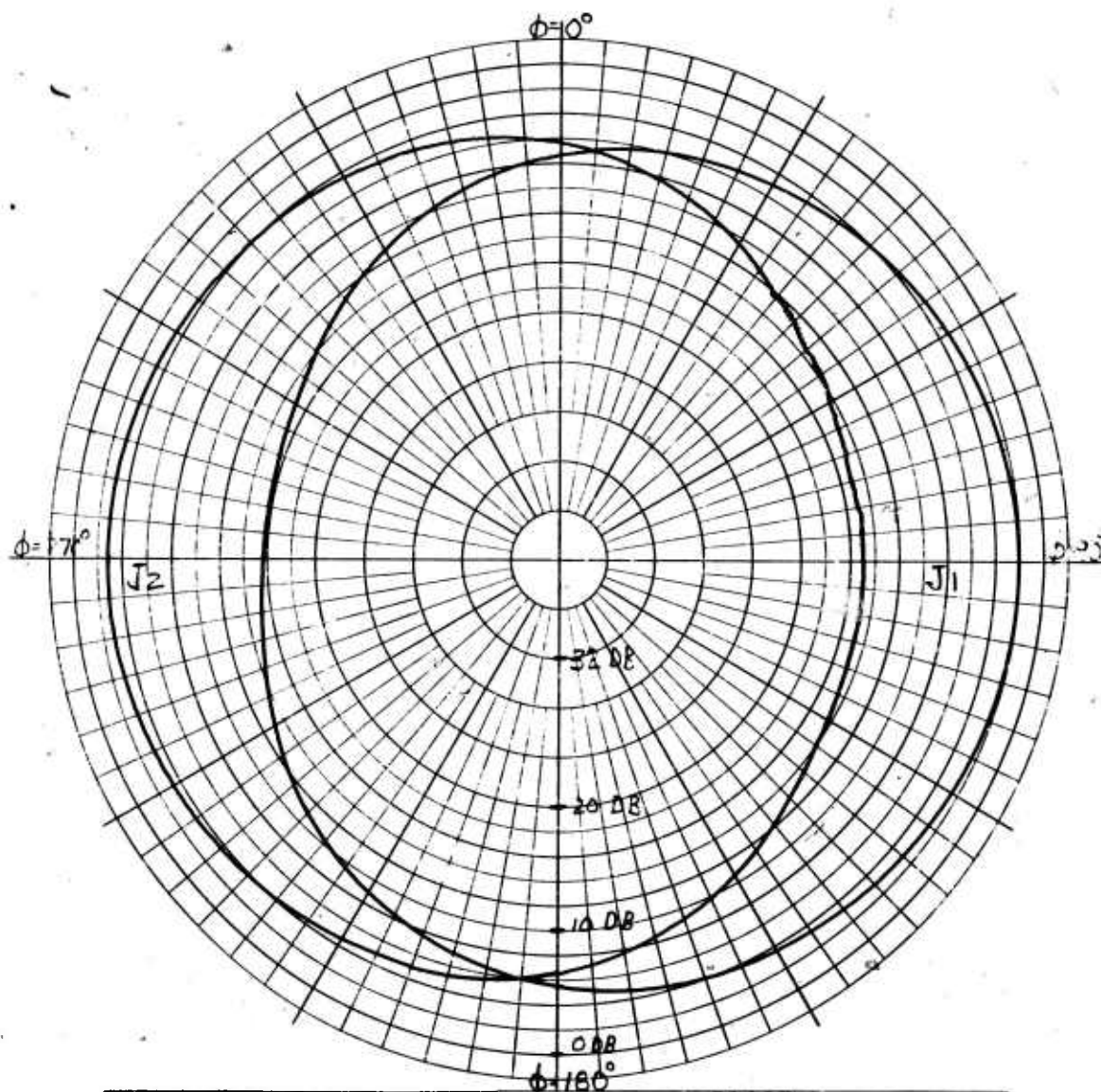


ANTENNA TYPE <u>HOMING</u>		LOCATION	USE <u>PPADS</u>
TEST MODEL: <u>UNIT #3</u>		FREQUENCY: <u>F0</u> MCS	
MODEL SCALE: <u>FULL</u>		SCALE FREQUENCY: _____ MCS	
CONDITIONS: _____		POLARIZATION: _____	
CURVES PLOTTED IN: <u>DB</u>		E $\phi$ : <u>✓</u>	
VOLTAGE: _____		E $\phi$ : _____	
POWER: _____		PATTERN AREA: _____	
ENGINEER <u>LDB</u>	OPERATOR <u>NMS</u>	FILE NO. <u>5</u>	DATE <u>9-3-68</u>

☐  $\phi$  CUTS  
☐ DEPRESSION 0°

ANTLAB # 36330

Figure 71.  $f_0$  Azimuth Pattern (0-Degree Depression)

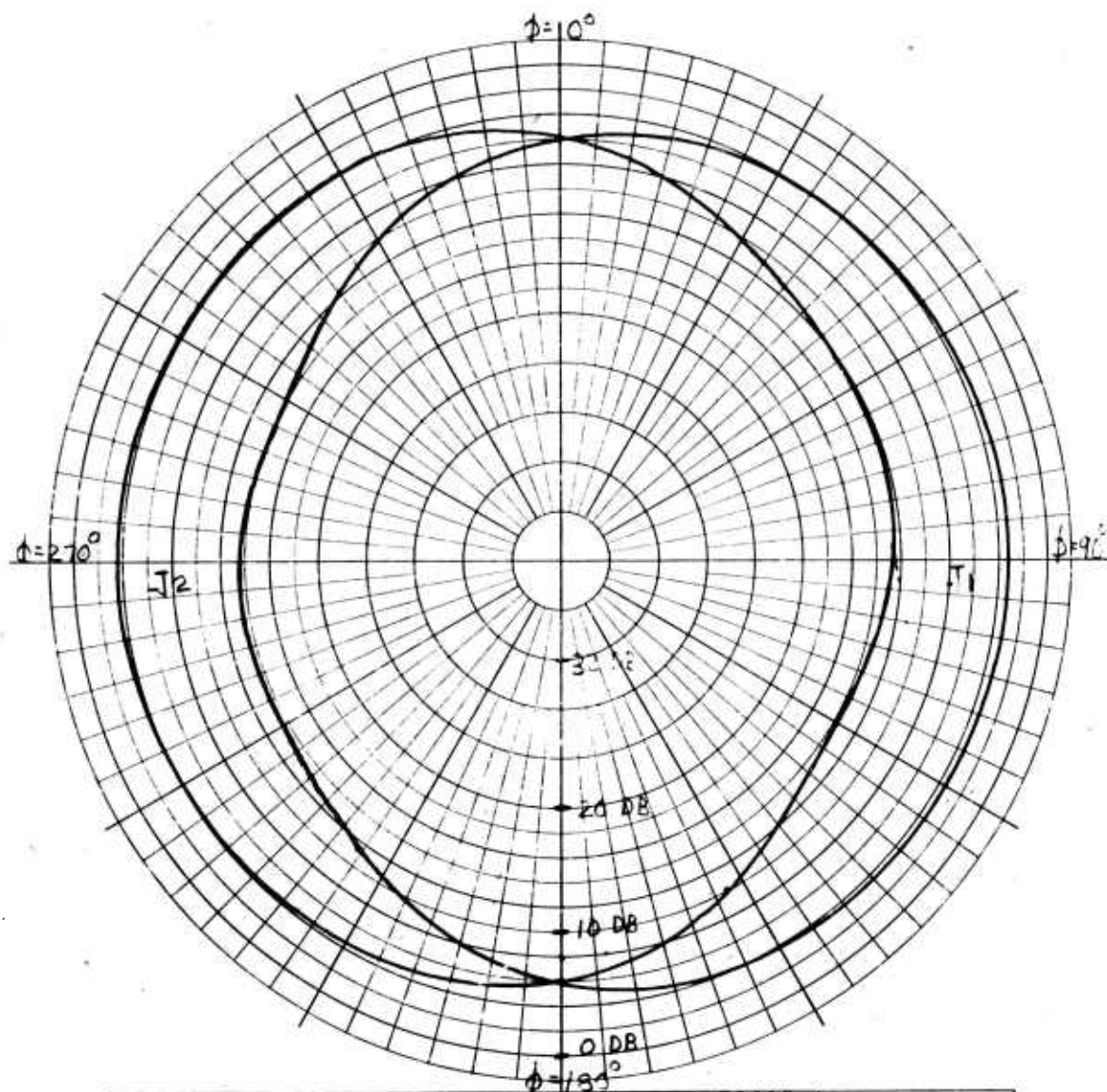


ANTENNA TYPE	HOMING	LOCATION	USE PPADS
TEST MODEL:	UNIT #3	FREQUENCY:	F <sub>0</sub> MCS
MODEL SCALE:	FULL	SCALE FREQUENCY:	MCS
CONDITIONS:		POLARIZATION:	
CURVES PLOTTED IN:	DB	E φ:	✓
VOLTAGE:		E φ:	
POWER:		PATTERN AREA:	
ENGINEER	LDR	OPERATOR	NMS
FILE NO.	6	DATE	9-3-68

ANTLAB # 36330

Figure 72.  $f_0$  Azimuth Pattern (15-Degree Depression)

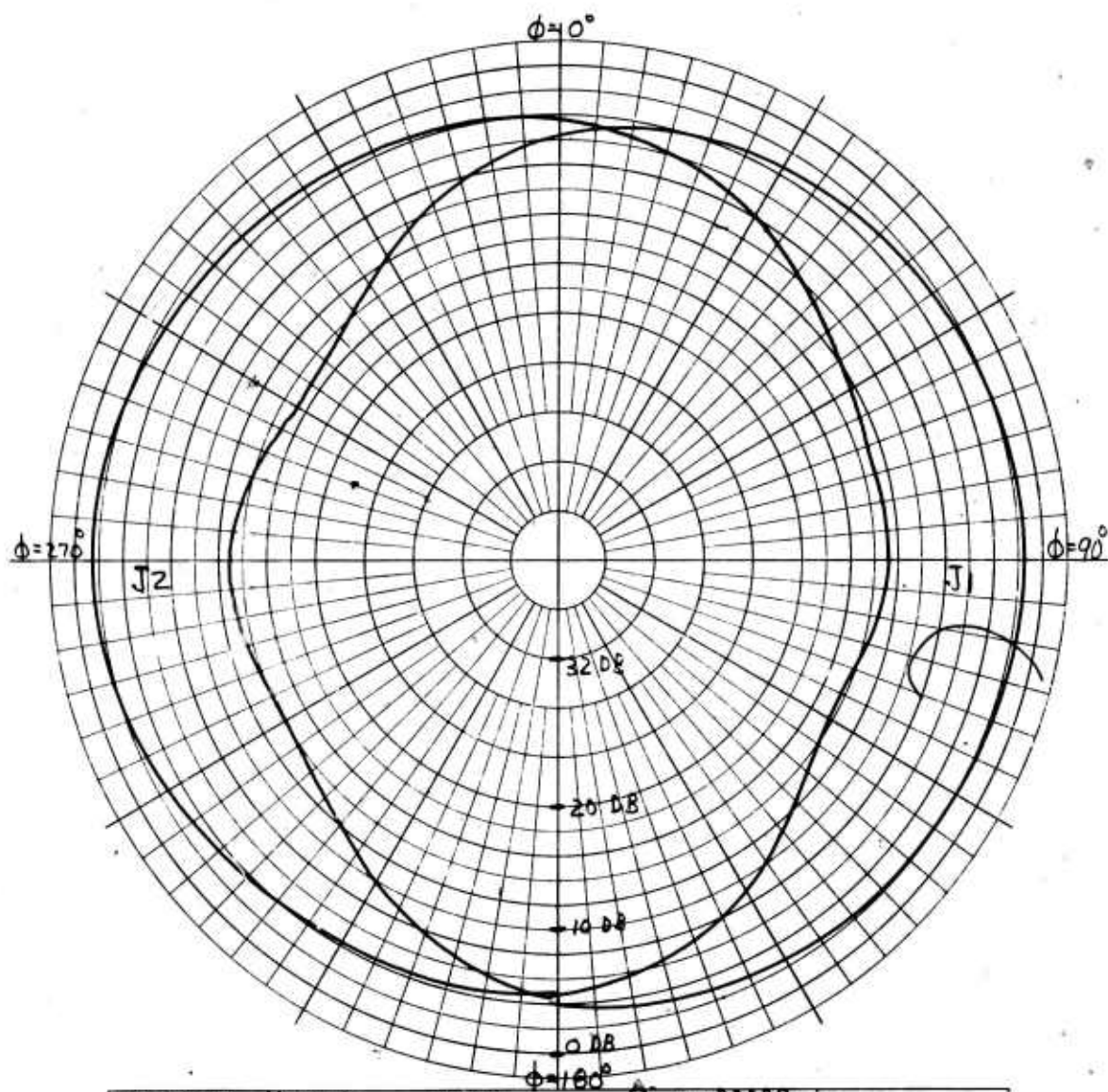




ANTENNA TYPE <u>HOMING</u>		LOCATION	USE <u>PPADS</u>
TEST MODEL: <u>UNIT #3</u>		FREQUENCY: <u>F0</u> MCS	
MODEL SCALE: <u>FULL</u>		SCALE FREQUENCY: _____ MCS	
CONDITIONS: _____		POLARIZATION: _____	
CURVES PLOTTED IN: <u>DB</u>		E $\phi$ : <u>✓</u>	
VOLTAGE: _____		E $\phi$ : _____	
POWER: _____		PATTERN AREA: _____	
ENGINEER <u>LDB</u>	OPERATOR <u>NMS</u>	FILE NO. <u>7</u>	DATE <u>8-29-68</u>

ANTLAB # 36330

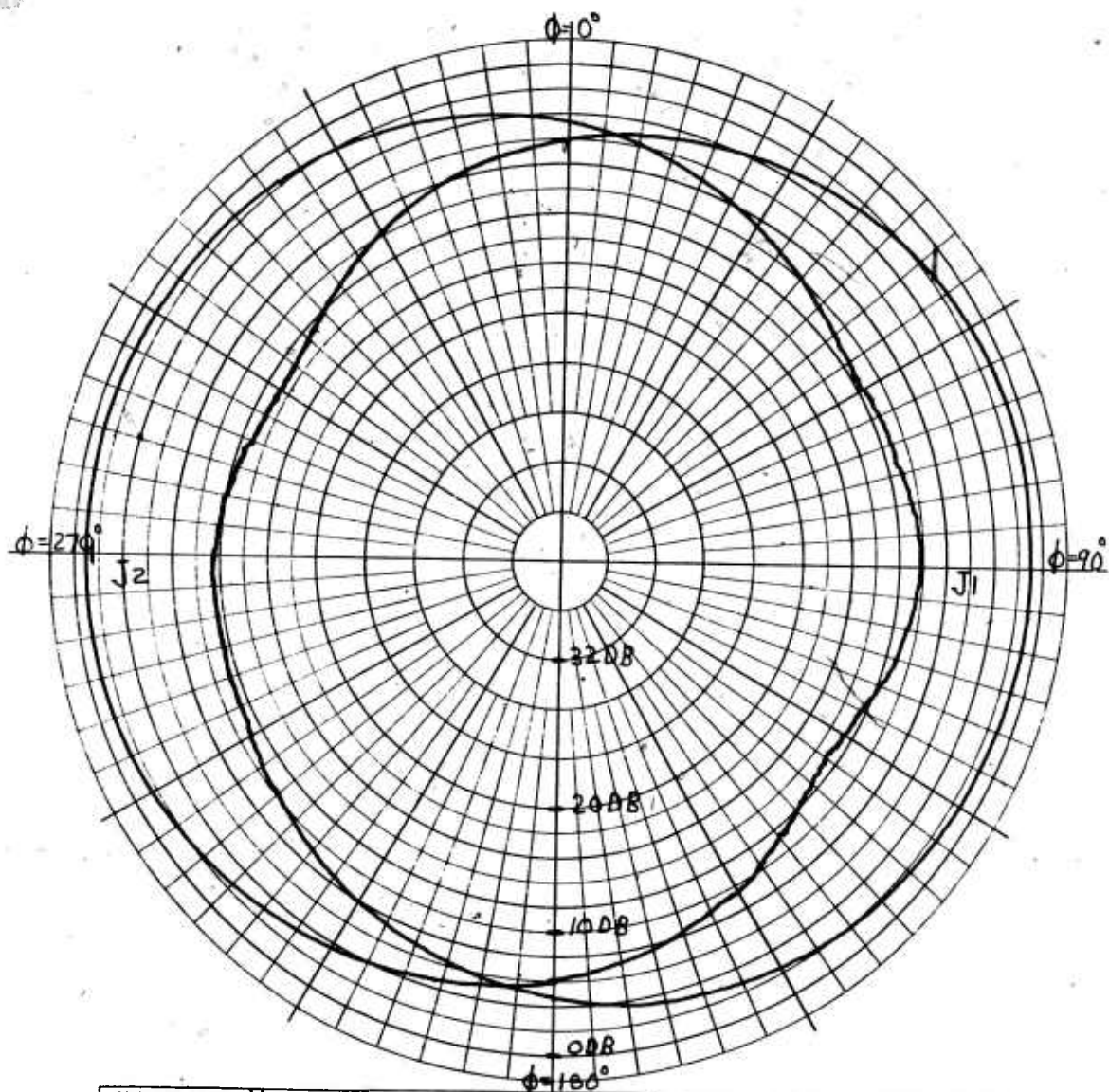
Figure 73.  $f_0$  Azimuth Pattern (45-Degree Depression)



ANTENNA TYPE	HOMING	LOCATION	USE PPADS
TEST MODEL:	UNIT #3	FREQUENCY:	F <sub>0</sub> MCS
MODEL SCALE:	FULL	SCALE FREQUENCY:	MCS
CONDITIONS:		POLARIZATION:	
CURVES PLOTTED IN:	DB	E $\phi$ :	<input checked="" type="checkbox"/>
VOLTAGE:		E $\phi$ :	
POWER:		PATTERN AREA:	
ENGINEER	LDB	OPERATOR	NMS
FILE NO.	8	DATE	9-3-68

ANTLAB # 36330

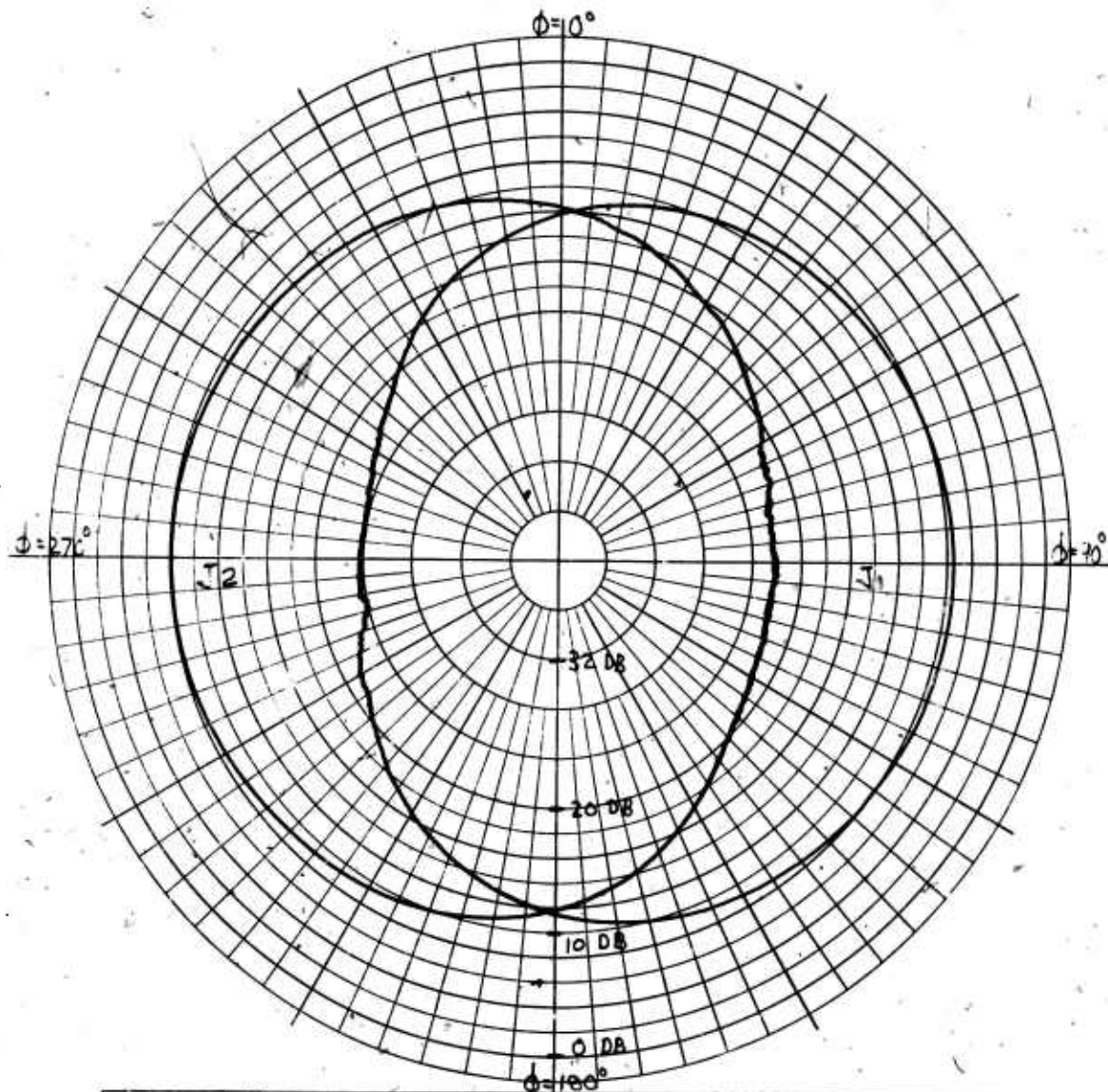
Figure 74.  $f_0$  Azimuth Pattern (60-Degree Depression)



ANTENNA TYPE <u>HOMING</u>	LOCATION	USE <u>PPADS</u>	<input type="checkbox"/> $\phi$ CUTS <input type="checkbox"/> DEPRESSION <u>0°</u>
TEST MODEL: <u>UNIT 3</u>	FREQUENCY: <u>F<sub>HI</sub></u> MCS	SCALE FREQUENCY: _____ MCS	
MODEL SCALE: <u>FULL</u>	POLARIZATION:	E $\phi$ : <input checked="" type="checkbox"/>	
CONDITIONS:	E $\phi$ : _____	PATTERN AREA: _____	
CURVES PLOTTED IN: <u>DB</u>	VOLTAGE:	POWER:	
ENGINEER <u>LDB</u>	OPERATOR <u>NMS</u>	FILE NO. <u>9</u>	DATE <u>9-3-68</u>

ANTLAB # 36330

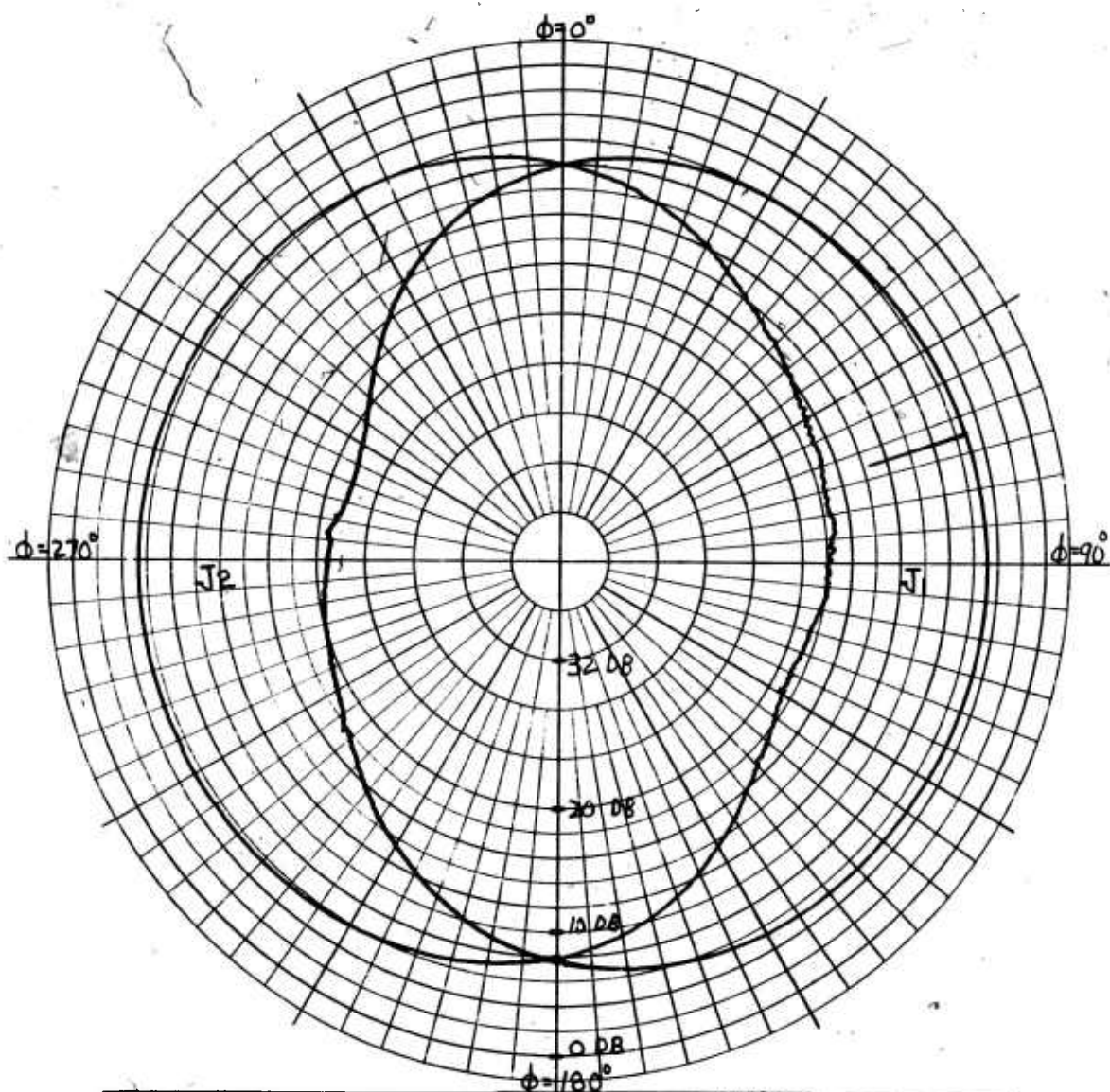
Figure 75.  $f_{hi}$  Azimuth Pattern (0-Degree Depression)



ANTENNA TYPE <u>HOMING</u>	LOCATION	USE <u>PPADS</u>	<input type="checkbox"/>
TEST MODEL: <u>UNIT #3</u>	FREQUENCY: <u>F-HI</u> MCS	SCALE FREQUENCY: _____ MCS	<input type="checkbox"/>
MODEL SCALE: <u>FULL</u>	POLARIZATION:	E $\phi$ : <u>✓</u>	<input type="checkbox"/>
CONDITIONS:	E $\phi$ : _____	PATTERN AREA:	<input type="checkbox"/>
CURVES PLOTTED IN: <u>DB</u>			
VOLTAGE:			
POWER:			
ENGINEER <u>LDB</u>	OPERATOR <u>NMS</u>	FILE NO. <u>10</u>	DATE <u>8-29-68</u>

ANTLAB # 36330

Figure 76.  $f_{h1}$  Azimuth Pattern (15-Degree Depression)

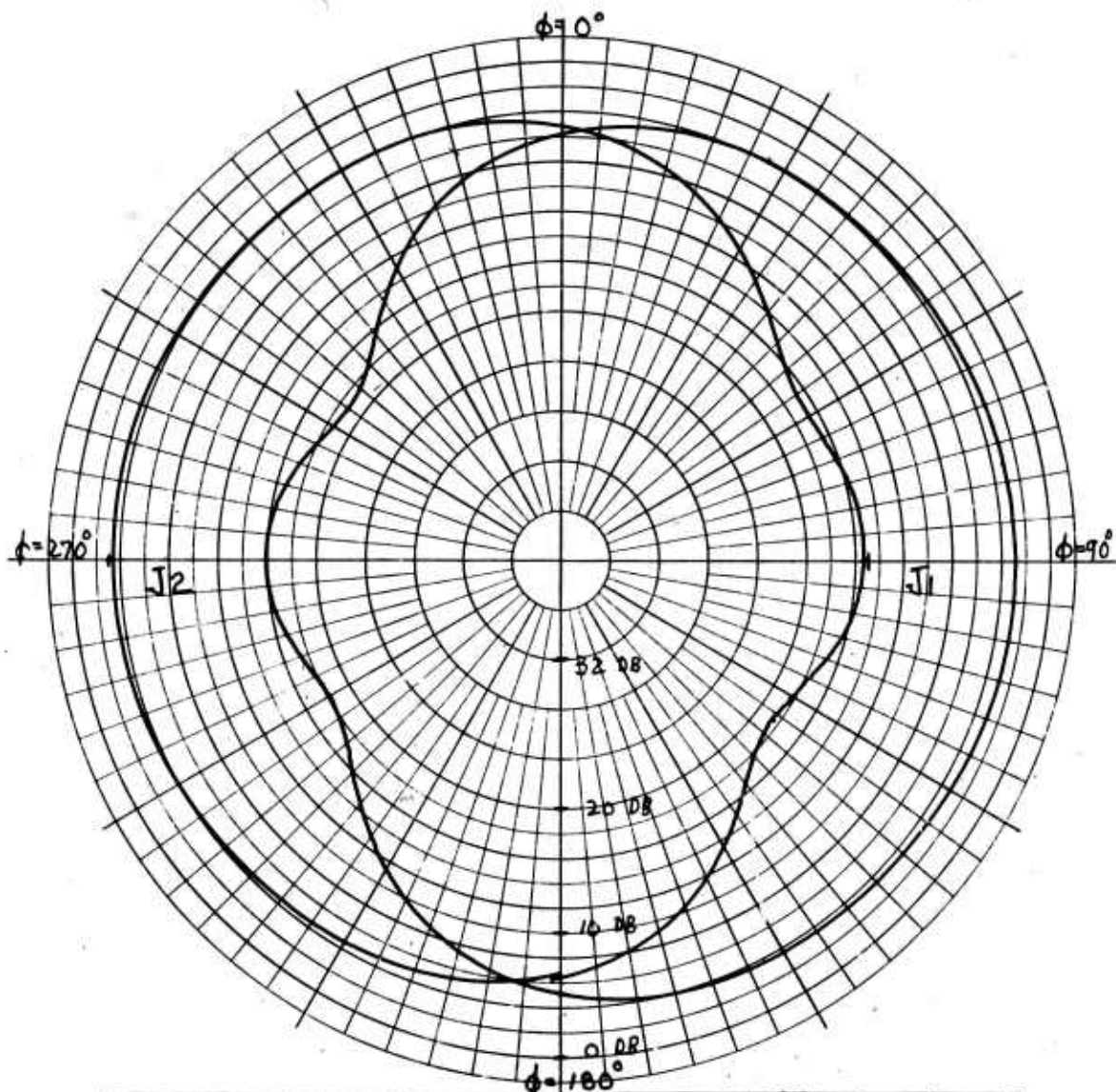


ANTENNA TYPE <u>HOMING</u>	LOCATION	USE <u>PPADS</u>	
TEST MODEL: <u>UNIT #3</u>	FREQUENCY: <u>F<sub>h1</sub></u> MCS	$\phi$ CUTS <input type="checkbox"/>	
MODEL SCALE: <u>FULL</u>	SCALE FREQUENCY: MCS	DEPRESSION <u>45°</u>	
CONDITIONS:	POLARIZATION:		
CURVES PLOTTED IN: <u>DB</u>	E $\phi$ : <input checked="" type="checkbox"/>		
VOLTAGE:	E $\phi$ :		
POWER:	PATTERN AREA:		
ENGINEER <u>LDB</u>	OPERATOR <u>NMS</u>	FILE NO. //	DATE <u>8-30-68</u>

ANTLAB # 36330

Figure 77.  $f_{h1}$  Azimuth Pattern (45-Degree Depression)





ANTENNA TYPE <u>HOMING</u>	LOCATION	USE <u>PPADS</u>	
TEST MODEL: <u>UNIT 3</u>	FREQUENCY: <u>F-H1</u> MCS	<input type="checkbox"/>	
MODEL SCALE: <u>FULL</u>	SCALE FREQUENCY: MCS	<input type="checkbox"/>	
CONDITIONS:	POLARIZATION: <input checked="" type="checkbox"/>	<input type="checkbox"/>	
CURVES PLOTTED IN: <u>DB</u>	E $\phi$ : <input checked="" type="checkbox"/>	<input type="checkbox"/>	
VOLTAGE:	E $\phi$ :	<input type="checkbox"/>	
POWER:	PATTERN AREA:	<input type="checkbox"/>	
ENGINEER <u>LDB</u>	OPERATOR <u>NMS</u>	FILE NO. <u>12</u>	DATE <u>9-3-68</u>

ANTLAB # 36330

Figure 78.  $f_{h1}$  Azimuth Pattern, (60-Degree Depression)

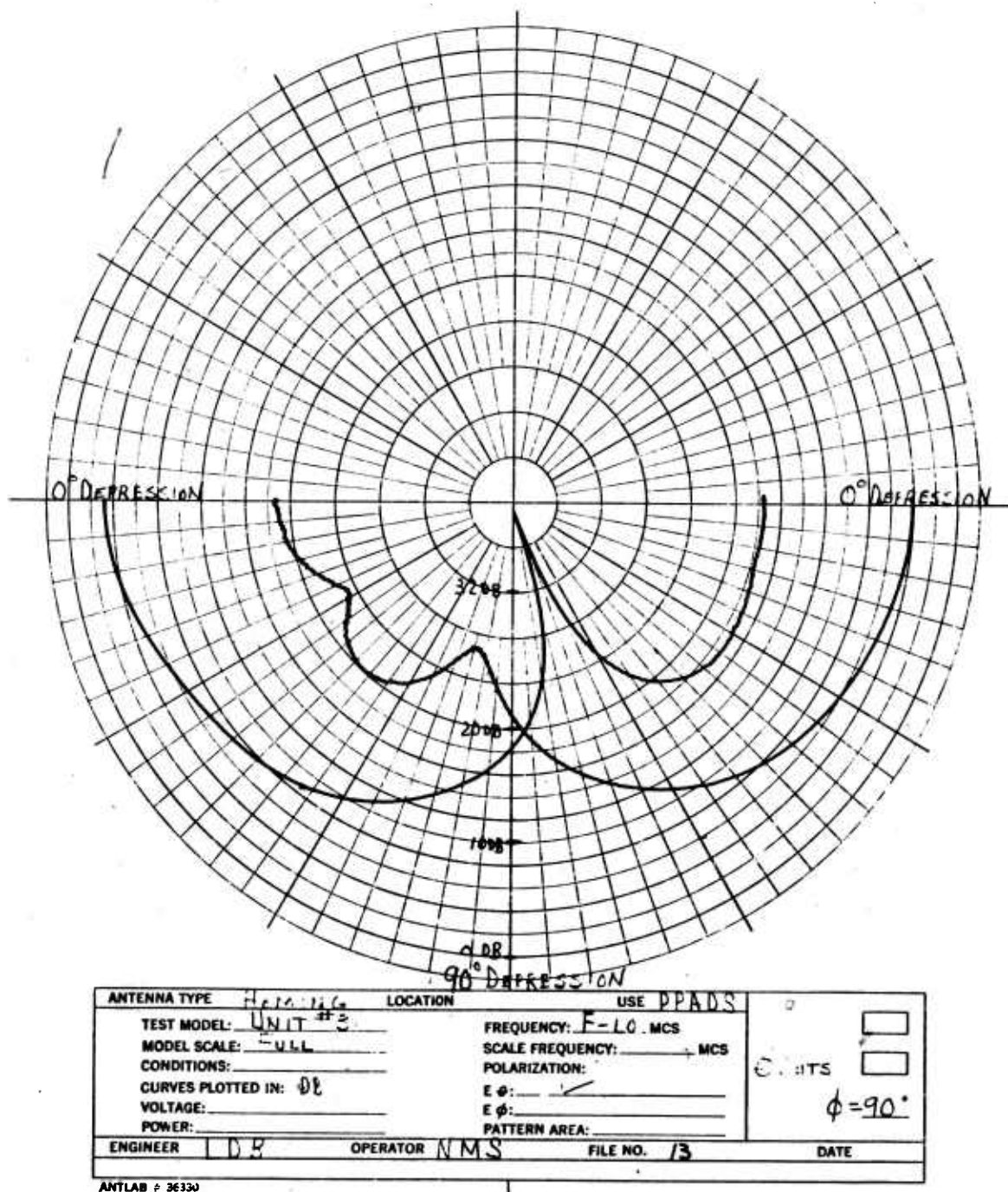
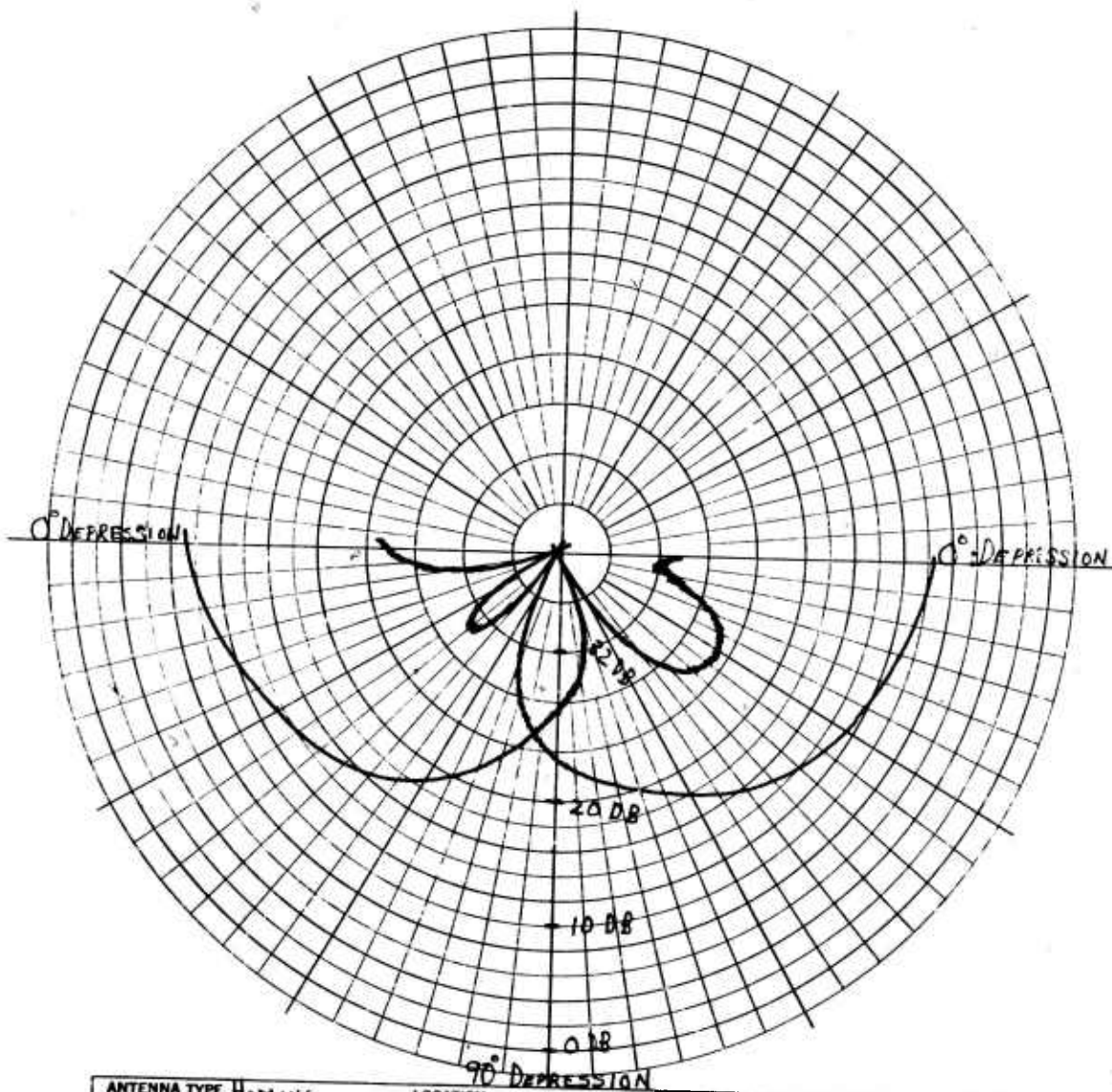


Figure 79.  $f_{10}$  Elevation Plane Pattern



ANTENNA TYPE <u>HOMING</u>	LOCATION	USE <u>PPADS</u>	
TEST MODEL: <u>UNIT #3</u>	FREQUENCY: <u>F<sub>0</sub></u> MCS		<input type="checkbox"/>
MODEL SCALE: <u>FULL</u>	SCALE FREQUENCY: MCS		<input type="checkbox"/>
CONDITIONS:	POLARIZATION:	$\Theta$ CUTS	<input type="checkbox"/>
CURVES PLOTTED IN: <u>DB</u>	E $\phi$ : <input checked="" type="checkbox"/>	$\phi = 90^\circ$	
VOLTAGE:	E $\phi$ :		
POWER:	PATTERN AREA:		
ENGINEER <u>LDR</u>	OPERATOR <u>NIA</u>	FILE NO. <u>14</u>	DATE

ANTLAB # 36330

Figure 80.  $f_0$  Elevation Plane Pattern



Figures 79 and 80 are elevation plane cuts taken from right to left on the control box. They were taken to assure that the side-lobe level did not increase to an unusable level at depression angles other than those used in azimuth plane measurements. The side-lobe level is 10 db down or greater for all depression angles up to approximately 75 degrees. Above 75 degrees, the side-lobe level increases rapidly.

#### TEST PLAN

A draft of the test plan for antenna system functional tests was prepared. It was the purpose of the plan to establish test procedures, equipment requirements, and the data to be obtained to determine adequate antenna system performance prior to installation of each system. Exact antenna performance specifications must be determined from further system analyses.

#### DISCUSSION

Although the antenna impedance is degraded somewhat by shortening, the antenna is reasonably well matched to the transmission line (cables), and very little system sensitivity is lost. The antenna length could be reduced further to allow recessing into the box. The impedance mismatch would be approximately the same as when the connectors were recessed 1/4 inch. System sensitivity would be degraded approximately 0.2 db at  $f_0$  and 0.3 db at  $f_{10}$  over the final length chosen in this report.

Grounding straps were connected from the antenna connectors and the control box cover during the impedance and pattern measurements. No change in impedance or radiation patterns with or without the straps was evident. It is recommended that the straps be retained to remove the possibility of radiation pattern jitter due to interruption of currents between the mounting bar and the control box cover.

The radiation pattern data, when compared to the scale model measurements (see Appendix IV) indicates some changes of characteristics. The course error signal at 5 degrees from electrical boresight averages 1.1 db for the full-scale antenna system as compared with 1.1 db for the scale model measurements. The course error signal at 12 degrees from electrical boresight averages 2.6 db for the full-scale antenna system as compared to 2.4 db for the scale model measurements. Thus, the course error signals compare quite favorably. The side-lobe levels of the full-scale antenna system were considerably higher than the measured values on the scaled version. The side-lobe levels were from 2.7 db to 17 db higher on the full-scale mockup at  $f_0$ ; however, the side-lobe level is still -10 db or greater over most of the lower hemisphere of radiation pattern coverage. There appear to be two reasons for the side-lobe level increase on the full-scale antenna. The signal received by the two antenna elements is slightly unbalanced in amplitude because of the hybrid loss unbalance. This would not allow the two antenna signals to cancel one another completely at broadside aspect angles to the control box and, thus, increase the side-lobe level. The

second reason is that the radiating element on the full-scale unit is not strictly a monopole antenna, but more a sleeve-type dipole. This is due to the method of construction where a type "N" connector is used as the lower part of the radiating element. Thus, the current distribution on the radiating element will be slightly different from that obtained on the scale-model monopole antennas. This could lead to an unbalance in received signal amplitude on the two antennas near broadside aspect angles and, again, not allow complete cancellation of signals for a low side-lobe level. A slightly different spacing of the antenna elements could possibly improve the side-lobe level if desired.

APPENDIX VI  
INSTRUMENTATION

GENERAL

The original instrumentation package was designed around a GFE recorder (CEC 5-118) and contained a high-speed 16mm movie camera to photograph the parawing during deployment and disreefing and in flight. The package also contained a 4-ampere-hour nickel-cadmium battery pack and the necessary signal conditioning circuits, etc. The instrumentation was designed to provide reason-for-failure data and certain engineering data for performance evaluation.

The initial setup provided six data channels to the recorder as follows:

<u>Channel</u>	<u>Function</u>
1	Motor Current
2	PAM Switch (16 Channels)
3	Control Line Load
5	Control Line Load
7	Roll Inclinator
9	Pitch Inclinator

Channel 2 provides recording time sharing via a commutator for the following.

PAM Switch Channels

1	Right Turn Relay	9	Amplifier Power
2	Left Turn Relay	10	Suspension Load
3	Loss Carrier Relay	11	Suspension Load
4	Receiver Battery	12	Suspension Load
5	Servo Battery	13	Suspension Load
6	22-Volt Regulator	14	Preset Voltage
7	Accelerometer	15	Servo Feedback
8	Hi-Level Steering	16	Instrumentation Battery

Other data-gathering means used during the flight test program were:

1. Fairchild analyzer was used for preliminary indications of effective L/D of the system. Two methods were considered for obtaining the data eliminating the effects of the wind:

- a. One method is to simply fly the system along the prescribed course both upwind and downwind, and then average the results for the L/D and the descent rate.
- b. The second method would entail the use of two auxiliary devices in addition to the basic parawing system:
  - (1) a drag device which will descend at the same rate as the parawing system and (2) a deadweight. The system test procedure would then include the release of the weight and the drag device simultaneously with the initiation of the test record. As a result, the deadweight would then provide a starting point, the drag device would provide an actual wind effect on the system, and the parawing system would impact at a point including the wind effect. Physical measurement of the locations of the three test components on the ground would then facilitate calculation of the actual performance of the system during no-wind conditions.

Laying out the course for use of the Fairchild analyzer is simple geometry depending on the portion of the flight to be recorded. The record obtained, due to the method of operation of the analyzer, can be roughly read by the use of an overlay to spot check the L/D and descent rate of the system.

2. Closed-circuit television for quick-look review data of deployment and flight performance.
3. Brinell block harness for maximum load measurements during deployment tests.
4. 16mm movies, both ground and airborne, with up to 40-inch lens for closeup views of deployments, etc.
5. Still photographs for documentation purposes.
6. Smoke bombs attached to payloads during test to facilitate tracking.
7. Personnel with spring scales to measure pull-in loads and for preliminary evaluation of parawing control characteristics.

The instrumentation package was used on three flights during the preliminary flight test phase and on ten flights during the deployment and control flight test phase. These flights were:

102 - 8 August 1968	212 - 2 December 1968	225 - 6 December 1968
108 - 9 August 1968	214 - 2 December 1969	229 - 9 December 1968
123 - 25 September 1968	217 - 3 December 1969	242 - 16 December 1968
204 - 22 November 1968	224 - 6 December 1969	244 - 17 December 1968
208 - 27 November 1968		

Flights 204 through 229 were deployment tests and used the instrumentation package in place of the control box. The others used the instrumentation box and the control box and were control flights.

A summary for each of the instrumented flights categorized according to the test being conducted follows:

#### PRELIMINARY FLIGHT TEST

1. Test 102 - 8 August 1968

- a. Manual control flight (interim receiver)
- b. Twin-catenary keel with tubular nylon lines
- c. Weight (lbs) Payload 100  
Control Box 67  
Instrumentation 112  
Total 279
- d. Snyder reefer
- e. System stable at approximately 25 seconds
- f. Pull-in: 6 inches in manual  
4 inches in loss carrier
- g. Post-flight check showed left servo cable tangled
- h. Instrumentation turned on 9 seconds after deployment
- i. Deployment 40 KIAS at 4000 feet
- j. Flight duration 275 seconds
- k. Pitch and roll data no good
- l. Relay closure monitor inoperative except loss carrier
- m. Alternate left and right manual turns were transmitted during flight
- n. No indication of loss carrier during flight

Figures 81 through 83 are portions of the data tape from flight 102.

Figure 81 starts 9 seconds after deployment and shows the suspension loads at 10 and 11 seconds after deployment. It also

shows the actuator current pulse for a left turn pull-in as indicated by the voltage levels of segment 14 (hi-level preset) and segment 15 (servo feedback).

The second figure (Figure 82) shows the actuator current for a 6-inch right turn pull-in and return to neutral. It also shows the right control line load during the right turn and the suspension loads during steady-state flight.

The third figure (Figure 83) shows the actuator current for a 6-inch left turn pull-in and for return to neutral. It also shows the left control cable load and the suspension loads.

It can also be noted that the control line load does not start to increase until approximately half of the pull-in time has elapsed.

See Table XLII for calibration data.

2. Test 108 - 9 August 1960

a. Manual control flight (interim receiver)

b. Weight (Lbs)	Payload	100
	Control box	67
	Instrumentation	<u>112</u>
	Total	279

c. Pull-in      6 inches in manual  
                 0 inch in loss carrier

d. Instrumentation turned on 9 seconds after deployment

e. Deployment 60 KIAS at 4000 feet

f. Flight duration 200 seconds

g. Pitch and roll data no good

h. Relay closure monitor inoperative

i. Alternate left and right turns transmitted during flight

j. Load cell for aft suspension load apparently damaged at deployment

k. Load cell for left suspension load open at approximately 55 seconds

Figures 84 through 86 are portions of the data tape from flight 108.

Figure 84 shows the suspension loads at 12 seconds and identifies the channels. It also shows the aft suspension load cell open when the instrumentation is turned on.

Figure 85 shows the servo actuator current and control cable load for a 6-inch right-turn pull-in and the actuator current for return to neutral.

Figure 86 shows the same information for a 6-inch left-turn pull-in (see Table XLII for calibration).

3. Test 123 - 25 September 1968

a. Automatic homing flight (final receiver)

b. Weight (Lbs):	Payload	300
	Control box	65
	Instrumentation	<u>112</u>
	Total	477

c. Pull-in: 6 inches manual  
3-1/4 inches automatic  
5 inches loss carrier

d. Instrumentation turned on 6 seconds after deployment

e. Deployment 40 KIAS at 7000 feet

f. Flight duration 138 seconds

g. Snyder reefer tangled in right leading-edge lines, causing a continuous tight right turn to impact

Since the reefer was tangled in the right lines, the wing stayed in a tight right turn to impact.

The data tape from flight 123 shows that the system was in automatic homing for the first 75 seconds and that the servo actuator functioned at least 85 times during this period. The right control line load was erratic during the flight and reached peaks in excess of 60 pounds. The system was switched to manual after 75 seconds, and right and left turns were transmitted.

The tape shows the delay from receiver power on to AGC buildup to be 7 seconds. The servo actuator current indicates pull-in times on the order of 1 second for 6-inch pull-in.

The suspension loads were erratic throughout the flight. Eight seconds before impact, the suspension loads were as follows:

Aft	450
Forward	300
Left	59
Right	<u>177</u>
Total	986 Lbs

The highest single suspension load was in the aft load cell at 50 seconds. The load was 510 pounds from the aft load cell alone. The others were forward 285 pounds, left 118 pounds, and right 70 pounds, for a total of 983 pounds.

Although the system was in a very tight right turn from deployment to impact, due to the tangled reefer, the data tape indicates that the control system was functioning normally throughout the flight in both the automatic homing and manual modes.

#### DEPLOYMENT TEST

##### 1. Test 204 - 22 November 1968

Test 204 was a deployment test using the deployment sleeve with "0" + 3/4 nose tuck reefing for 4 seconds. The payload weighed 500 pounds, and the instrumentation package used in place of the control box weighed 85 pounds. A Brinell block was used between the payload and instrumentation package for peak load indication, and load cells were used in each suspension line group to obtain the load/time history. Figure 87 is a portion of the data tape covering the first 7 seconds of the flight. It shows a peak load in the reefed mode of about 1995 pounds or 3.4 g and a peak load in the disreefed mode of about 4160 pounds or 7.1 g, while the Brinell block indicated a peak load of 3700 pounds or 7.4 g. Since the drop was uncontrolled, a right turn was tied into the wing. The turn result was a tight, right turn as indicated by static loads of:

Aft	378
Forward	416
Left	215 at 50 sec
Right	<u>252</u>
Total	1261 Lbs or 2.15 g

Total flight time was 56 seconds. Deployment was 3000 feet at 80 KIAS.



2. Test 208 - 27 November 1968

Test 208 was a deployment test using the deployment bag with "0" + 3/4 nose tuck reefing for 4 seconds. The payload weighed 500 pounds, and the instrumentation package used in place of the control box weighed 85 pounds. A Brinell block was used between the payload and the instrumentation package for peak load indications, and load cells were used in each suspension line group to obtain the load/time history. Figure 88 is a portion of the data tape covering the first 10 seconds of the flight. It shows a peak load in the reefed mode of 1445 pounds or 2.5 g and a peak load in the disreefed mode of 2245 pounds or 2.85 g, while the Brinell block indicated a peak load of 1900 pounds or 3.8 g. Total flight time was 120 seconds. Deployment was 3000 feet at 80 KIAS.

3. Test 212 - 2 December 1968

Test 212 was a deployment test using the deployment sleeve with "0" + 1/2 nose tuck reefing for 4 seconds. The payload weighed 500 pounds, and the instrumentation package used in place of the control box weighed 85 pounds. A Brinell block was used between the payload and the instrumentation package for peak load indications, and load cells were used in each suspension line group to obtain the load/time history. Figure 89 is a portion of the data tape covering the first 8 seconds of flight. It shows a peak load in the reefed mode of 1860 pounds or 3.2 g and a peak load in the disreefed mode of 2185 pounds or 3.75 g, while the Brinell block indicated a peak load of 3300 pounds or 6.6 g.

The accelerometer shows a peak in excess of 6 g, but no corresponding loading appears on the data tape. Deployment was 3000 feet at 80 KIAS.

4. Test 217 - 3 December 1968

Test 217 was a deployment test using the deployment sleeve with a drogue chute and "0" + 1/2 nose tuck reefing. Delays were 2 seconds on the drogue chute and 2 seconds in the reefed mode. The payload weighed 500 pounds, and the instrumentation package used in place of the control box weighed 85 pounds. A Brinell block was used between the payload and the instrumentation package for peak load indication, and load cells were used in each suspension line group for the load/time history. Figure 90 is a portion of the data tape covering the first 6 seconds of flight. The reefing line used on this flight was a MIL-W-5625 1000-pound web. The reefing line broke, and the resulting load as indicated by the Brinell block was 7200 pounds or 14.4 g. All four of the load cells used on the suspension line groups were damaged beyond reuse. Deployment was 3000 feet at 80 KIAS.

5. Test 224 - 6 December 1968

Test 224 was a deployment test using the deployment bag and "O" + 1/2 nose tuck reefing for 4 seconds. The payload weighed 500 pounds, and the instrumentation package used in place of the control box weighed 85 pounds. This test used a single load cell located between the payload and the instrumentation package for the load/time history, and a similarly located Brinell block was used for peak load indication. Figure 91 is a portion of the data tape covering the first 6 seconds of the flight. It shows a peak load in the reefed mode of 2485 pounds or 5 g and a peak load in the disreefed mode of 3000 pounds or 6 g, while the Brinell block indicated a peak load of 3600 pounds or 7.2 g. Total flight time was 148 seconds, 3000 feet at 80 KIAS.

6. Test 225 - 6 December 1968

Test 225 was a deployment test using the deployment bag with a drogue chute and "O" + 1/2 nose tuck reefing using 2-second delays. The payload weighed 500 pounds, and the instrumentation package weighed 85 pounds. A single load cell was used between the payload and the instrumentation package for load/time history, and a Brinell block was used for peak load indication. The type M21, 2-second delay reefing line cutter used to release the drogue chute and deploy the parawing failed; thus, the package impacted with only the drogue chute deployed, and the instrumentation package was destroyed. When the reefing line cutter fired, the rear end blew out of the cutter, and the knife did not move far enough to cut the line. Figure 92 is a portion of the data tape covering the first 6 seconds of flight, 3000 feet at 80 KIAS.

7. Test 229 - 9 December 1968

Test 229 was a deployment test using the deployment bag with a drogue chute and "O" + 3/4 nose tuck reefing using 2-second delay on the drogue and the reefing line. This test used a rebuilt instrumentation package and a single load cell between the 85-pound instrumentation package and a 500-pound payload. Figure 93 is a portion of the data tape covering the first 8 seconds of the flight. It shows a peak load on the drogue chute of 1700 pounds or 3.4 g, a peak load in the reefed mode of 2100 pounds or 4.2 g, and a peak load in the disreefed mode of 3600 pounds or 7.2 g, while the Brinell block showed a peak load of 3700 pounds or 7.4 g. Total flight time was 135 seconds, 3000 feet at 80 KIAS.

CONTROL FLIGHT

Test 242 - 16 December 1968

Test 242 was a control flight using 1-1/2 inches pull-in in all modes. The 90-pound instrumentation package was mounted on top of the 65-

pound control box and load cells were used in the control lines only. The payload weighed 500 pounds, for a total suspended weight of 655 pounds. The data items on the instrumentation package for this flight were:

1. Left control line load
2. Right control line load
3. Hi-level preset voltage
4. Servo feedback voltage
5. Receiver AGC
6. Receiver proportional output
7. Relay closure monitor
8. 1-second timing pulse

The wing had a built-in left turn which could just be overcome by the 1-1/2-inch pull-in. The control system functioned normally in all modes. Figure 94 is a portion of the data tape showing the first 20 seconds of the flight. It shows a control line load peak in the reefed mode at about 2 seconds and a second peak load following dis-reefing at about 5.5 seconds. The time delay relay closes in 6 seconds, and the system goes into a loss carrier right turn during which the right control line load stabilizes around 35 pounds. The receiver AGC builds up to the receiver on point (3.5v) in about 7 seconds after the time delay closes, and the system goes to neutral followed by three right/left turn cycles in the automatic homing mode. The system then stays in automatic homing right turn to T + 56 seconds.

Figure 95 is a portion of the data tape covering the time span from 125 to 140 seconds. This figure starts with the system in automatic homing right turn and ends in an automatic homing left turn. The control line loads are seen to be

<u>Left</u>	<u>Right</u>	
0	31	right turn
27	0	left turn
7	17	neutral

The average time for the 1-1/2-inch pull-in is 0.35 second. The figure also shows the proportional output voltage at turn relay pull-in to be approximately 2v for left or for right turn.

The data tape for this test also shows the following AGC condition:

From power on to receiver operate (3.5v)	7.6 sec
From power on to AGC maximum (9v)	20.7 sec
From RF on to receiver operate	0.35 sec
From RF on to stable 3.5v	0.95 sec

Total flight time was 352 seconds from a drop altitude of 10,000 feet.

TABLE XLII. DATA REDUCTION (SENSITIVITY)

TABLE XLII. DATA REDUCTION (SENSITIVITY)		
Channel	Scale Factor	Data Item
1	$5.5 \text{ amp}/1.07'' = 5.15 \text{ amp}/''$	Actuator current
3	$66.4 \text{ \#}/.91'' = 73 \text{ \#}/''$	Control load (left)
5	$72.5 \text{ \#}/.92'' = 78.5 \text{ \#}/''$	Control load (right)
7	<div><div>Pitch and roll</div><div>calibration not valid</div></div>	Roll inclinometer
9		Pitch inclinometer
2 PAM		
1		Right turn relay operation
2		Left turn relay operation
3		Loss carrier relay operation
4	$20 \text{ v}/.55'' = 36.4 \text{ v}/''$	Receiver battery voltage
5	$20 \text{ v}/.55'' = 36.4 \text{ v}/''$	Servo battery voltage
6	$20 \text{ v}/.81'' = 24.6 \text{ v}/''$	Regulated 22 v
7	$4.16 \text{ G}/.84'' = 4.95 \text{ G}/''$	Accelerometer
8	$20 \text{ v}/.81'' = 24.6 \text{ v}/''$	Hi-level steering
9	$10 \text{ v}/.4'' = 25 \text{ v}/''$	Proportional output
10	$185 \text{ \#}/.83'' = 222 \text{ \#}/''$	Riser load aft
11	$188 \text{ \#}/.85'' = 226 \text{ \#}/''$	Riser load forward
12	$189 \text{ \#}/.85'' = 228 \text{ \#}/''$	Riser load left
13	$193 \text{ \#}/.85'' = 230 \text{ \#}/''$	Riser load right
14	$20 \text{ v}/.80'' = 25 \text{ v}/''$	Preset voltage
15	$20 \text{ v}/.80'' = 25 \text{ v}/''$	Servo feedback voltage
16	$5 \text{ v}/.52'' = 9.6 \text{ v}/''$	Regulated 5 VDC (instrumentation)

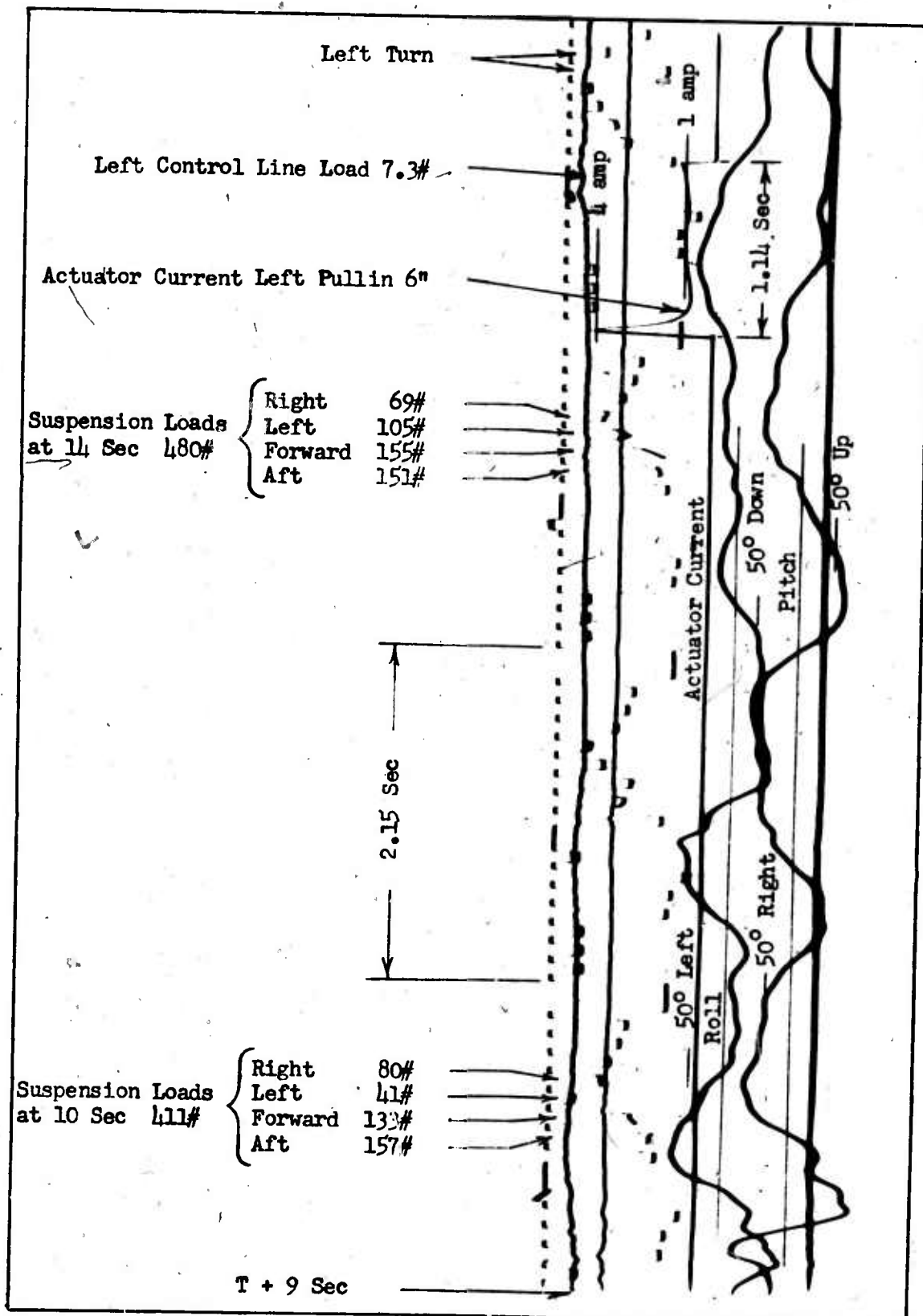


Figure 81. Instrumentation Data Test 102

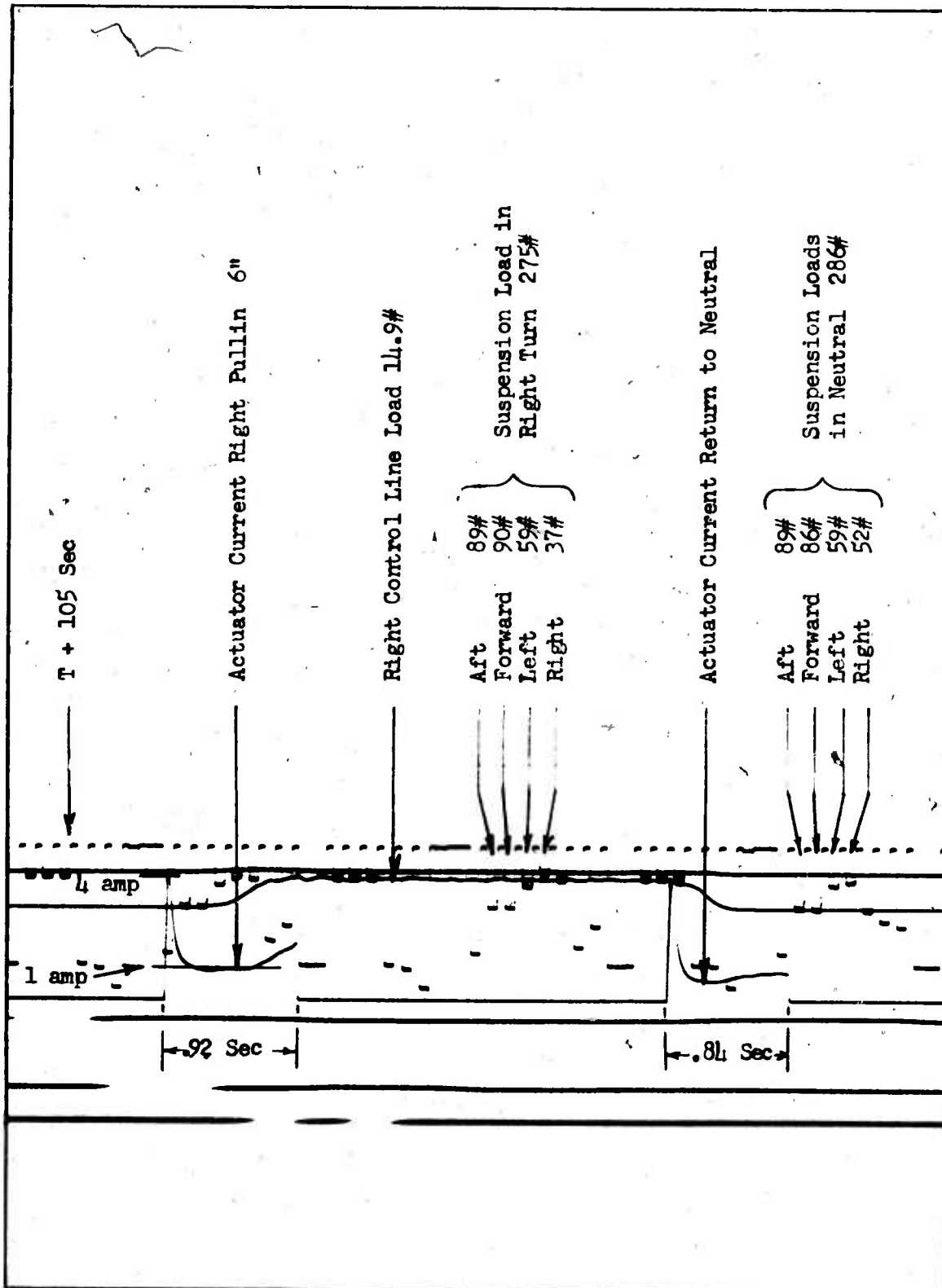


Figure 82. Instrumentation Data Test 102

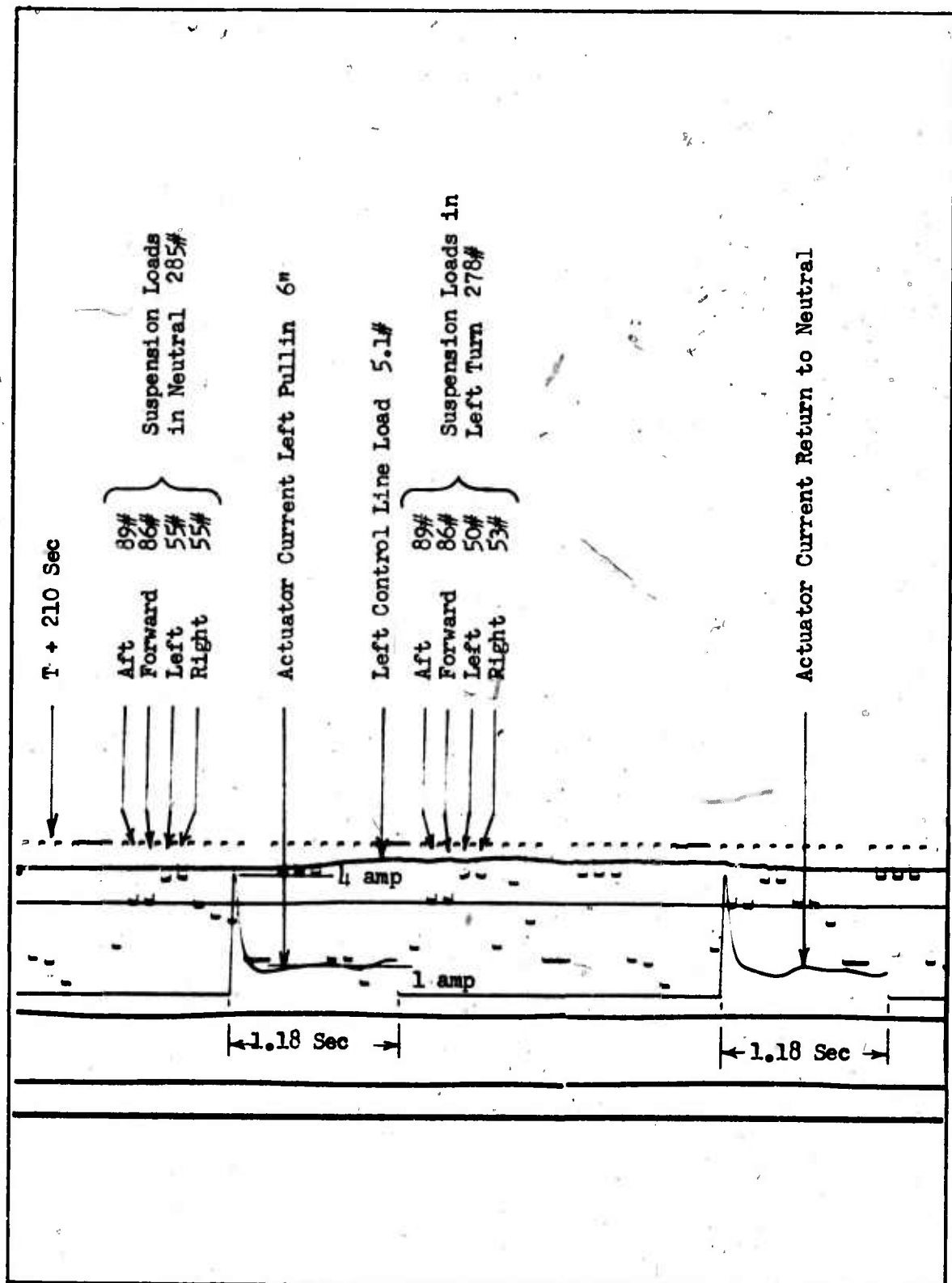


Figure 83. Instrumentation Data Test 102

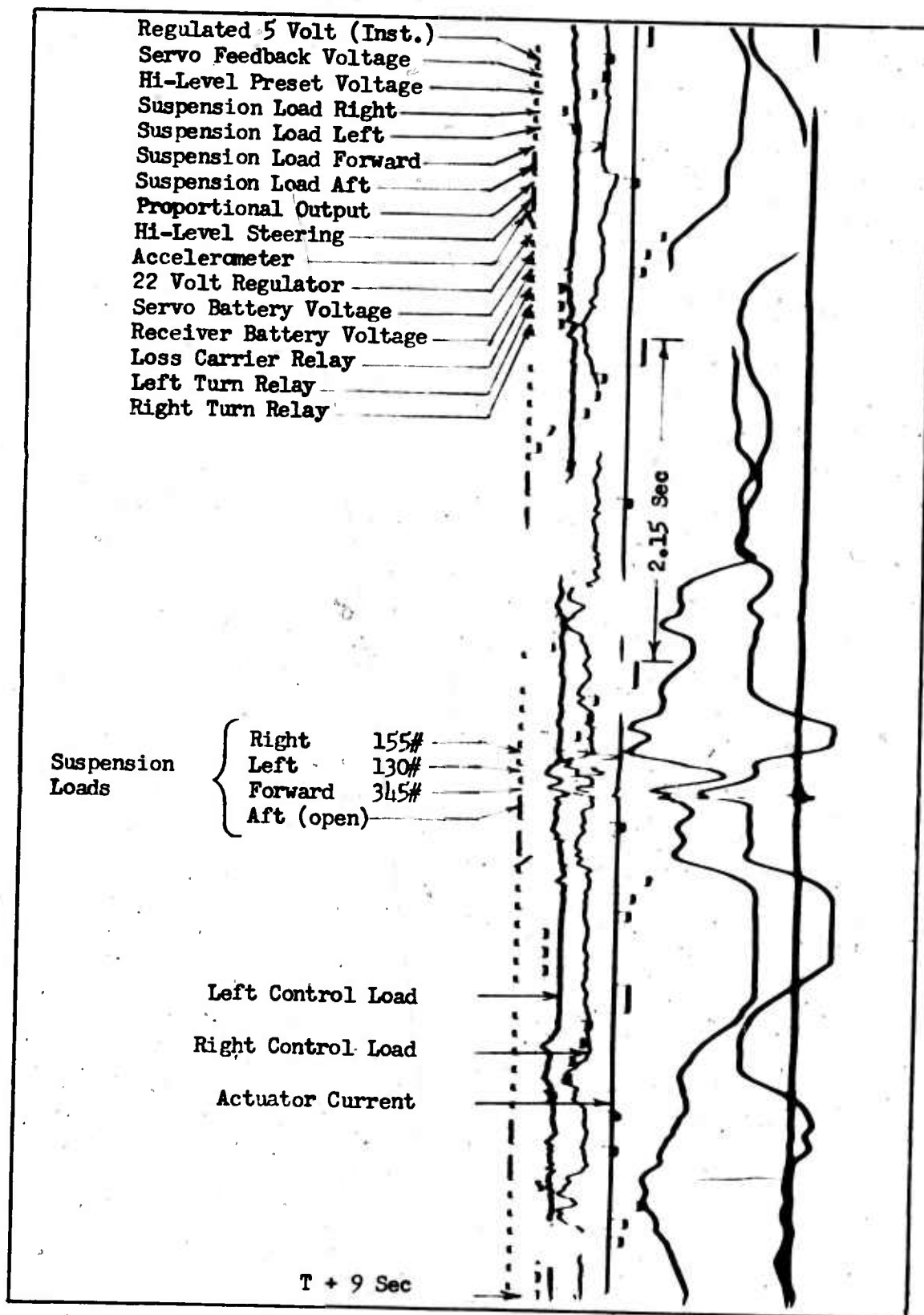


Figure 84. Instrumentation Data Test 108



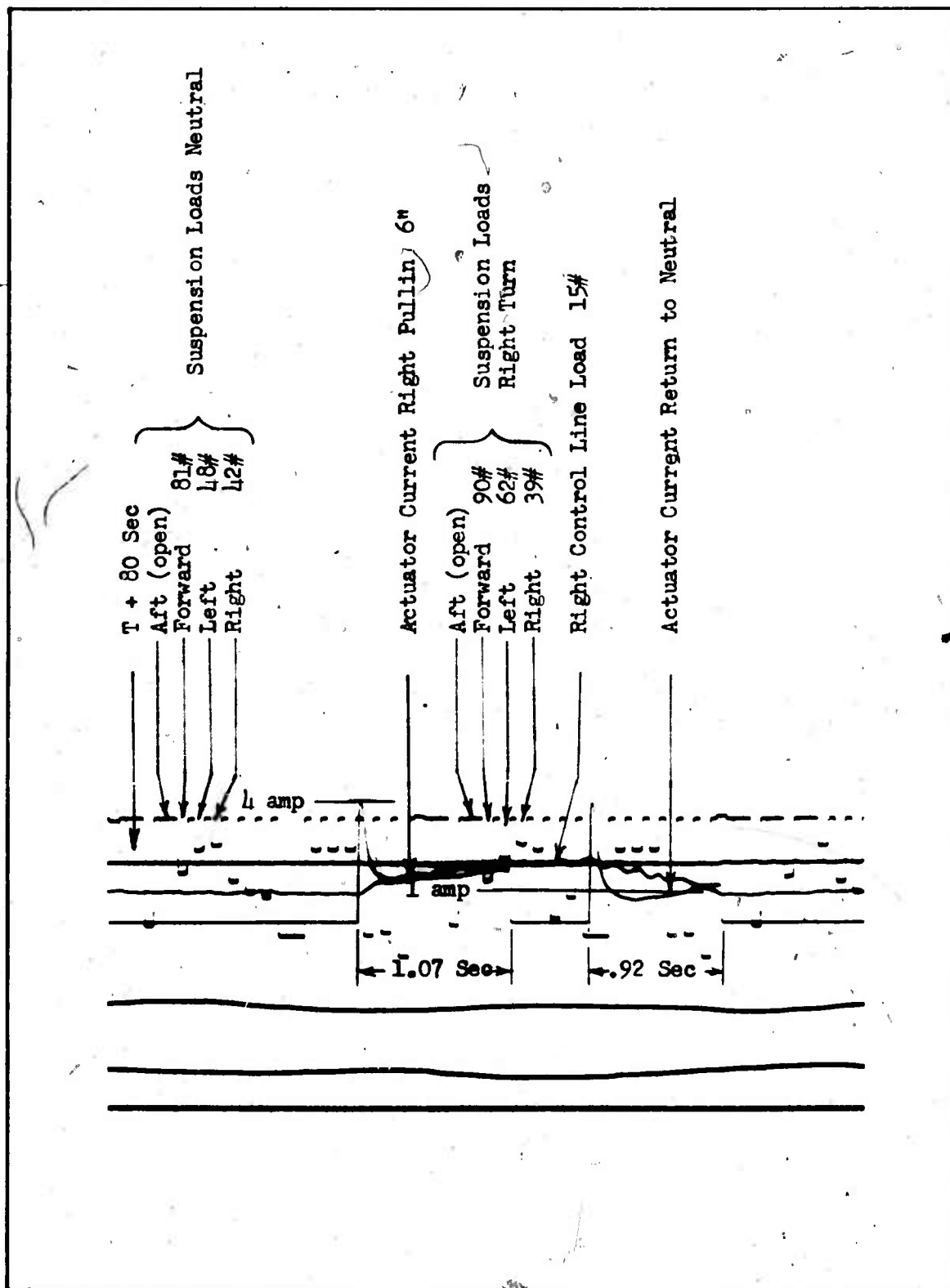


Figure 85. Instrumentation Data Test 108

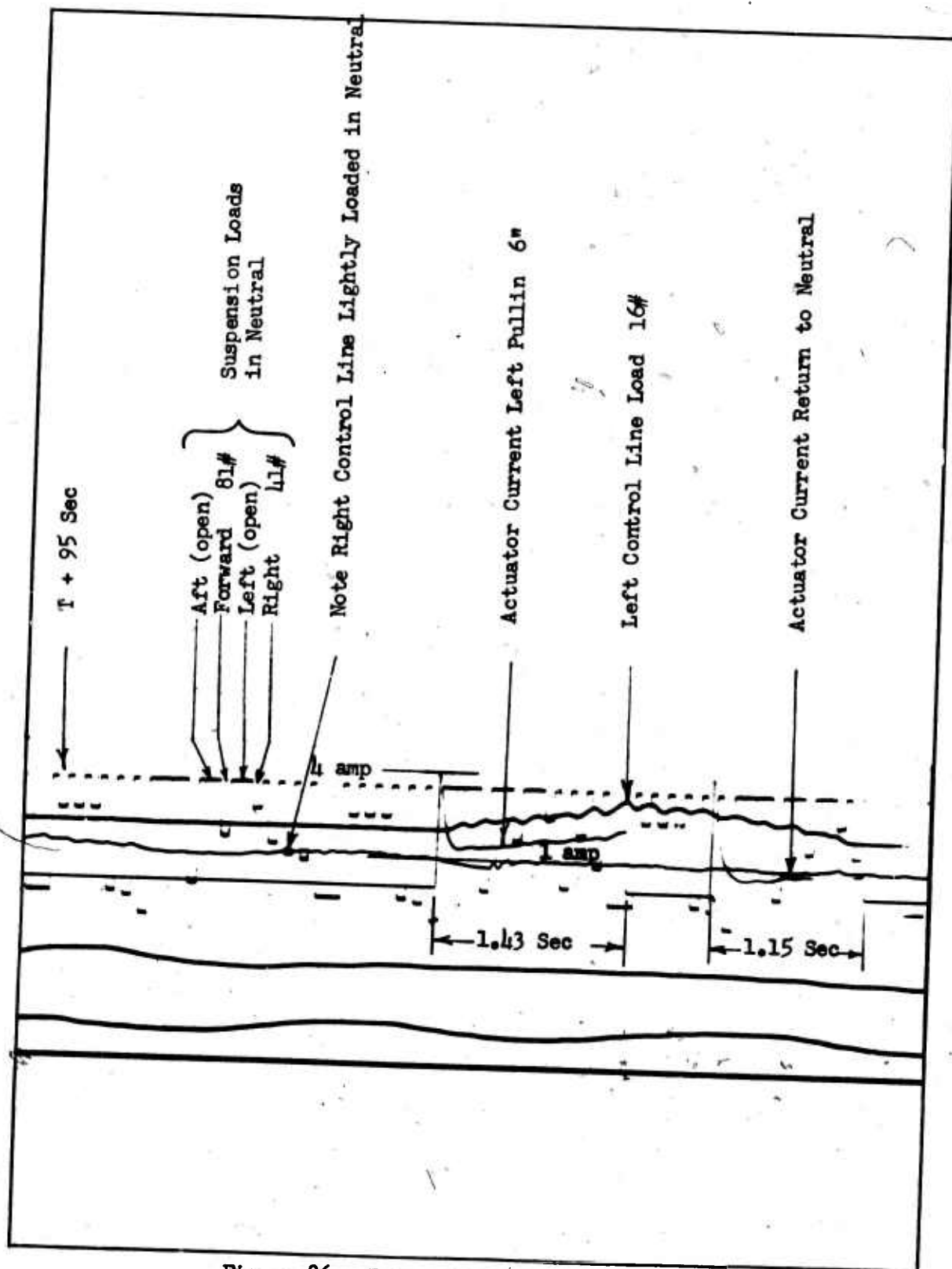


Figure 86. Instrumentation Data Test 108

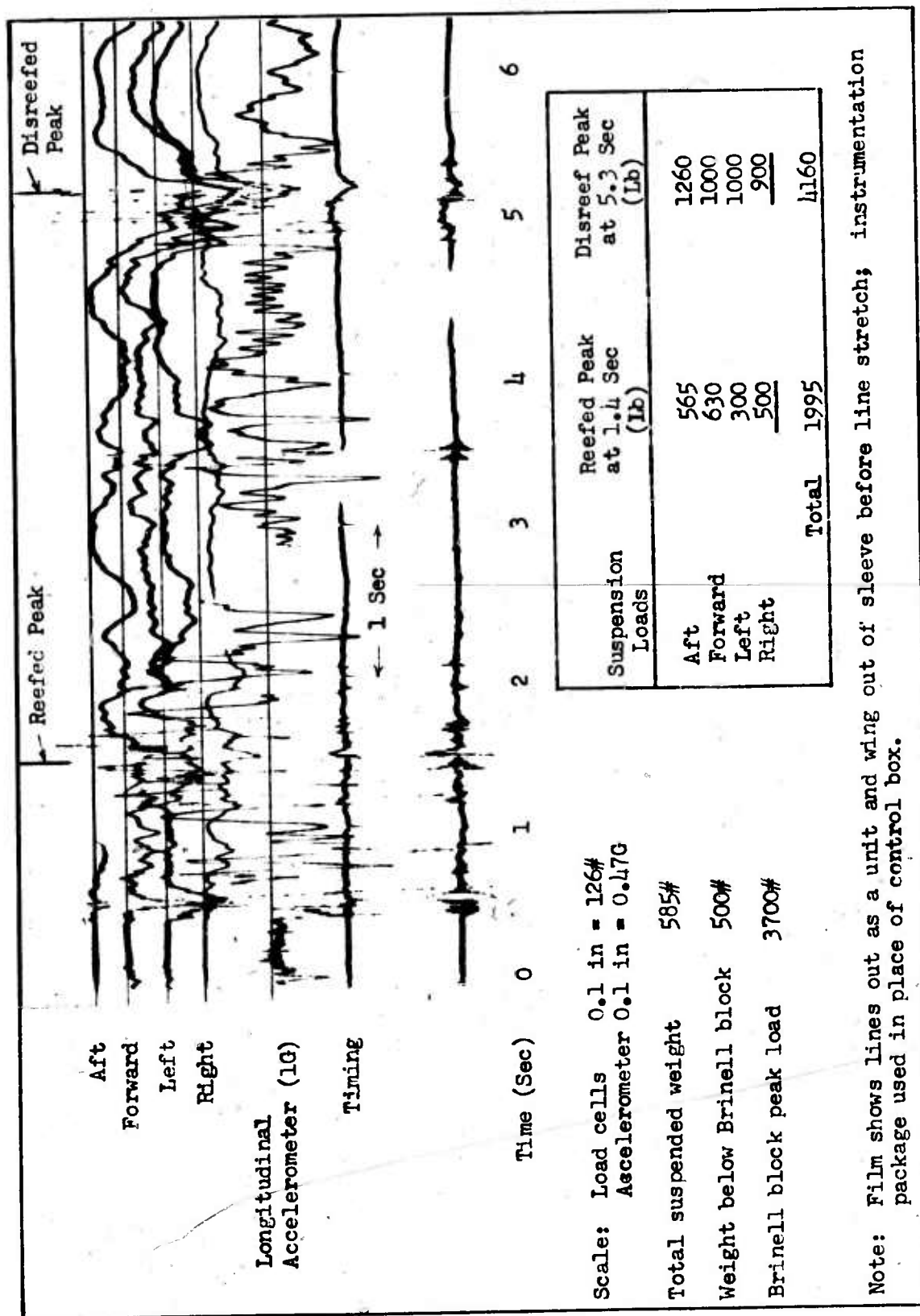


Figure 87. Instrumentation Data Test 204

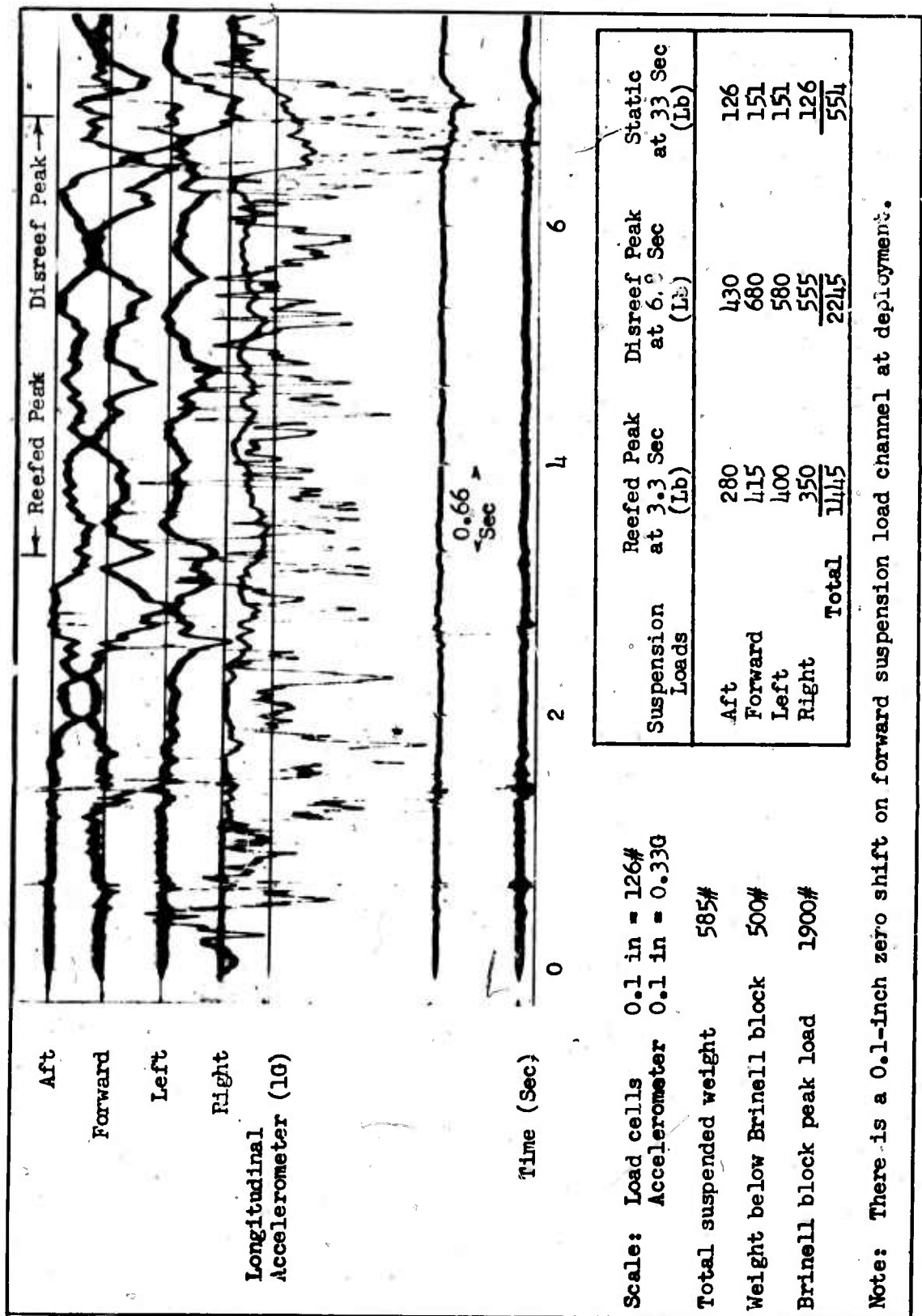


Figure 88. Instrumentation Data Test 208

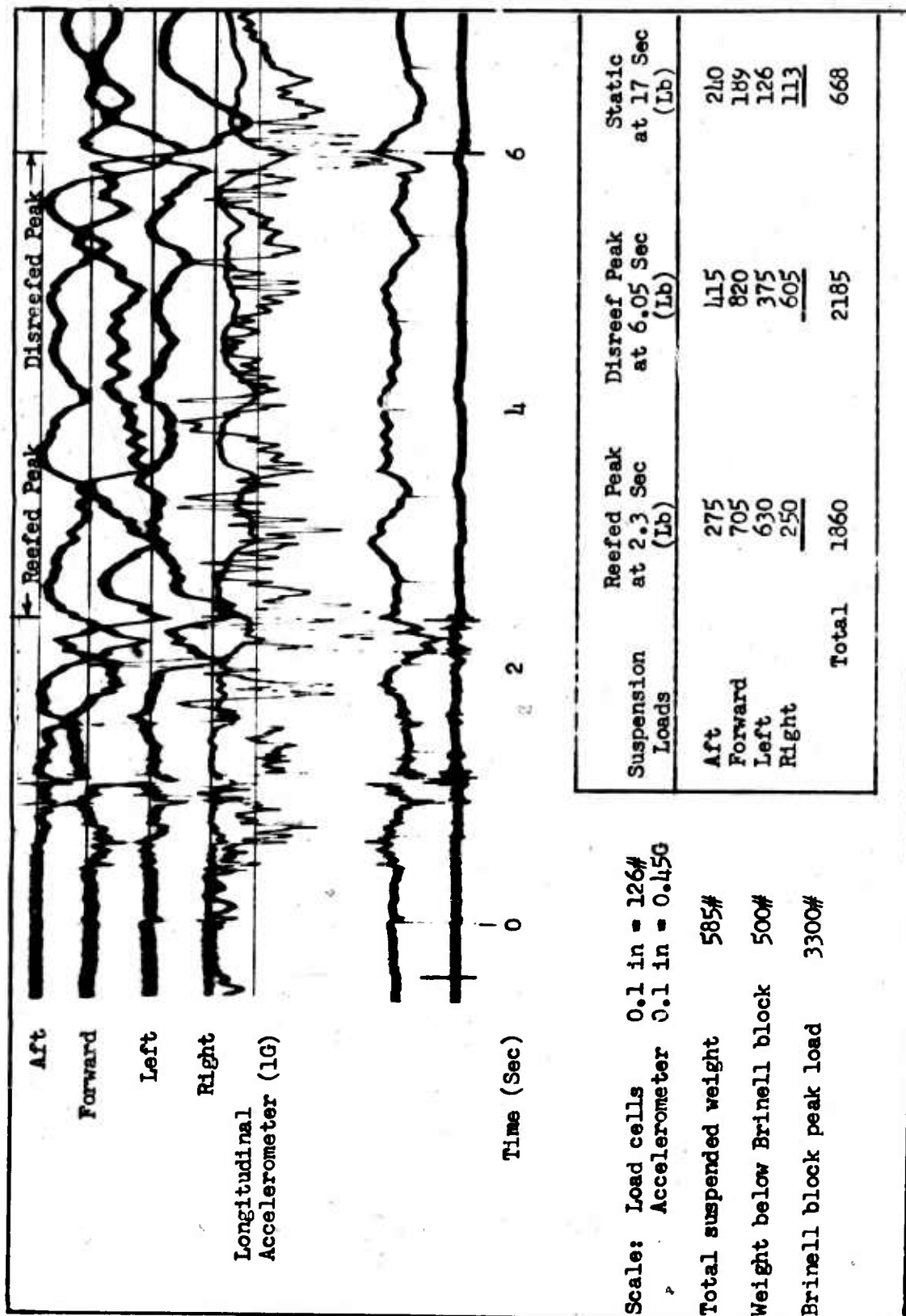
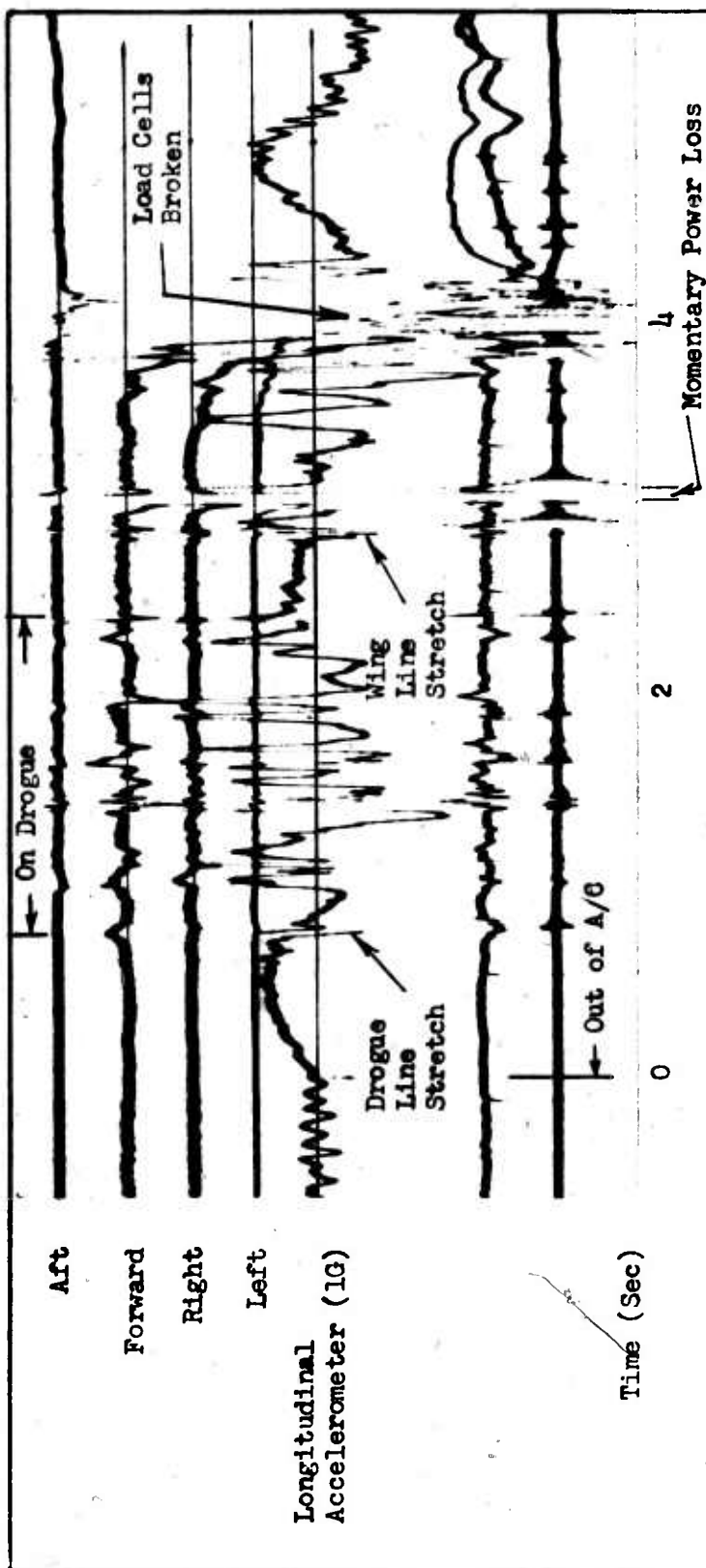


Figure 89. Instrumentation Data Test 212



Scale: Load cells 0.1 in = 126#  
Accelerometer 0.1 in = 0.47G

Brinell block peak load 7200#

Note: The MIL-W-5625, 1000-pound reefing line broke shortly after wind deployment resulting in a peak load of 7200 pounds as measures by the Brinell block. The yield point of the dog bones used in the load cells was 1200 pounds per cell, and all four cells were damaged beyond reuse. There was no other damage to the system.

Figure 90. Instrumentation Data Test 217

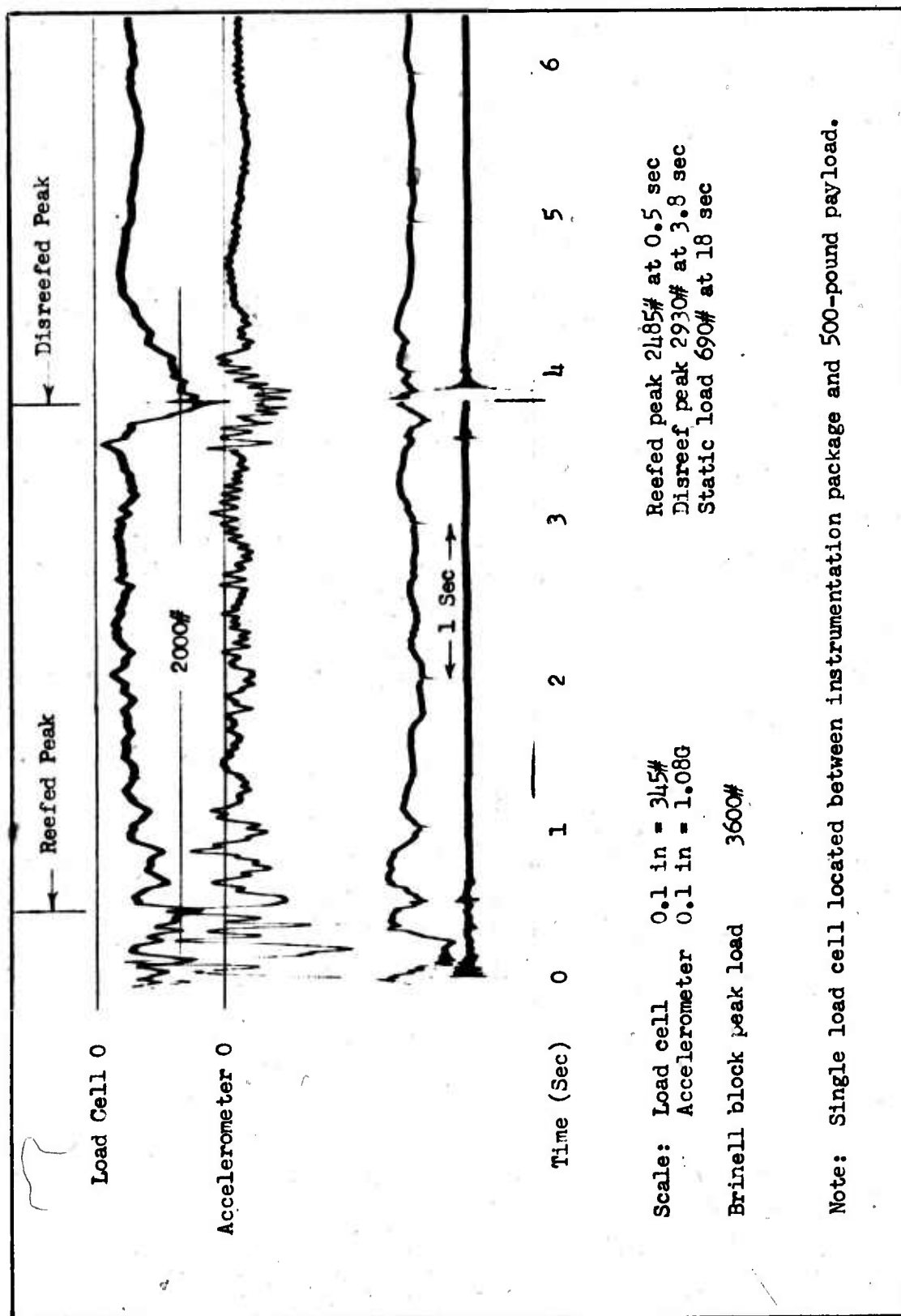


Figure 91. Instrumentation Data Test 224

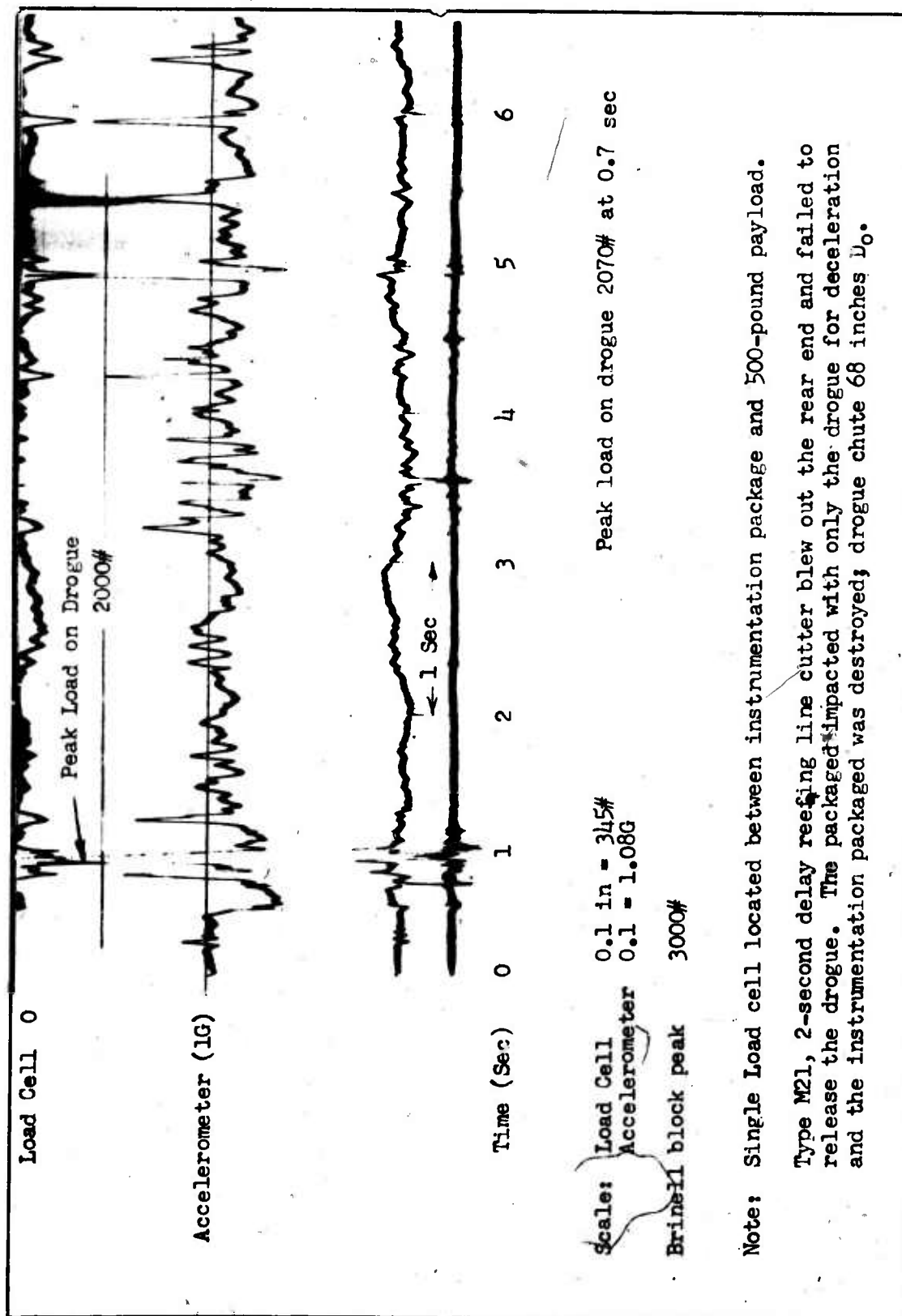


Figure 92. Instrumentation Data Test 225



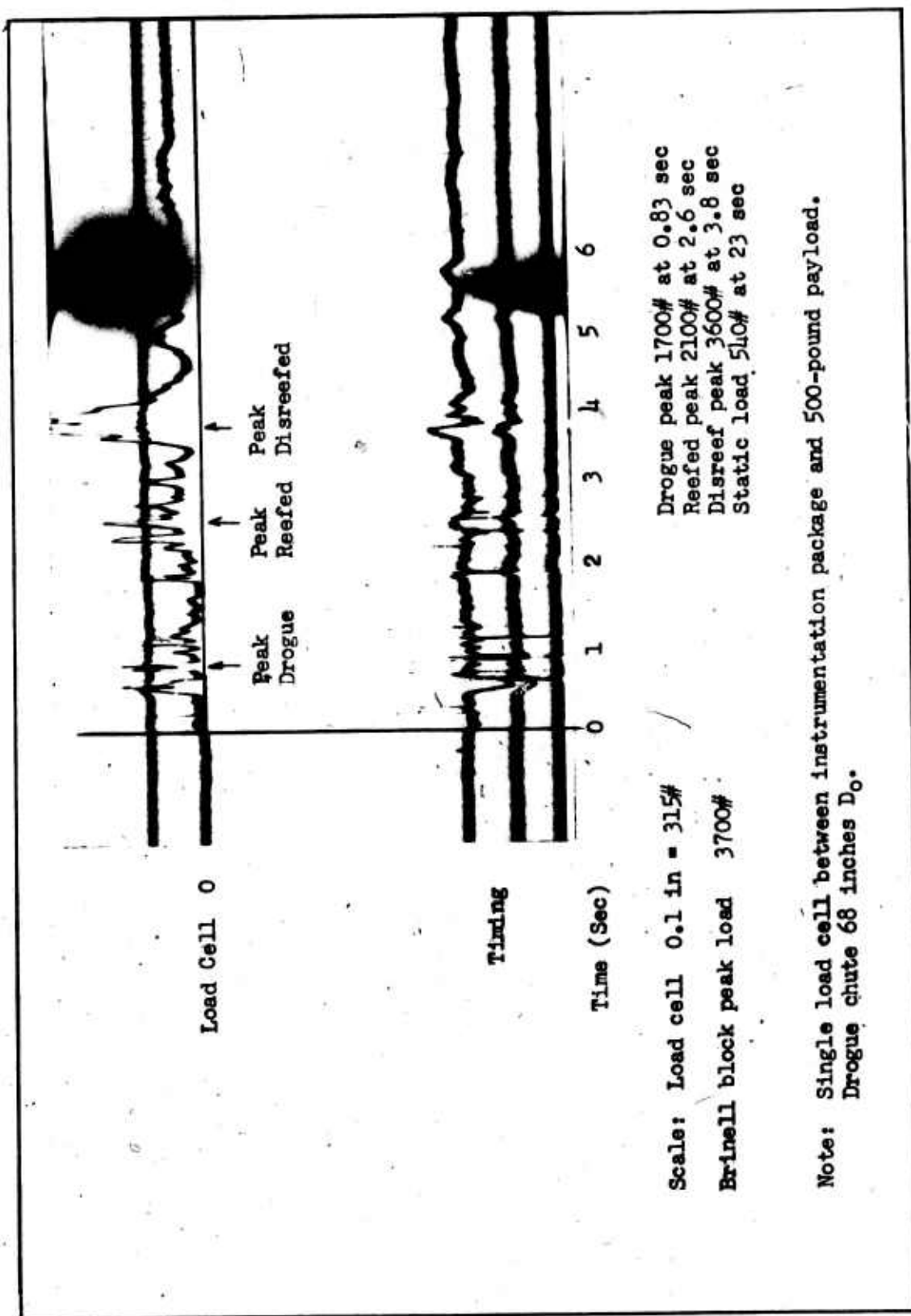


Figure 93. Instrumentation Data Test 229

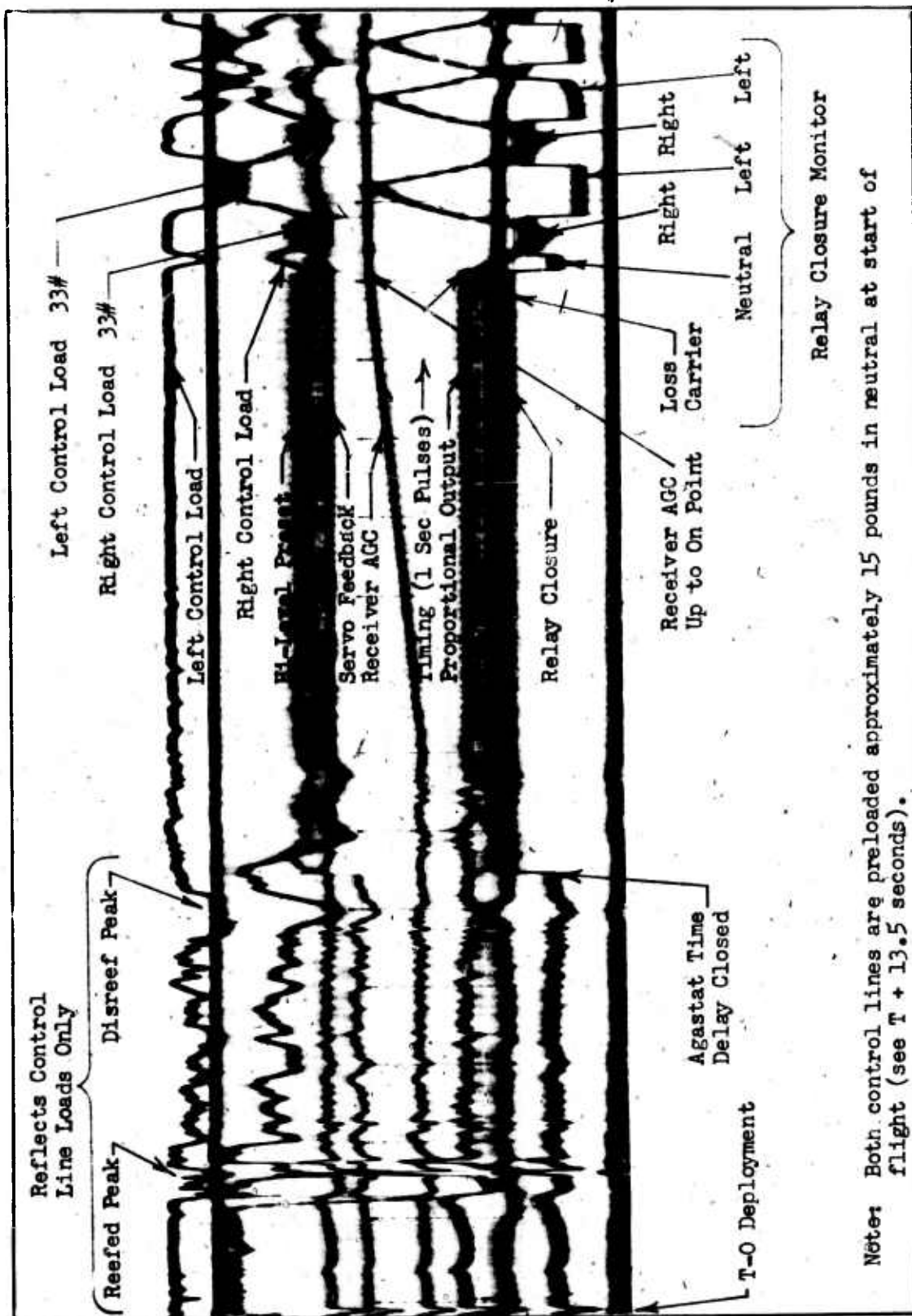


Figure 94. Instrumentation Data Test 242

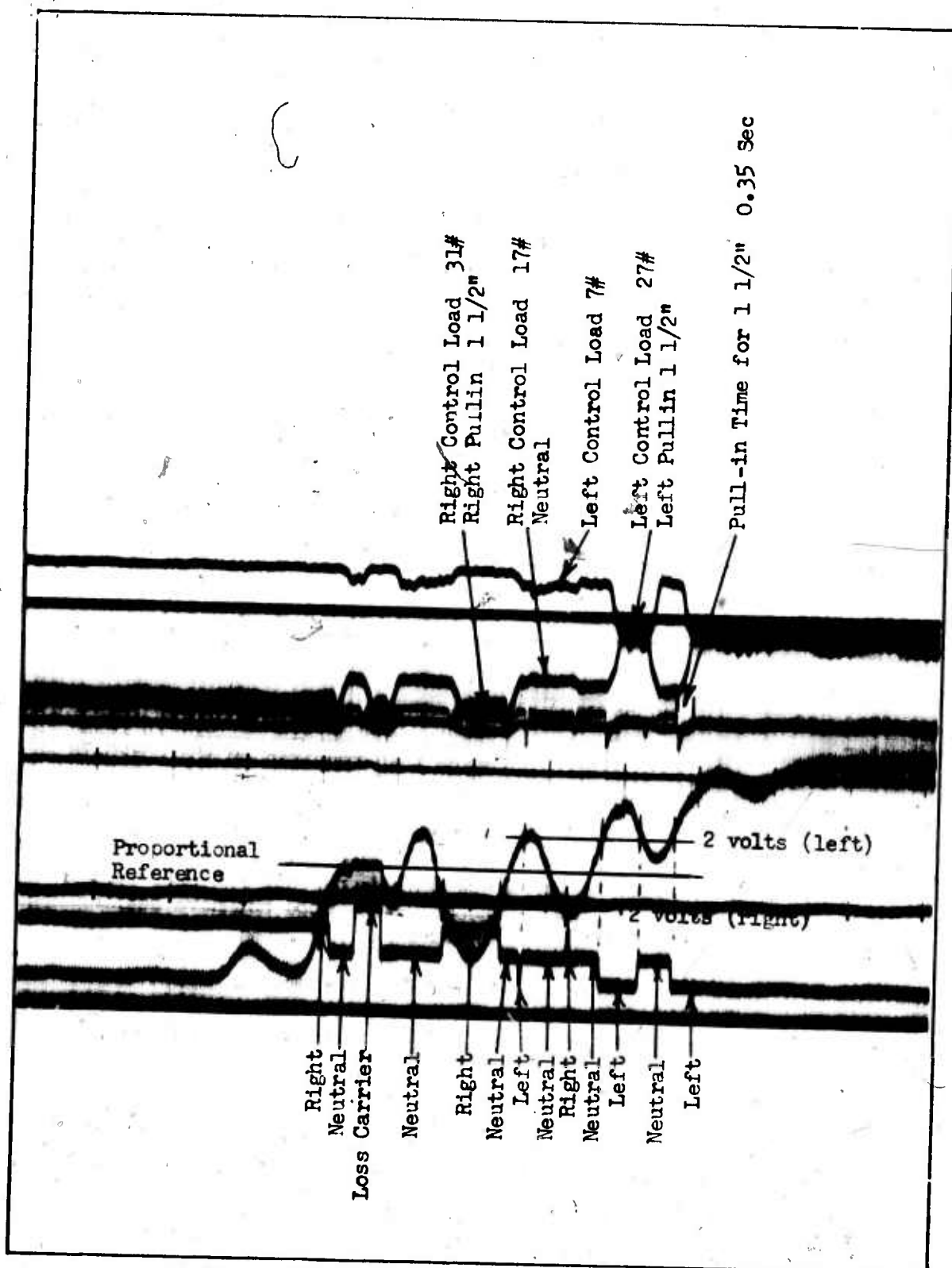


Figure 95. Instrumentation Data Test 242

**APPENDIX VII**  
**EXEMPT PARTS LIST**

<u>Part No. and Name</u>	<u>Mfg Code</u>	<u>Reason</u>
C177 Connector	59730	Nearest applicable spec is MS20659-28, which does not provide a terminal for 5/8-inch studs that will accommodate No. 12 AWG wire
8661-50 Shielding	70903	Equivalent to federal spec QQ-B-575
DAC-15P Connector	71468	Part selected because of space requirements; nearest standard part is M24308/2-2; no QPL for MIL-C-24308
80GB5-4-A-5X Relay	98927	Part recommended by Ryan Aeronautical as compatible with their radio equipment
79GB10R4-A600 Relay	98927	Part recommended by Ryan Aeronautical as compatible with their radio equipment
CA3108ER20-7S Connector	71468	Part provides potting feature (for sealing and strain relief) in less space than required by MS3108R20-7S with M53057 strain relief clamp
703PBI Switch	91929	703PBI is made up of MS27216-1 (MIL-S-8805/8) sensitive switches which are sealed; nearest MIL spec part M8805/23-003 does not have sealing feature
DAC-15S Connector	71468	Part selected because of space requirements; closest applicable spec MIL-C-24308; no QPL for MIL-C-24308
DBC-25S Connector	71468	Part selected because of space requirements; closest applicable spec MIL-C-24308; no QPL for MIL-C-24308
DCC-37S Connector	71468	Part selected because of space requirements; closest applicable spec MIL-C-24308; no QPL for MIL-C-24308

<u>Part No. and Name</u>	<u>Mfg Code</u>	<u>Reason</u>
34002-6-63 Terminal Block	98410	Part selected because of space requirements; closest equivalent standard part is Class 40TB of MIL-T-55164/4
2112DH3N (.05-10 sec) Time Delay Relay	98403	No time delay relays qualified under MIL-R-5757
PT06SE-12-10S Connector	77820	Commercial equivalent to MS3126E12-10S; future procurements will be to MIL-C-26482
JS5 Switch Actuator	92993	No standard switch actuator available for this application

Unclassified

Security Classification

## DOCUMENT CONTROL DATA - R &amp; D

(Security classification of title, body of abstract and indexing annotation must be entered when the overall report is classified)

## 1. ORIGINATING ACTIVITY (Corporate author)

Goodyear Aerospace Corporation  
1210 Massillon Rd.  
Akron, Ohio 44315

## 2a. REPORT SECURITY CLASSIFICATION

Unclassified

## 2b. GROUP

## 3. REPORT TITLE

500-Pound Controlled Airdrop Cargo System

## 4. DESCRIPTIVE NOTES (Type of report and inclusive dates)

Final Report

## 5. AUTHOR(S) (First name, middle initial, last name)

Robert G. Slayman  
Herbert Q. Bair  
Thomas W. Rathbun

## 6. REPORT DATE

September 1970

## 7a. TOTAL NO. OF PAGES

253

## 7b. NO. OF REFS

6

## 8a. CONTRACT OR GRANT NO.

DAAJ02-68-C-0040 NEW

## 9a. ORIGINATOR'S REPORT NUMBER(S)

USAAVLABS Technical Report 70-31

## 8b. PROJECT NO.

1F164204D158

## 9b. OTHER REPORT NO(S) (Any other numbers that may be assigned this report)

GER-13801

## 10. DISTRIBUTION STATEMENT

This document is subject to special export controls, and each transmittal to foreign governments or foreign nationals may be made only with prior approval of US Army Aviation Materiel Laboratories, Fort Eustis, Virginia 23604.

## 11. SUPPLEMENTARY NOTES

## 12. SPONSORING MILITARY ACTIVITY

U.S. Army Aviation Materiel Laboratories  
Fort Eustis, Virginia

## 13. ABSTRACT

The purpose of this work was to develop and furnish to the Army (USAAVLABS) a flexible-wing delivery system for all-weather airdrop of 500 pounds of cargo with both automatic and command homing capability. These systems are for use in military engineering and service tests.

A detailed design analysis and trade-off was accomplished, followed by a full-scale wind-tunnel test program and flight test evaluation effort which resulted in the selection of a twin-keel catenary parawing, airborne control box, and suspension system. This final system was then tested for reliability and landing accuracy.

This report presents the results and findings of the work accomplished.

DD FORM 1473

1 NOV 66 REPLACES DD FORM 1473, 1 JAN 64, WHICH IS OBSOLETE FOR ARMY USE.

Unclassified

Security Classification

14.

KEY WORDS

LINK A

LINK B

LINK C

ROLE

WT

ROLE

WT

ROLE

WT

Cargo Delivery

All-flexible Parawing

Twin-catenary-keel Parawing

Automatic Homing

Manual Control Homing

Loss Subcarrier

"0" + 3/4 Nose Tuck Reefing